TIME DOMAIN SIMULATION OF SWATH SHIP MOTIONS

by

Erik K. Arthur. B.Sc.

Thesis submitted for the Degree of Master of Science

Department of Naval Architecture and Ocean Engineering
University of Glasgow

May 1988

To my Parents, who have taught and inspired me since the day I was born

and, to my good friend James

DECLARATION

Except where reference is made to others, this thesis presents the author's original work.

ACKNOWLEDGEMENTS

Studies of this nature require the support of a large number of people. I would particularly like to thank the following :

Professor D. Faulkner, Head of Department, for providing the research opportunity and, for his confidence in me,

Dr. R. C. McGregor, my Supervisor, for allowing me freedom of approach and for proposing me to the Department,

Dr. Atilla Incecik, Superintendent at the Hydrodynamics Laboratory, for his enthusiastic advice and co-operation,

James MacGregor, research colleague and authority on SWATH, with whom I have enjoyed a special rapport,

Dr. Neil Bose, for his valuable guidance and friendship during my early days at the Department,

Koon Tong, for his expert opinion on Hydrodynamics,

My colleagues in research, for lively debate and especially Muhittin Soylemez for sharing his knowledge of time domain analysis,

Ho Hwan Chun, for his direct comment and for helping make a home of Acre House,

Bob Christison and the technicians at the Hydrodynamics Laboratory, for their warm spirit and buoyant goodwill.

Finally, I would like to pay tribute to the University of Glasgow trusting that by their indulgence, they will have profited in some small way.

Happy to have completed this research, it is with great regret that I take leave of my colleagues.

ABSTRACT

This thesis presents a technique for predicting the coupled heave and pitch motions of SWATH vessels in the time domain. The emphasis is on completing the essential foundation work required for developing a fully comprehensive, non-linear time domain model.

A procedure for solving the coupled motion equations is developed for linear motions and then validated using predictions obtained from equivalent frequency domain analysis. Hydrodynamic quantities are calculated using a two dimensional strip theory method which involves solving source distribution boundary value conditions using the Frank Close-Fit technique. The methods employed for introducing some non-linear effects caused by the time dependency of motion coefficients and wave exciting forces and moments are described. Results from a computer program written to perform the time domain calculations are used to illustrate the non-linear phenomena and to demonstrate the improved correlation with model test data that can be achieved using non-linear time domain analysis.

Further development work is proposed. The influence of motion control fins and the occurrence of cross-Structure slamming require careful consideration in SWATH ship design. Suitable approaches to introducing these non-linear effects into the simulation are suggested.

CONTENTS

LIST OF FIGURES

CHAPTER 4

CHAPTER 5

CHAPTER 6

LIST OF TABLES

CHAPTER 1

CHAPTER 6

NOMENCLATURE

a	Wave amplitude.
a_{jk}	Strip section added mass coefficient.
a_{33f}	Control fin added mass.
a^{m}	Mean component of sectional added mass coefficient.
a^{os}	Oscillatory component of sectional added mass coefficient.
b_{jk}	Strip section damping (potential) coefficient.
b^{m}	Mean component of sectional damping coefficient.
b^{os}	Oscillatory component of sectional damping coefficient.
c_{aN}	N^{th} order coefficient of sectional added mass coefficient polynomial.
c_{bN}	N^{th} order coefficient of sectional damping coefficient polynomial.
c_r	Fin root chord length.
c_t	Fin tip chord length.
f_{nI}	Imaginary part of sectional heave force.
f_{nR}	Real part of sectional heave force.
f_D	Fin cross flow drag heave force.
f_I	Inertia component of fin heave force.
f_L	Fin lift heave force.
f_T	Total fin heave force.
$f^{K}_{(3)}$	Froude-Krylov (Incident) component of sectional heave force.
$f^{D}_{(3)}$	Diffraction component of sectional heave force .
g	Acceleration due to gravity.
i_N	N^{th} order coefficient of sectional force (imaginary) polynomial.
j	Mode of excitation.
k	Mode of motion.
k_o	Wave number.
m_f	Fin mass.

n	Hull section no.
n_i	Segment outward unit normal vector.
p_D	Diffraction hydrodynamic pressure component at a point on a strip section contour.
p_I	Incident wave hydrodynamic pressure component at a point on a strip section contour.
p_w	Net hydrodynamic wave excitation pressure at a point on a strip section contour.
r_N	N^{th} order coefficient of sectional force (real) polynomial.
t	Time (secs.).
u	Water particle velocity vector.
V_{zf}	Relative vertical velocity of control fin.
w_z	Vertical velocity of incident wave.
x_f	Longitudinal fin location.
x_n	Position of hull section n w.r.t. G.
A_e	Fin aspect ratio.
A_f	Fin face area.
A_{jk}	Added mass coefficient for whole vessel.
B_{jk}	Damping (potential) coefficient for whole vessel.
C_D	Drag coefficient.
$C_{L\sigma}$	Fin lift coefficient.
C_{jk}	Hydrostatic restoring coefficient.
C_n	Average normal load coefficient.
I_{55}	Pitch mass moment of inertia of ship.
E_n	Water surface elevation.
E_h	Heave motion component of water surface elevation.
E_p	Pitch motion component of water surface elevation.
E_w	Wave profile component of water surface elevation.

F_{jf} Forcing function correction due to fin effects.

F_j Amplitude of linear complex forcing function.

F'_j Amplitude of non-linear complex forcing function.

$F_j(t)$ Linear complex forcing function.

$F'_j(t)$ Non-linear complex forcing function.

F_{jI} Imaginary part of linear complex forcing function.

F'_{jI} Imaginary part of non-linear complex forcing function.

F_{jR} Real part of linear complex forcing function.

F'_{jR} Real part of non-linear complex forcing function.

F_T Total heave restoring force of control fin system.

$F^K_{(j)}$ Froude-Krylov (Incident) component of total wave excitation.

$F^D_{(j)}$ Diffraction component of total wave excitation.

G Centre of gravity.

L Hull length, overall.

LCB Longitudinal centre of buoyancy w.r.t. G.

M_T Total pitch restoring moment of control fin system.

M_{33} Ship mass.

REST3 Heave restoring force.

REST5 Pitch restoring moment.

R(t) Ramp function.

S_k Motion displacement in k^{th} mode.

$\dot{S}_k$ Motion velocity in k^{th} mode .

$\ddot{S}_k$ Motion acceleration in k^{th} mode.

S_{kR} Real part of motion displacement amplitude.

S_{kI} Imaginary part of motion displacement amplitude.

T Duration of time domain simulation.

U Ship forward speed.

* Denotes parameter in its non-dimensionalised form.

α_k	Phase Angle of complex motion response.
ε	Fin sweep-back angle.
ϕ_j	Phase angle of complex forcing function.
ϕ_D	Diffraction velocity potential component.
ϕ_I	Incident wave velocity potential component.
ϕ_R	Radiation velocity potential component.
ϕ_T	Velocity potential.
ϕ_w	Net wave excitation velocity potential.
γ	Controllable fin angle.
λ	Wave length.
σ	Controllable fin in angle of attack.
ω	Wave frequency.
ω_e	Wave encounter frequency.
μ	Wave heading angle.
∇	Differential operator.
∇_v	Volume of Ship displacement.

CHAPTER 1

INTRODUCTION

1.1 Introduction

Through the experiences of seafarers and the findings of marine theoreticians it has long been known that if the buoyant volume of a vessel can be kept well below the water surface, that vessel will be less lively in a seaway. This is the fundamental idea behind the SWATH ship concept.

SWATH is an acronym for Small Water-Plane Area, Twin Hull craft. The configuration has been actively exploited over the last two decades in the pursuit of improved operation capability. Activities have attracted interest from both commercial and military representatives who recognise the SWATH ship potential. The US Navy's active involvement in SWATH ship technology has included the design construction and full scale analysis of full-scale prototypes[24]. Other SWATH ships have been built and operated successfully on a commercial basis[60][61]. Many proposed conceptual designs have been published, the most recent of which is a commercial passenger ferry for Norwegian waters[47].

Attractive features of the concept when compared with a conventional monohull equivalent include improved seakeeping performance, higher speed capability in rough seas and reduced slamming and deck wetness. As a consequence the SWATH ship provides improved operational capabilities in extreme seas whilst maintaining acceptable levels of comfort and safety for crew and passengers.

The active development of the SWATH ship concept is in its early days. Recent studies have shown[45][48] that, as in the case of many new technologies, the concept itself has history which dates back many years. It cannot therefore be claimed that SWATH ships are a new invention.

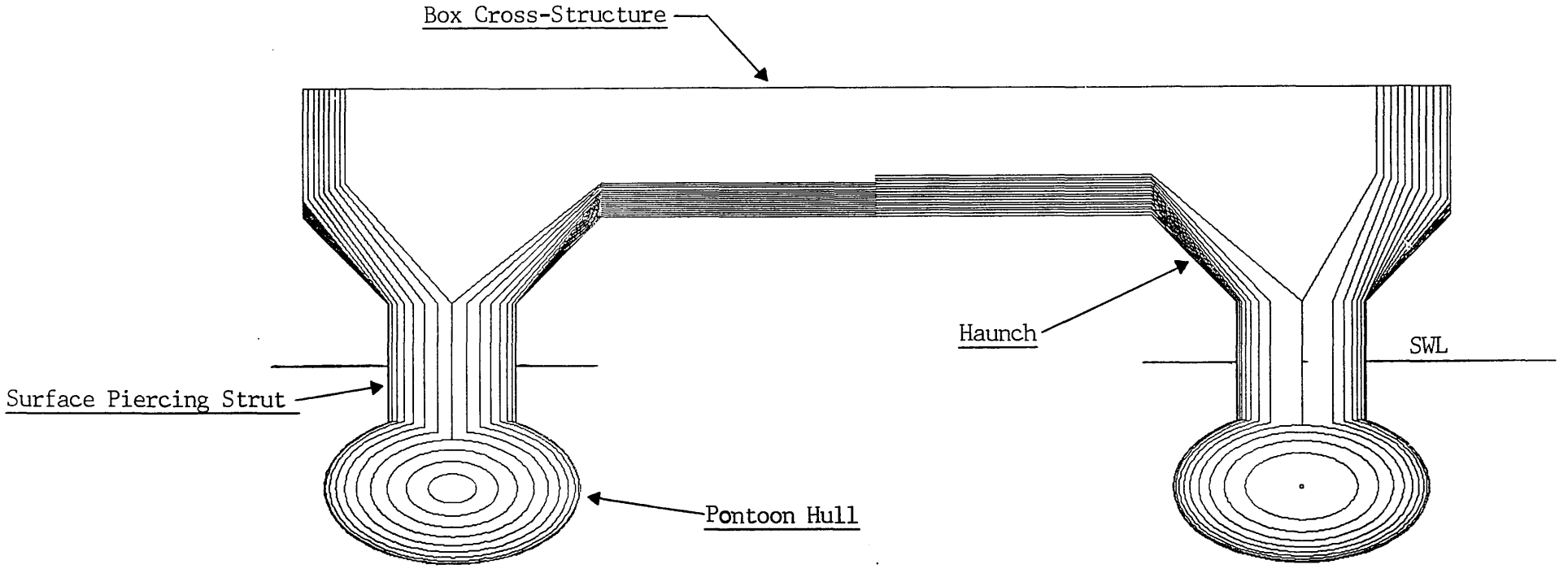

Figure 1.1 SWATH Ship Form

1.2 SWATH Ship Geometry

Limited experiences gained from the performances of prototypes and the results obtained from many SWATH design studies have led to the evolution of what are currently accepted as practical SWATH designs. Although the operational role will have a significance on design solutions, the general geometric proportions of a SWATH vessel can be described (Figure1).Most of the displaced volume, which consists of between 70 and 85 percent of the total is contained in the pontoon hulls. The hulls are slender and are circular or, more recently, elliptical in form. They have length to diameter ratios in the range of around 14 for smaller vessels and closer to 20 for designs of 15,000 tonnes and greater. Prismatic coefficient values for the hulls commonly lie within the range 0.7 to 0.9. Submerged portions of each surface piercing strut provide the remaining displaced volume. At the water surface the struts are fine with vertically prismatic section. Strut thickness is normally 30 to 60 per cent of the pontoon hull beam. The two distinct strut configuration options are either single strut per hull or twin struts per hull. Above their prismatic waterplane sections struts are flared. The inboard flare, running the length of the cross box structure, is known as the haunch. The box upon which superstructure is housed, connects the two struts and is positioned well clear of the water surface.

1.3 Seakeeping Characteristics

Monohull and SWATH ship motions differ both in magnitude and acceleration. The behaviour of monohulls is characterised by oscillations of large magnitude and high acceleration.These motions are the cause of crew discomfort, slamming occurrences and general degradation of operability. In contrast, the angular motions of SWATH vessels are low in both magnitude and acceleration. Consequently degradation of their operability occurs only in the more extreme sea conditions.

The seakeeping qualities of the SWATH concept has been impressively demonstrated by existing ships such as the Kaimalino[26] and Suave Lino[27]. Trials conducted by the US Navy have further demonstrated the seakeeping advantages of SWATH craft compared with equivalent monohulls.

The key feature which causes improved behaviour in waves is the small water-plane area. This has the effect of minimising wave exciting forces which act on the ship and results in the vessel describing long natural periods of motion. Since the high energy waves at most operation locations have short periods, the motions of SWATH vessels in moderate conditions are comparatively low. Measures taken to further improve performance include fitting active fin stabilisers. These lift generating devices are normally located on the inboard side of the pontoon hulls and provide restoring in the heave, pitch and role modes of motion.

There are some drawbacks associated with the small water-plane area configuration. When travelling at forward speed all craft experience a destabilising pitch effect known as the Munk moment. As SWATH ships have small restoring in pitch this effect which is proportional to the heave added mass times the square of the ship speed, may cause the vessel to become unstable at higher speeds and in certain following sea conditions.

Although SWATH ships tend to slam less frequently than conventional monohulls, the wave impacts that do occur on the underside of the cross deck can cause main structural damage, hull vibrations and crew discomfort. Raising the cross-deck higher above the water may appear to be a simple solution, however, this would result in raising the centre of gravity and further reduce the pitch and roll restoring arms.

The combination of tender behaviour and complex geometry of this concept gives great scope for designing both very good seakeepers and - very bad ones.

1.4 Theoretical Analysis of SWATH Seakeeping.

As the behaviour of SWATH ships in waves is substantially different to that of conventional monohull craft, there has been a requirement for the development of new design tools.

Seakeeping performance represents the principle design criterion for SWATH craft and, as a result, theoretical techniques for predicting SWATH motions are essential requirements in the development of SWATH design technology. SWATH motions are particularly sensitive to small changes in many of their design parameters. As a result, motions analysis carried out early in the design stage using validated techniques will allow the unfamiliar Naval Architect to proceed with a higher degree of confidence.

As commercial and military interest in SWATH technology increases there have been many seakeeping studies which have resulted in the development of numerical simulation methods for predicting SWATH ship motions and wave loads. Works by Lee and Curphey[11], Atlar[3] and Zheng[9] are good examples. Extensive studies have been carried out by the US Navy who are keenly pursuing the development of SWATH ships for combatant roles. Most recent of their published works is that by McCreight[28].

The University of Glasgow Department of Naval Architecture and Ocean Engineering has been involved in a long term programme of research into the development of SWATH ship technology. This has attracted interest and financial backing from both military and commercial sources. Products of the research have included the development of two prediction techniques which model motions response and primary structural loading. Both of these methods use applications of potential flow theory. One employs a two dimensional strip theory approach[3] whereas the other tackles the problem in three dimensions by using a distribution of surface panels[9].

Until recently, SWATH motion prediction techniques have, on the whole, been restricted to analysis in the frequency domain. Implicit in such analysis is the assumption that motions are linear. This limits their application to response in small amplitude waves and within this limited scope predictions have shown satisfactory agreement with test measurements.

In reality, as displaced geometry changes during a wave cycle, motions are non-linear. Closer correlation with reality can be sought by introducing the effects of non-linearity into prediction. To this end there is a requirement for time domain simulation of SWATH motion.

1.5 Study Objectives

The aim of this study has been to develop a theoretical model for predicting the coupled heave and pitch motions of SWATH vessels in the time domain. Throughout, the emphasis has been on technique development. The coupled heave and pitch simulation presented represents essential foundation work for the development of a fully comprehensive, non-linear time domain model.

As time domain analysis provides a means for including motion non-linearities it can be used for predicting SWATH behaviour and wave loading in the more extreme conditions which are beyond the scope of valid linear analysis. Although time domain analysis is computationally more demanding than linear frequency domain analysis, it can be used to assess effects such as slamming, fin stabilizer control, viscous damping, manoeuvring and damage condition performance .

The principle of the time sequence model is to define as accurately as possible the hydrodynamic and hydrostatic conditions experienced by the oscillating craft at a point in time. Having established these conditions , the coupled differential equations of

motion which define the force system can be solved. The values of motion displacements obtained and the altered position of the incident wave define a revised submerged geometry which represents the condition for the next solution time step.

The core development described here incorporates three non-linear effects. It has been suitably structured to enable the systematic introduction of further non-linearities and additional modes of motion.

Although the capacities of digital computers have advanced dramatically in recent years, solving non-linear differential equations of motion can present a demanding task. For this reason, and in order to make the development process more manageable, some necessary simplifications and assumptions have been incorporated.

Solving the hydrodynamic force problem to determine wave excitation and added mass and wave (potential) damping represents the most complex part of wave induced motion simulation.

At present the theoretical models available, such as those described in references (1) and (2), use applications of linear hydrodynamic theory and are based on the assumption that motions described by the vessel are small amplitude harmonic oscillations about a fixed mean position.

Until a general, computationally efficient, solution is available for the time-varying hydrodynamic forces on a body undergoing arbitrarily large motions in steep waves, these techniques based on linear theory remain the only practical alternative and it is necessary to make this somewhat intuitative simplification in modelling the hydrodynamic forces.

The technique used in this study was developed specifically for application to SWATH-type geometries. It has been applied in frequency domain predictions of SWATH ship motions. Comparisons made with model test results show that the technique provides good approximations of the hydrodynamic coefficients and wave

exciting force. In a time domain solution it is important to minimise the number of calculations performed at each time step . This is to avoid the requirement of excessive computer CPU time. Computationally lengthy hydrodynamic calculations are impractical to apply during the time sequence. This problem has been overcome by developing a technique which involves the use of a pre-generated database of sectional hydrodynamic properties.

Restoring force and moment variations are modelled by defining the submerged hull-strut geometry at each time step and calculating values for the associated instantaneous vessel displacement and LCB position.

A systematic approach has been adopted for this work. First , a basis solution procedure was developed and validated for linear motions. Then, non-linear effects due to the time dependencies of wave excitation, restoring, added mass and damping were introduced in turn.

1.6 Model 'SWATH11'

For each development stage in this study, validation has been sought by , comparing the time domain predictions with results obtained from frequency domain analysis and model seakeeping trials.

Previous work carried out at the University of Glasgow Department of Naval Architecture and Ocean Engineering Hydrodynamics Laboratory[8] has involved extensive physical model tests to study the behaviour of the SWATH11 design. This model has been used for validation during the development of existing SWATH motion prediction technique at the department. Comprehensive information on the behaviour of this design is therefore readily available. Owing to the ensuing facts and the shortage of alternative SWATH model test data generally, SWATH11 has been a natural choice for the test case.

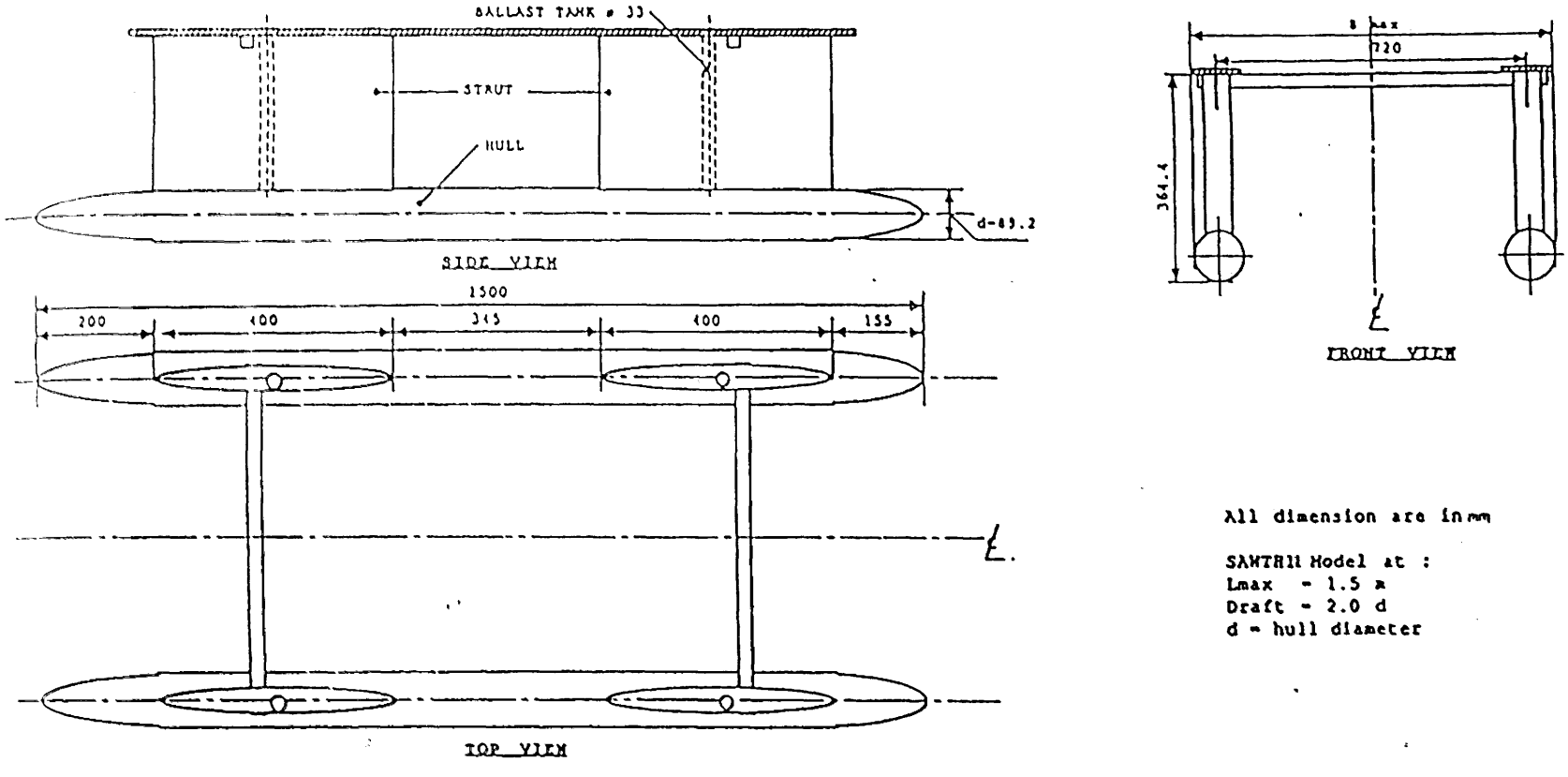

Figure 1.2 Model SWATH11 - General Arrangement and Principle Dimensions

Weight	21.8 Kg
Hull Length (L)	1.500 m
Strut Length	0.400 m
Hull Diameter (D)	0.089 m
Draught (2xD)	0.178 m
Hull Spacing between Centres of the Hull	0.720 m
Waterplane Area	0.054 m^2
Longitudinal Distance from Nose of the Hull to the Forward Strut End	0.155 m
Longitudinal Distance from Tail of the Hull to Rear Strut End	0.200 m
Longitudinal Metacentre above Keel (KM_L)	0.429 m
Transverse Metacentre above Keel (KM_T)	0.512 m
Centre of Gravity above Keel (KG)	0.176 m
Vertical Centre of Bouyancy (VCB)	0.064 m
Longitudinal Centre of Gravity (LCG)	0.752 m
Longitudinal Metacentre above Centre of Gravity (GM_L)	0.252 m
Transverse Metacentre above Centre og Gravity (GM_T)	0.327 m

Table 1.1 SWATH11 Hydrostatic Particulars

Figure 1.2 shows the general arrangement and principle dimensions of SWATH11. It has circular section pontoon hulls and has a twin strut per hull configuration. The hulls have paraboloid and tapered ends. All four struts are prismatic vertically and have a fine aerofoil section. Hydrostatics particulars for the design are given in table 1.1.

1.7 Simplifications and Assumptions

The mathematical model described is restricted to coupled heave and pitch motions of a SWATH ship advancing in regular head seas. Heave and pitch motions are assumed to be free oscillations which refer to the systems of axes described below.

Extreme situations such as the occurrence of cross-deck structure slamming and submerged hulls breaking the water surface are not included at this stage.

Designs under analysis should possess longitudinal centre plane symmetry and should rest in still water in their upright position.

A brief description of the method is given in section 4.0. The technique used to perform the hydrodynamic calculations is restricted to determining first order oscillatory wave forces which are proportional to incident wave amplitude. Second order wave forces, proportional to the square of the wave amplitude, are not included.

Only potential wave damping is accounted for. The effects of viscosity could be introduced relatively easily at a later stage as a subject of further development work.

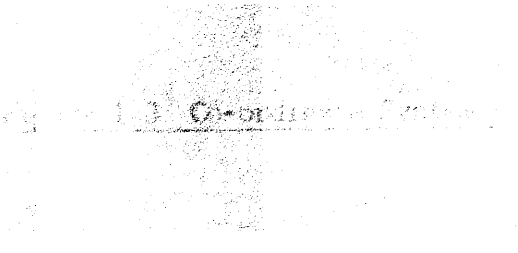

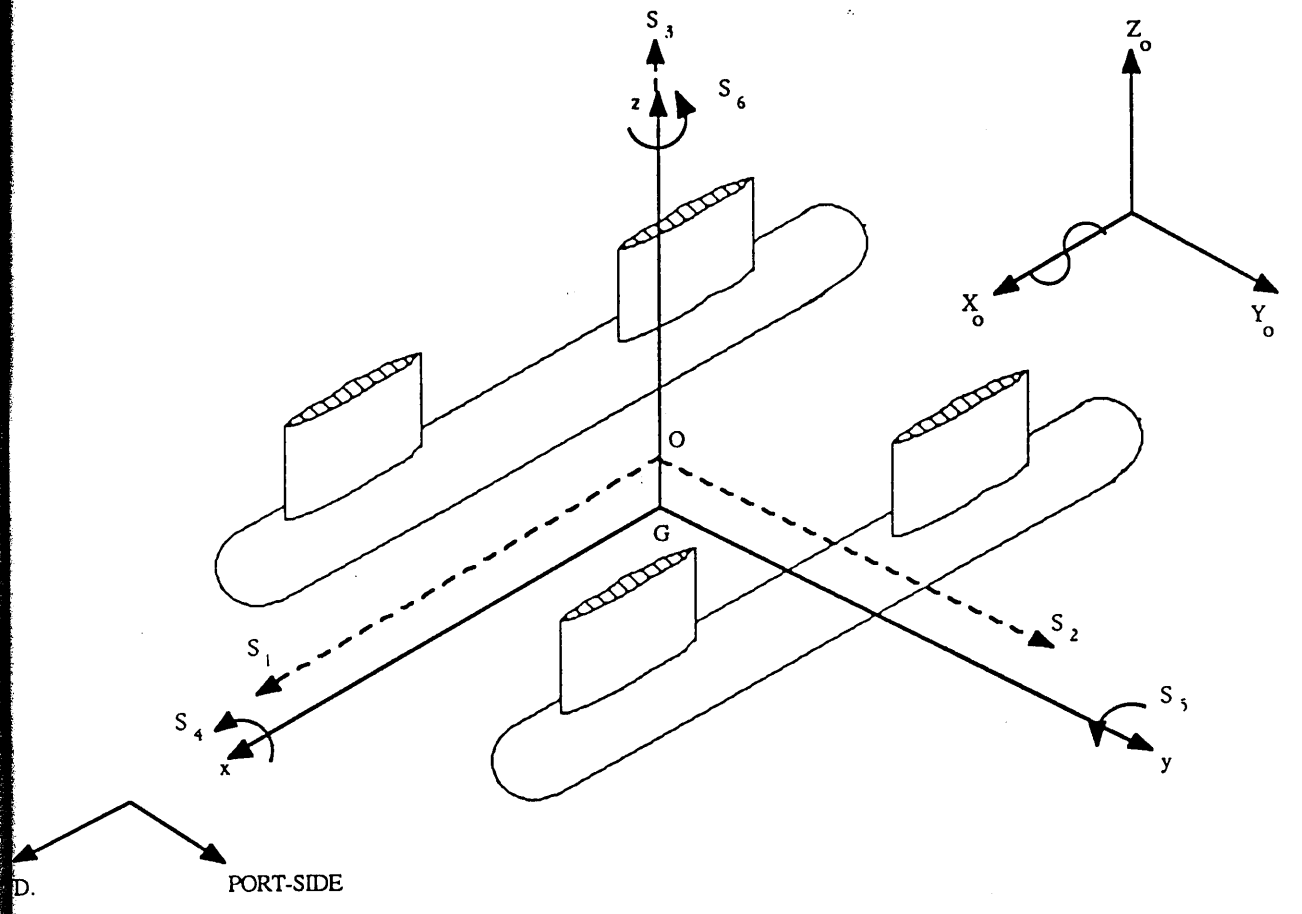

Figure 1.3 Co-ordinate Systems

1.8 Co-ordinate Systems

Expressions for heave and pitch motions and for fluid force components refer to the following orthogonal, right handed, co-ordinate systems (Figure 1.3) : -

(i) earth-fixed axes (O-XoYoZo) are fixed with respect to the earth.Their origin is located at the calm water surface,

(ii) body-fixed axes (G-xyz) have their origin at the centre of gravity of the body and are coincident with the intersections of the principle planes of inertia,

(iii) space-fixed or mean body axes (O-XYZ) originate at the mean position of the body centre of gravity and are used to describe the body oscillations. This system is parallel to the earth-fixed axes but translates with ship speed,U.

1.9 Coupled Heave and Pitch Motions

Motions of the rigid-body SWATH ship are linear and angular displacements of the body axes with reference to the space fixed axes (O-XYZ).

The general, six-degree of freedom, expression for linear coupled motions of a floating body which is subjected to sinusoidal wave excitation can be written as : -

$$\sum_{k=1}^{6} (M_{jk} + A_{jk})\ddot{S}_k + B_{jk}\dot{S}_k + C_{jk}S_k = F_j \qquad (1.2)$$

where,

k = mode of motion and has values 1, 2, 3, 4, 5 and 6 which refer to surge, sway, heave, roll, pitch and yaw respectively,

j = mode of excitation and has the values of k for corresponding modes,

M_{jk} = mass matrix containing the mass, mass moment of inertia and products of inertia of the body,

A_{jk} = added mass and added moment of inertia matrix

B_{jk} = damping force and moment matrix per unit linear and angular velocity,

C_{jk} = hydrostatic restoring force and moment matrix per unit linear or angular displacement,

F_j = complex wave exciting force or moment amplitude , and

S_k = complex motion displacement amplitude ,

Equations (1.1) are linear, coupled differential equations. These can be solved using frequency domain analysis where added mass, damping and restoring coefficients are constant values and wave force amplitudes are constants proportional to wave amplitude. As the vessel has longitudinal centre plane symmetry, the vertical plane modes, heave and pitch, can be uncoupled from the horizontal plane modes. The coupled heave and pitch equations of motion then become :

$$\begin{aligned}
&(M_{33} + A_{33})\ddot{S}_3 + B_{33}\dot{S}_3 + C_{33} S_3 + A_{35}\ddot{S}_5 + B_{35}\dot{S}_5 + C_{35} S_5 = F_3 \\
&(I_{55} + A_{55})\ddot{S}_5 + B_{55}\dot{S}_5 + C_{55} S_5 + A_{53}\ddot{S}_3 + B_{53}\dot{S}_3 + C_{53} S_3 = F_5
\end{aligned} \qquad (1.2)$$

1.10 Hydrodynamic and Hydrostatic Regimes

Equations (1.2) represent the coupled heave and pitch motions force system which is composed of hydrostatic, hydrodynamic and inertial forces and moments due to the vessel's mass.

M_{33} and I_{55} represent the inertial forces and moments which are proportional to the acceleration of heave and pitch motions respectively.

The coefficients C_{33},C_{35},C_{55} and C_{53} represent the hydrostatic restoring forces and moments which are proportional to motion displacement and act in opposition. These are caused by the changes in the immersed buoyant volume and centre of buoyancy resulting from motions and travelling wave position.

The relatively straight forward method employed to calculate the hydrostatic forces and moments is covered in Chapter 5. The method adopted for calculating the hydrodynamic coefficients and the wave exciting forces and moments is detailed in the following Chapter.

CHAPTER 2

HYDRODYNAMIC FORCES

2.1 Introduction

Wave exciting forces and the hydrodynamic coefficients of added mass and wave (potential) damping are calculated using a method which has been employed at Glasgow University[3] specifically for application to SWATH-type geometries. Beam-wise, two-dimensional strip theory and the Frank Close-fit technique[4] are applied for solving the boundary value, source distribution problem . Ideal fluid flow is assumed.

The boundary conditions for calculating added mass and damping coefficients are defined by assuming that the vessel oscillates with small amplitude unit motions in still water. Wave exciting forces and moments are calculated by assuming the vessel is rigidly fixed in an incident unit amplitude sinusoidal wave

Components of velocity potential represent the hydrodynamic system. The potential due to disturbance of the fluid caused by rigid body motions is known as the radiation potential and represents the added mass and damping forces. The incident wave potential and the potential due to the wave being diffracted by the rigidly held vessel represent wave excitation.

The two-dimensional Green's Function Integral equation method introduced by Frank (1967) involves representing the velocity potential by a distribution of sources over two dimensional strip sections. The unknown function of the density of sources along a section contour is determined from integral equations which are obtained by satisfying the kinematic boundary conditions. Hydrodynamic pressures are obtained from the velocity potential by using the linearised Bernoulli equation. Integration of these pressures over the immersed section yields

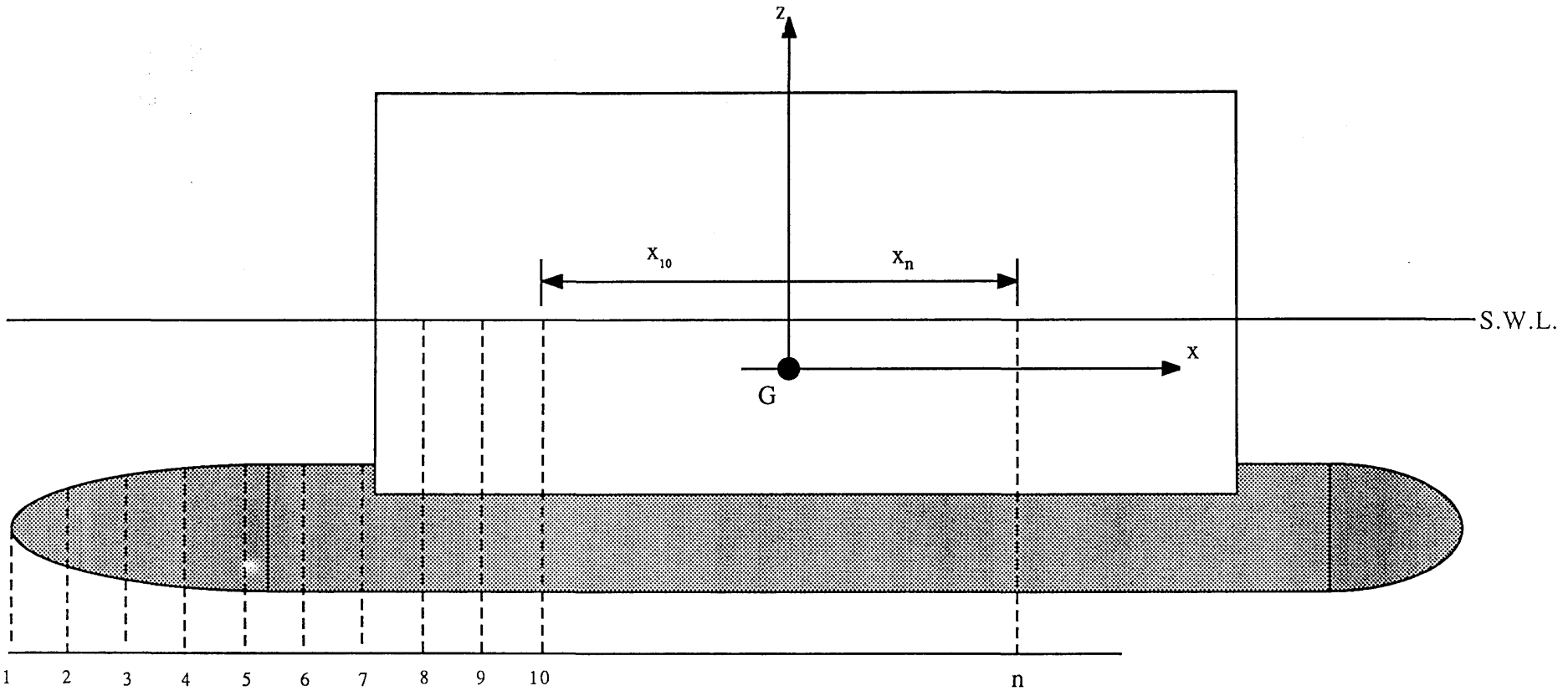

Figure 2.1 Beamwise Strip Sections

the hydrodynamic coefficients and wave exciting forces and moments.

The technique described in this chapter applies to vessels with longitudinal centre-plane symmetry and accounts for the hydrodynamic interference between the cross elements of the underwater geometry and the effects of the surface piercing strut sections.

2.2 Strip Sections and their Segmentation

In the two-dimensional strip theory approach to predicting wave induced and motion induced forces, the hydrodynamic system is analysed for separate beam-wise strip sections which are suitably distributed along the vessel length. The sectional forces calculated are then integrated longitudinally to obtain the net hydrodynamic forces for the whole vessel. Figure 2.1 illustrates a typical distribution of beam-wise strip sections for a tandem strut SWATH design.

Strictly speaking the two-dimensional strip theory approach to hydrodynamic motions and wave load modelling only applies to slender bodies where interaction between strip domain sections in the the third dimension can be assumed to be negligibly small. For submerged geometries or any part of that geometry which are not slender, significant three-dimensional effects can be expected and it is important to increase the number of longitudinal two-dimensional sections so that errors caused by 3-D effects can be minimised. Owing to their almost prismatic wetted form in the longitudinal sense , SWATH ships are good examples of slender bodies and are particularly suitable for 2-D strip theory analysis.

Applying the Frank Close-fit technique involves defining the contour of each strip section as a number of straight line elements. A typical segmented strip section contour for a surface piercing SWATH section is shown in figure 2.2. Figure 2.3 defines the individual segment notation which is referred to in the following theory. Pulsating source potentials are located at the mid-length of each segment, $P(y_j,z_j)$. The corresponding hydrodynamic pressures due to these

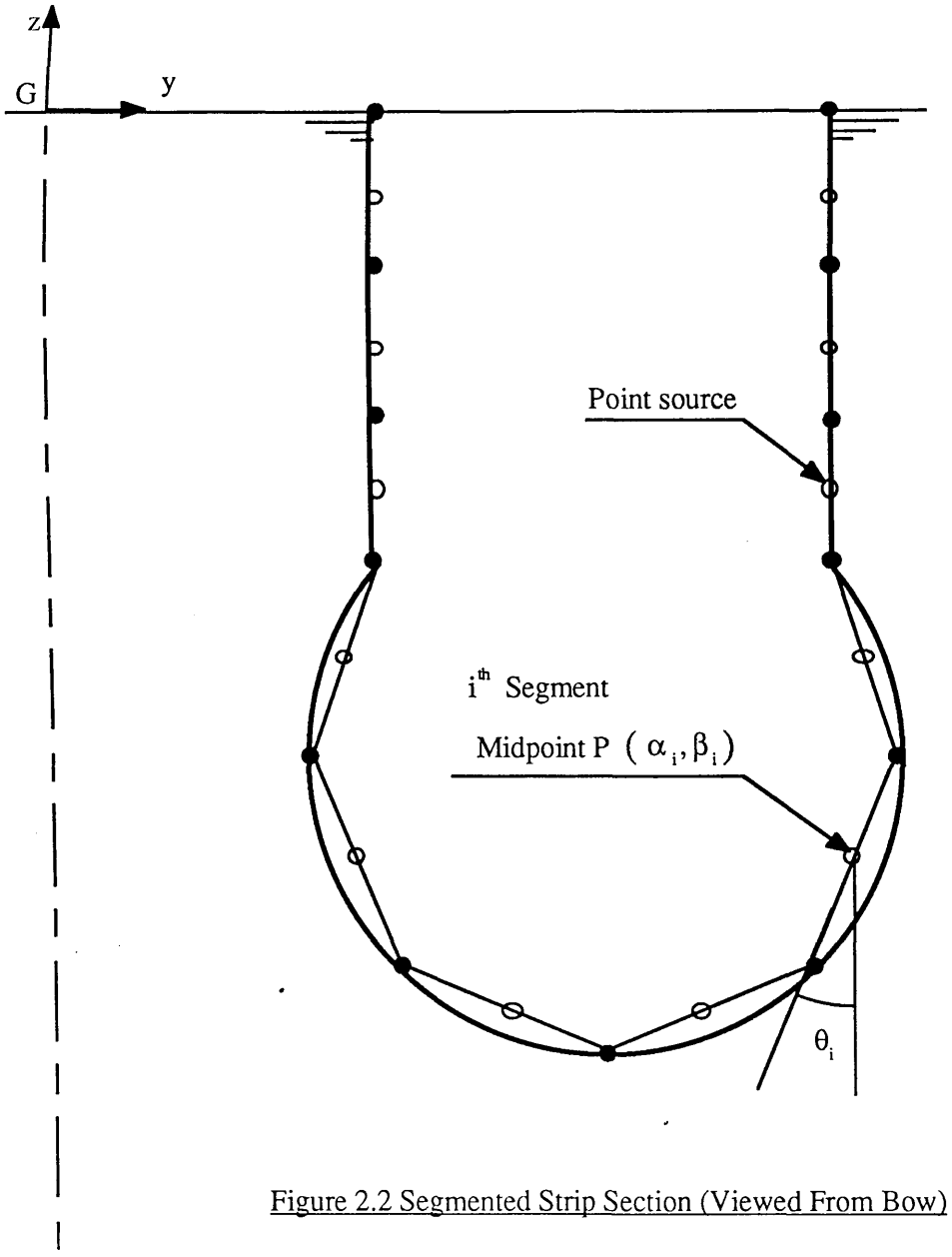

Figure 2.2 Segmented Strip Section (Viewed From Bow)

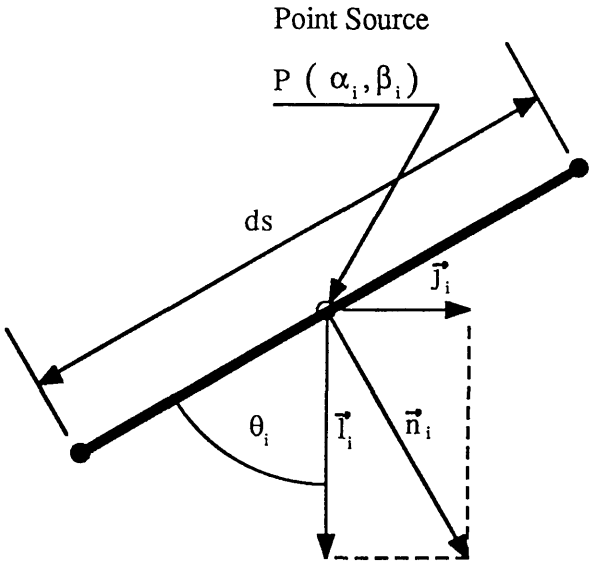

Figure 2.3 Segment Notation

source potentials are then calculated and assumed to be mean values which are evenly distributed along the segment length. Integrating these segment pressures around the strip section wetted surface yields the total hydrodynamic forces for that section.

2.3 Components and Conditions of the Hydrodynamic System

The motions of fluid particles due to an oscillating vessel in an ideal fluid can be described in terms of the particle velocity vector, u and a (scalar) velocity potential[12], ϕ_T. These will depend on the body-fixed co-ordinates (x,y, z) and time.

$$u = \nabla \phi_T(x, y, z, t) \tag{2.1}$$

where ∇ is the differential operator

ϕ_T can be regarded as the net velocity potential due to a combination of hydrodynamic effects. As the fluid motion is assumed to be simple harmonic motion , the velocity potential can be expressed with its time dependence as :

$$\phi_T(x, y, z, t) = \phi_T(x, y, z)\, e^{-i\omega t} \tag{2.2}$$

Assuming that the incident wave amplitude and the induced motions are small, the total velocity potential for a floating vessel amongst waves can be given as follows :

$$\phi_T(x, y, z, t) = \left[\phi_I(x, y, z) + \phi_D(x, y, z) + \phi_R(x, y, z)\right] e^{-i\omega t} \tag{2.3}$$

The first two terms in equations (2.3) are due to the incident wave and the diffraction of the wave on impact with the vessel's surface. These terms represent the total wave excitation potential , ϕ_W :

$$\phi_W(x,y,z,t) = \left[\phi_I(x,y,z) + \phi_D(x,y,z)\right] e^{-i\omega t} \qquad (2.4)$$

and are obtained by assuming the vessel is fixed in position. The third term, known as the radiation potential, is due to the disturbance caused by the vessel's rigid body motions. This term represents the added virtual mass and wave (potential) damping components of the hydrodynamic system.

2.4 Wave Exciting Forces from the Incident and Diffraction Potentials

Wave exciting forces and moments for the complete vessel can be obtained by determining sectional values of ϕ_W and calculating the dynamic pressure at each section using the linearised Bernoulli equation :

$$p_W(y,z,t) = -\rho \frac{\partial \phi_W(x,y,z)}{\partial t} e^{-i\omega t} \qquad (2.5)$$

where ρ is the water density.The component incident and diffraction potentials of ϕ_W are therefore required.

2.41 Boundary Conditions

As the vessel is assumed to be rigidly fixed in position when subjected to wave

action, the velocity in any direction on the wetted surface is zero The conditions on each section contour can therefore be defined.

Given that d/dn is the normal derivative at a point on the contour surface, the first condition is :

$$\frac{\partial \phi_W}{\partial n} = 0 \qquad (2.6)$$

where

$$\frac{\partial \phi_W}{\partial n} = \nabla \phi_W \cdot n = \frac{\partial \phi_W}{\partial x} n_x + \frac{\partial \phi_W}{\partial y} n_y + \frac{\partial \phi_W}{\partial z} n_z \qquad (2.7)$$

The following relationships :

$$\phi_W = \phi_I + \phi_D \quad \text{and} \quad \frac{\partial \phi_W}{\partial n} = \frac{\partial \phi_I}{\partial n} + \frac{\partial \phi_D}{\partial n} \qquad (2.8)$$

yield the second condition.

$$\frac{\partial \phi_I}{\partial n} = -\frac{\partial \phi_D}{\partial n} \qquad (2.9)$$

Equations (2.6) and (2.9) represent the kinematic boundary conditions at the hull surface. Other boundary conditions[33] [34] which must be satisfied by the diffraction

potential, ϕ_D and the incident potential , ϕ_I are :

(i) The Laplace continuity of fluid mass equation

$$\nabla^2 \phi_D = 0 \qquad (2.10)$$

(ii) The condition at the sea bed

$$\frac{\partial \phi_D}{\partial z} = 0 \qquad (2.11)$$

(iii) The linearised free surface condition

$$\frac{\partial \phi_D}{\partial z} - \frac{\omega^2}{g} \phi_D = 0 \qquad (2.12)$$

and in addition, for ϕ_D ,

(iv) The radiation condition distant from the vessel

$$\lim_{r \to \infty} r^q \frac{\partial \phi_D}{\partial r} - \frac{i\omega}{c} \phi_D = 0 \qquad (2.13)$$

where $q = (n-1)/2$ (n= no. of dimensions) and the radial distance 'r' and wave celerity 'c' are given by :

$$r = \sqrt{x^2 + y^2}$$

$$c = \lambda / T$$

2.42 Incident Component

Excitation forces due to the incident wave potential , ϕ_I are known as the Froude-Krylov forces .

The incident wave velocity potential, ϕ_I, in deep water is given by :

$$\phi_I(x, y, z, \mu, t) = \phi_I(y, z)\, e^{i(k_o x \cos \mu - \omega t)}$$

where (2.14)

$$\phi_I(y,z) = -\frac{i g a}{\omega} e^{(k_o z)}\ e^{(i k_o y \sin \mu)}$$

In this equation the term $e^{(i k_0 x \cos \mu)}$ accounts for the longitudinal phase shift at the strip section relative to the incident wave origin and $e^{(i k_0 y \sin \mu)}$ represents the wave component resolved in the 2-D strip section domain.

Equation (2.14) , which satisfies the above boundary conditions , represents the incident wave potential for all modes of motion. By breaking the equation down into its real and imaginary parts and omitting the time factor, the even and odd components of ϕ_I in the beam-wise strip domain are obtained :

$$\phi_I^{(o)}(y,z) = \mathrm{Re}[\phi_I(y,z)] = \frac{g a}{\omega} e^{(k_o z)} \sin (k_0 y \sin \mu)$$

(2.15)

$$\phi_I^{(e)}(y,z) = \mathrm{Im}[\phi_I(y,z)] = -\frac{g a}{\omega} e^{(k_o z)} \cos (k_0 y \sin \mu)$$

The even component , $\phi_I^{(e)}$, contributes to wave excitation in the heave mode and the odd component , $\phi_I^{(o)}$, contributes to wave excitation in the sway and roll modes. As this work is concerned with the vertical plane modes of motion , the strip sectional incident wave forces due to $\phi_I^{(e)}$ are required. The contribution to pitch can be obtained once the section heave forces have been calculated simply by applying the section lever about the body axes origin .

From equation (2.5) it can be seen that the induced incident wave pressure at a point on the section contour is given by :

$$p_I = -\rho \frac{\partial \phi_I}{\partial t} e^{-i\omega t} \qquad (2.16)$$

By substituting equation (2.15), in which the time factor is omitted, the time independent part of heave pressure is written :

$$\frac{p_I^{(3)}}{a} = \rho g e^{(k_o z)} \cos (k_o y \sin \mu) \qquad (2.17)$$

The superscript denotes the heave mode.

It is assumed that at each segment on a section contour, the dynamic pressure is evenly distributed and acts at the segment midpoint. The total strip section heave force is therefore given by :

$$f^K_{(3)}(x) = \int_{S(x)} p_I^{(3)} n_i^{(3)} ds \qquad (2.18)$$

where,

- i denotes the i^{th} segment ,
- $f^K_{(3)}$ is the sectional Froude-Krylov heave component per unit wave amplitude,
- ds is the segment length,
- $n_i^{(3)}$ is the outward unit normal for heave at the ith segment (= $\cos \theta_i$),
- $Z_{S(x)}$ is the anti-clockwise surface integral at section x.

Substituting (2.17) into (2.18) and omitting the time factor gives :

$$f^{K}_{(3)}(x) = \rho g \int_{S(x)} e^{k_0 z} \cos(k_0 y \sin \mu)\, dy \qquad (2.19)$$

By and integrating along the vessel length and taking into account the phase of each section, the Froude-Krylov heave force for the total vessel per unit wave amplitude becomes :

$$F^{K}_{(3)} = \int_{L} f^{K}_{(3)}(x)\, e^{ik_0 x \cos \mu}\, dx \qquad (2.20)$$

and, integrating moments of the sectional values gives the total Froude-Krylov pitch moment per unit wave amplitude is given by :

$$F^{K}_{(5)} = -\int_{L} f^{K}_{(3)}(x)\, e^{ik_0 x \cos \mu}\, x\, dx \qquad (2.21)$$

where L denotes the lengthwise integral.

2.43 Diffraction Component

The general equation for the diffraction potential is :

$$\phi_D(x, y, z, \mu, t) = \phi_D(y, z)\, e^{i(k_0 x \cos \mu - \omega t)} \qquad (2.22)$$

where , as for the incident potential, $e^{i k_0 x \cos\mu}$ represents the phase of each section in relation to the incident wave which has incidence μ and wave number k_0.

An expression for ϕ_D can be obtained by using the method first suggested by Frank[4] which involves the distribution of pulsating source potentials at each segment mid-length around the strip section contour. The distribution of sources is represented by Greens function[12]of unit strength point sources[4] [29], $G(y,z;\alpha_i,\beta_i,k_0)$. The Greens function representing a distribution of pulsating point sources is described in references (4), (35), (36), and (37) and is not discussed here. The strength of each source , $Q(\alpha_i,\beta_i)$ is determined by a set of integral equations. These equations are governed by the kinematic boundary conditions (equations 2.6 & 2.9) imposed under the assumption that the vessel is held fixed . Thus, the general equation for the total diffraction potential at each section is written :

$$\phi_D^{(m)}(y,z) = \int_S Q^{(m)}(\alpha_i,\beta_i)\ G(y,z;\alpha_i,\beta_i,k_0)\ ds \qquad (2.23)$$

where 'ds' is the differential surface area of the strip section and (α_i,β_i) is the segment mid-length location and 'm' denotes the mode of motion

Using the boundary condition (2.9) and by writing :

$$\frac{\partial}{\partial n} = \vec{n_i}\vec{\nabla} = \left(\sin\theta_i \frac{\partial}{\partial z} - \cos\theta_i \frac{\partial}{\partial y}\right) \qquad (2.24)$$

where (as shown in figure 2.3)

n_i is the outward unit outward normal vector at the i^{th} segment mid-length,

θ_i is the angle made by the segment with the z axis,

the normal derivative of the real and imaginary parts of the incident potential can be written :

$$\frac{1}{a}\frac{\partial \phi_I^{(o)}}{\partial n} = \omega\, e^{k_o z}[\sin\mu \cos(k_o y \sin\mu)\sin\theta - \sin(k_o y \sin\mu)\cos\theta]$$

$$\frac{1}{a}\frac{\partial \phi_I^{(e)}}{\partial n} = \omega\, e^{k_o z}[\sin\mu \sin(k_o y \sin\mu)\sin\theta + \cos(k_o y \sin\mu)\cos\theta]$$

(2.25)

Expressing the diffraction potential (2.23)in its real and imaginary part form gives :

$$\phi_D^{(m)} = \int_S (Q_R^{(m)} + i\,Q_I^{(m)})(G_R + i[-G_I])\,ds$$

$$= \int_S [(Q_R^{(m)} G_R + Q_I^{(m)} G_I) + i(G_R Q_I^{(m)} - G_I Q_R^{(m)})]\,ds$$

(2.26)

Thus by replacing the surface integral by a summation over a number of N segments the normal derivative of ϕ_D for a section contour is given as :

$$\frac{\partial \phi_D^{(m)}}{\partial n} = \left[\sum_{j=1}^{N} Q_j^{(m)} I_{ij} + \sum_{j=1}^{N} Q_{N+j}^{(m)} J_{ij}^{(m)}\right]$$

$$+ i\left[\sum_{j=1}^{N} Q_j^{(m)} J_{ij}^{(m)} - \sum_{j=1}^{N} Q_{N+j}^{(m)} I_{ij}^{(m)}\right] \qquad (2.27)$$

From equation (2.27) the normal derivatives of the real and imaginary parts of the source potential are given as :

$$\begin{aligned} I_{ij}^{(m)} &= \left(\vec{n} \cdot \vec{\nabla}\right) \int G_R \, ds \\ J_{ij}^{(m)} &= \left(\vec{n} \cdot \vec{\nabla}\right) \int G_I \, ds \end{aligned} \qquad (2.28)$$

and the unknown source strength real and imaginary parts are given as :

$$\begin{aligned} Q_j^{(m)} &= Q_R^{(m)} \\ Q_{N+j}^{(m)} &= Q_I^{(m)} \end{aligned} \qquad (2.29)$$

By substituting the normal derivative expressions for ϕ_D and ϕ_I given by (2.25) and (2.27) into the kinematic boundary condition equation given in (2.9), expressions for the potential of each mode of motion m can be obtained. For the heave force, which is associated with the even (or imaginary) wave potential derivative ,this yields :

$$\sum_{j=1}^{N} Q_j^{(m)} I_{ij} + \sum_{j=1}^{N} Q_{N+j}^{(m)} J_{ij}^{(m)} = 0$$

$$\sum_{j=1}^{N} Q_j^{(m)} J_{ij}^{(m)} - \sum_{j=1}^{N} Q_{N+j}^{(m)} I_{ij}^{(m)}$$

$$= \omega e^{k_o z} [\sin \mu \sin (k_o y \sin \mu) \sin \theta + \cos (k_o y \sin \mu) \cos \theta]$$

(2.30)

This algebraic system can be solved to yield the odd part of the complex source strength diffraction potential corresponding to the even incident wave potential (2.15). The diffraction potential for heave can be written in its final form as :

$$\phi_D = \left[\phi_D^{(o)} + i \phi_D^{(e)}\right] e^{i(k_o x \cos \mu - \omega t)} \qquad (2.31)$$

In the same manner as shown for the incident wave dynamic pressure in equation (2.16), the time independent part of hydrodynamic pressure due to wave diffraction is given by :

$$p_D = -\rho \frac{\partial \phi_D}{\partial t}$$

$$= i\rho\omega \left(\phi_D^{(o)} + i \phi_D^{(e)}\right) e^{ik_o x \cos \mu} \qquad (2.32)$$

and again, by integrating around the section surface, the sectional heave forces due to diffraction are obtained :

$$f^{D}_{(3)}(x) = i\rho\omega \int_{S(x)} \phi^{(e)}_{D}(y,z,k_0,\mu)\, dy \qquad (2.33)$$

Taking into account the phase of each section in relation to the wave origin, these sectional values are then integrated along the vessel length to give the total diffraction heave force and pitch moment per unit wave amplitude :

$$F^{D}_{(3)}(k_0) = \int_{L} f^{D}_{(3)}(x,k_0,\mu)\, e^{ik_0 x \cos\mu}\, dx$$

$$F^{D}_{(5)}(k_0) = -\int_{L} f^{D}_{(3)}(x,k_0,\mu)\, e^{ik_0 x \cos\mu}\, x\, dx \qquad (2.34)$$

where k_0 is the wave number at zero ahead speed.

In summary, the total wave exciting heave forces and pitch moments due to the incident wave and the diffraction of that wave are thus given by equations (2.20), (2.21) and (2.34). These expressions represent the heave force and pitch moment amplitudes per unit wave amplitude for the vessel due to wave excitation. Under the linearity assumption which is applied in this theory, the excitation for a given sinusoidal wave is obtained by multiplying the above by the wave amplitude, a.

2.44 Forward Speed Corrections

Reference (1) gives an approximate theory for introducing corrections to the wave excitation terms due to the effects of forward speed of the vessel.

As the Froude-Krylov component of wave excitation due to the incident wave is independent of the vessel's presence, forward speed corrections only apply to the

diffraction component. In the theory presented by Kim et al. the correction is applied by first of all calculating the diffraction component using the wave encounter frequency and then applying additional terms which are functions of speed and encounter frequency.

Work carried out by Atlar [38] at the University of Glasgow Hydrodynamics Laboratory has shown that by including forward speed corrections in the theoretical model, the motion predictions obtained disagree with the model test results presented in reference (1).

The inclusion of forward speed corrections to the wave excitation terms is known to be controversial[13], especially if excitation is predominantly due to the incident wave , Froude-Krylov component. Because of this, the foregoing, forward speed corrections have not been applied

2.5 Added Mass and Damping Coefficients from the Radiation Potential

The added mass and wave damping coefficients are associated with the radiation potential, ϕ_R which is part of the total potential, ϕ_T, as shown in equation (2.3).

2.51 Boundary Conditions

In order to solve for the hydrodynamic coefficients it is assumed that the vessel oscillates with small amplitude, simple harmonic motions of unit velocity and acceleration in still water about its mean, at rest, position. The kinematic boundary conditions on the wetted surface of the section contour therefore represents the only difference between conditions assumed for determining the radiation and diffraction potentials. This condition is given as :

$$V_n^{(m)} = \vec{n} \vec{\nabla} \phi_R^{(m)} (x, y, z; t) \qquad (2.35)$$

where V_n is the velocity component normal to the contour surface and, as before, n and m represent the outward unit normal vector and mode of motion respectively.

2.52 Radiation Potential

The free surface boundary condition (2.12) is in fact a function of encounter frequency, however this 'zero-speed' expression, in terms of wave frequency, is obtained by assuming that the vessel speed is small.

It has been shown [2] that the unsteady, 2-D strip section radiation potentials corresponding to each mode of motion can be expressed in terms of the zero-speed potentials. For the heave mode (m=3) this gives :

$$\phi_R^{(3)} = \phi_{Ro}^{(3)} \qquad (2.36)$$

where $\phi_{R_0}(y,z)$ is a speed independent potential which satisfies the kinematic boundary condition.

In the same manner as described in section 2.43 earlier, for the diffraction potential (2.23), the radiation potential can be expressed in terms of a distribution of sources around the wetted surface of each strip section as follows :

$$\phi_R^{(m)}(y,z;t) = \mathrm{Re}\left[\int_S Q^{(m)} G \, ds \; e^{-i\omega t} \right] \qquad (2.37)$$

which includes the harmonic time component.

$Q^{(m)}$ the unknown source strength is obtained by applying the kinematic boundary condition (2.35).

The complex functions $Q^{(m)}$ and G can be written in terms of their real and

imaginary parts :

$$Q^{(m)} = Q_R^{(m)} + iQ_I^{(m)}$$
$$G = G_R + iG_I \qquad (2.38)$$

and by substituting these equations into (2.37) and omitting the time factor we obtain :

$$\phi_R^{(m)} = \int_S \left[\left(Q_R^{(m)} G_R - Q_I^{(m)} G_I \right) + i\left(Q_R^{(m)} G_I + Q_I^{(m)} G_R \right) \right] ds \qquad (2.39)$$

The normal velocity component of motion can be written as :

$$\sum_{m=2,3,4} V_n = V^{(m)} \cos(n,m) = \omega S^{(m)} \cos(n,m) \qquad (2.40)$$

where $S^{(m)}$ and cos(n,m) are the motion displacement amplitude and directional cosines at the contour surface for the mode m respectively.

Substituting (2.39) and (2.40) into the kinematic boundary condition (2.35) gives the following linear coupled integral equations for the real and imaginary part of the unknown source strengths :

$$\left(\vec{n} \cdot \vec{\nabla}\right) \int_S \left(Q_R^{(m)} G_R - Q_I^{(m)} G_I\right) \, ds = \omega S^{(m)} \cos(n, m)$$

$$\left(\vec{n} \cdot \vec{\nabla}\right) \int_S \left(Q_R^{(m)} G_I + Q_I^{(m)} G_R\right) \, ds = 0 \qquad (2.41)$$

Frank's numerical method for solving these integral equations is described in reference (4). The method has been applied by Atlar to SWATH-type geometries and is fully described in reference (29).

Having obtained the velocity potential ϕ_R the added mass and damping forces are determined by using the linearised Bernoulli's equation to obtain segment pressures and then integrating these pressures around the section wetted surface.

2.53 Coupled Added Mass and Damping Coefficients

The general expression for the radiation forces for each mode of motion, j, due to the velocity and acceleration of all six modes of motion, k, can be written as :

$$F_j^R = \rho \sum_{k=1}^{6} s_k \iint_S n_j \left[i\omega + U\frac{\partial}{\partial x}\right] \phi_R \, ds \qquad (2.42)$$

where

S_k is the motion displacement.

F_j^R is the total radiation force for the j^{th} mode of motion at a strip section.

By introducing the sectional coefficients of added mass and wave damping a_{jk} and b_{jk}

which are the section radiation forces per unit acceleration and unit velocity respectively, equation (2.42) becomes :

$$F_j^R = -\sum_{k=1}^{6} \left[a_{jk} \ddot{s}_k + b_{jk} \dot{s}_k \right] \qquad (2.43)$$

This expression represents the sectional hydrodynamic forces due to rigid body motion accelerations and velocity. The subscripts j and k represent the motion induced forces and moments in the j^{th} mode of motion due to the coupling effect of motions in the k^{th} mode.

2.54 Speed Corrected Heave and Pitch Hydrodynamic Coefficients

The added mass and damping coefficients for the complete vessel can be obtained by integrating the sectional values along the hull length, L. Under the slender body assumption, the vertical plane heave and pitch modes of motion can be decoupled from the horizontal plane modes and by applying the forward speed correction approximations described by Kim et. al.(1) the net coupled heave and pitch coefficients for the vessel are given as :

$$A_{33} = \int_L a_{33} dx + \frac{U}{\omega^2} b_{33}(x) \Big|_L$$

$$B_{33} = \int_L b_{33} dx - U a_{33}(x) \Big|_L$$

$$A_{35} = -\int_L a_{33} x\, dx + \frac{U}{\omega^2} B^o_{33}(x) - \frac{U}{\omega^2} x b_{33}(x) \Big|_L$$

$$B_{35} = -\int_L b_{33}xdx - UA^o_{33}(x) + Uxa_{33}(x)\Big|_L$$

$$A_{55} = \int_L a_{33}x^2dx + \frac{U^2}{\omega^2}A^o_{33} - \frac{U^2}{\omega^2}xa_{33}(x)\Big|_L + \frac{U}{\omega^2}x^2b_{33}(x)\Big|_L$$

$$B_{55} = \int_L b_{33}x^2dx + \frac{U^2}{\omega^2}B^o_{33} - Ux^2a_{33}(x)\Big|_L - \frac{U^2}{\omega^2}xb_{33}(x)\Big|_L$$

$$A_{53} = A^o_{35} - \frac{U}{\omega^2}B^o_{33} + \frac{U^2}{\omega^2}a_{33}(x)\Big|_L - \frac{U}{\omega^2}xb_{33}(x)\Big|_L$$

$$B_{53} = B^o_{53} + UA^o_{33} + Uxa_{33}(x)\Big|_L + \frac{U^2}{\omega^2}b_{33}(x)\Big|_L$$

(2.44)

The first term of each of the above expressions is speed independent and corresponds to the vessel in waves with zero ahead speed. The last term accounts for the cross sectional area of the end sections and disappears if these are zero. The superscript 'o' denotes the zero speed value.

2.6 Comments on the Hydrodynamic Forces

As shown in the foregoing theoretical model, under the assumptions upon which the model is based, the hydrodynamic forces due to wave excitation and rigid body motions are dependent on wave frequency and the depth of submergence of each hull section.

In linear, frequency domain motion simulation, time is omitted and the constant submerged geometry of the craft under analysis is defined by the still water, at rest

condition.

In time domain analysis the time dependency of the submerged geometry can be introduced and the wave excitation force and motion amplitudes and the hydrodynamic coefficients become variables of the simulation.

2.7 Computer Routines for Performing the Calculations

Computer subroutines developed at the University of Glasgow Hydrodynamics Laboratory (39) for SWATH-type geometries have been modified to perform the calculations for the hydrodynamic forces associated with coupled heave and pitch motions . The subroutines are based on the theoretical model described above and give predictions for individual 2-Dimensional sections of a defined hull/strut geometrical configuration. Modifications to the original routines AYHANR and BURAK were required in order to obtain predictions for the decoupled vertical plane heave and pitch mode hydrodynamic values. AYHANR, gives predictions for the wave exciting force and moment complex amplitudes due to the incident and diffraction potentials and BURAK gives the corresponding coupled added mass and damping coefficients (Radiation potential).

Additional subroutines have been incorporated to obtain the total hydrodynamic values for the complete vessel by integrating the strip sectional values along the vessel length as described in section 2.54.

Figure 2.4 illustrates the computational procedure. Geometry offset data which refers to the sectional co-ordinate system shown in figure 2.2 are required for a number of equally spaced hull sections. This information , together with the wave frequency, the still water draught and the degree of segmentation required for each section contour are used as input data Feeder routines are then applied to calculated the nodal co-ordinates of the segments of each section before AYHANR and BURAK are run. The routines INTWEX and INTADM integrate the sectional hydrodynamic values to give net , coupled coefficients and wave excitation complex amplitude values for the whole

vessel. The values obtained are zero speed values which require correction as described earlier for forward speed cases.

Reference (40) gives some results of computations performed on various submerged and surface piercing sections using the subroutines AYHANR and BURAK. Further computational heave and pitch results are presented in Chapters 4 and 5 of this work for hull sections of model SWATH11.

Solving the hydrodynamic force system using the Frank Close-fit technique is computationally demanding. Because of this, large amounts of computer CPU-time are required to run the subroutines AYHANR and BURAK. Unless computing charge rates are high, this is of no great concern for frequency domain motions analysis. However in the case of time domain simulation, problems are presented and these have influenced the approach adopted in this work.

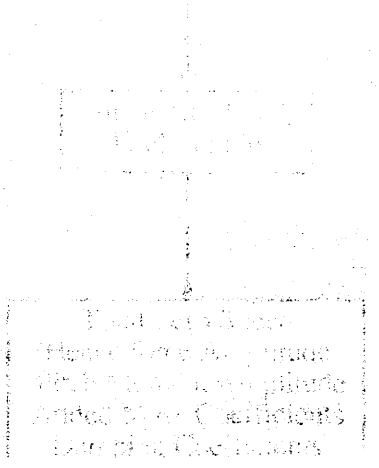

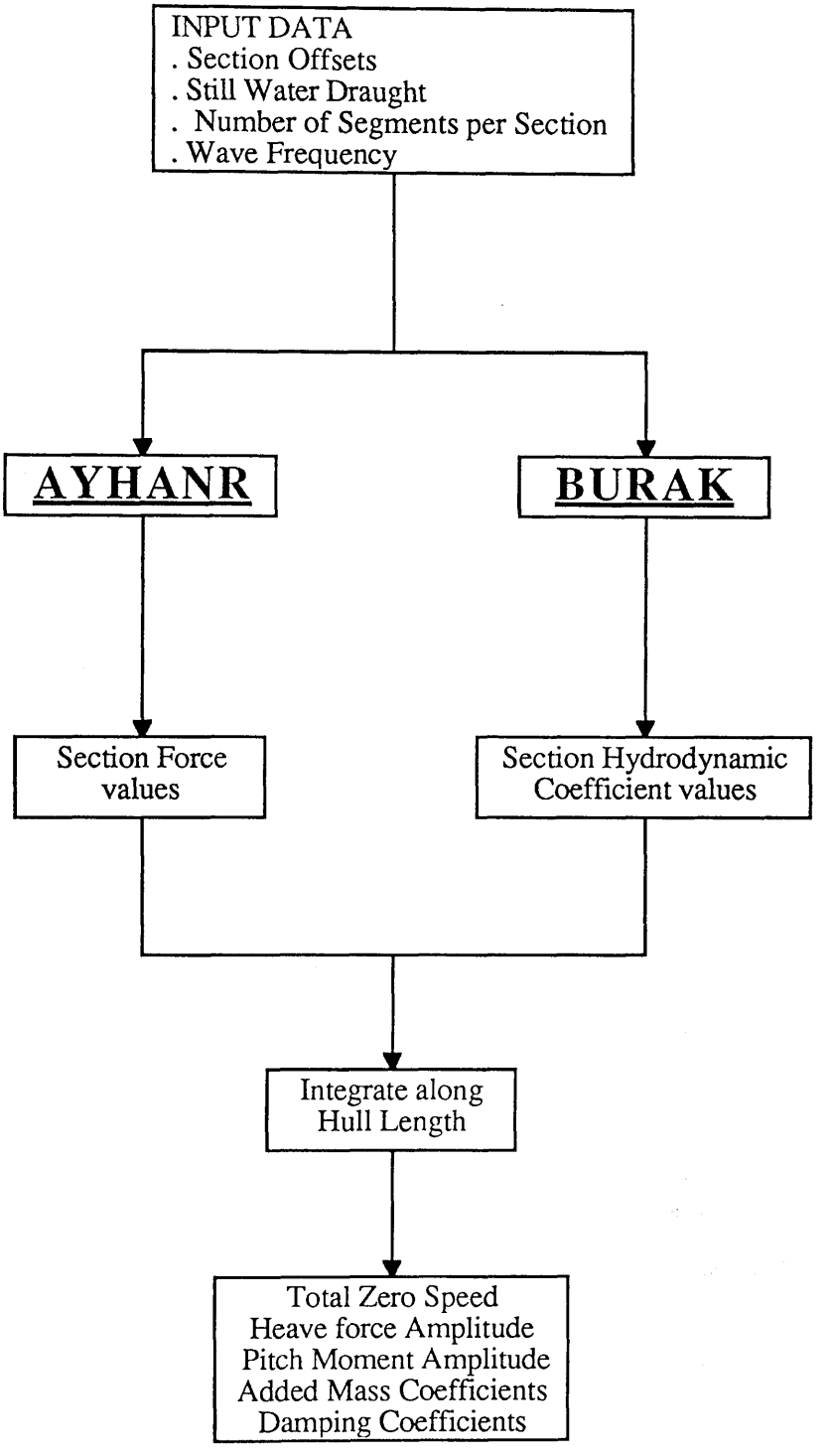

Figure 2.4 Hydrodynamic Force Computation Procedure

CHAPTER 3

LINEAR MOTIONS ANALYSIS

3.1 Introduction

As explained earlier, the approach adopted in this study has been, to develop a time domain solution technique by concentrating on linear motions, to validate the technique using equivalent linear frequency domain analysis and then, to move on to introducing some non-linear effects.

This chapter outlines how coupled heave and pitch motions are solved first in the frequency domain and then in the time domain. A computer program written to perform the time domain calculations is described. Comparisons made between the predictions obtained from this program and those obtained from the frequency domain equivalent provide the means for validation.

3.2 Frequency Domain Solution

In Chapter 1 it was shown how, for vessels with vertical centre-plane symmetry , the vertical plane modes of motion, heave and pitch, can be uncoupled from the horizontal plane modes. Expressions for the linear coupled heave and pitch motions system are given in equations (1.2).

Terms on the left-hand side of the equations represent the radiation forces due to rigid body motion response and the hydrostatic forces due to motion displacement. The motion coefficients are constant values and are assumed to correspond to the vessels at rest, still water condition . This is assumed to be the vessel's mean condition during its oscillatory motions.

Equations (1.2) are written in a time independent form. Here, the forcing functions, which
represent the excitation right-hand side of the equations, are given as complex amplitude values. The response displacement S_3 and S_5 are, correspondingly, complex amplitude values. In regular waves, the forcing functions oscillate harmonically and can be written with their time dependency as : .

$$F_3(t) = RE\left(F_3\, e^{-i\omega_e t}\right)$$
$$F_5(t) = RE\left(F_5\, e^{-i\omega_e t}\right) \qquad (3.1)$$

Equations (1.2) can then be written :

$$(M_{33}+A_{33})\ddot{S}_3(t)+B_{33}\dot{S}_3(t)+C_{33}S_3(t)+A_{35}\ddot{S}_5(t)+B_{35}\dot{S}_5(t)+C_{35}S_5(t) = F_3(t)$$
$$(I_{55}+A_{55})\ddot{S}_5(t)+B_{55}\dot{S}_5(t)+C_{55}S_5(t)+A_{53}\ddot{S}_3(t)+B_{53}\dot{S}_3(t)+C_{53}S_3(t) = F_5(t) \qquad (3.2)$$

As the wave exciting force and moment terms given in equations (3.2) are complex, the motion displacements S_3 and S_5 must also be complex and can be written as :

$$S_3(t) = RE\left(S_3 e^{-i\omega_e t}\right)$$
$$S_5(t) = RE\left(S_5 e^{-i\omega_e t}\right) \qquad (3.3)$$

S_3 and S_5 can be expressed in terms of their real and imaginary parts :

$$S_3 = S_{3R} + i S_{3I}$$
$$S_5 = S_{5R} + i S_{5I} \qquad (3.4)$$

These complex terms have trigonometrical relationships and can be written in terms of amplitude, |S|, and phase, α :

$$S_3 = |S_3| e^{-i\alpha_3}$$
$$S_5 = |S_5| e^{-i\alpha_5} \qquad (3.5)$$

where

$$|S_3| = \sqrt{S_{3R}^2 + S_{3I}^2}$$
$$|S_5| = \sqrt{S_{5R}^2 + S_{5I}^2} \qquad (3.6)$$

and

$$\alpha_3 = \tan^{-1}\left(\frac{S_{3I}}{S_{3R}}\right)$$
$$\alpha_5 = \tan^{-1}\left(\frac{S_{5I}}{S_{5R}}\right) \qquad (3.7)$$

The phase expressions given in (3.7) represent the positional shifts of motion displacements relative to the incident wave axes.

By combining equations (3.5) with (3.3) the following expressions for the complex heave and pitch displacements are obtained :

$$\begin{aligned} S_3 &= RE\left\{ |S_3| e^{i(\alpha_3 - \omega_e t)} \right\} \\ S_5 &= RE\left\{ |S_5| e^{i(\alpha_5 - \omega_e t)} \right\} \end{aligned} \qquad (3.8)$$

or

$$\begin{aligned} S_3 &= S_{3R} \cos \omega_e t + S_{3I} \sin \omega_e t \\ S_5 &= S_{5R} \cos \omega_e t + S_{5I} \sin \omega_e t \end{aligned} \qquad (3.9)$$

Equations (3.3) and their first and second differentials represent the displacements, velocities and accelerations of heave and pitch motions. These are written :

$$\begin{aligned} S_3(t) &= S_3 e^{-i\omega_e t} \\ S_5(t) &= S_5 e^{-i\omega_e t} \\ \dot{S}_3(t) &= -i\omega_e S_3 e^{-i\omega_e t} \\ \dot{S}_5(t) &= -i\omega_e S_5 e^{-i\omega_e t} \\ \ddot{S}_3(t) &= -\omega_e^2 S_3 e^{-i\omega_e t} \\ \ddot{S}_3(t) &= -\omega_e^2 S_3 e^{-i\omega_e t} \end{aligned} \qquad (3.10)$$

Substituting equations (3.10) into equations (3.2) and omitting the time factor will yield the following relationships between complex excitation forces and moments and complex motion displacements :

$$\left[\left(M_{33}+A_{33}\right)\left(-\omega_e^2\right) + B_{33}\left(-i\omega_e\right) + C_{33}\right] S_3 + \left[A_{35}\left(-\omega_e^2\right) + B_{35}\left(-i\omega_e\right) + C_{35}\right] S_5 = F_3$$

$$\left[\left(M_{55}+A_{55}\right)\left(-\omega_e^2\right) + B_{55}\left(-i\omega_e\right) + C_{55}\right] S_5 + \left[A_{53}\left(-\omega_e^2\right) + B_{53}\left(-i\omega_e\right) + C_{53}\right] S_3 = F_5$$

(3.11)

By substituting equations (3.4) and the complex force and moment relationships :

$$F_3 = F_{3R} + i F_{3I}$$

$$F_5 = F_{5R} + i F_{5I}$$

(3.12)

into equations (3.11).and by rearranging the left and right-hand sides in terms of their real and imaginary parts, the matrix form of the coupled system is obtained :

$$\begin{pmatrix} C_{33}-\omega_e^2(M_{33}+A_{33}) & C_{35}-\omega_e^2 A_{35} & \omega_e B_{33} & \omega_e B_{35} \\ C_{53}-\omega_e^2 A_{53} & C_{55}-\omega_e^2(I_{55}+A_{55}) & \omega_e B_{53} & \omega_e B_{55} \\ -\omega_e B_{33} & -\omega_e B_{35} & C_{33}-\omega_e^2(M_{33}+A_{33}) & C_{35}-\omega_e^2 A_{35} \\ -\omega_e B_{53} & -\omega_e B_{55} & C_{53}-\omega_e^2 A_{53} & C_{55}-\omega_e^2(I_{55}+A_{55}) \end{pmatrix} \begin{pmatrix} S_{3R} \\ S_{5R} \\ S_{3I} \\ S_{5I} \end{pmatrix} = \begin{pmatrix} F_{3R} \\ F_{5R} \\ F_{3I} \\ F_{5I} \end{pmatrix}$$

(3.13)

Using matrix solution techniques equations (3.13) can be solved to give the real and imaginary parts of the of motion displacements. The amplitude and phase of linear heave and pitch motion displacements are then obtained from equations (3.6) and (3.7).

As the excitation terms are forces and moments per unit wave amplitude, the corresponding responses are linear and angular displacements per unit wave amplitude , more commonly known as the Response Amplitude Operators (RAO's).

3.21 Frequency Domain Calculations

Previous work carried out at the University of Glasgow Department of Naval Architecture and Ocean Engineering has involved the development of a computer program which gives frequency domain. predictions of SWATH ship coupled heave and pitch motions.

The program which is called HP2, applies wave excitation and the hydrodynamic coefficient data obtained using original versions of the subroutines AYHANR and BURAK. These routines were discussed in section 2.6.

Figure 3.1 illustrates the structure of the frequency domain procedure. Initial input data consists of transverse strip section geometry offsets and a range of wave frequencies for which solutions are required. Sectional wave exciting forces and hydrodynamic coefficients are

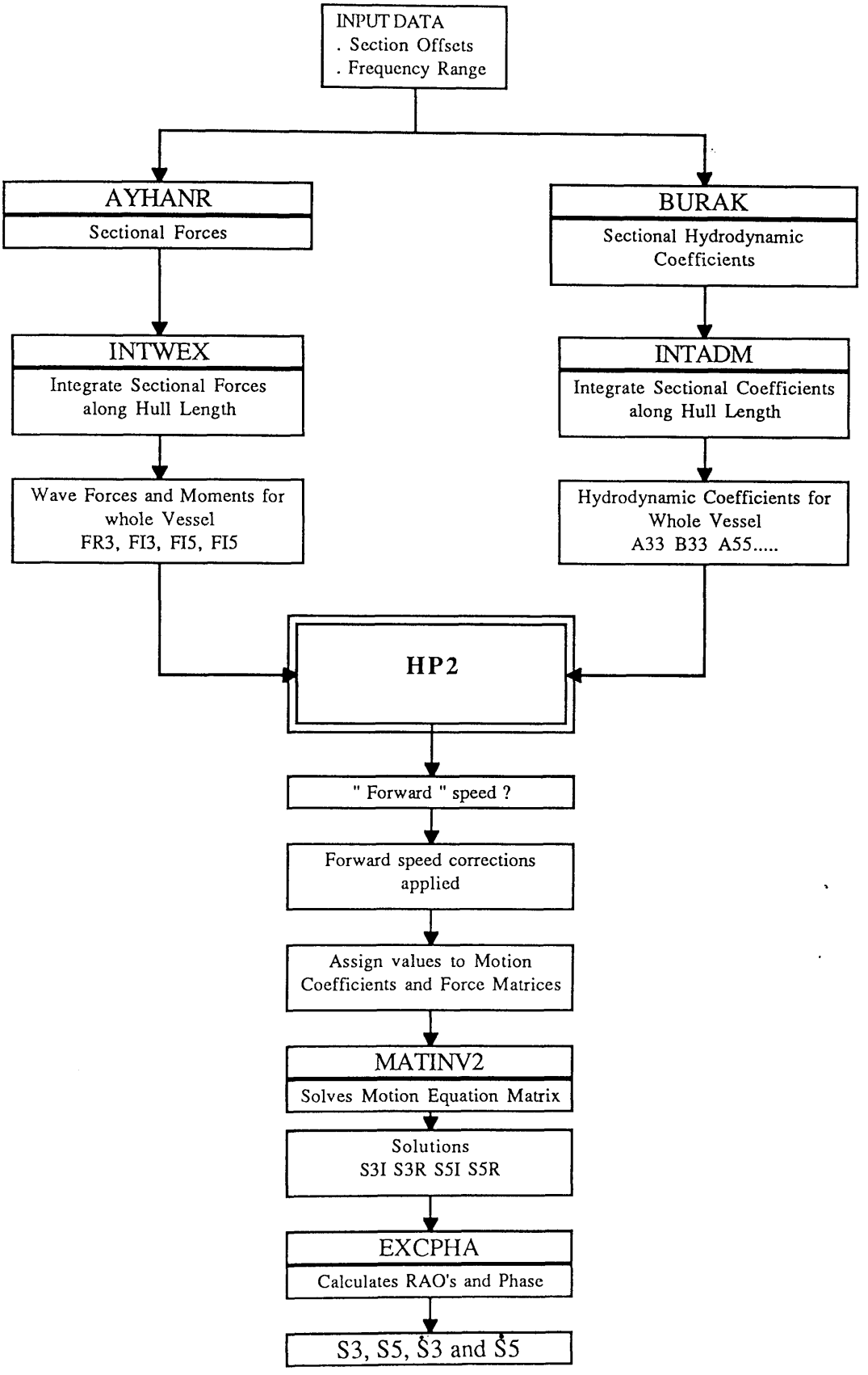

Figure 3.1 Frequency Domain Computational Procedure

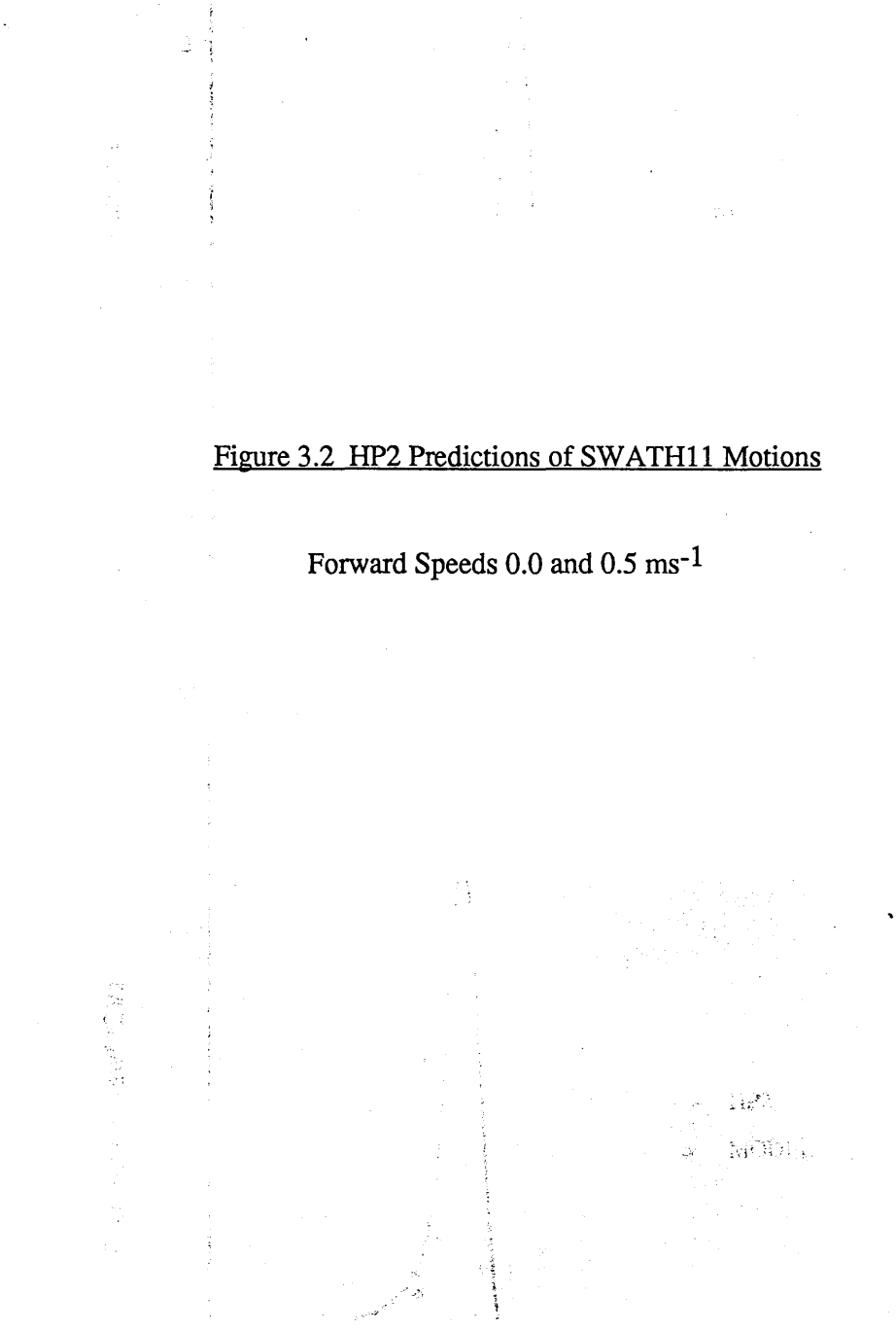

Figure 3.2 HP2 Predictions of SWATH11 Motions

Forward Speeds 0.0 and 0.5 ms^{-1}

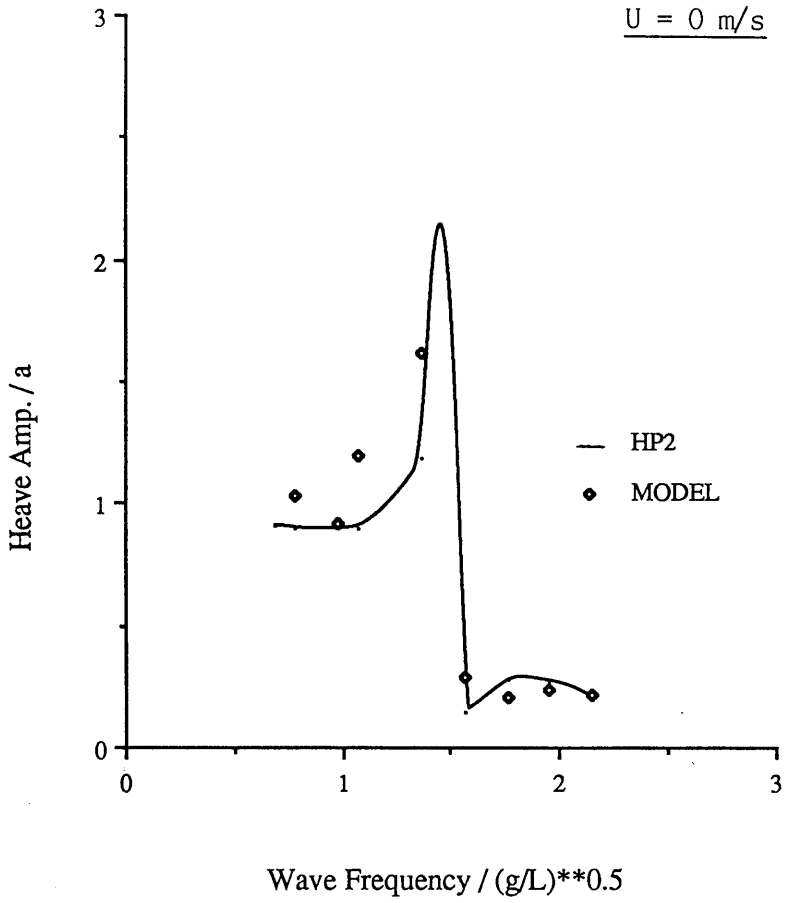
U = 0 m/s
Heave Amp. / a
HP2
MODEL
0
1
2
3
Wave Frequency / (g/L)**0.5

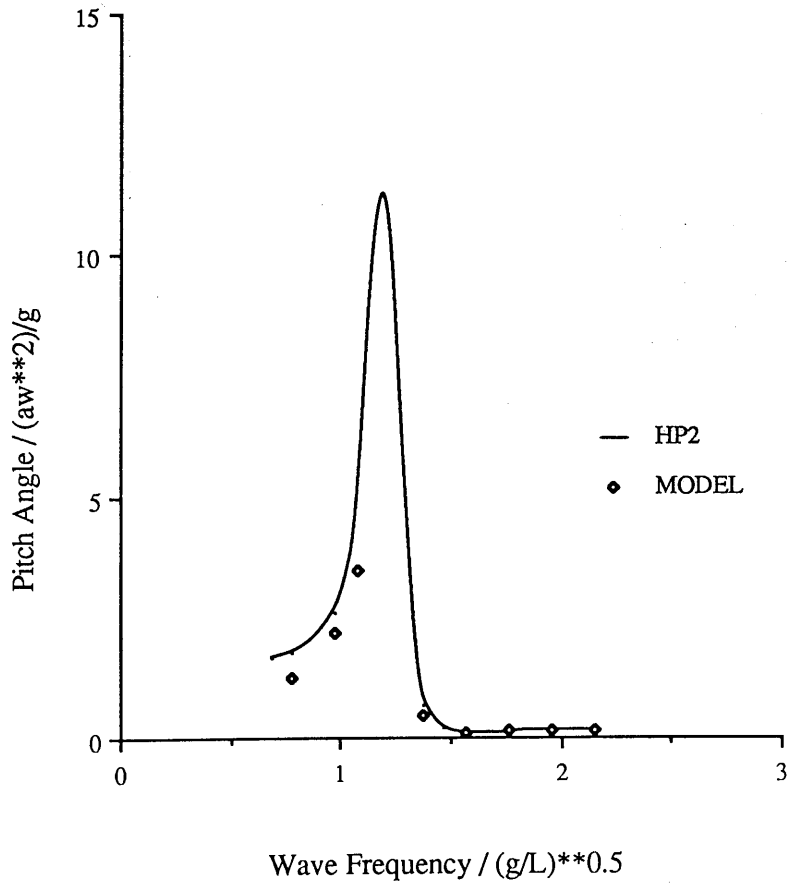
Pitch Angle / (aw**2)/g
HP2
MODEL
0
5
10
15
0
1
2
3
Wave Frequency / (g/L)**0.5

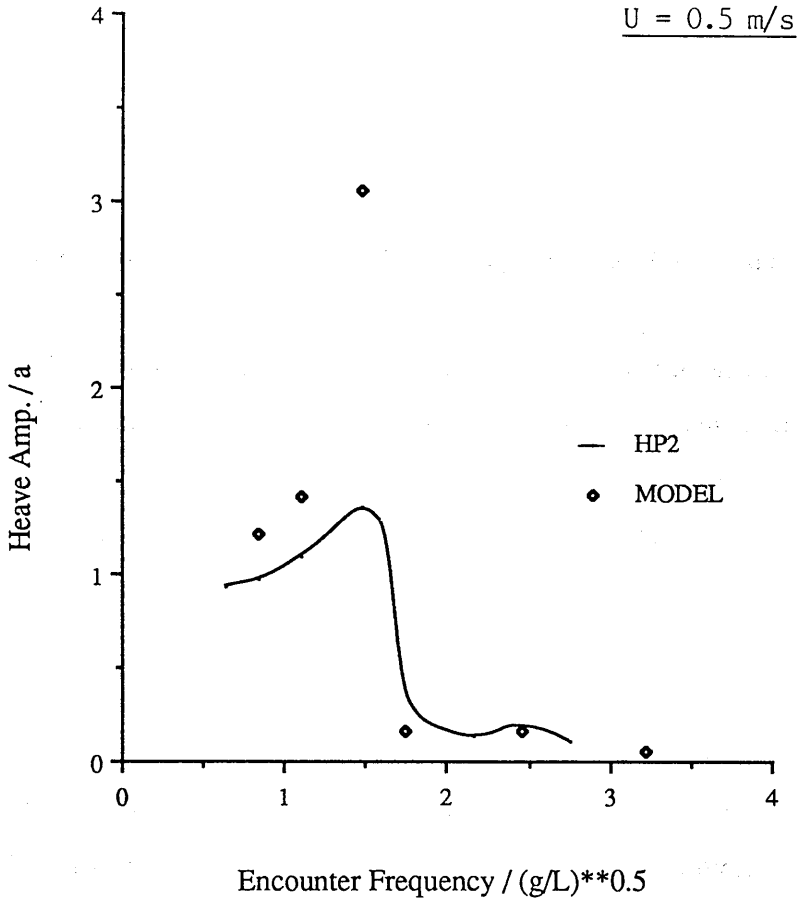
U = 0.5 m/s
Heave Amp. / a
HP2
MODEL
Encounter Frequency / (g/L)**0.5

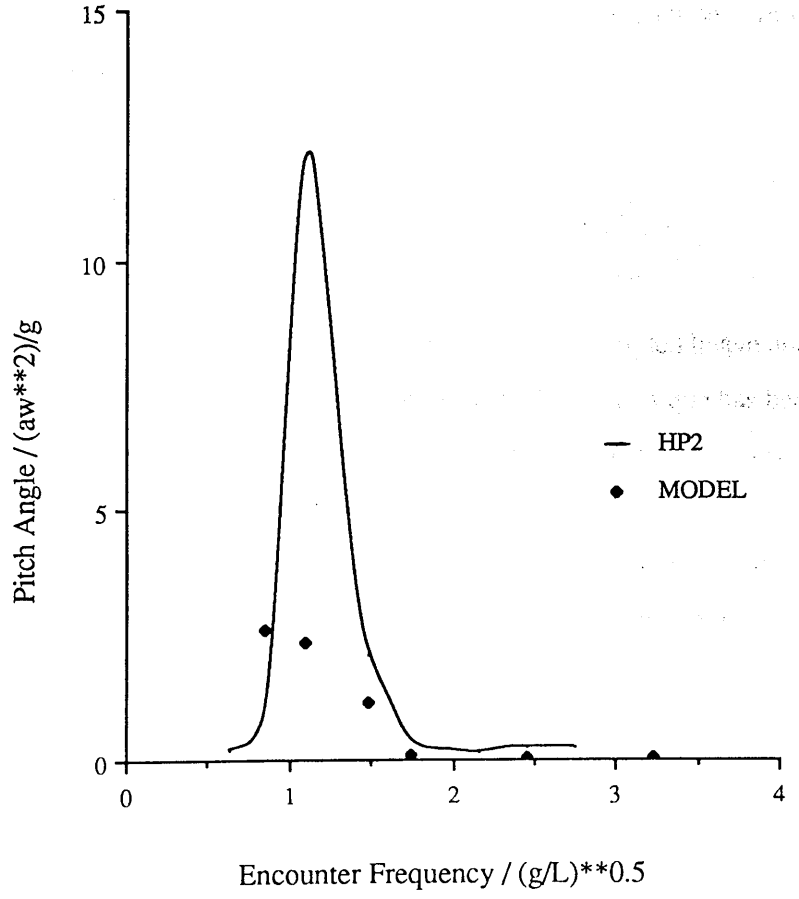
Pitch Angle / (aw**2)/g
HP2
MODEL
Encounter Frequency / (g/L)**0.5

calculated in AYHANR and BURAK. Total values for the whole vessel are obtained using subroutines INTADM and INTWEX. These integrate the sectional values along the vessel length .

Within HP2, forward speed corrections are applied to the hydrodynamic coefficients before components of the motion equations matrix are assigned. MATINV2 inverts the coefficients matrix and solves the matrix system yielding the real and imaginary parts of the motion displacements. Heave and pitch RAO's and their phase shifts calculated in the subroutine EXCPHA.

3.22 Analysis of SWATH11

HP2 has been used to analyse the motions of SWATH11 in head seas for a range of wave frequencies. Figure 3.2(i) and 3.2(ii) show some heave and pitch predictions obtained for the zero and 0.5 ms^{-1} forward speed cases. Results are compared with measurements obtained from physical model seakeeping tests (8) . These comparisons illustrate the good quality of the predictions.

3.3 Time Domain Solution

This section describes a technique for solving the linear coupled heave and pitch system in the time domain . A computer program based on the technique has been written as a core routine to which non-linear effects are added later in the study. The program has been validated using results obtained from 'HP2'.

In the time domain, the time dependency of motion coefficients and wave force and moment amplitudes can be introduced and equations (3.2) form a set of non-linear differential equations. The terms A_{jk}, B_{jk}, C_{jk}, S_k and F_j then become time dependent variables. However, for the purpose of developing and validating a basis solution procedure linear motions are

assumed and these terms remain constant values corresponding to the still water, submerged geometry.

By combining equation (3.1) and (3.2), the motion equations can be written :

$$(M_{33}+A_{33})\ddot{S}_3(t)+B_{33}\dot{S}_3(t)+C_{33}S_3(t)+A_{35}\ddot{S}_5(t)+B_{35}\dot{S}_5(t)+C_{35}S_5(t)=F_3 e^{-i\omega_e t}$$

$$(I_{55}+A_{55})\ddot{S}_5(t)+B_{55}\dot{S}_5(t)+C_{55}S_5(t)+A_{53}\ddot{S}_3(t)+B_{53}\dot{S}_3(t)+C_{53}S_3(t)=F_5 e^{-i\omega_e t}$$

(3.14)

These represent the coupled differential equations of motion in their second order form. The harmonic time function applied to the excitation forces and moments has frequency and phase according to wave encounter frequency ω_e and wave start position.

A time history of solutions to equation (3.14) will show harmonically varying heave and pitch values with amplitudes equal to those obtained from frequency domain analysis.

The solution procedure involves reducing the coupled equations to their first order differential form.

By writing,

$$y_1 = S_3, \quad y_2 = \dot{S}_3, \quad y_3 = S_5, \quad \text{and} \quad y_4 = \dot{S}_5$$

the first order form is given as :

$$\dot{y}_1 = y_2 \quad (=\dot{S}_3(t)) \qquad \dot{y}_3 = y_4 \quad (=\dot{S}_5(t))$$

$$\dot{y}_2 = \left[\frac{M_{55}+A_{55}}{(M_{33}+A_{33})(M_{55}+A_{55})-A_{35}A_{53}}\right][\,F_3(t)-B_{33}y_2-C_{33}y_1-B_{35}y_4$$

$$-C_{35}y_3-(F_5(t)-B_{55}y_4-C_{55}y_3-B_{53}y_2-C_{53}y_1)\left(\frac{A_{35}}{M_{55}+A_{55}}\right)\,]$$

$$\dot{y}_4 = \left[\frac{M_{55}+A_{55}}{(M_{55}+A_{55})(M_{33}+A_{33})-A_{53}A_{35}}\right][\,F_5(t)-B_{55}y_4-C_{55}y_3-B_{53}y_2$$

$$-C_{53}y_1-(F_3(t)-B_{33}y_2-C_{33}y_1-B_{35}y_4-C_{35}y_3)\left(\frac{A_{53}}{M_{33}+A_{33}}\right)\,] \qquad (3.15)$$

3.31 Solution of First Order differential Equations

NAg Library subroutines [6] cover the solution of any number of coupled first order differential equations. The routines apply various different numerical techniques for solving a range of problem types. Equations (3.15) represent an initial value problem which can be solved by setting initial values of the time-dependent variables S_3, S_5, $\dot{S}_3$ and $\dot{S}_5$ and integrating with respect to time in a step by step manner.

The NAg library manual recommends carrying out a problem classification procedure for establishing the nature of the differential equation system. This involves applying the routine D02BDF which determines whether or not the problem is 'stiff' - that is , a system with rapidly decaying transients[41]

The classification of this particular problem resulted in the selection of D02BBF which applies a Runge-Kutte numerical technique(7).

3.32 Motions Solution Procedure

Figure 3.3 illustrates the motions solution procedure. From the geometry offset data, added mass and damping and wave excitation values corresponding to the still-water submerged geometry are calculated by applying the theoretical techniques described in Chapter 2. Values of S_3, S_5, $\dot{S}_3$ and $\dot{S}_5$ are set at zero to represent the initial conditions of the simulation. Next, a forward speed is selected, and the added mass and damping coefficient corrections given in equations (2.44) are applied. These values are inserted into the coupled motion equations. Harmonic time function of wave encounter frequency are then applied to the wave exciting forces and moments. Solutions obtained for the first time step represent the initial conditions for the next. The same procedure is repeated for subsequent solution steps until constant amplitude, 'steady' solutions for heave and pitch displacements are obtained.

3.33 Application of Ramp Functions

Before settling to steady state values the heave and pitch solutions experience a transient period due to the 'impact' effect of the initial values of the motion equation components. During this period frequencies other than that of the encountered wave can be seen in the solutions. The stiffness of the system determines at what rate these transients are damped out to leave steady simple harmonic solutions.

Solutions will diverge if the damping characteristics of the coupled system are insufficient to cope with the initial conditions. Figure 3.4 shows an example of a diverging solution. This clearly illustrates that, regardless of the number of solution cycles, a steady state solution will not be achieved.

The characteristics of divergence depend on the numerical solution technique employed, the wave encounter frequency and the magnitude of the speed corrected motion equation coefficients.

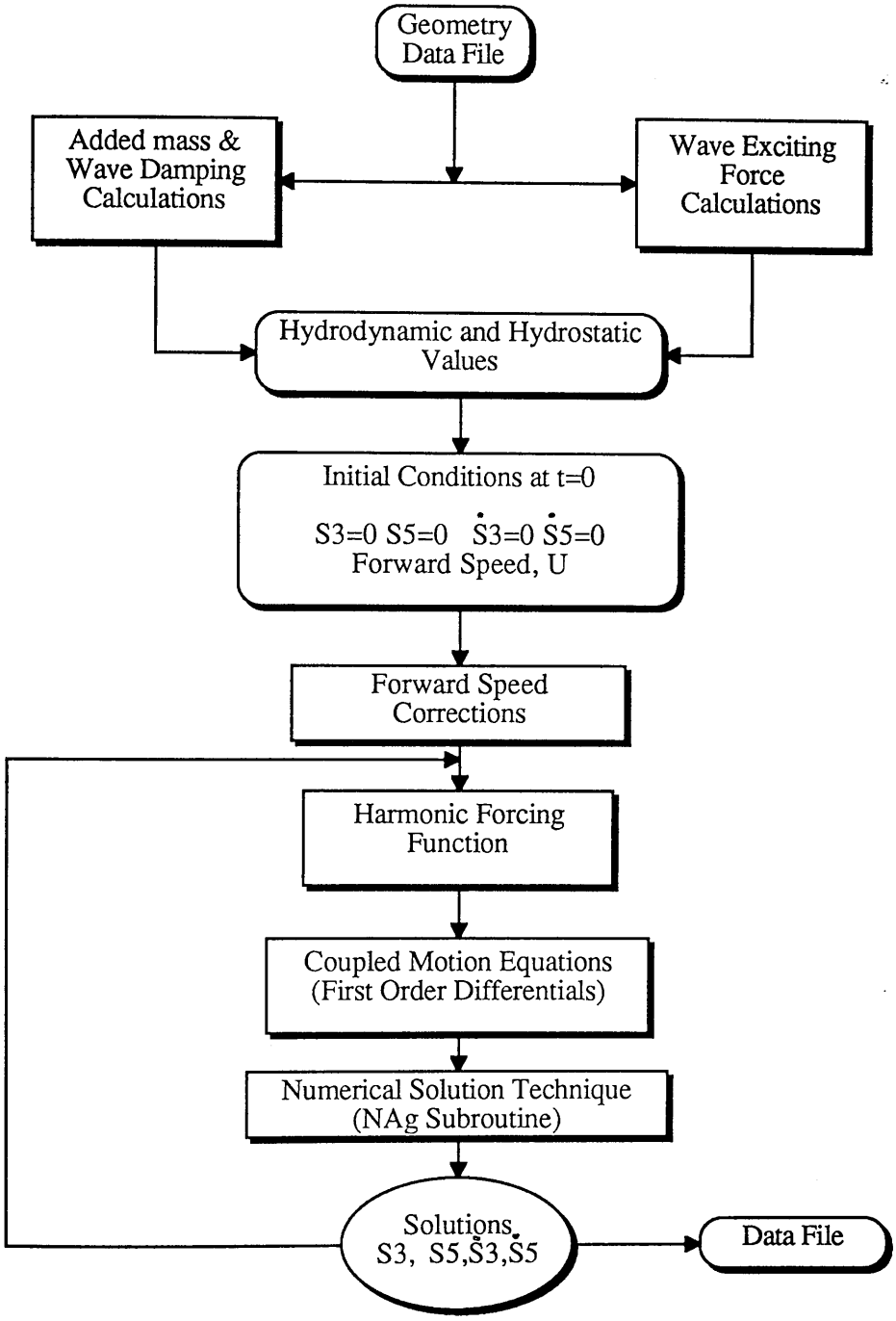

Figure 3.3 Time Domain Solution Procedure

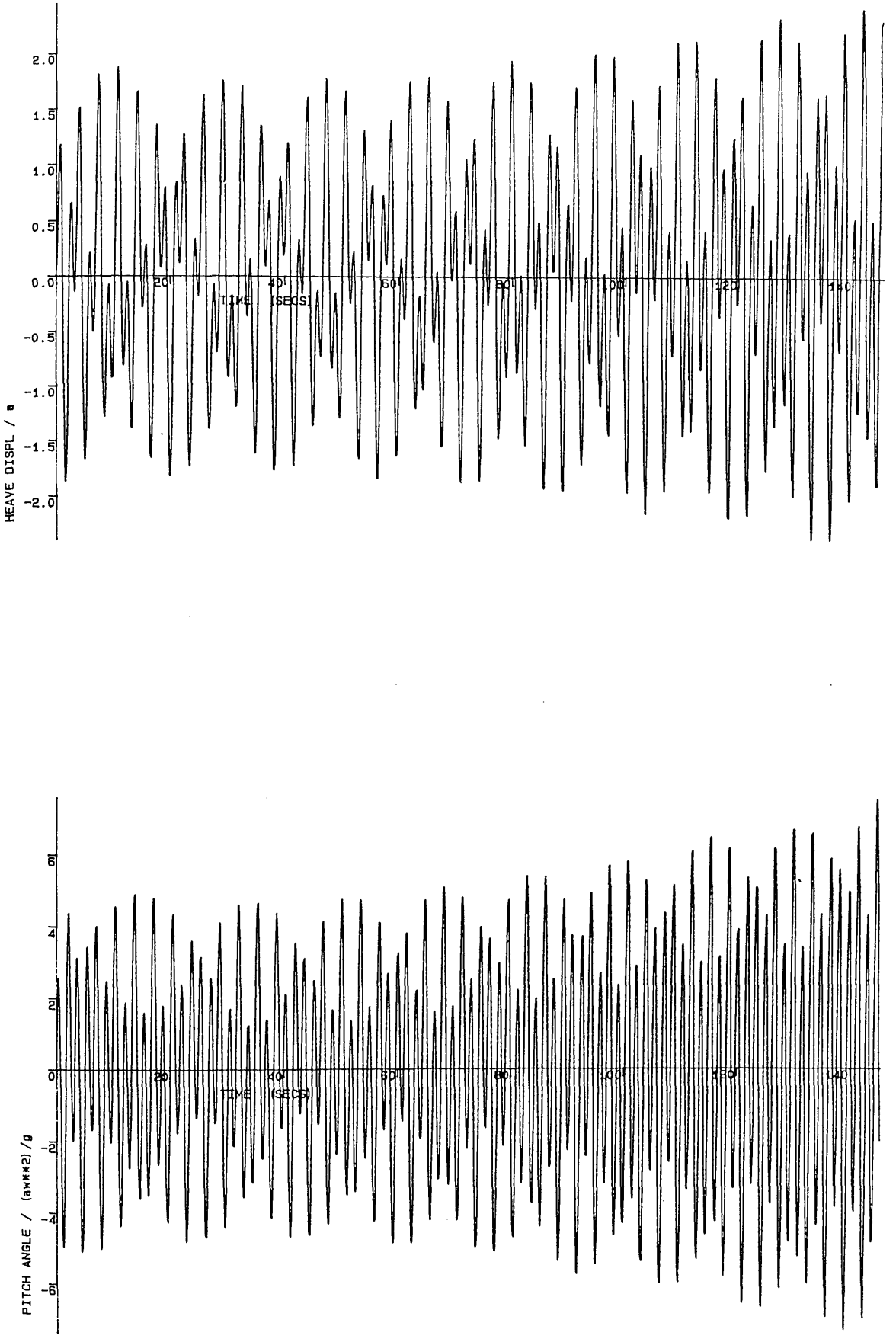

Figure 3.4 Diverging Solutions

In essence however, divergence can be avoided if the harmonic forcing functions are gradually amplified from zero to their true values over an initial period of the simulation.

This is done by using a ramp function R(t) which is applied to the forcing functions as follows :

$$F_3(t)_{ramp} = F_3(t)\ R(t)$$
$$F_5(t)_{ramp} = F_5(t)\ R(t) \qquad (3.16)$$

The time dependency of R(t) is such that after an initial period, its value is unity. The following exponential ramp function is illustrated in figure 3.5.

$$R(t) = 1 - e^{-A\,t^2} \qquad (3.17)$$

This shows R(t) to increase from zero at $t = 0$, to unity at $t = T/2$, where T is the duration of the the simulation and

$$A = \log_e (1000) / (T/2)^2. \qquad (3.18)$$

3.34 Structure of Computer Routine

A computer program named TDSOL has been written to perform the time domain calculations. Its position in the solution routine is shown in figure 3.6

Using transverse section offsets and wave frequency data, hydrodynamic coefficient and wave excitation sectional values are calculated within subroutines BURAK2 and AYHANR2. These values are integrated along the vessel length in TOTADM and TOTWEX yielding total values for the whole vessel.

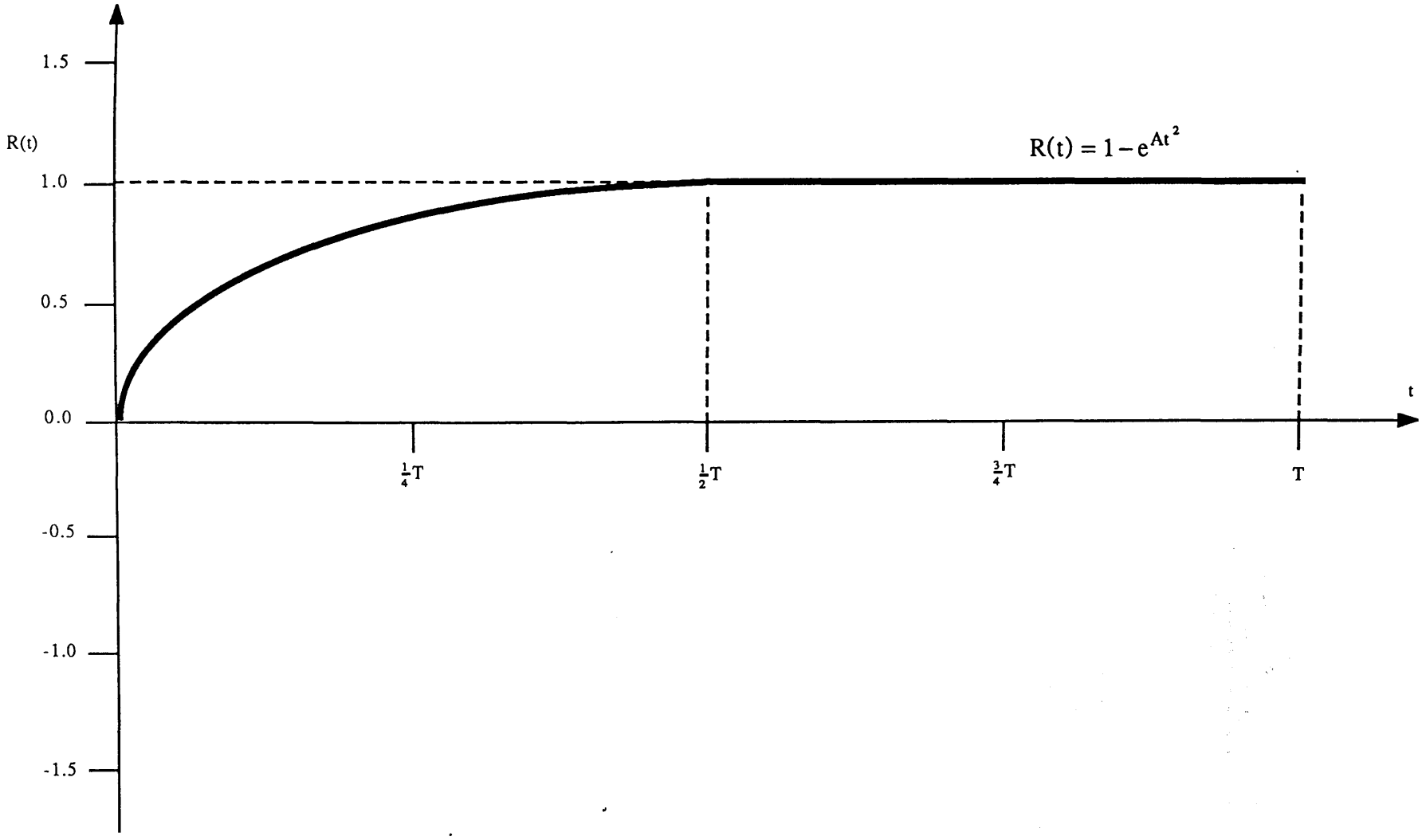

Figure 3.5 Exponential Ramp Function

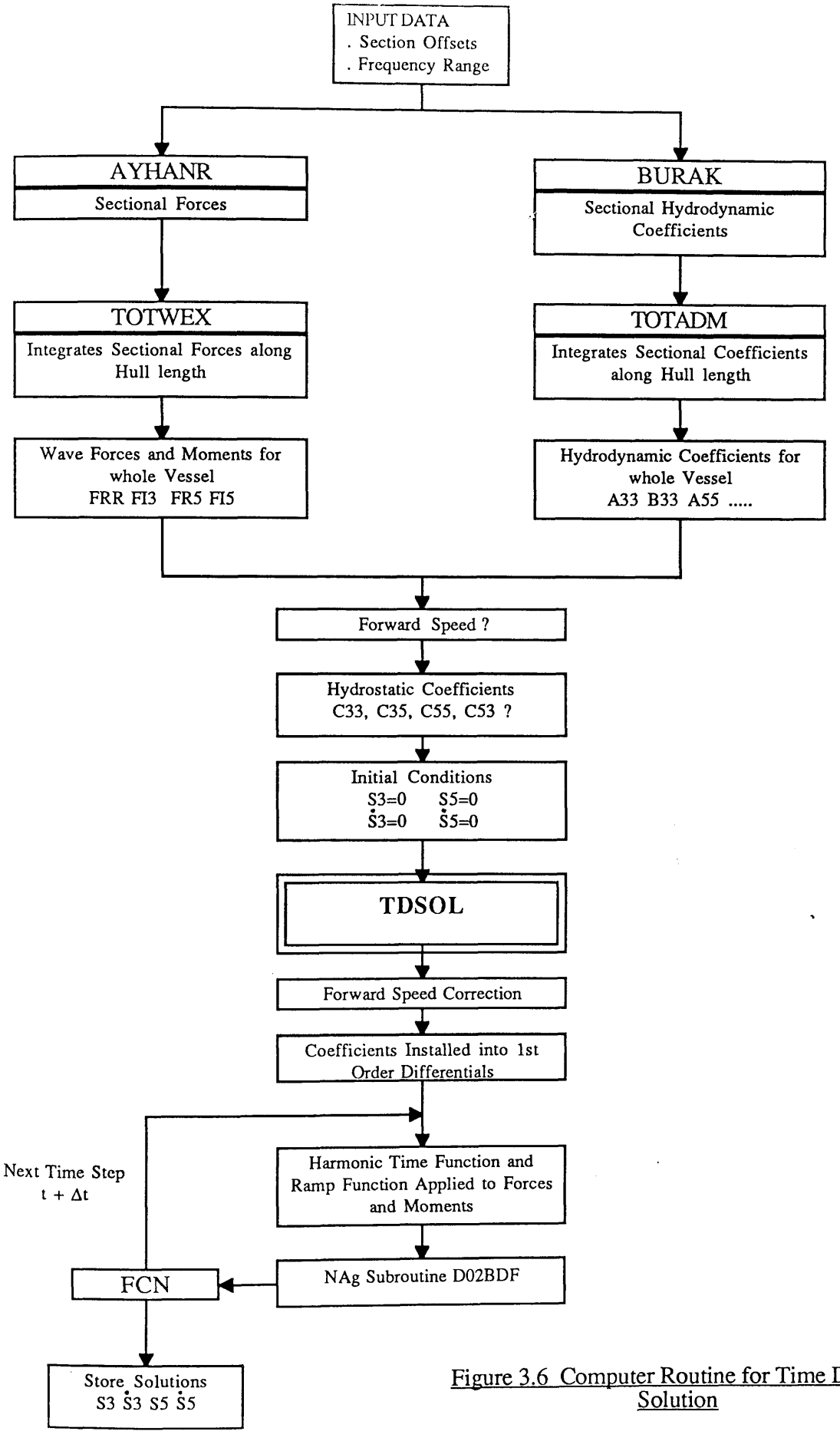

Figure 3.6 Computer Routine for Time Domain Solution

Additional items of input data which are required include the ship forward speed and previously determined hydrostatic coefficients for the vessel. Initial values of S_3, S_5, $\dot{S}_3$ and $\dot{S}_5$ are set to zero. Within TDSOL, first the hydrodynamic coefficients corrections for forward speed (described in section 2.54) are applied. Then, initial motion and motion coefficient values are installed into the coupled first order differentials (3.15) and ramp functions are applied to the forcing functions. NAg subroutine solutions obtained for the first time step are used as input conditions for the next time step at t+ dt .Before repeating the process, excitation force and moment values corresponding to t = t + dt are obtained via the reconditioning subroutine FCN. This time stepped process is repeated until simple harmonic heave and pitch oscillations are obtained.

3.4 Validation

Both the time domain model and the frequency domain model use subroutines based on the same theoretical technique for performing hydrodynamic force calculations. Assuming that restoring coefficient data used is common , the techniques can be regarded as alternative ways to solve an identical linear motions force system.

Heave and pitch predictions obtained from each method should therefore be in exact agreement and comparisons made between the two provide a means for validating the time domain solution technique.

Time histories of SWATH11 heave and pitch motions are shown in figures 3.7. Results over a range of wave frequencies, for two forward speed cases are given. The exponential ramp function, (3.17), has been applied and its resulting effects can be seen in the early part of the solutions.

Figure 3.8 shows predictions obtained from the frequency domain and time domain analysis of SWATH11 advancing at 0.3 ms^{-1} in head seas. The results illustrate exact agreement between the two techniques. The same agreement has been

achieved for a range of conditions and has confirmed the validity of the linear model.

This validated technique can now be developed to introduce some non-linear characteristics of motion.

Figures 3.7 Time Domain Solutions for Linear Motions

SWATH11, Forward Speeds: 0.0 and 0.5ms-1

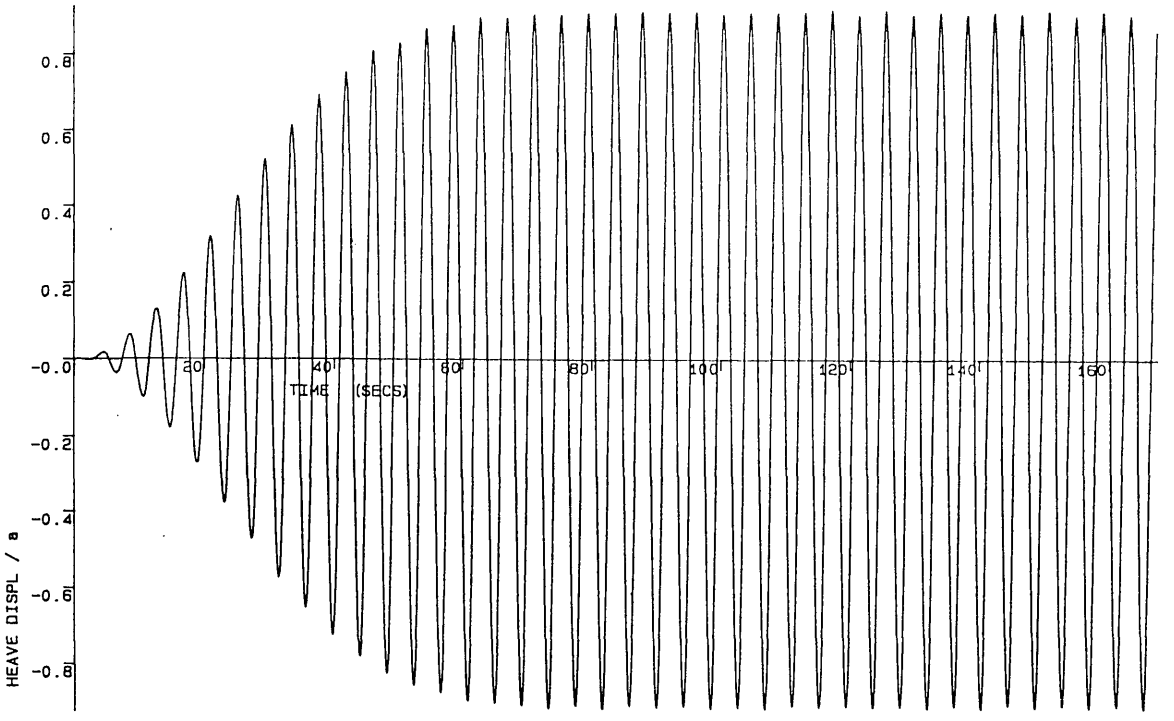

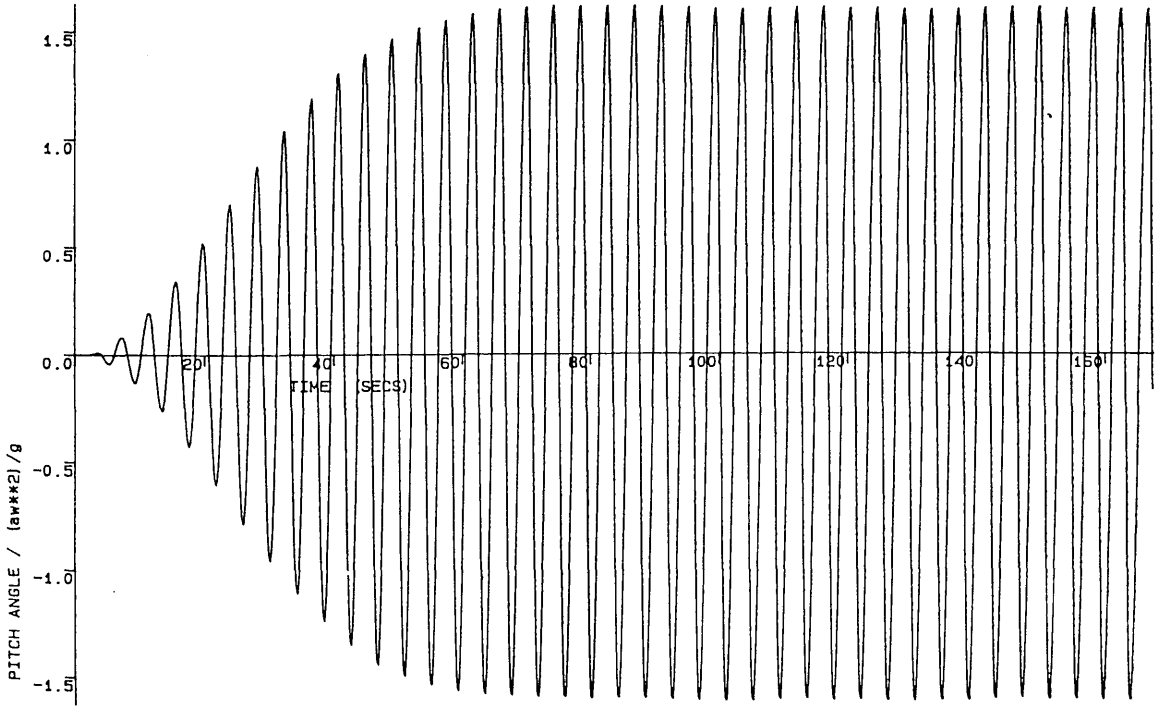

U = 0 m/s w = 1.5 rad/s

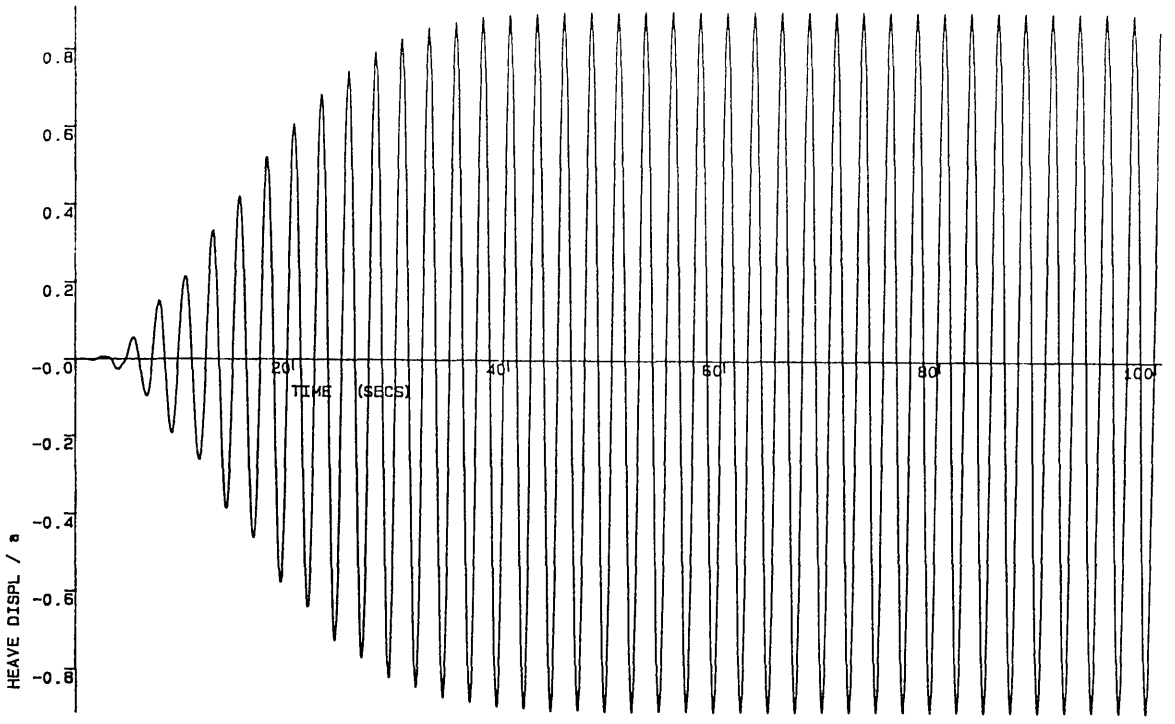

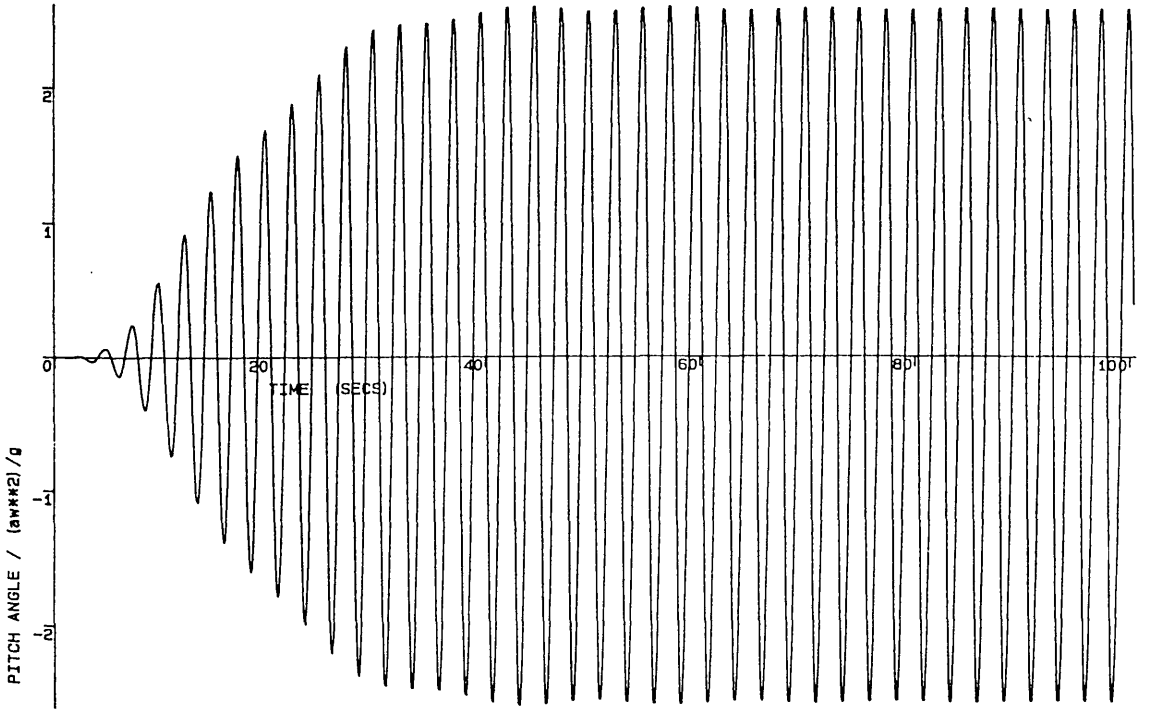

U = 0 m/s w = 2.5 rad/s

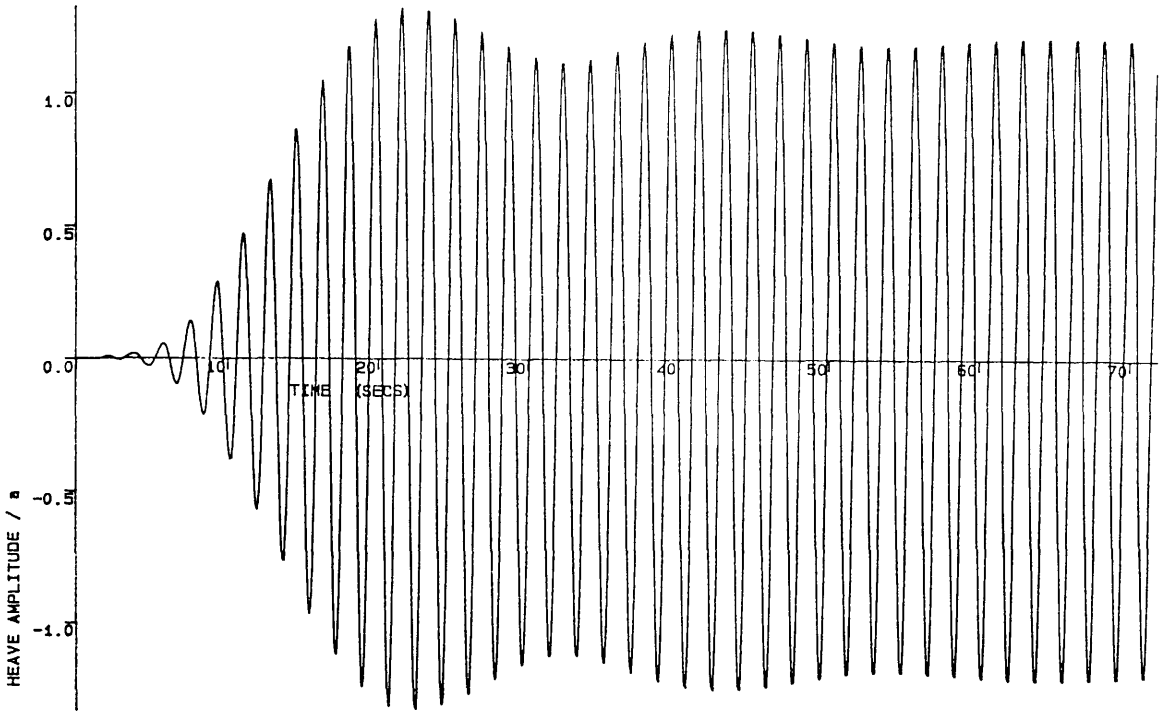

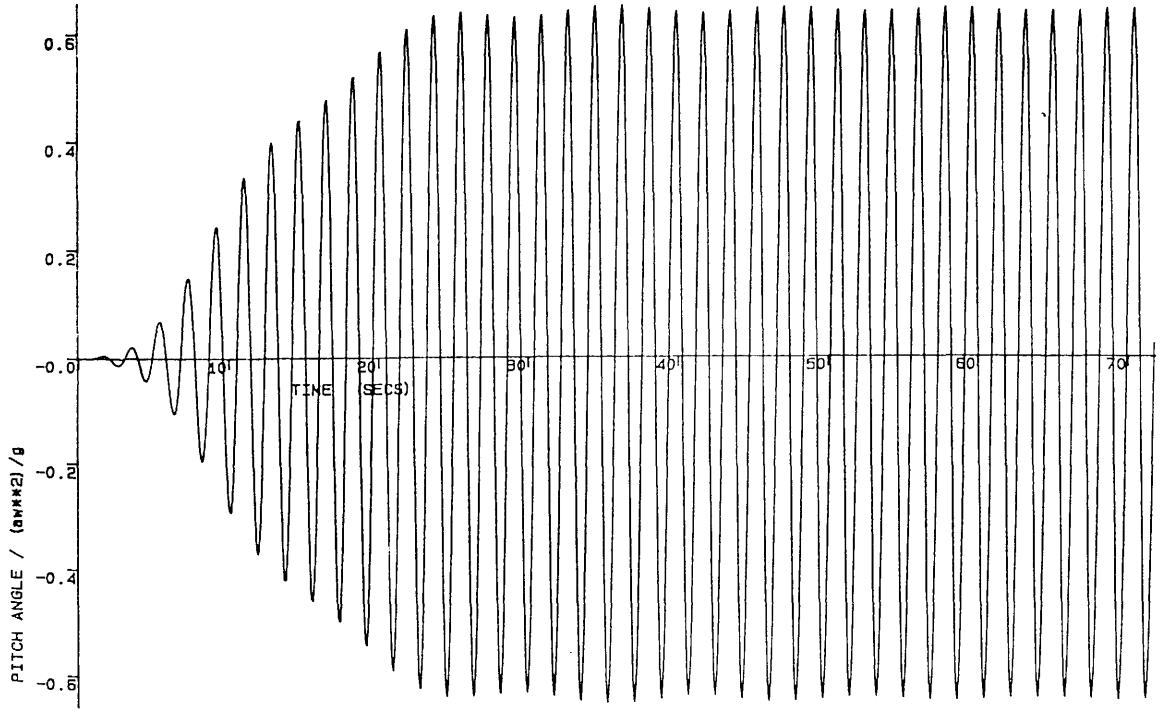

U = 0 m/s w = 3.5 rad/s

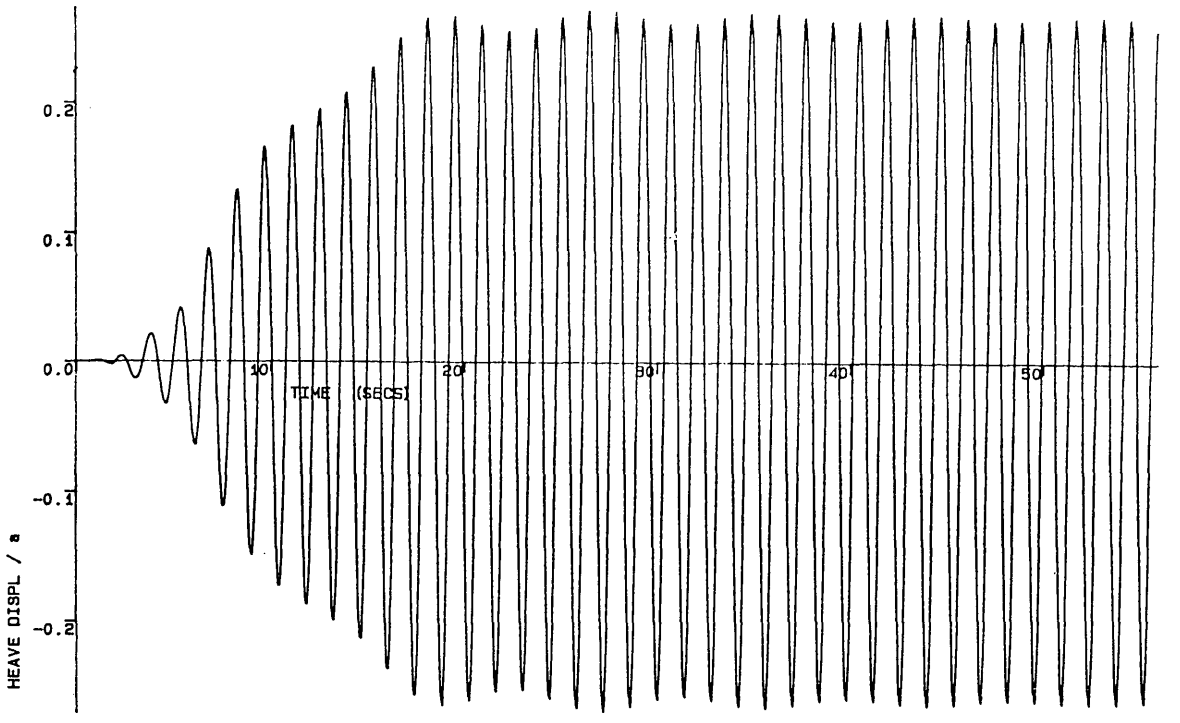

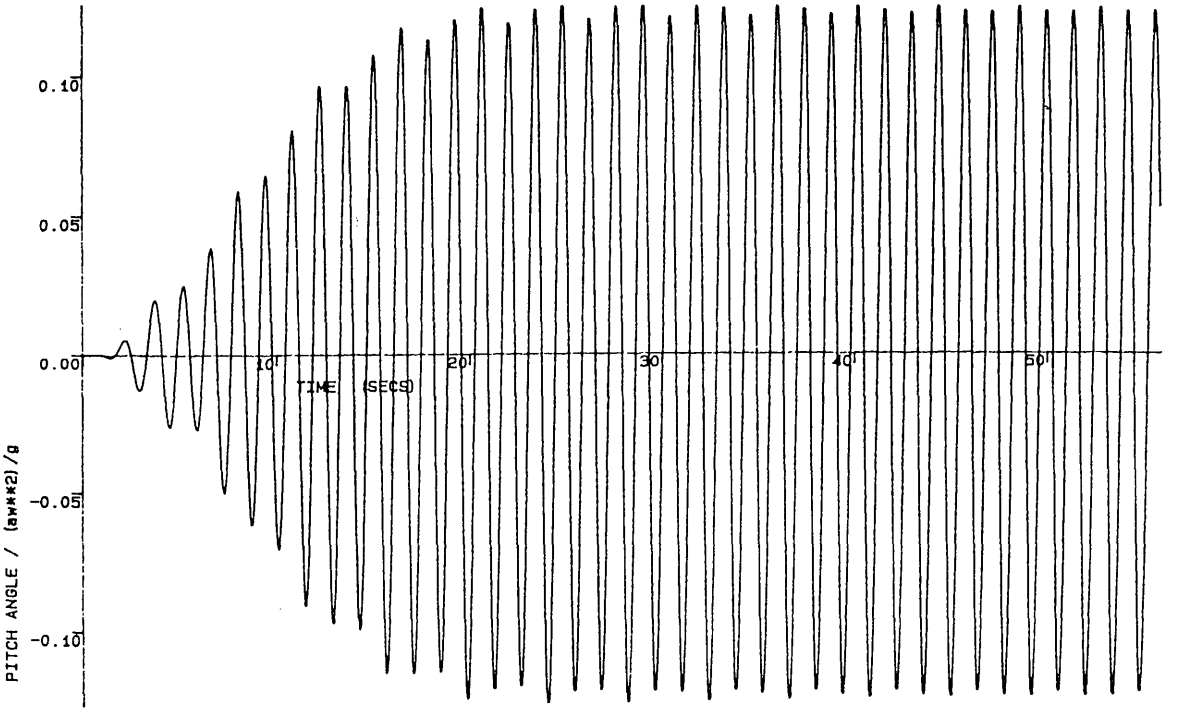

U = 0 m/s w = 4.5 rad/s

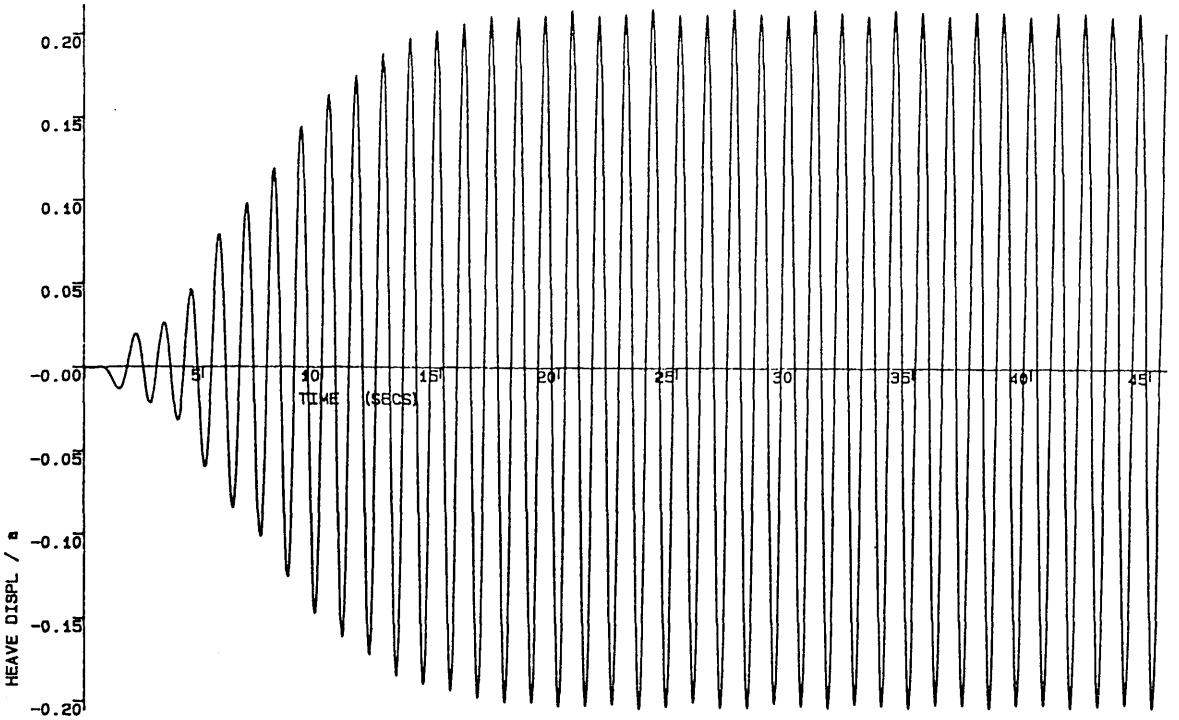

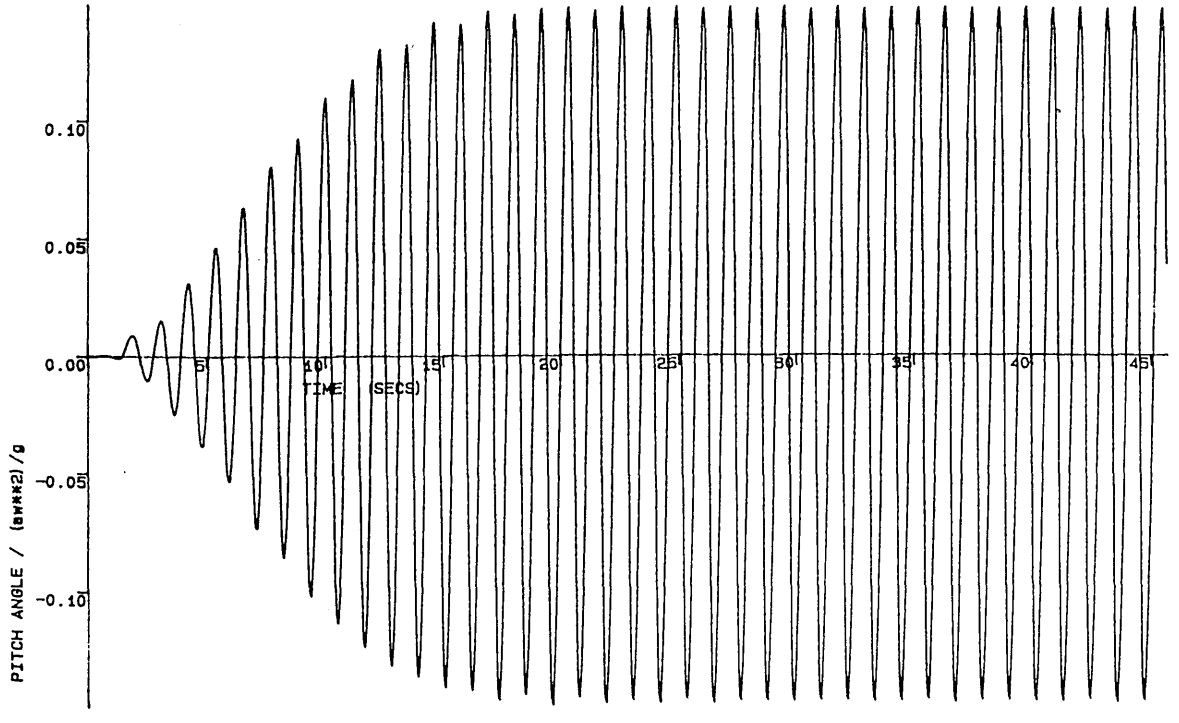

U = 0 m/s w = 5.5 rad/s

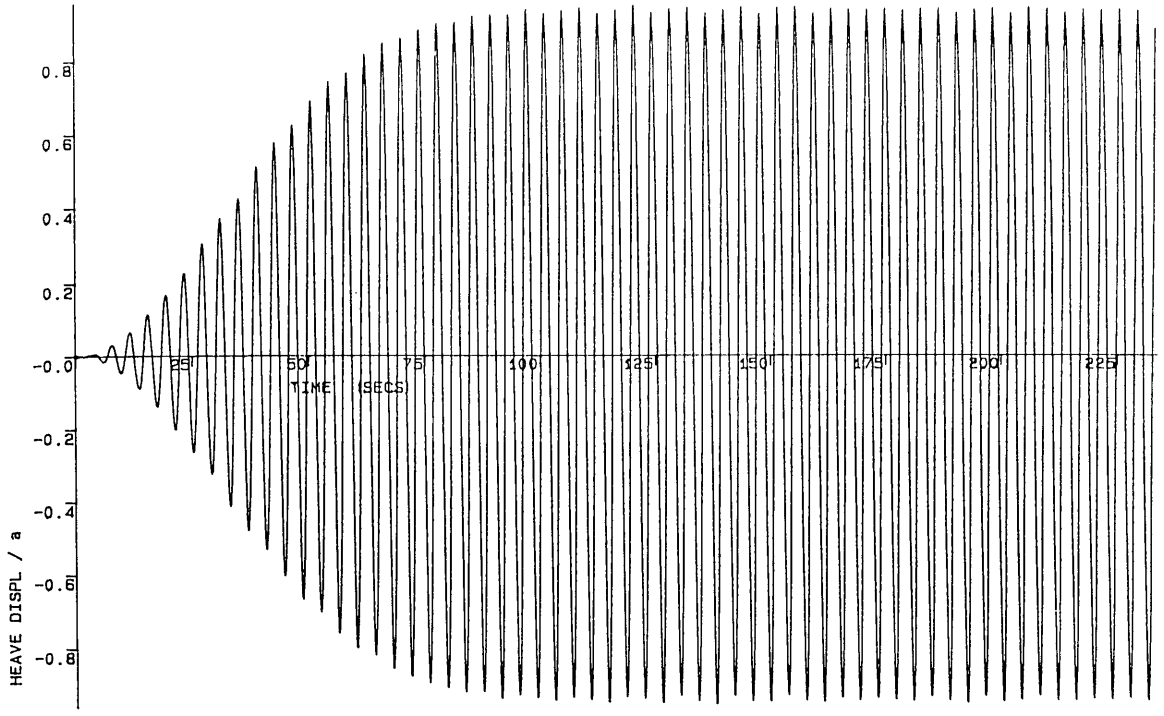

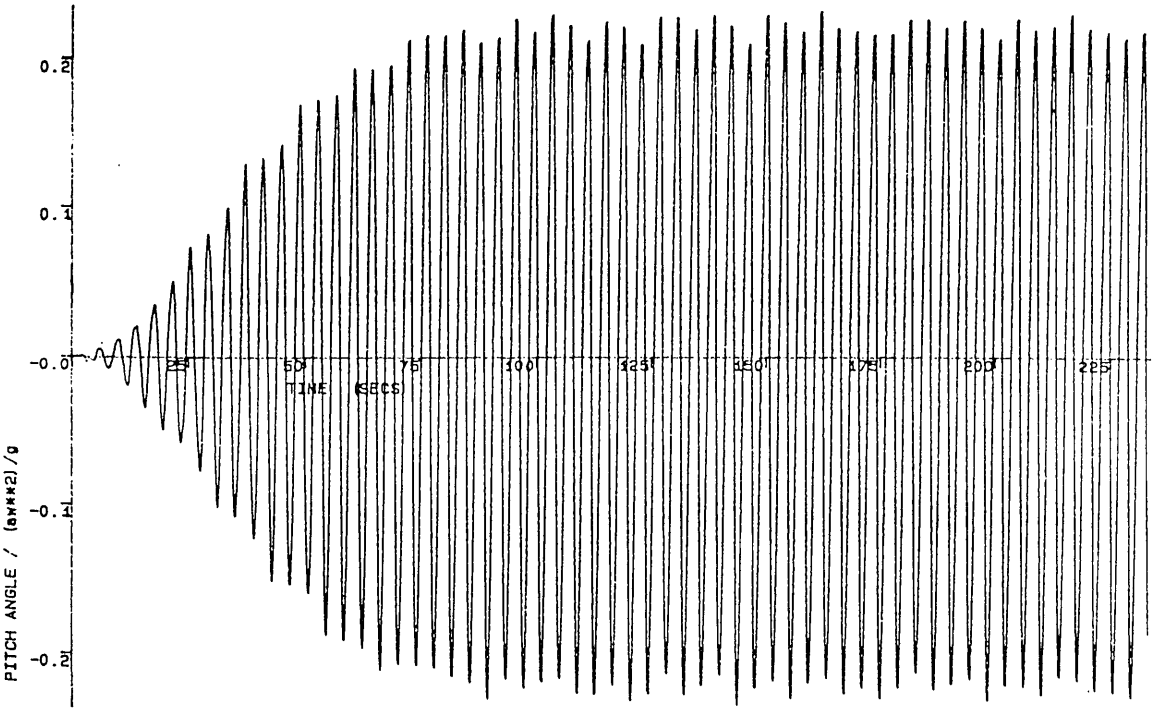

U = 0.5 m/s w = 1.5 rad/s

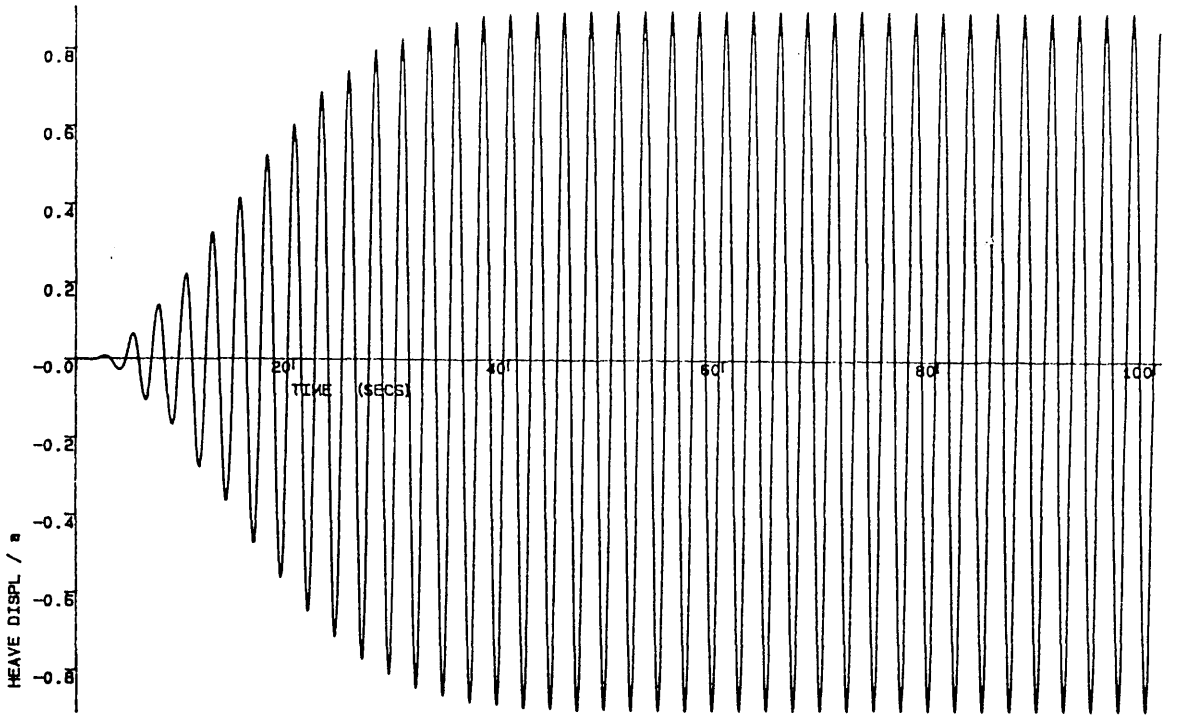

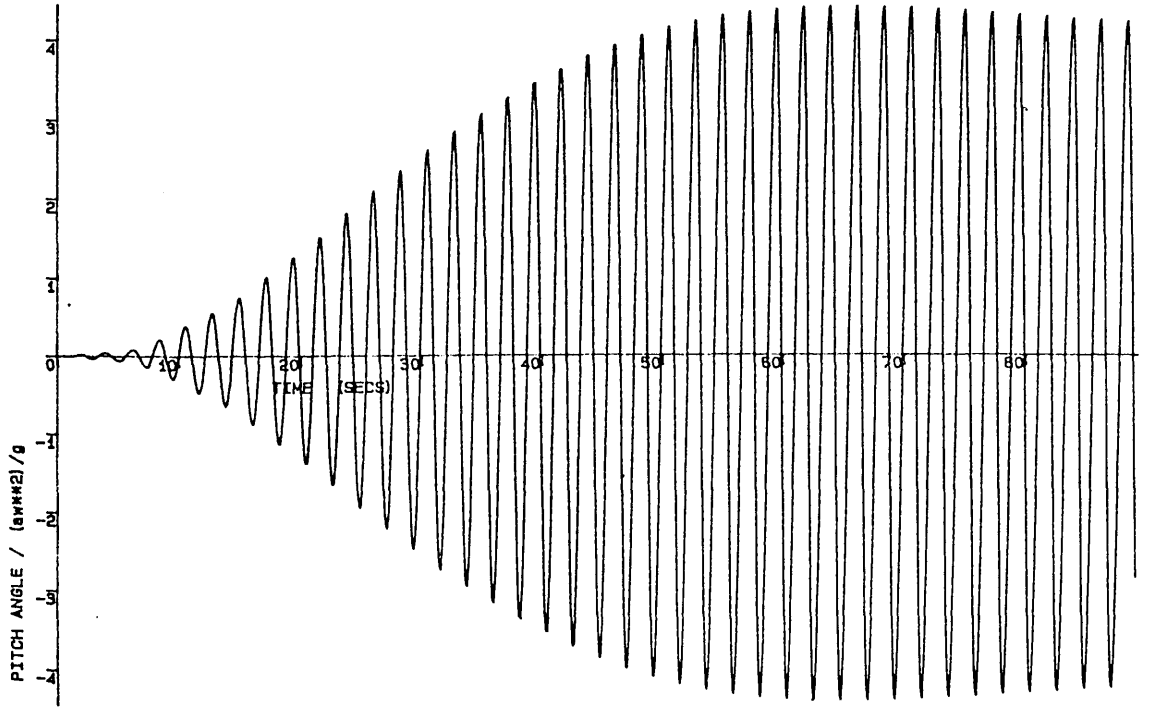

U = 0.5 m/s w = 2.5 rad/s

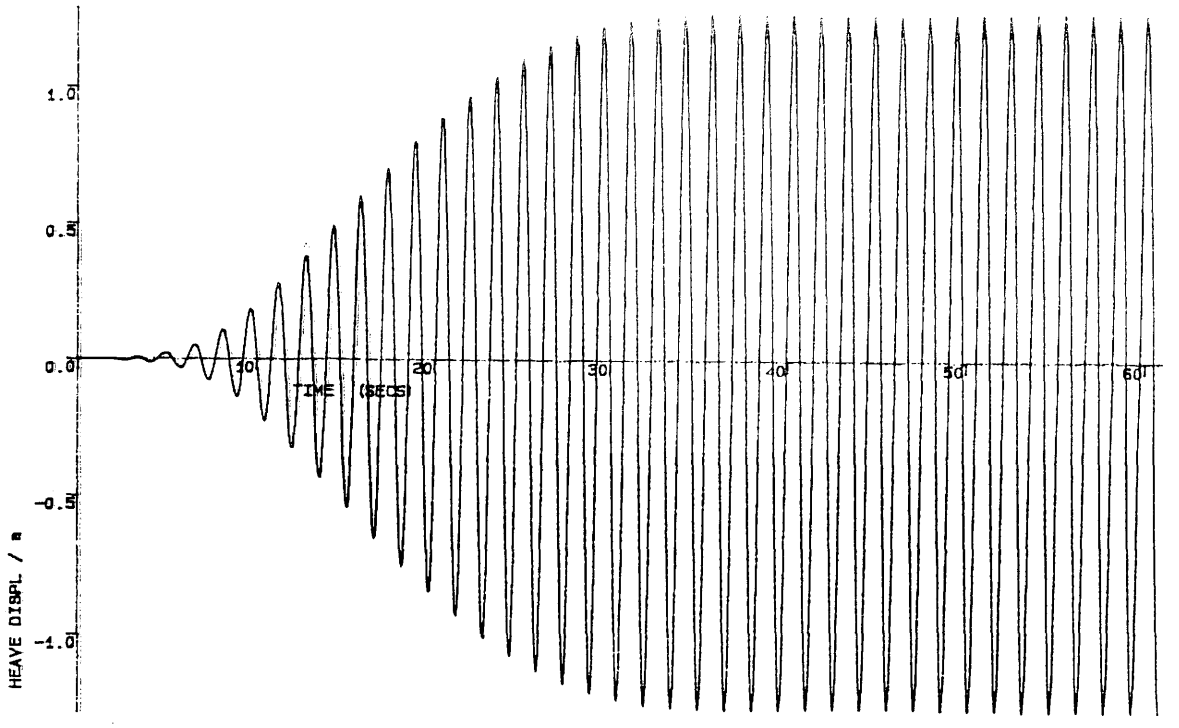

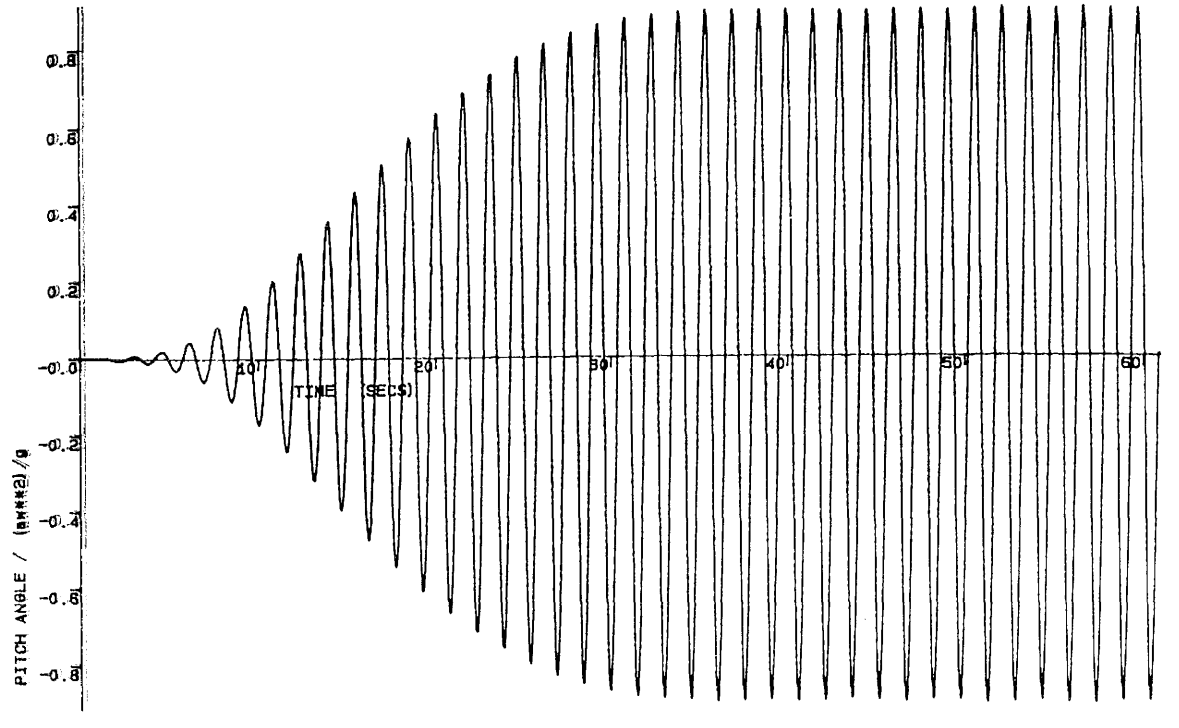

U = 0.5 m/s w = 3.5 rad/s

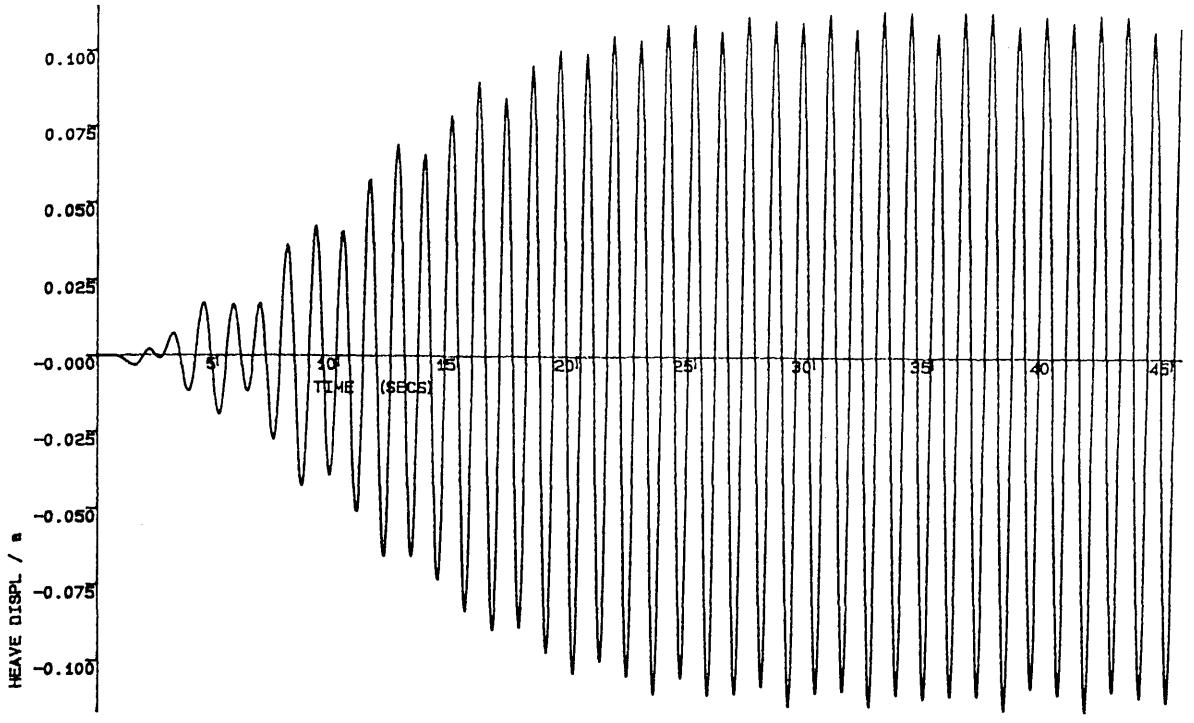

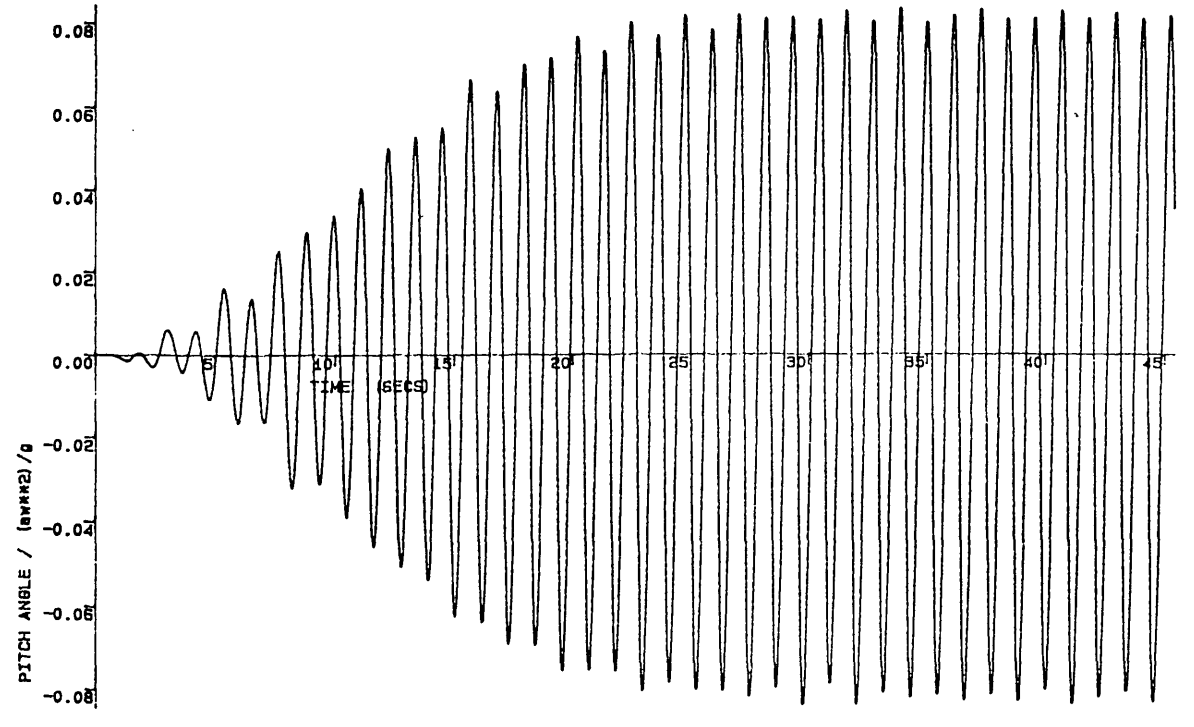

U = 0.5 m/s w = 4.5 rad/s

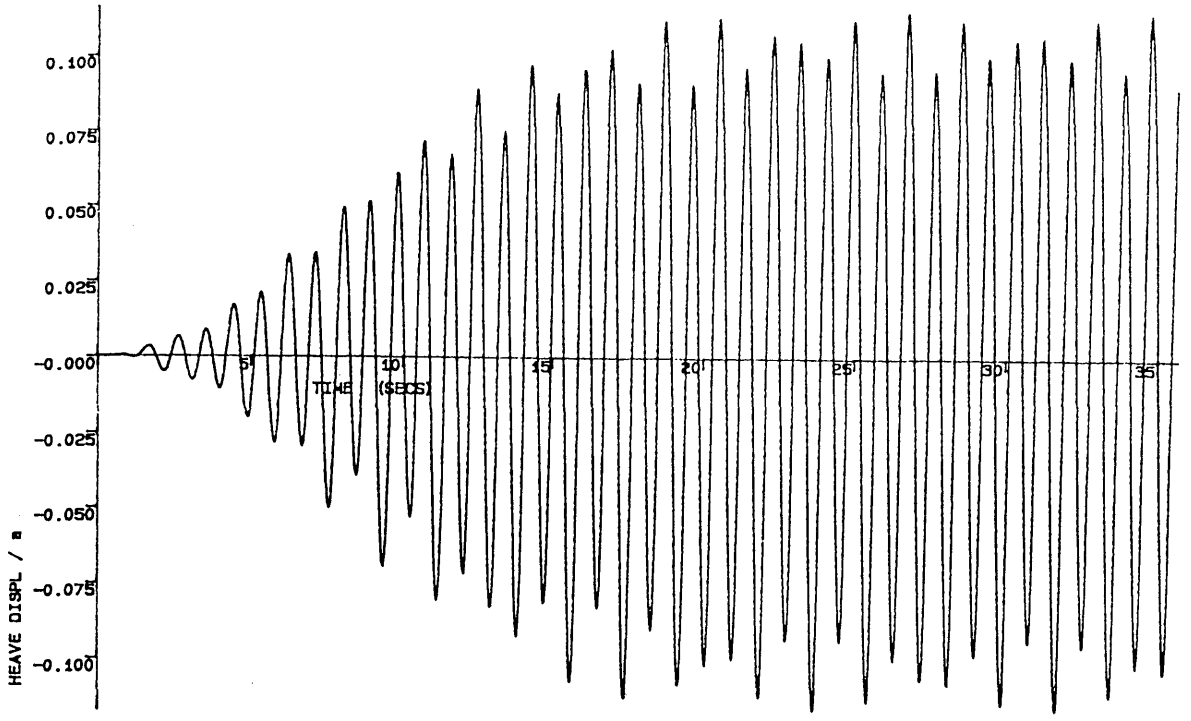

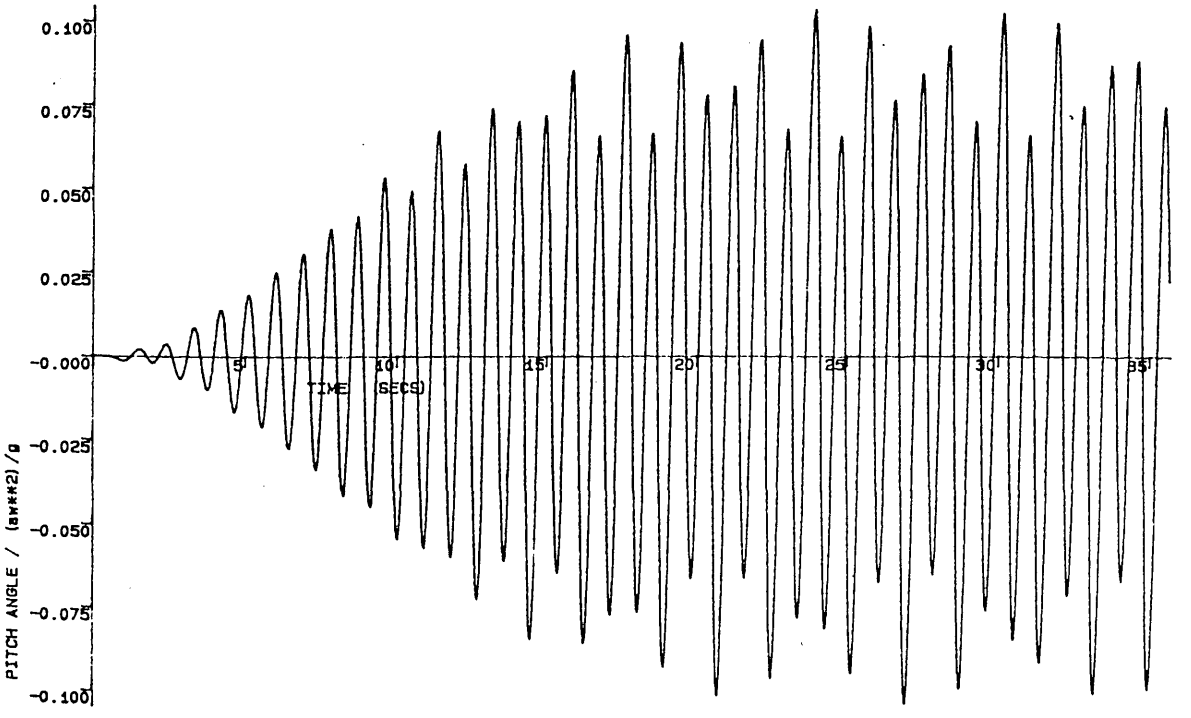

U = 0.5 m/s w = 5.5 rad/s

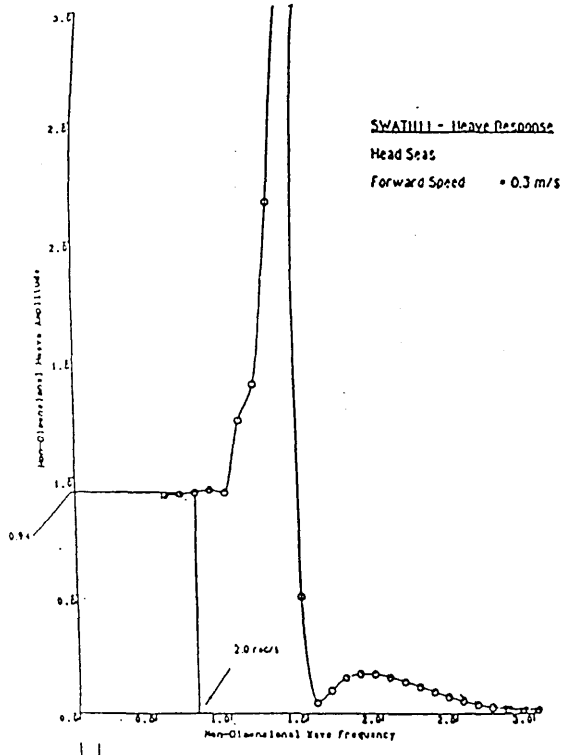

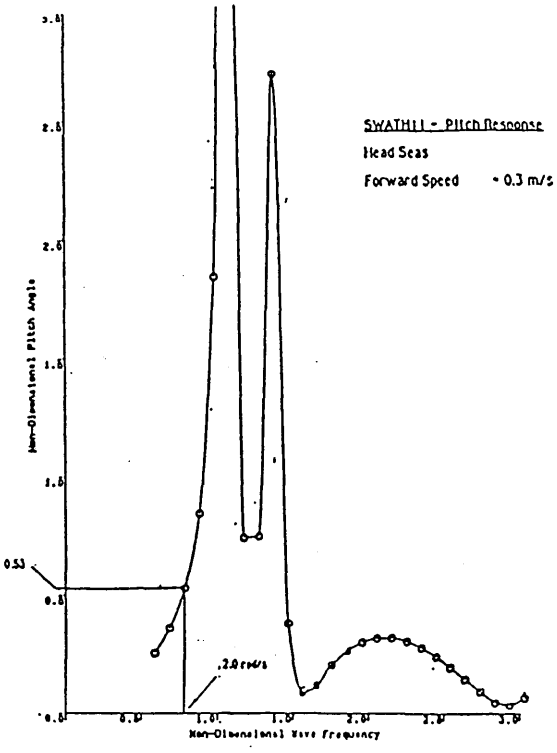

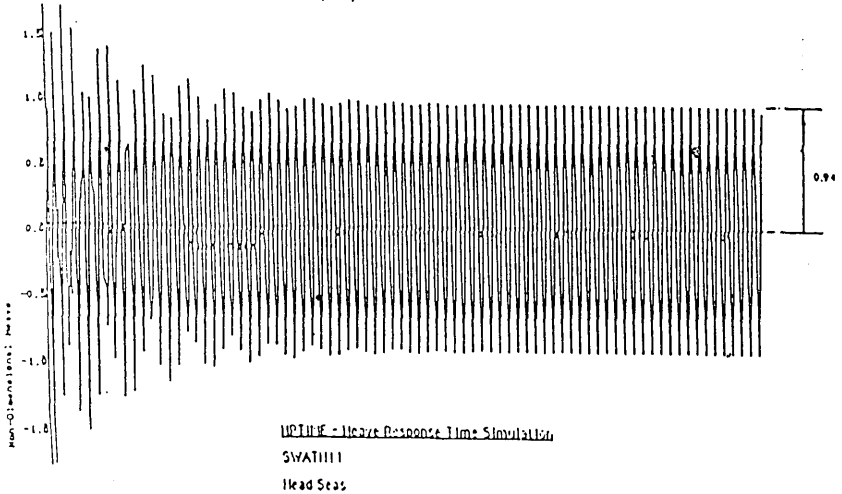

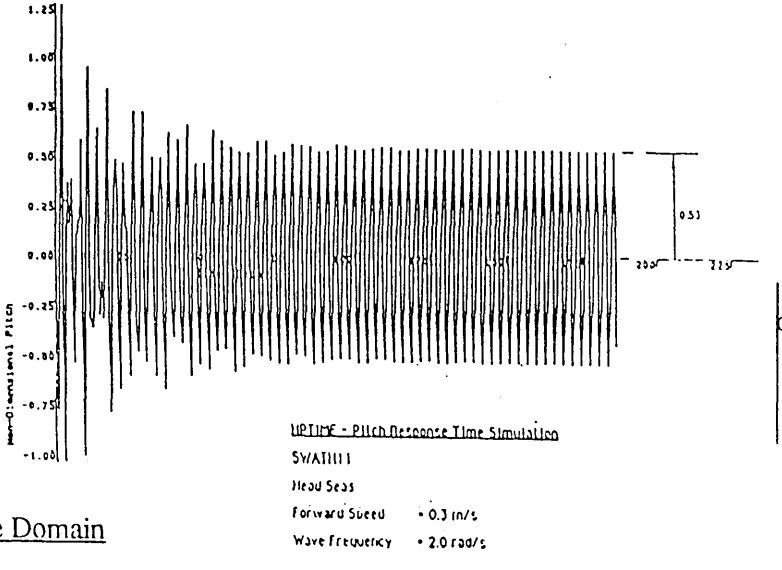

Agreement between Linear Time Domain

and Frequency Domain Predictions

Figure 3.8

CHAPTER 4

INTRODUCTION OF NON-LINEAR WAVE EXCITATION

4.1 Introduction

Previous work carried out at the University of Glasgow Department of Naval Architecture and Ocean Engineering[10][40] has involved investigating variations in wave excitation amplitudes for different types floating vessels. In these studies theoretical predictions were obtained for a range of fully submerged and surface piercing section geometries using versions of the same Frank close-fit method as applied here. The results given that wave excitation force and moment amplitudes can vary considerably with changes in submerged geometry. Amongst the conclusions drawn are suggestions that the effect of the vessel's oscillatory heave and pitch motions in particular, can cause significant variations in these values.

4.2 Some Non-linear Aspects of Wave Induced Motions

Before introducing the first non-linearity into the simulation it is important to consider the effects which are overlooked when the vessel motions system is linearised. Highly non-linear effects due to slamming occurrences, motion control fins and random seas are covered in Chapter 6 and are not discussed here. The fundamental omissions can be summarised as follows :

(i) Large Motion Displacement Effects on Restoring

As the vessel oscillates in the presence of the encountered wave its water

plane area is continuously varying. Linear analysis is restricted to small amplitude motions and the effects of this are regarded as negligible. Heave and pitch restoring (spring) coefficients are therefore assumed to be constants. In time domain analysis, the time dependency of the restoring coefficients can be introduced. This non-linear hydrostatic effect is covered in Chapter 5 .

(ii) Large Motion Displacement Effect on Hydrodynamic Forces

Hydrodynamic forces are dependent on the submerged geometry changes of each motion cycle. Beyond small amplitude motions therefore, variations in the hydrodynamic coefficients and wave exciting forces and moments have to be accounted for. This chapter deals with non-linear wave force effects. The time dependencies of the the added mass and damping coefficients are covered in Chapter 5.

(iii) Effects of Viscous Damping

In the theoretical model for hydrodynamic force calculations described in Chapter 2, ideal (irrotational) fluid theory is applied and viscous damping is not considered. Non-linear viscous effects are related to the square of motion velocity and can only be approximated in linear analysis by using an equivalent linearisation method.(3) Time domain modelling provides the means for introducing viscous terms of the form :

$$F_v = \frac{1}{2} \rho C_D \dot{S}_k \left| \dot{S}_k \right|$$

where 'k' denotes the mode of motion and C_D is the drag coefficient. Introducing velocity squared terms is outside the scope of this study.

(iv) Hydrodynamic Pressure due to the Square of Velocity Potential

In linear theory , the total fluid pressure acting on the vessel is given by the linearised form of Bernoulli's equation :

$$p = -\rho\frac{\partial\phi_T}{\partial t} - \rho gz$$

where the velocity potential term ϕ_T represents the hydrodynamic pressure and ρgz, the hydrostatic pressure.However, Bernoulli's equation includes a hydrodynamic component due to the square of the velocity potential :

$$p = -\rho\frac{\partial\phi_T}{\partial t} - \frac{1}{2}\rho\,\nabla\phi_T\cdot\nabla\phi_T - \rho gz$$

(v) Free Surface Boundary Condition.

In the linear hydrodynamic model, boundary conditions of the system are defined in order to solve for the unknown pulsating source strengths. The linearised form of the free surface condition :

$$\frac{\partial^2\phi_T}{\partial t^2} + g\frac{\partial\phi_T}{\partial z} = 0$$

is used.

It is assumed that this condition applies at the mean, still water, free surface. The exact free surface condition however, is given as (12) :

$$\frac{\partial^2\phi_T}{\partial t^2} + 2\nabla\phi_T\,\nabla\frac{\partial\phi_T}{\partial t} + \nabla\phi_T\,\nabla\left(\nabla\phi_T\right)^2 + g\frac{\partial\phi_T}{\partial z} = 0$$

and should be applied at the true, wave free surface.

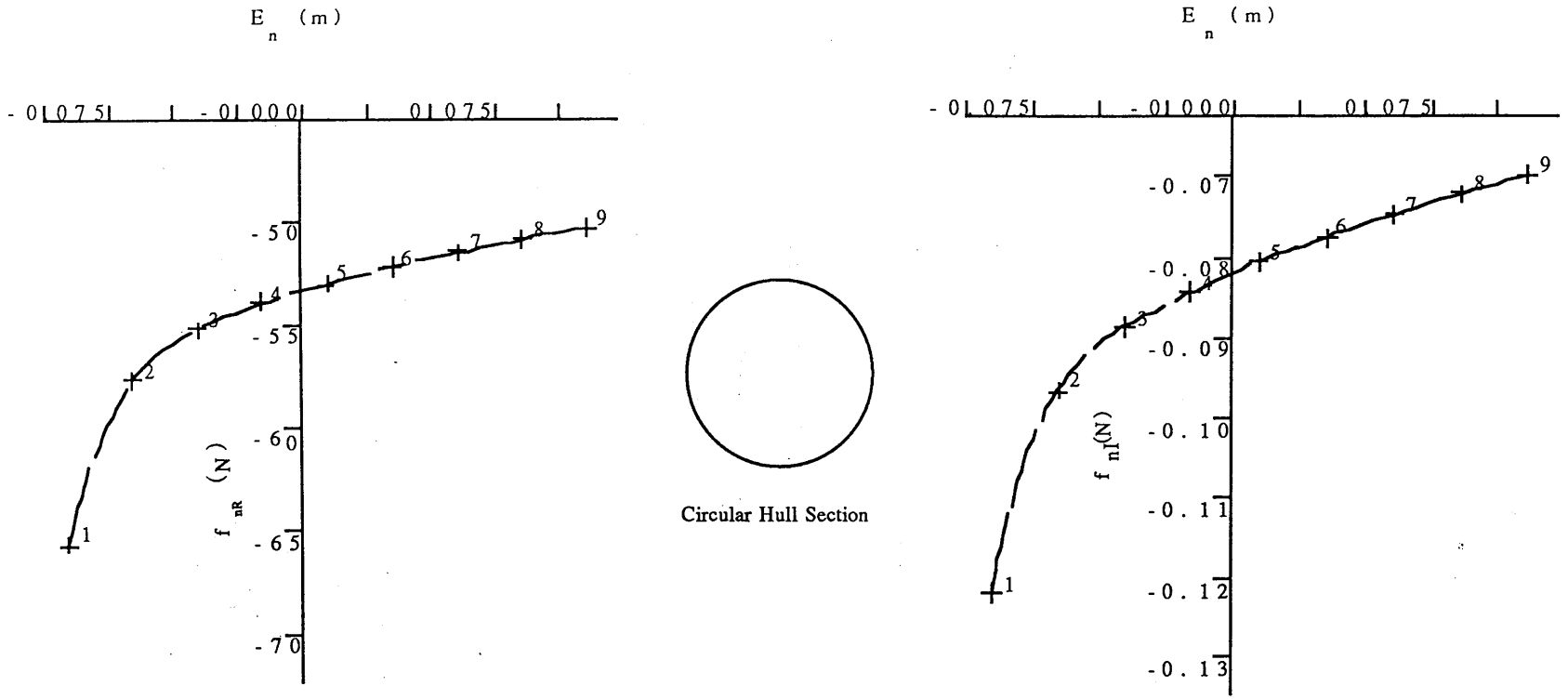

Figure 4.1 Variation of section forces with 'E_n'

At present there are no computationally efficient theoretical models available which take account of the last two items, (iv) and (v) and Simplified methods such as the one applied in this work therefore remain the only practical means for predicting the hydrodynamic forces.

4.3 Non-linear Wave Excitation Effects

In this chapter, the non-linear behaviour of wave excitation due to the motion related changes in hull section geometry are introduced into the simulation. The implications of this modification may be seen in time histories of both the excitation forces and moments and in the motion predictions obtained from the modified simulation.

4.31 Sectional Force Variations With Submergence Depth

By studying the expression derived in Chapter 2 for the incident (Froude-Krylov) component of wave excitation , the dependence of section force on submergence depth can be demonstrated. Equation (2.19) includes the term , $e^{k_o z}$. This term represents an exponential variation of force in the z direction A typical trend with submergence depth for a fully submerged SWATH circular hull section is shown in figure 4.1

The extent of this exponential characteristic will depend on the relative significance of the incident and diffraction components of wave excitation.

Generally,the Froude-Krylov component is expected to be the most significant in the lower and higher bands of normal operation wave spectra. In the mid range however, the diffraction component can predominate and the dependency on submergence depth could show different characteristics. In such cases the force-depth relationship will be governed by the nature of section wetted geometry changes.

4.32 Harmonic Components of Wave Excitation

When dealing with single regular waves in motion simulation, the frequency of motion response to wave excitation will be equal to the frequency of wave encounter. The natural frequency or resonance in any mode of motion will not feature in steady state response predictions obtained unless, of course, the encounter frequency coincides with a motion resonant frequency. In Chapter 3 an initial transient feature of the time domain motion solutions was discussed. This feature was ascribed to the impulse effect of the initial applied excitation at the start of the simulation. Unless a suitable ramp function is applied to the forcing functions,as described, this impulse effect can cause excitation at at heave and pitch resonant frequencies. However this is an artificial effect which is damped out with time.

As the vessel oscillates in heave and pitch , the amplitudes of wave excitation forces and moments are expected to show harmonic variations with time. This effect is due to their depth of submergence dependency described above. It can be seen that, under the harmonic motions of the craft and the passing of the incident wave, the submergence depth at each hull section is time dependent. A net effect of sectional variations will be evident in the total heave forces and pitch moments for the vessel.

Referring to Equations(3.14) the right-hand side wave excitation terms can be expressed with their time dependency as :

$$F_3(t) = F_3\, e^{-i\omega_e t}$$

$$F_5(t) = F_5\, e^{-i\omega_e t} \qquad (4.1)$$

As the excitation amplitudes, F_5 and F_3 are themselves time dependent, they can be written :

$$F_3' = F_3^m + F_3^{os}\, e^{-i\omega_e t}$$

$$F_5' = F_5^m + F_5^{os}\, e^{-i\omega_e t} \qquad (4.2)$$

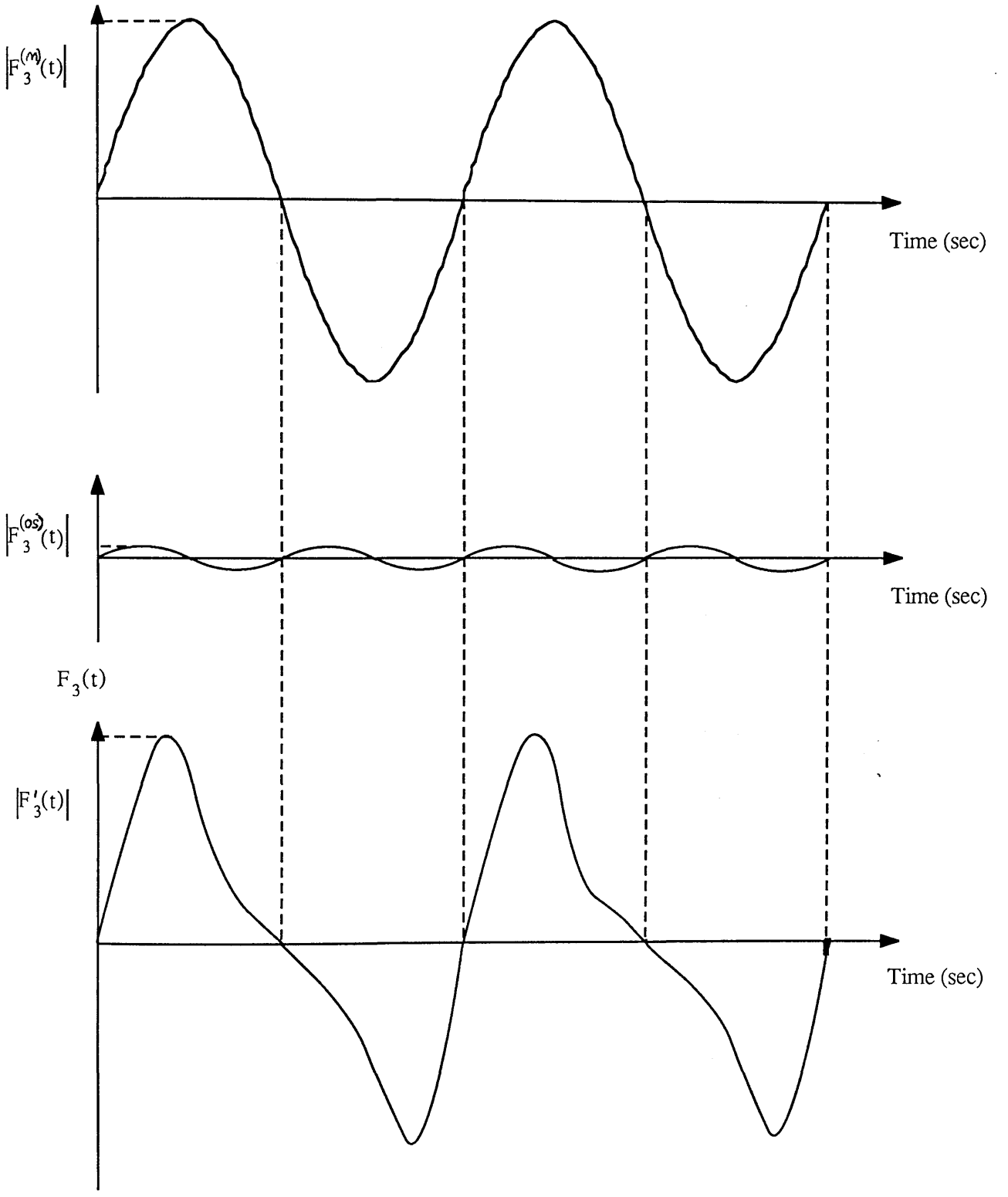

Figure 4.2 Secondary Component of Wave Excitation

where ' m 'denotes the mean component and 'os' an oscillatory component. By inserting equations (4.2) into equations (4.1), the time dependent forcing functions become non-linear and are :

$$F_3'(t) = (F_3^m + F_3^{os} e^{-i\omega_e t}) e^{-i\omega_e t} = F_3^m e^{-i\omega_e t} + F_3^{os} e^{-i\,2\omega_e t}$$

$$F_5'(t) = (F_5^m + F_5^{os} e^{-i\omega_e t}) e^{-i\omega_e t} = F_5^m e^{-i\omega_e t} + F_5^{os} e^{-i\,2\omega_e t}$$

(4.3)

These expressions show the two harmonic time components of excitation. The primary effect will be due to the mean component which oscillates with the same frequency , ω_e, as the encountered wave. The secondary component of excitation which is causedby submerged geometry variations will only be significant at larger amplitude motions and will oscillate at twice the frequency of encounter, $2\omega_e$. Figure 4.2 shows a schematic illustration of how the secondary component, which has been magnified in amplitude, could appear in a time history of excitation.

The significance of the higher frequency component will also depend on the hull / strut geometry. SWATH vessels are, in principle, designed to experience minimal wave excitation, and the secondary effect is expected to be small and maybe even difficult to detect.

As the nature of the vessel's motions are dependent on the nature of excitation ,the secondary effect, if of any significance, should be detectable during response analysis.

Re-writing the motion equations to include the non-linear wave excitation effects gives :

$$(M_{33} + A_{33})\ddot{S}_3(t) + B_{33}\dot{S}_3(t) + C_{33}S_3(t) + A_{35}\ddot{S}_5(t) + B_{35}\dot{S}_5(t) + C_{35}S_5(t) = F_3'(t)$$

$$(I_{55} + A_{55})\ddot{S}_5(t) + B_{55}\dot{S}_5(t) + C_{55}S_5(t) + A_{53}\ddot{S}_3(t) + B_{53}\dot{S}_3(t) + C_{53}S_3(t) = F_5'(t)$$

(4.4)

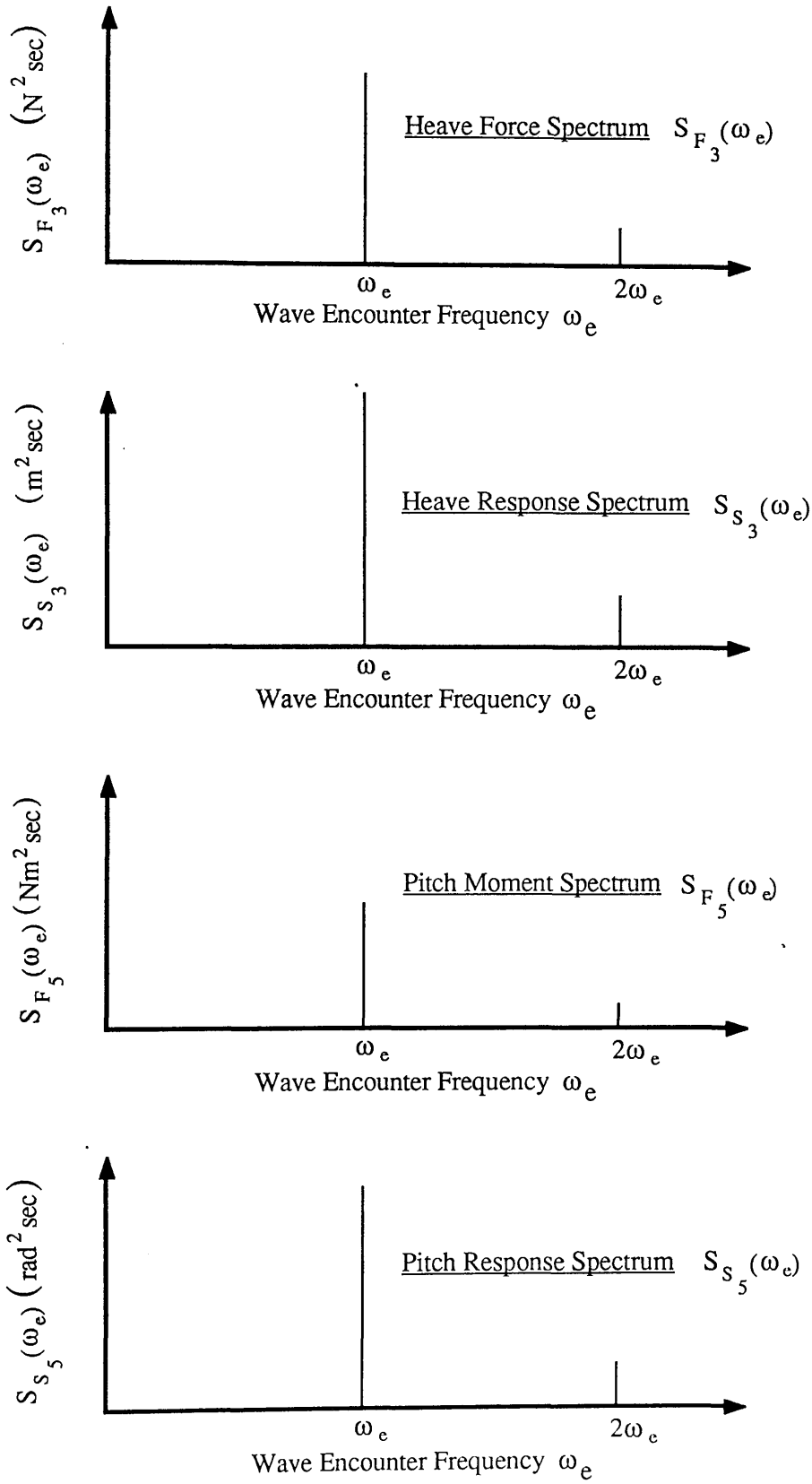

Figure 4.3 Non-Linear Wave Excitation Harmonic Components

or, by inserting (4.3) into(4.4)

$$(M_{33}+A_{33})\ddot{S}_3(t)+B_{33}\dot{S}_3(t)+C_{33}S_3(t)+A_{35}\ddot{S}_5(t)+B_{35}\dot{S}_5(t)+C_{35}S_5(t)$$

$$= F_3^m e^{-i\omega_e t} + F_3^{os} e^{-2i\omega_e t}$$

$$(I_{55}+A_{55})\ddot{S}_5(t)+B_{55}\dot{S}_5(t)+C_{55}S_5(t)+A_{53}\ddot{S}_3(t)+B_{53}\dot{S}_3(t)+C_{53}S_3(t)$$

$$= F_5^m e^{-i\omega_e t} + F_5^{os} e^{-2i\omega_e t}$$

(4.5)

An investigation of right-hand side harmonic components could be carried out by applying spectral analysis. Figure 4.3 illustrates spectra which might be, typically, expected.

4.33 Steady Motion Offset

The Froude-Krylov exponential behaviour of sectional wave forces with submergence depth described above can cause a steady offset in the vessels motion response. This effect which is illustrated in figure 4.4 can be significant for the angular motions of some floating configurations.(42)

4.34 Sectional Phase Shift Variations caused by Pitching Motion

It has been shown, sections 2.42 and 2.43, that the phase shift associated with the wave exciting forces and moments at each hull section is due to the longitudinal position of that section in relation to the space fixed origin of the encountered wave. In linear analysis this phase shift is assumed to be constant for each section which results in a constant phase shift for each mode of excitation for the whole vessel.

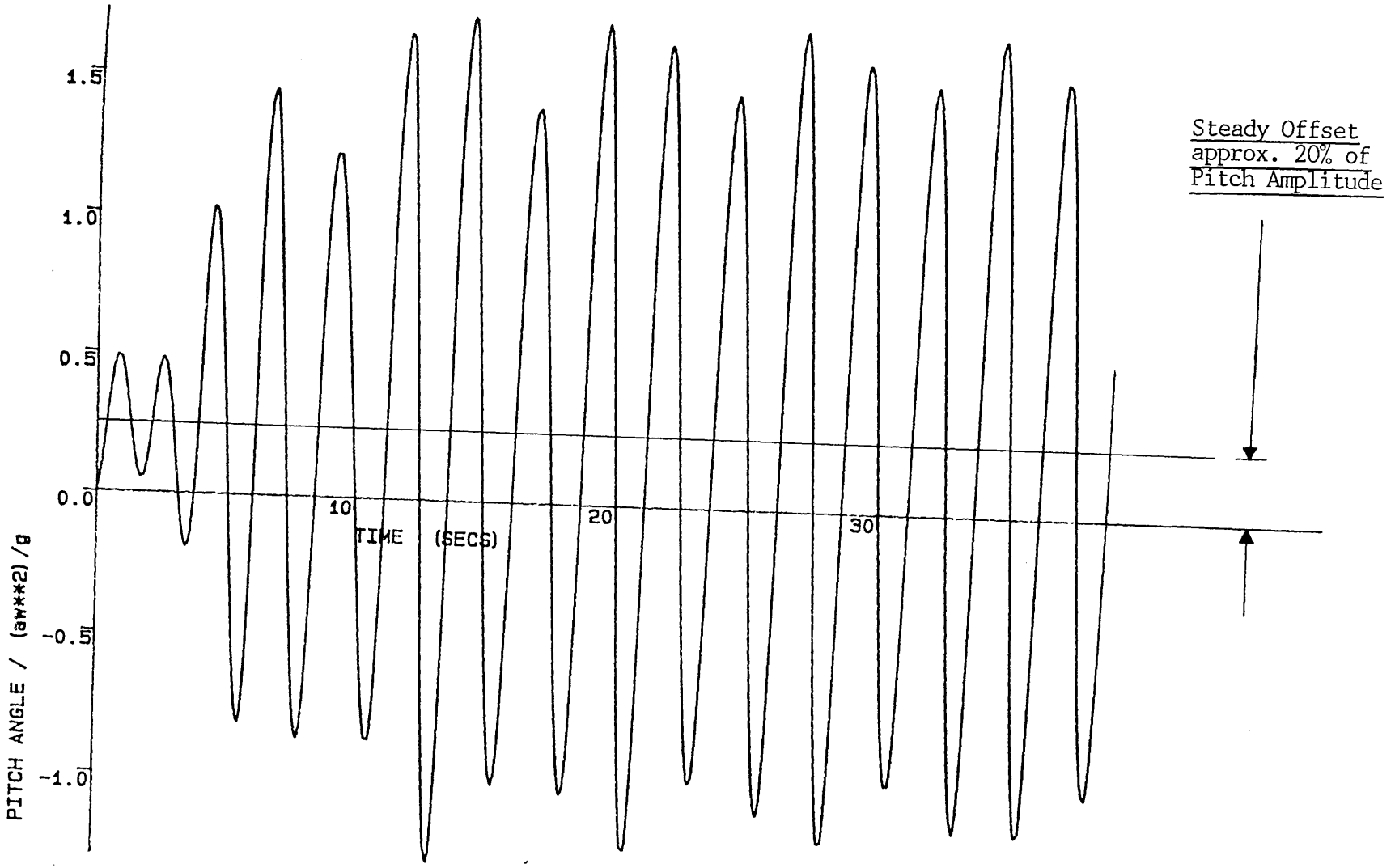

Figure 4.4 Steady Motion Offset

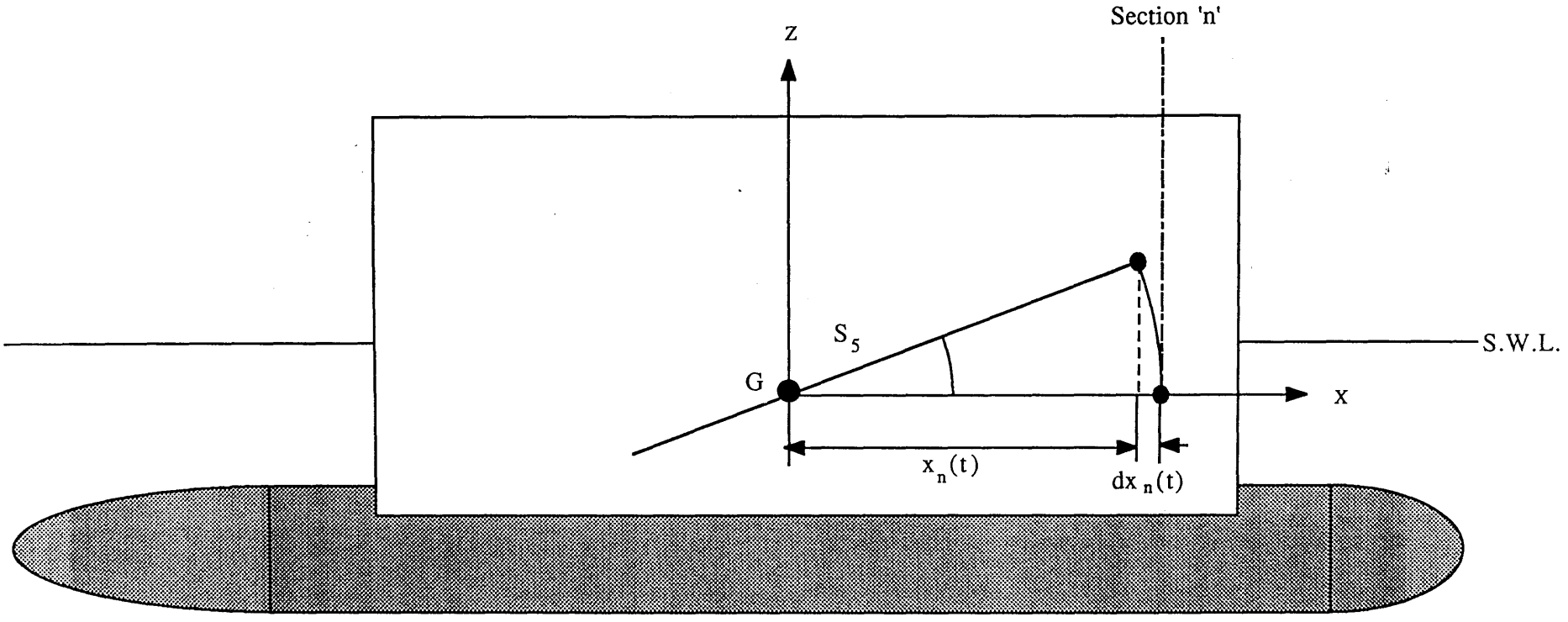

Figure 4.5 Variation in Phase shift due to Pitch Motion

Equations (2.14) and(2.22) show how the term, $e^{i k_0 x \cos \mu}$, accounts for the phase of each section in the expressions for the incidence and diffraction potentials of hydrodynamic excitation.

In reality, the longitudinal position of the section which is represented by x is a harmonic function of time due to the sinusoidal pitch motion charateristics. Therefore , x becomes x(t) and the section phase term becomes, $e^{i k_0 x(t) \cos \mu}$

Figure 4.5 illustrates the nature of this variation in x and, as shown in this simplified, level water surface case x(t) is given by :

$$x(t) = x_0 \cos S_5(t) \qquad (4.6)$$

and the magnitude of change, dx :

$$dx(t) = x_0 (1-\cos S_5(t)) \qquad (4.7)$$

where x_0 is the still water section position.

These two equations show that the variations in sectional phase shift are dependent on the pitch motion angular displacement and will be correspondingly small. For this reason and in order to avoid significant complication, the effect has not been incorporated in the wave excitation theoretical model.

4.4 Submerged Geometry Definition

As the vessel oscillates in heave and pitch, its volume of displacement is continuously varying. A method for defining the instantaneous submerged geometry is required so that the associated hydrostatic and hydrodynamic properties of that condition can be calculated.

It has been shown in Chapter 2 that the determination of added mass, damping and wave

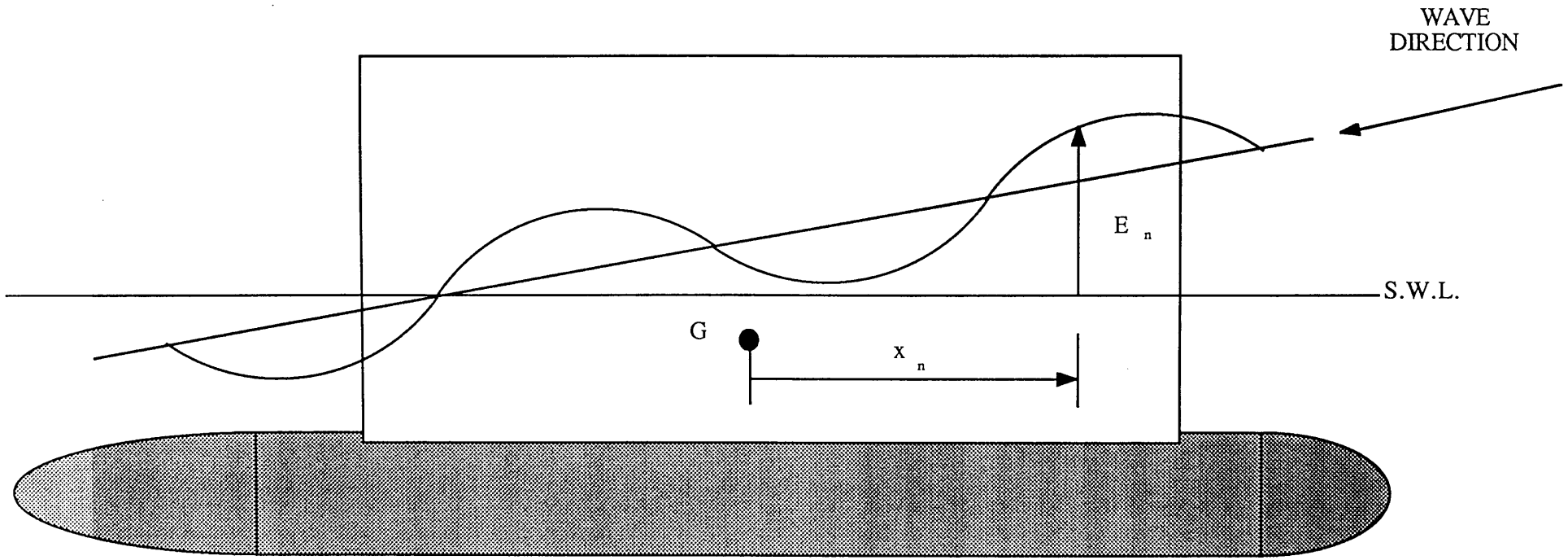

Figure 4.6 Water Surface Elevation E_n

excitation values for the complete wetted surface involves calculating sectional values and then integrating along the vessel length. This approach can also be adopted for determining the vessels hydrostatic condition. Sectional values are a function of submerged geometry and a method for defining submergence depths at each section during the vessel's motions in waves is therefore required. In defining these time dependent geometries it is necessary to account for the effects of the travelling encountered wave profile and the effects of motions in both the heave and pitch modes.

Figure 4.6 shows a SWATH ship in regular head seas. The example surface piercing section illustrates the time dependent variable E_n where 'n' denotes the station number. E_n is measured from the at rest, still water line and can be described as the water surface elevation at station n, due to the combined effects of heave and picth motion displacements and the encountered wave elevation.

The contributions to E_n from linear heave displacement and angular pitch displacement are :

$$E_h(t) = S_3(t) \tag{4.8}$$

and

$$E_p(x,t) = x_n \tan S_5(t) \tag{4.9}$$

respectively.

The wave profile component of E_n is given by :

$$E_w(x,t) = a \cos (k_o x_n - \omega_e t) \tag{4.10}$$

where,

k_o = wave number

a = wave amplitude

and

ω_e = wave encounter frequency

Combining equations (4.5), (4.6) and (4.7) yields the general expression for the water surface elevation at station n which is distance x_n from the LCG position :

$$E_n(x,t) = a \cos(k_0 x_n - \omega_e t) + x_n \tan S_5(t) - S_3(t) \qquad (4.11)$$

For given values of time, heave and pitch motion displacements from rest and wave encounter frequency, equation (4.8) can be used to define the vessel's submerged geometry at that instant.

4.5 Solution Procedure with Time Dependent Wave Excitation

Using the method described above, the depths of submergence values for pre-defined hull sections can be calculated at each simulation time step. Corresponding sectional forces and their phase with position can therefore be determined and integrated along the vessel length to give the total instantaneous force and moment amplitudes of the harmonic forcing functions.

Chapter 3 describes how a computer subroutine selected from the NAg library [6] is used to obtain numerical solutions for the set of time dependent first order differential equations of motion (3.15). Solutions are obtained by applying the Runge-Kutte technique which involves an iterative integration procedure during each simulation time step. A feature of the NAg routine is that the conditions of the system of differential equations can be modified at the beginning of each solution cycle. The subroutine FCN (figure 4.7) is available for this purpose and it provides the means for updating the time dependent components of the motion equation. Any number of calculations can therefore be performed under the control of FCN to establish the new conditions. The CPU time requirement however for each time step solution is directly related to the number of calculations performed. In order to obtain steady state solutions within a reasonable period of time it is therefore important to minimise the degree of

computation. A drawback of the NAg routines is that instead of calculating and memorising the new differential equation conditions prior to carrying out the integration itterations, subroutine FCN is called for every integration. The CPU time requirement is therefore magnified accordingly. The NAg routines are inacessible and it is not possible to make any suitable modifications in order to avoid this problem.

In Chapter 2 the computational demands of the Frank Close-fit technique were discussed. Early in this part of the study attempts were made to employ the technique directly during the time sequence. This however presented an enormous computational burden for the VAX 11/730 machine and it was clear that an alternative method for updating the wave force and moment amplitudes was required.

A technique which makes use of polynomial expressions obtained from pre-generated wave exciting force and moment data has been developed and the simulation procedure for including non-linear wave excitation effects is described as follows.

Each defined hull/strut section is analysed in turn. Hydrodynamic calculations are performed to obtain real and imaginary parts of the wave exciting force for E_n values ranging over the strut depth between the top side of the pontoon hull and the still water surface, for fully submerged sections. A polynomial curve fit routine is then applied to relate the force components with E_n and expressions of the form :

$$f_{nR} = r_1 + r_2 E_n + r_3 E_n^2 + \ldots. \qquad (4.12)$$

and

$$f_{nI} = i_1 \sigma + i_2 E_n + i_3 E_n^2 + \ldots..$$

are obtained for the real and imaginary parts at each hull section 'n'.

From the at rest initial conditions, at $t = 0$, motion displacements are set tozero . It can be seen therefore from equation (4.10) and (4.11) that the wave surface elevation values E_n are equal to E_w. With values of E_n established, real and imaginary parts of section wave forces are obtained by using the polynomials fnR and fnI. Integrating these values and their moments along the vessel length will yield total values for the real and imaginary parts of the heave force and pitch moment :

$$F'_{3R} = \sum_{n=1}^{\text{no.of sec}} f_{nR}$$

$$F'_{3I} = \sum_{n=1}^{\text{no.of sec}} f_{nI} \qquad (4.13)$$

$$F'_{5R} = \sum_{n=1}^{\text{no.of sec}} x_n f_{nR}$$

$$F'_{5R} = \sum_{n=1}^{\text{no.of sec}} x_n f_{nI}$$

where

$$F'_3 = \sqrt{F'^{2}_{3R} + F'^{2}_{3I}}$$

$$F'_5 = \sqrt{F'^{2}_{5R} + F'^{2}_{5I}} \qquad (4.14)$$

are the heave force and pitch moment amplitudes, and

$$\phi_3 = \tan^{-1}\left(\frac{F'_{3I}}{F'_{3R}}\right)$$

$$\phi_5 = \tan^{-1}\left(\frac{F'_{5I}}{F'_{5R}}\right) \qquad (4.15)$$

are their phases with position.

By introducing the harmonic time component , the instantaneous heave force and pitch moment for the time step are obtained :

$$F'_3(t) = F'_3 e^{-i\omega_e t} = F'_{3R}\cos\omega_e t + F'_{3I}\sin\omega_e t$$

$$F'_5(t) = F'_5 e^{-i\omega_e t} = F'_{5R}\cos\omega_e t + F'_{5I}\sin\omega_e t \qquad (4.16)$$

Solutions can be obtained by substituting values from equations (4.16) into the motion equations(3.15) and solving using the Runge-Kutte technique described in Chapter 3. It is important to remember that although the wave excitation values are now time dependent variables, the hydrodynamic and hydrostatic coefficients on the left-hand side of the motion equation are at this stage assumed to be linear values which correspond to the still water condition . These solutions represent the initial conditions for the next time step at $t = t + dt$ and, together with the altered wave position, define the new submerged geometry.

4.6 Computations

Computer subroutines written to incorporate the non-linear wave excitation effects have been combined with the core solution procedure TDSOL, described in Chapter 3.

Time domain predictions have been obtained for model SWATH11 and comparedwith results from linear analysis to assess the significance of non-linear wave excitation effects.

4.61 Structure of Computer Routine

Figure 4.7 shows a flow diagram which illustrates the modified structure of the complete program. As shown, the linear model TDSOL is used as the core solution routine.

The simulation is started using a control command file which contains the necessary input data and activates the main program. Items of design data required include hull section geometry files, longitudinal body axes position of each hull section X_n and vessel overall length, L. Data specifying the conditions of the simulation include wave frequency, 'ω', wave amplitude, 'a', and the number of solution cycles required. Mean, still water hydrodynamic and hydrostatic coefficient values complete the required information .

In opting for non-linear analysis, the subroutine DATABASE, which calculates the polynomial expressions for the real and imaginary parts of section wave forces, is called. Areturn to the main program will result if force polynomials have been previously calculated. Subroutines SECMOD and AYHANR2 are used to modify the geometry data according to a range of E_n values and to calculate the corresponding real and imaginary parts of heave exciting force for each section. Polynomial relationships (of order specified by the user) are fitted to the generated section data by subroutine FITTER. Polynomial coefficients defining f_{nR} and f_{nI} are stored for use during the solution process. Screen graphics are usedto show section force variations over the E_n range.

On the return to the main program, initial zero motion displacements of the simulation at time t = 0 are set. Subroutine ELEVATION calculates the E_n values for the first time step which correspond to the the zero displacement conditions and the encountered wave start position (crest at the body axis origin). If linear analysis has been opted for then all En values are set to zero to define the mean, still water submerged geometry. Real and Imaginary parts of the sectional heave exciting forces are calculated in SECFOR . This routine applies the f_{nR} and f_{nI} coefficients and the E_n obtained from ELEVATION.

Section heave force values and their moments about the body axes origin are integrated along the hull length in subroutine TOTWEX to yield the real and imaginary parts of heave force and pitch moment amplitudes (F'_{3R} , F'_{3I}, F'_{5R} and F'_{5I}) for the whole vessel.

TDSOL which incorporates the core time domain model is called to start the motions solution cycle. First of all, forward speed corrections are applied to the coupled hydrodynamic coefficients (Section 2.54). The harmonic time functions are then applied to the wave excitation force and moment amplitudes to obtain $F'_3(t)$ and $F'_5(t)$.

The subroutine RAME applies the exponential ramp function given in equation (3.17) to the wave excitation forcing functions for an initial period of the total run duration. All parameters are inserted into the first order differential equations of motion and heave and pitch displacement solutions for the first time step are calculated in the NAg subroutine DO2BBF. Using the service subroutine FCN, discussed earlier, heave and pitch values and any other infomation of interest such as F'_3 and F'_5 values, are stored as output data. Also FCN calls the subroutines ELEVATION, SECFOR and TOTWEX which use the motion solutions to calculate the revised submerged geometry condition and the corresponding excitation amplitudes for the next time step, at t+dt.

Iterations of this solution procedure are continued until the required number of motion cycles to obtain steady state solutions, have been completed.

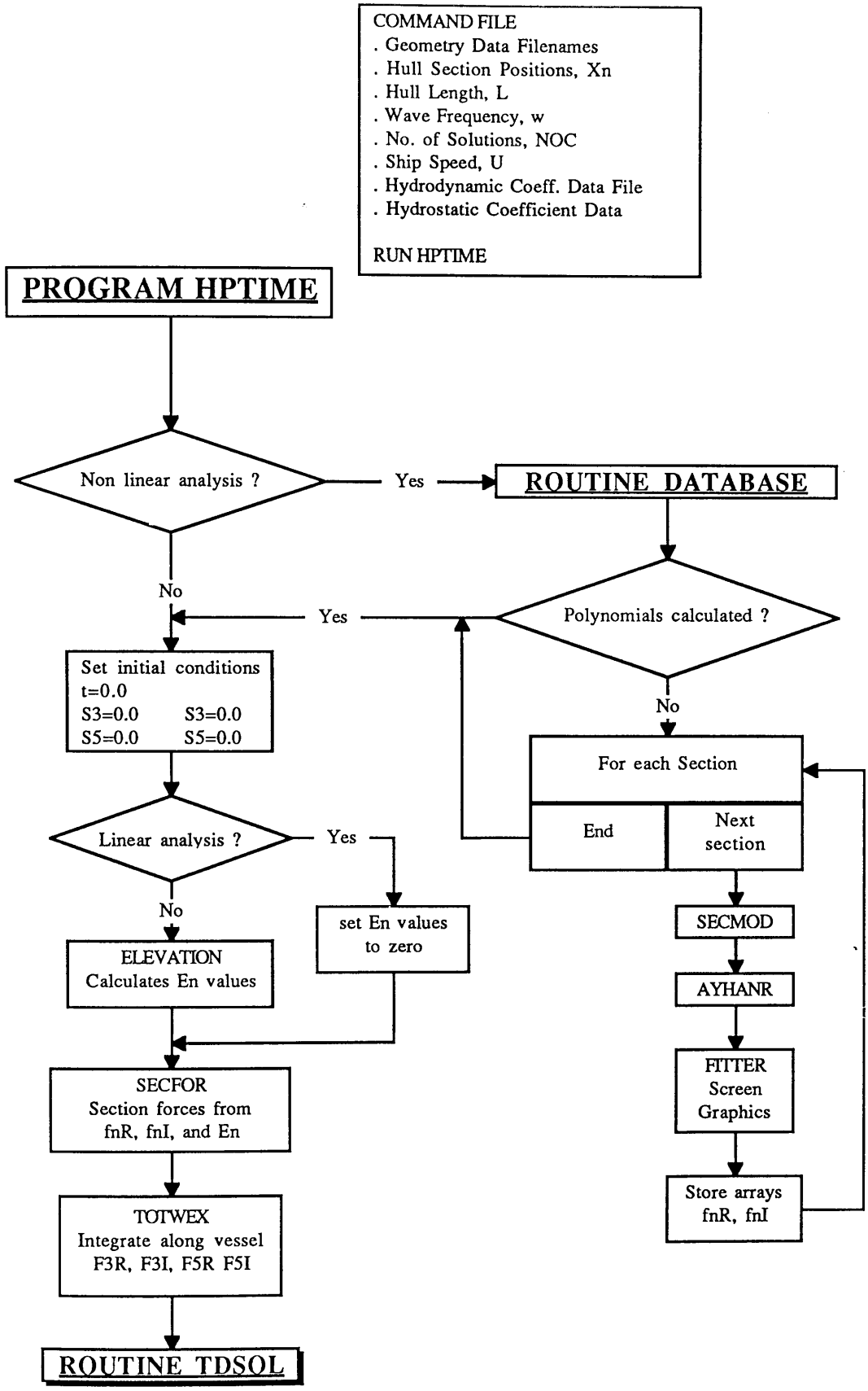

Figure 4.7 Structure of Computer Routine HPTIME with Non-linear Wave Excitation

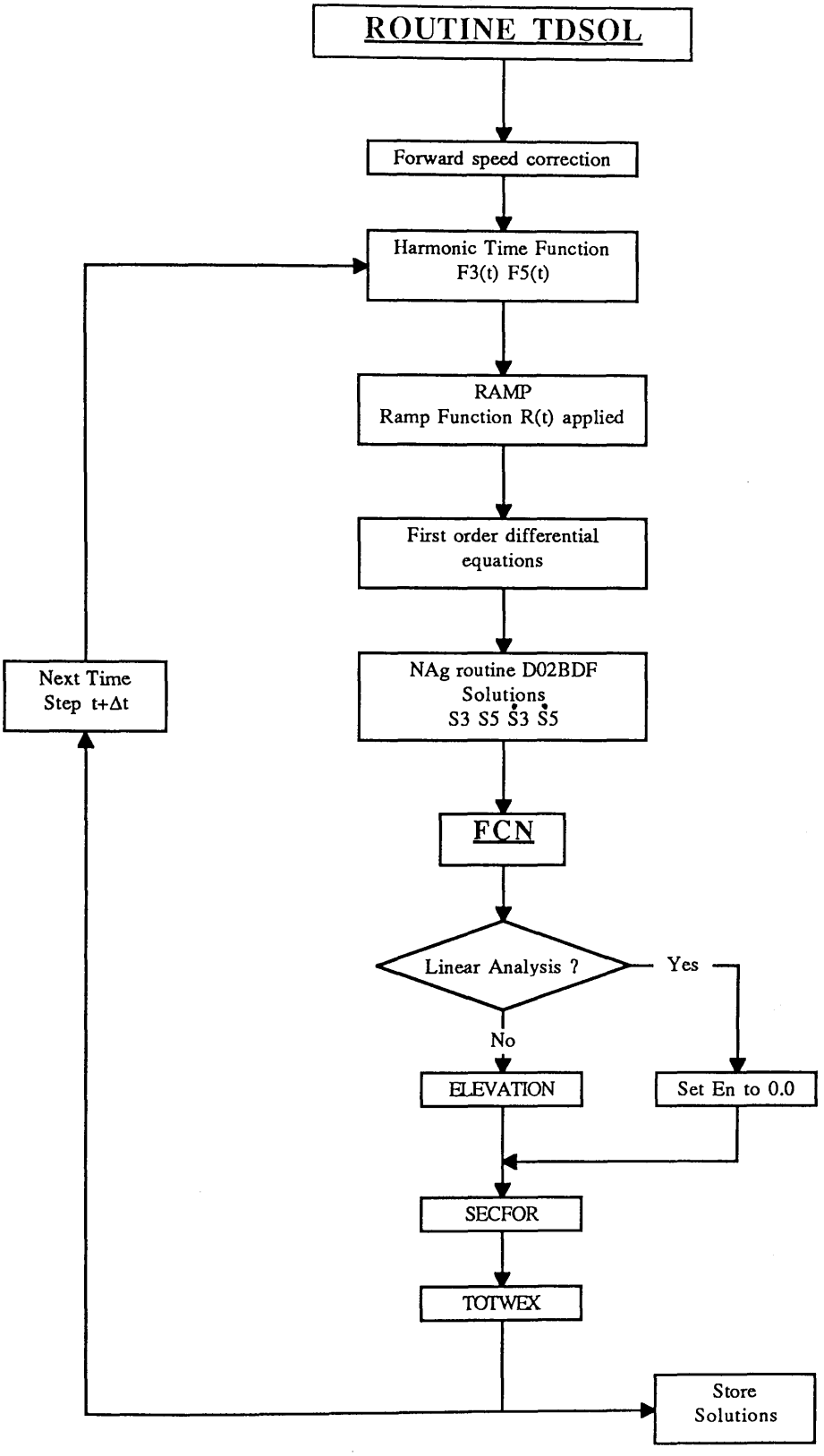

Figure 4.7 (cont..)

4.62 Analysis of SWATH11

Heave and pitch motions of the model SWATH11 have been analysed using the computer program described above. Tests were carried out for a range of wave frequencies and forward speeds. Since non-linear effects are of interest, responses were assessed for large amplitude waves which correspond with the 'high' wave condition of the SWATH11 physical model tests described in reference (8).

4.63 Sectional Heave Force Amplitude Variations

Figures 4.8 show the variations of real and imaginary parts of heave force for sections number 3, 4, 5 and 6. Sections number 3 and number 4 are fully submerged whereas 5 and 6 are surface piercing. Forces corresponding to wave frequencies of 1.5 and 3.5 rads^{-1} are presented. For the sections where variations with water surface elevation are more significant, the exponential relationship discussed in section 3.21 can be seen.

4.64 Heave, Pitch and Wave Excitation Time Histories

Results for the analysis of SWATH11 with forward speeds of 0 and 0.5 ms^{-1} are presented in figures 4.9 for a range of wave frequencies between 1.5 to 5.5 rads^{-1} Time histories of heave displacement, pitch displacement, heave exciting force and pitch exciting moment are shown for each case. Variations in the complex force and moment amplitudes are also given These results correspond to a wave amplitude of 10 cm. Heave and pitch response amplitudes have been non-dimensionalised :

$$S_3^* = S_3 / a$$

$$S_5^* = S_5 / (a\omega^2)/g$$

and then plotted against non-dimensional wave frequency ,ω':

$$\omega^* = \omega / (g/L)^{0.5}$$

The effect the exponential ramp function can be clearly seen in the initial period of the wave excitation and the motion response records.

Figures 4.10 represent each forward speed case and show the time domain, non-linear wave excitation values plotted against the equivelent freqeuncy domain results which were used for validation purposes in Chapter 3.

4.7 Concluding Remarks

These results from the analysis of SWATH11 show that the non-linear wave excitation effects are detectable but are too small to significantly influence the motions of this particular design. Because of this , the test case has not provided a dramatic illustration of how non-linear wave excitation can influence ship motions behaviour. On the other hand, SWATH11 is suitable for validating the simulation method. Since previous analysis of SWATH11 has shown its motions to be approximately linear, any substantial deviations from the linear predictions would have been treated with suspicion.

As the results illustrate, this particular design does not experience the steady effects in heave or pitch motion displacements discussed in section 4.33. If any steady component were apparent its significance would depend on the extent of non-linearity. Time histories of wave excitation amplitudes in the heave and pitch modes which are given in figures 4.9 show that SWATH11 experiences almost linear excitation.

The magnitudes of the complex force amplitude fluctuations are very small. It is difficult to draw any conclusions about the harmonic components of wave excitation due to this fact. Some of the force amplitude time histories show components of lower frequency than that of the motions. This is an artificial effect due to the transient influence of the initial applied excitation. In time the system damping causes these low frequency oscillations to disappear.

Figures 4.8 Sectional Heave Force Variations - Real and Imaginary Parts

SWATH11 Section Nos. 3, 4, 5 and 6

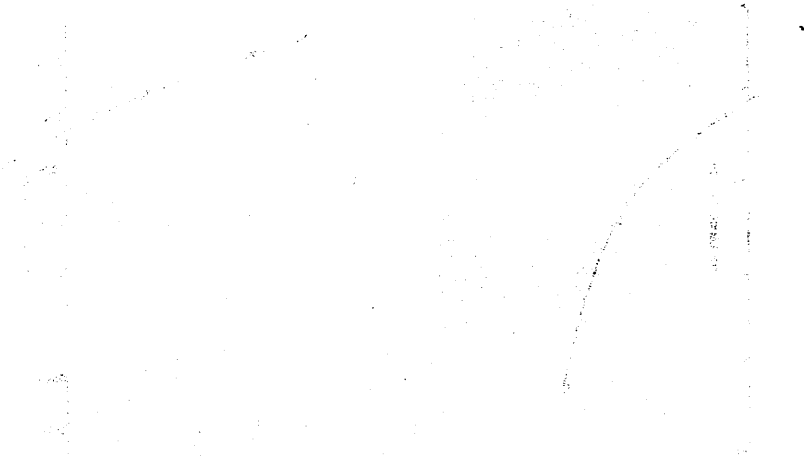

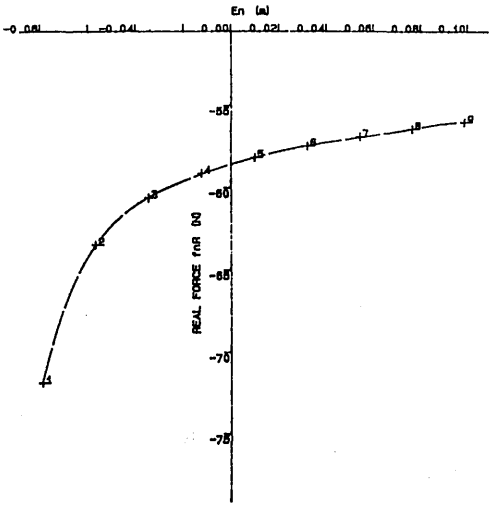

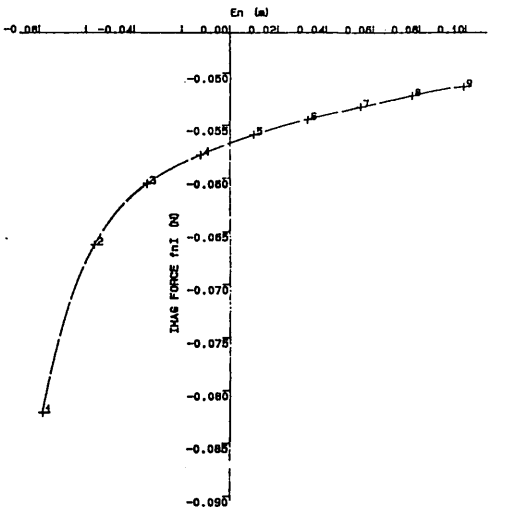

w = 1.5 rad/s

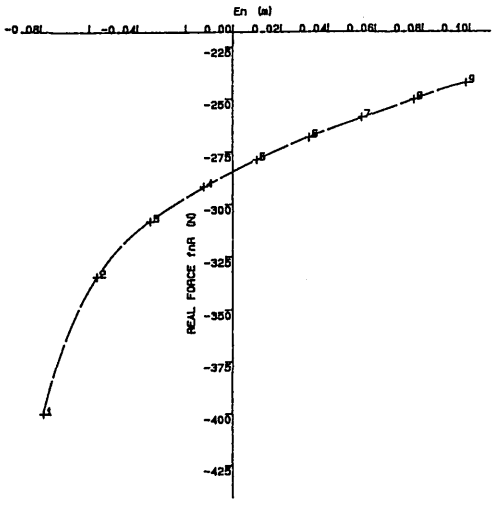

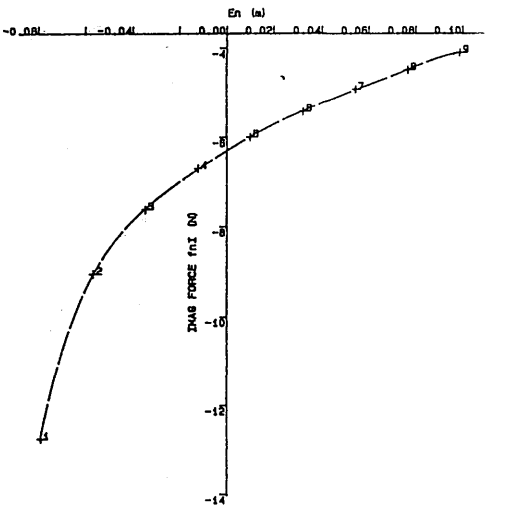

w = 3.5 rad/s

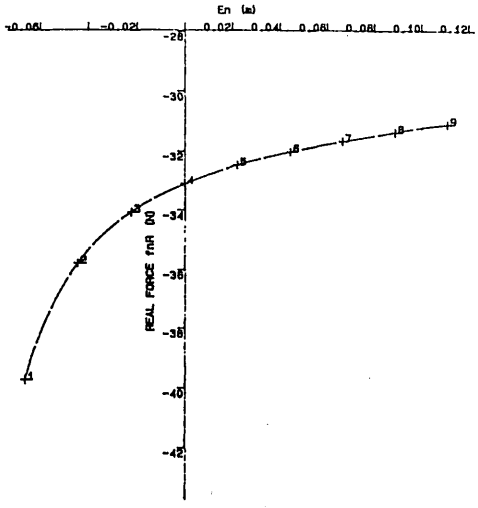

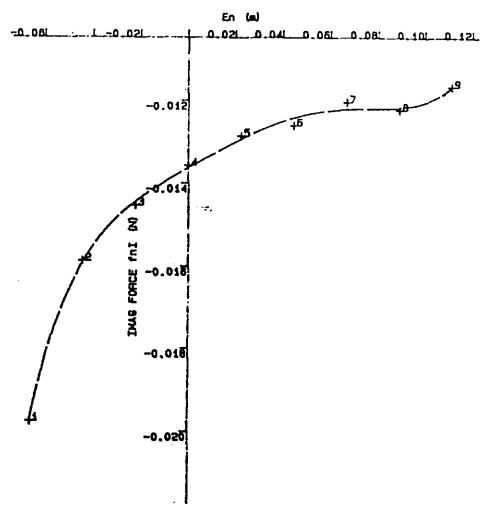

w = 1.5 rad/s

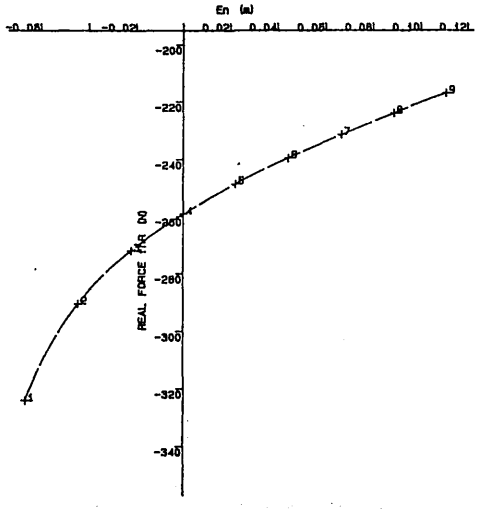

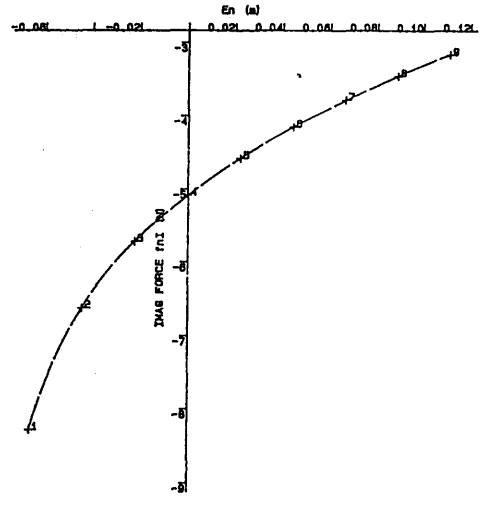

w = 3.5 rad/s

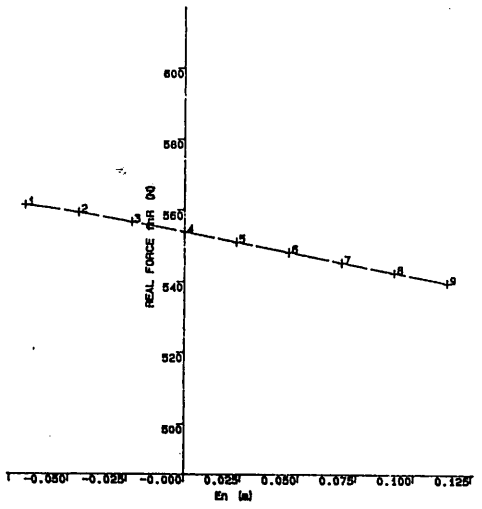

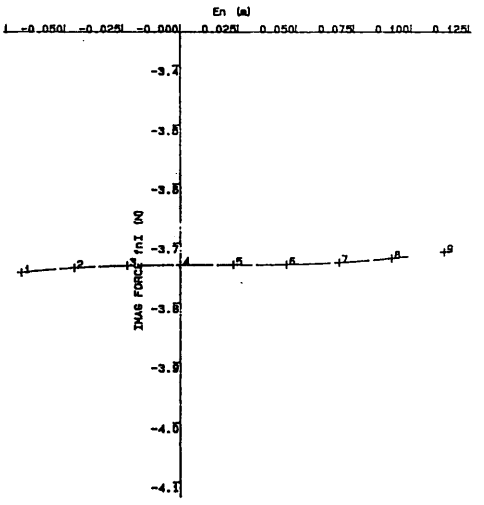

w = 1.5 rad/s

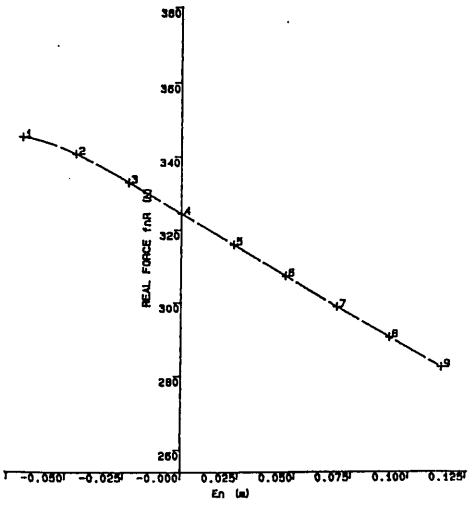

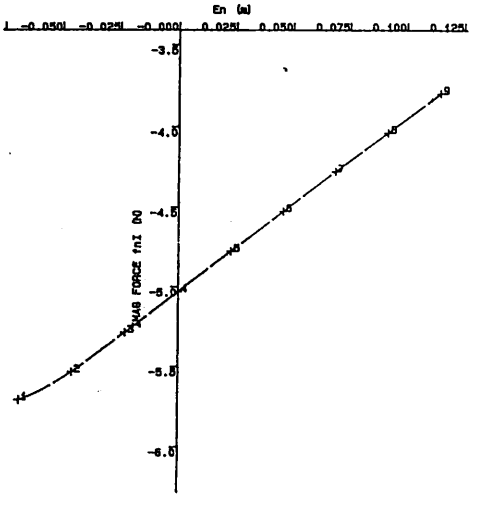

w = 3.5 rad/s

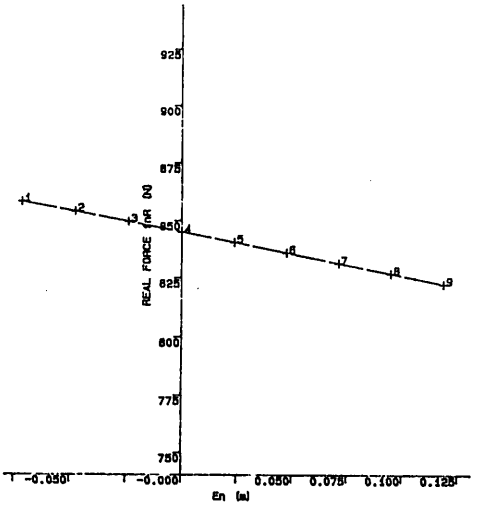

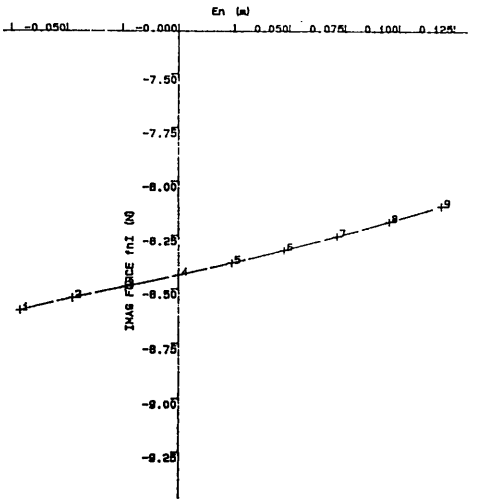

w=1.5 rad/s

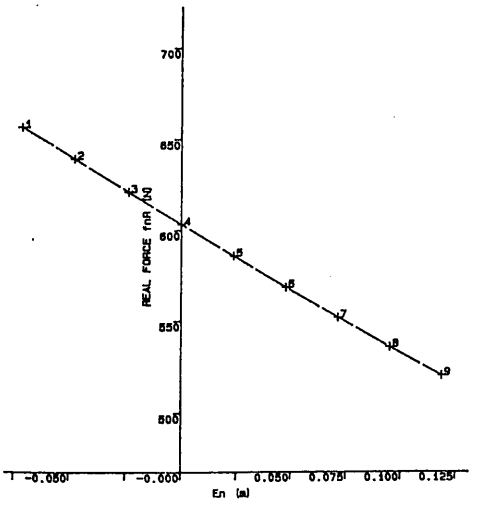

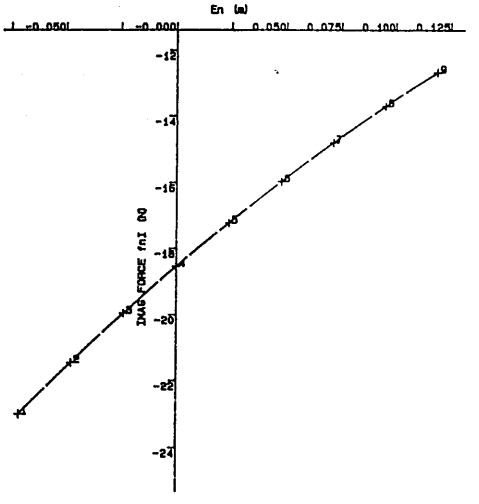

w = 3.5 rad/s

Figure 4.9 Time Domain Solutions with Non-Linear Wave Excitation

SWATH11, 0.0 and 0.5ms^{-1}

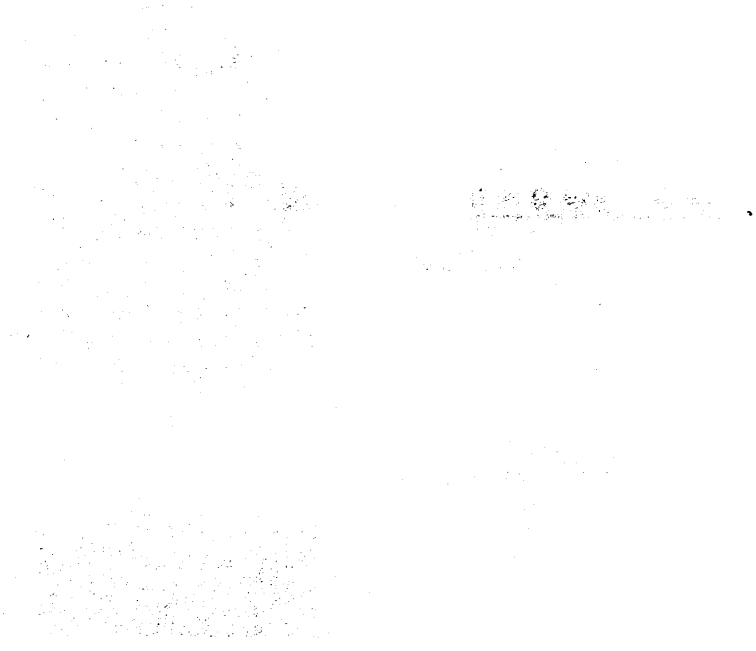

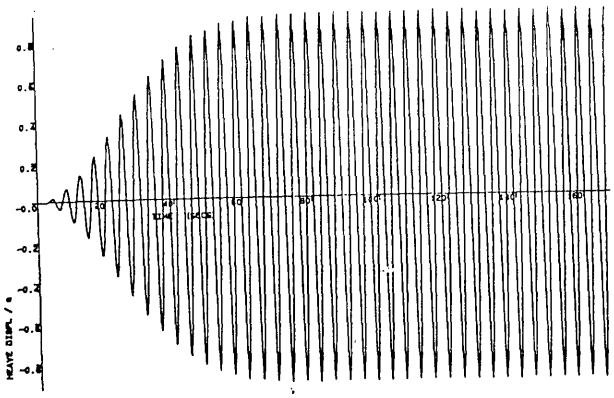

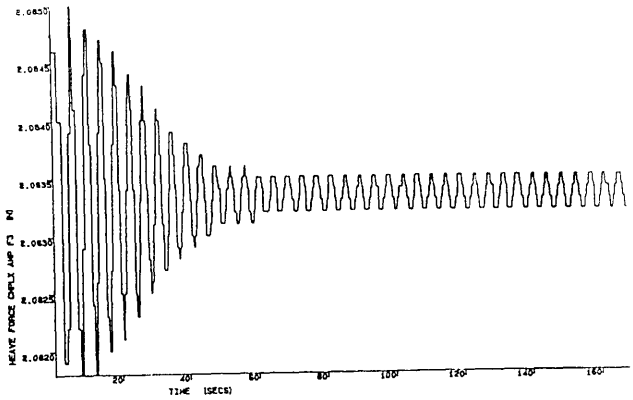

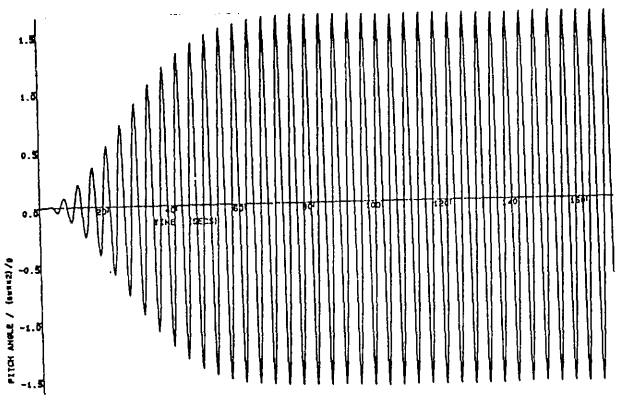

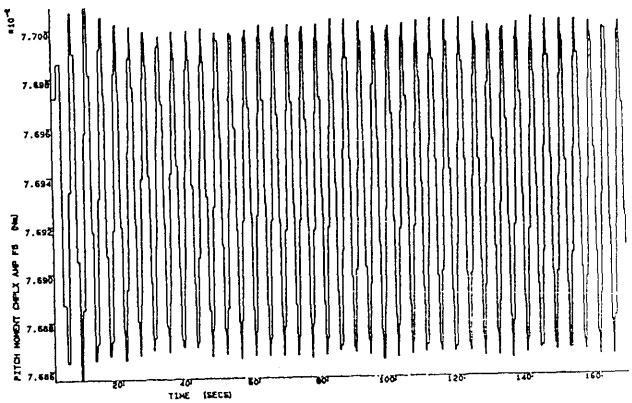

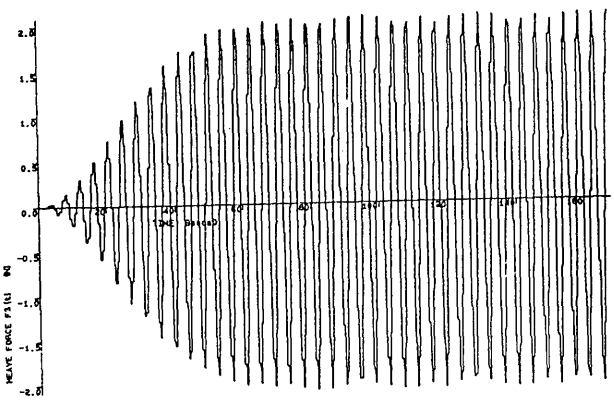

U = 0 m/s w =1.5 rad/s

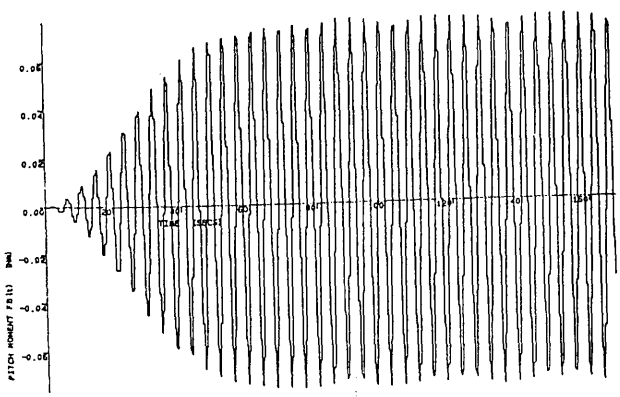

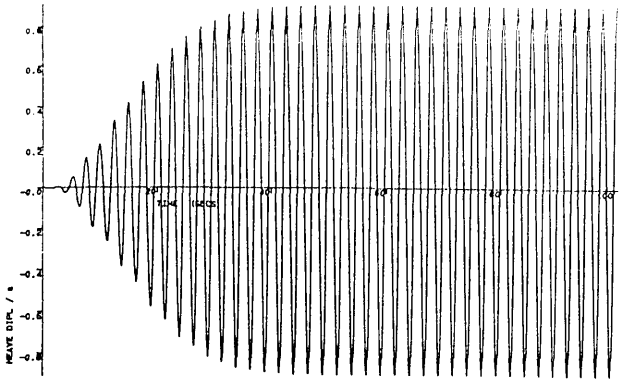

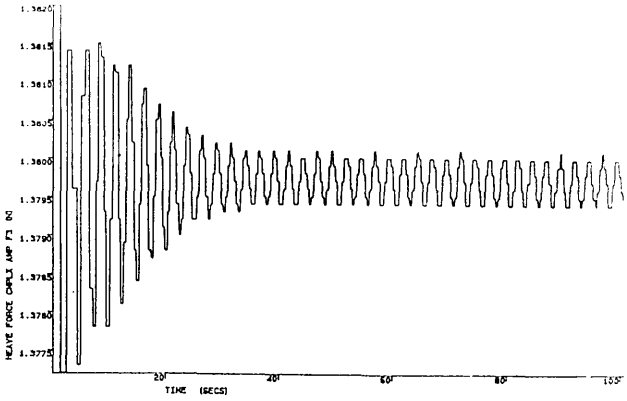

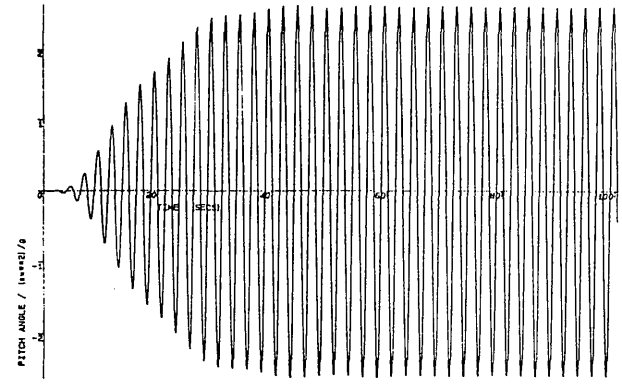

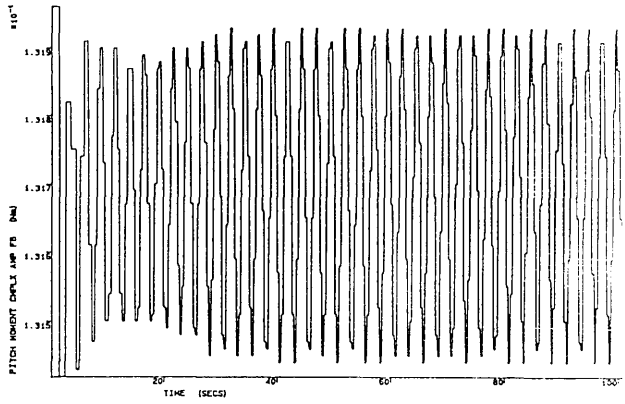

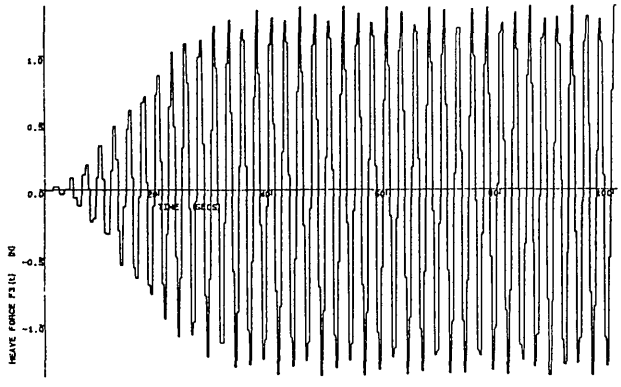

U = 0 m/s w = 2.5 rad/s

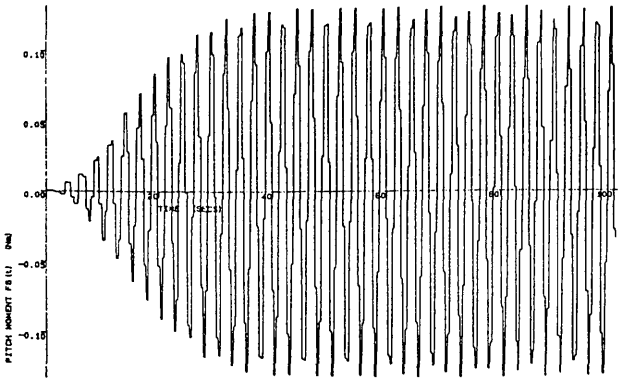

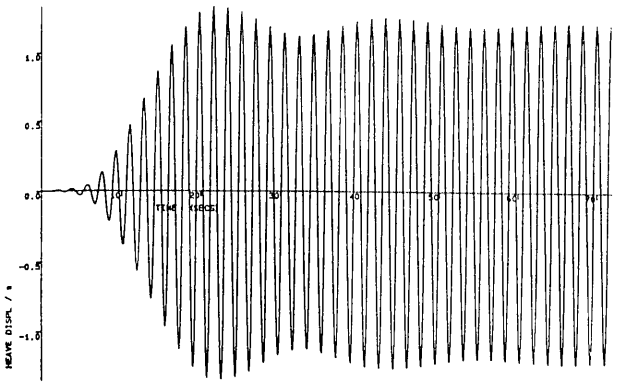

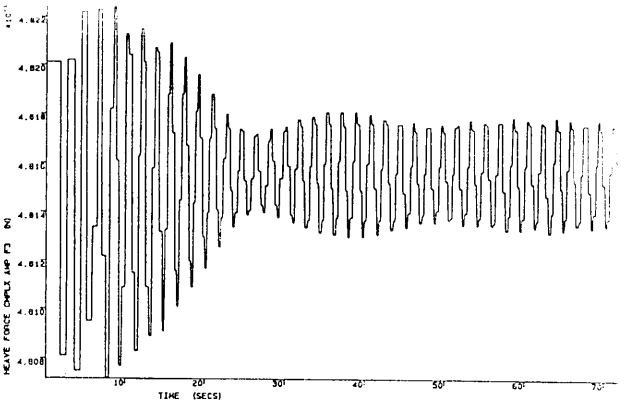

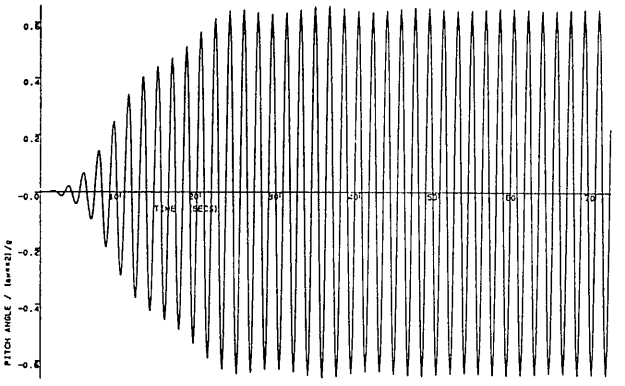

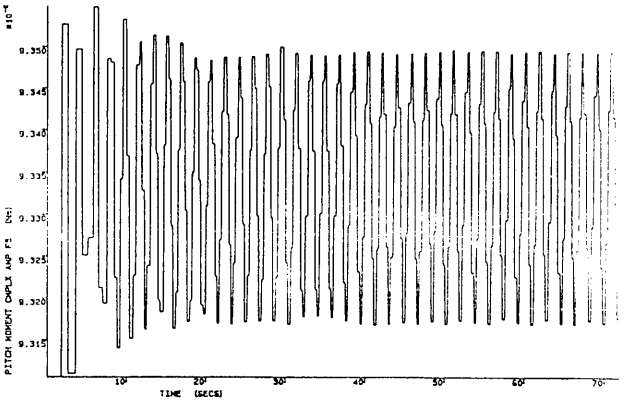

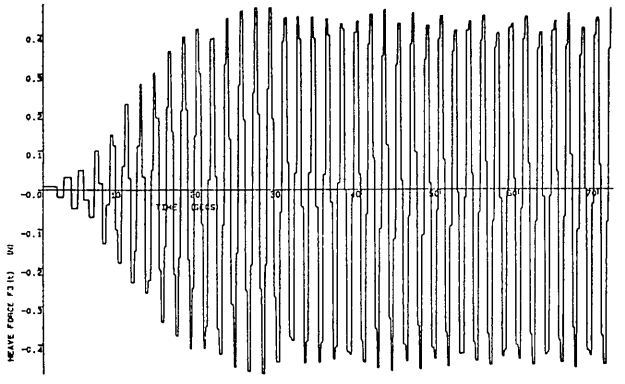

U = 0 m/s w = 3.5 Rad/s

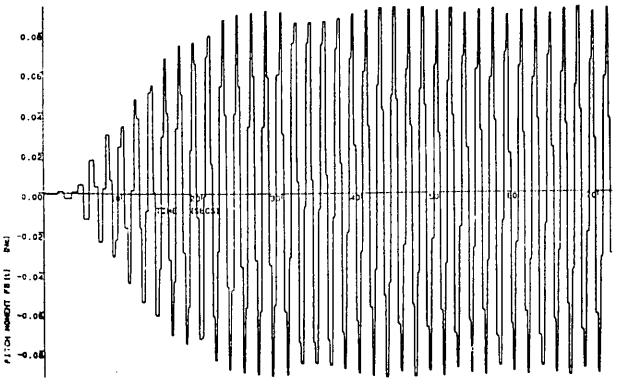

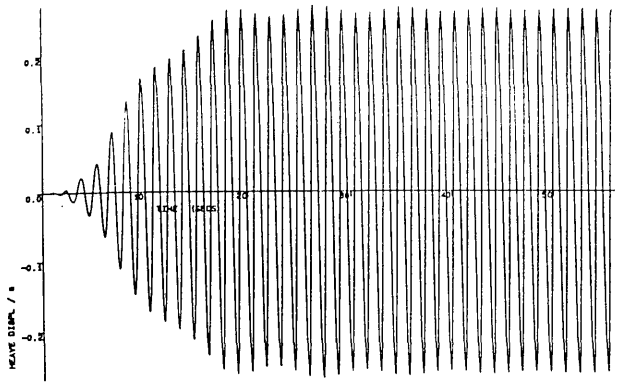

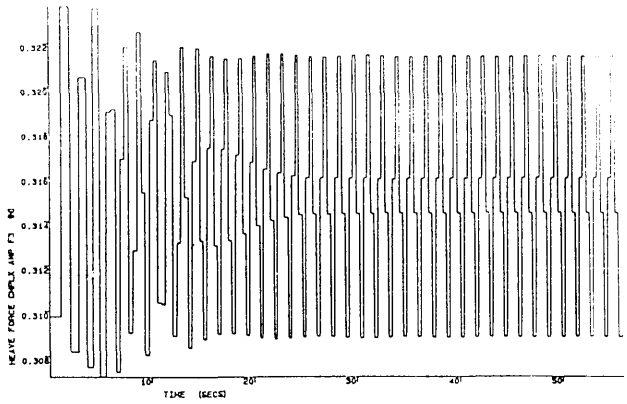

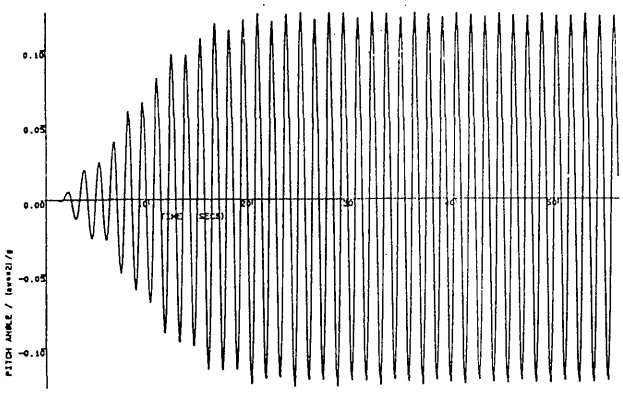

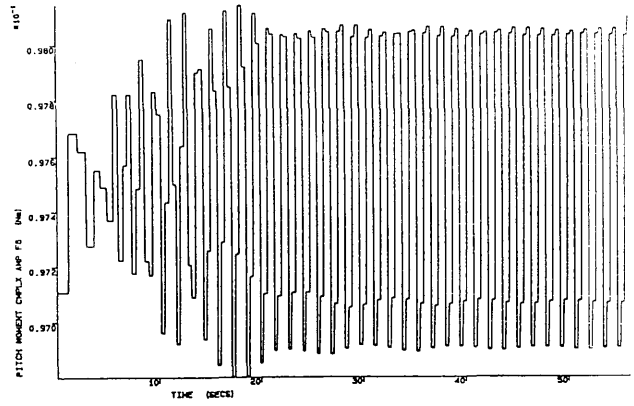

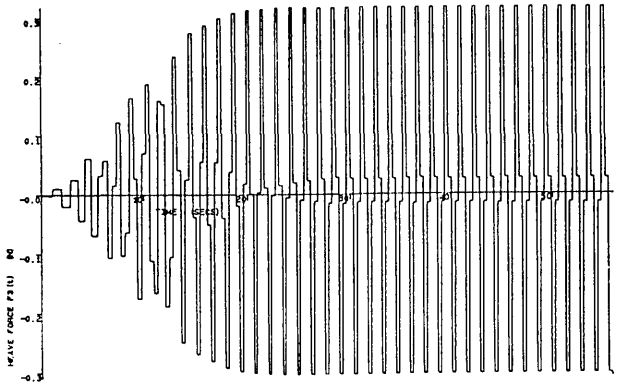

U = 0 m/s w = 4.5 rad/s

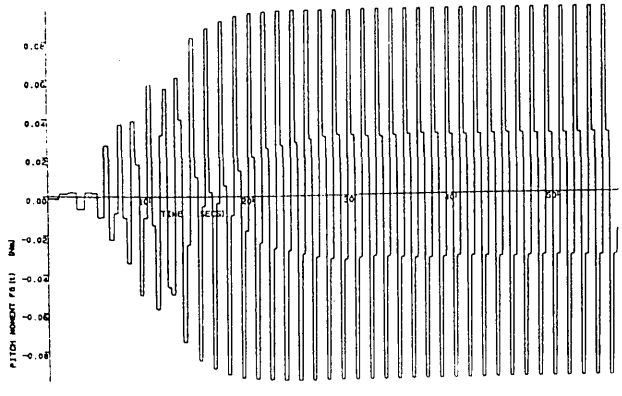

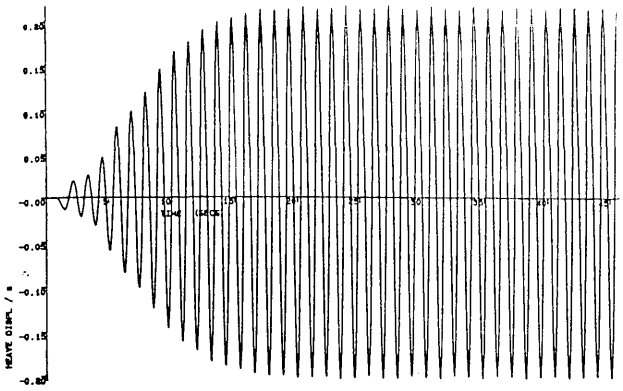

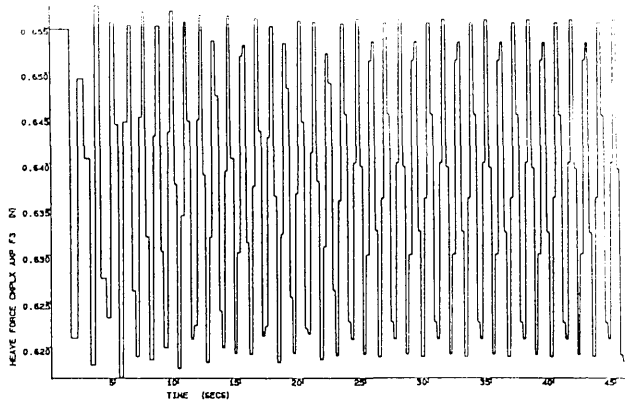

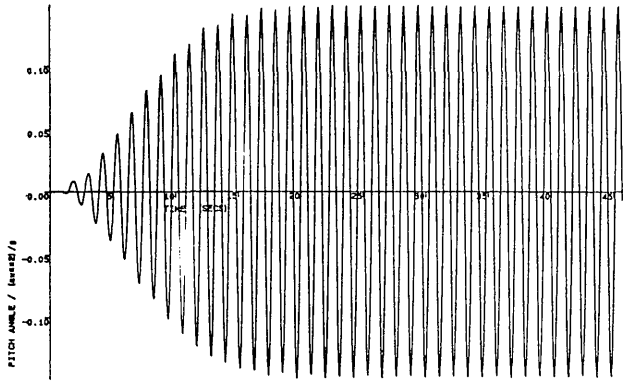

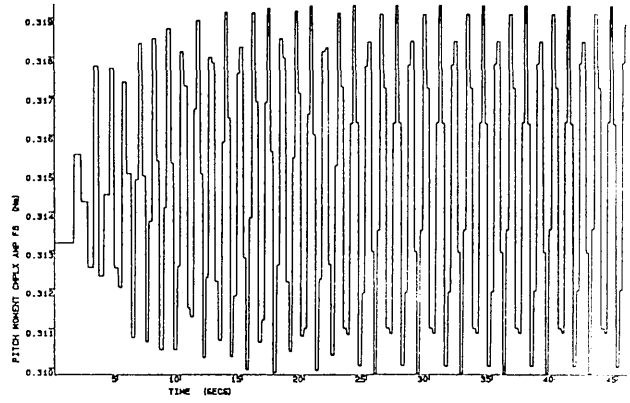

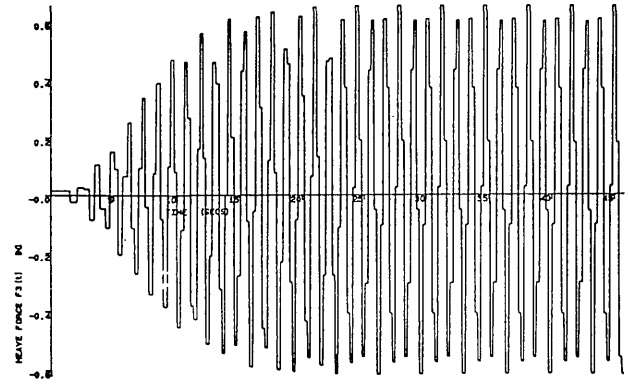

U = 0 m/s w = 5.5 rad/s

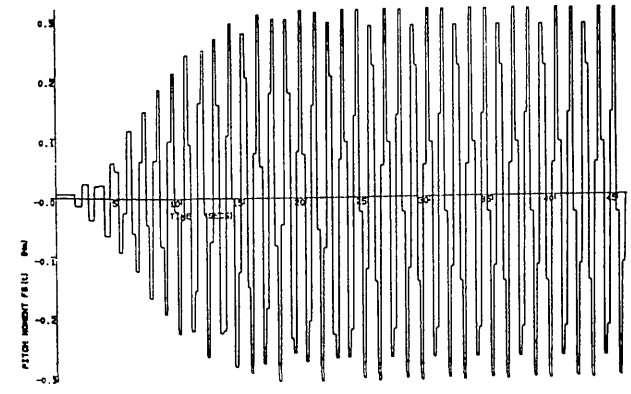

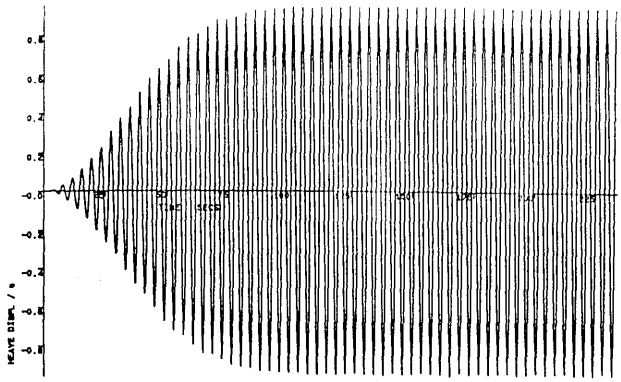
HEAVE DISPL / a
TIME (SECS)

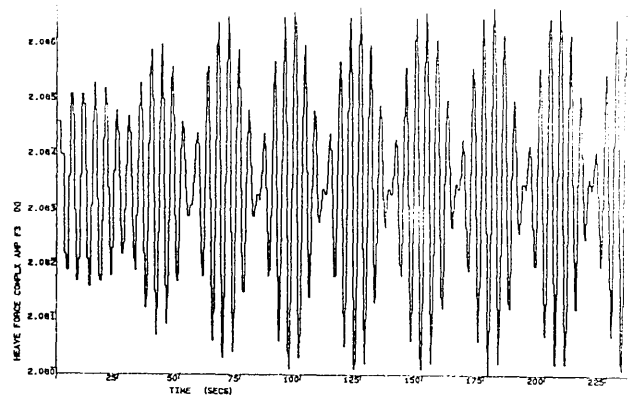
HEAVE FORCE COMPLX AMP F3 DO
TIME (SECS)

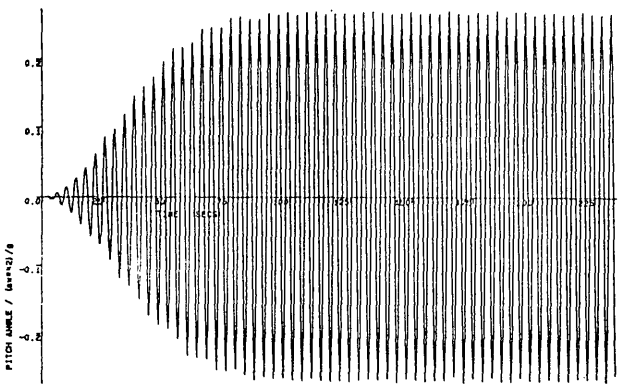
PITCH ANGLE / (ak**2)/a
TIME (SECS)

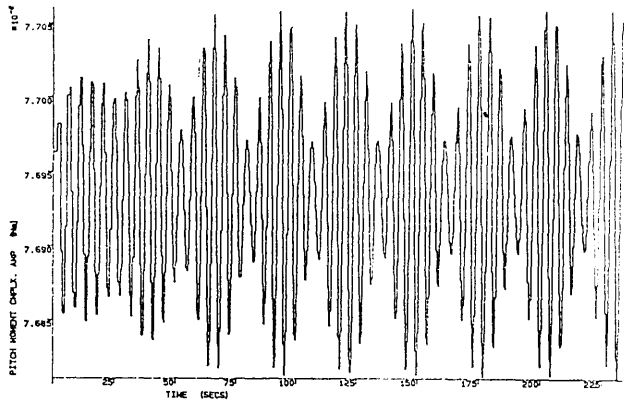
PITCH MOMENT CMPLX. AMP (Nm)
TIME (SECS)

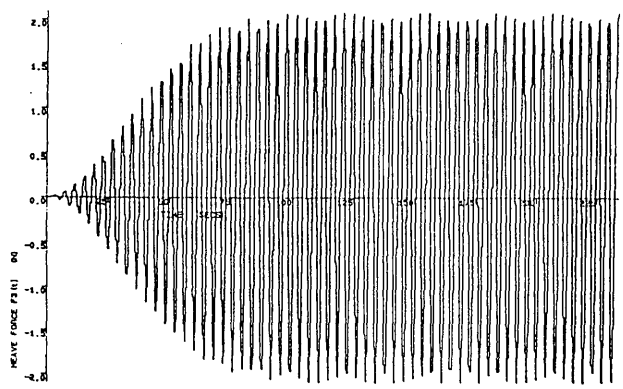
HEAVE FORCE F3(t) DO

U = 0.5 w = 1.5 rad/s

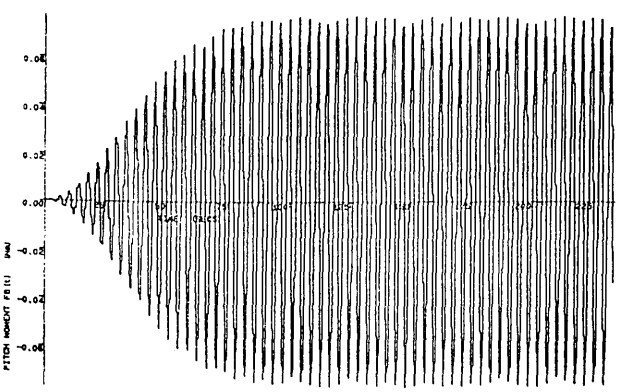
PITCH MOMENT F5(t) (Nm)

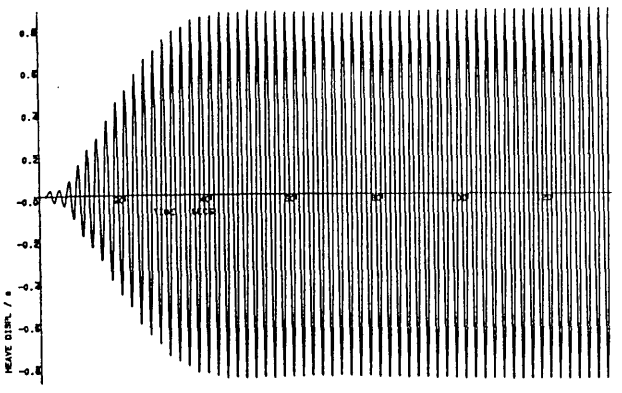

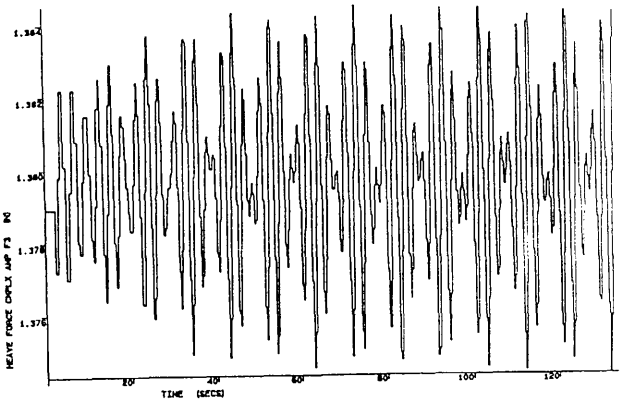

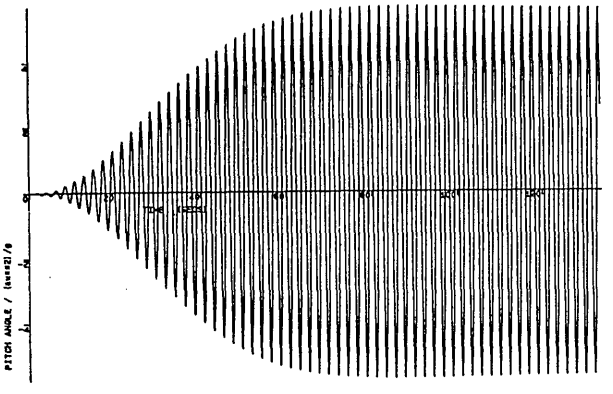

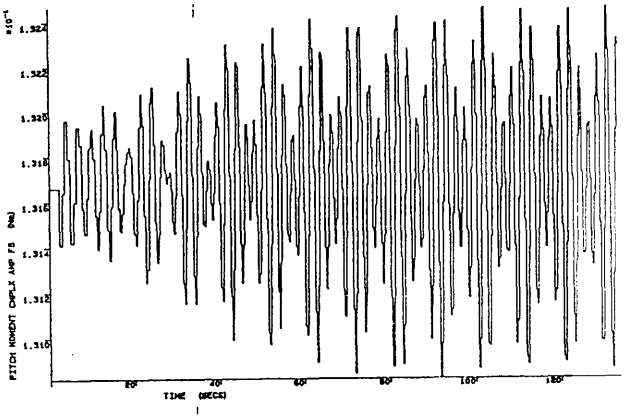

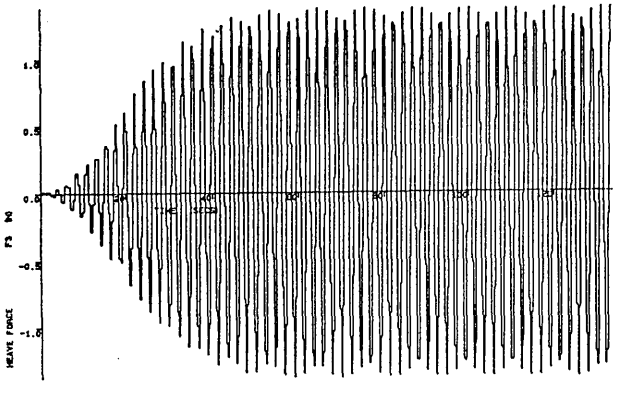

U = 0.5 m/s w = 2.5 rad/s

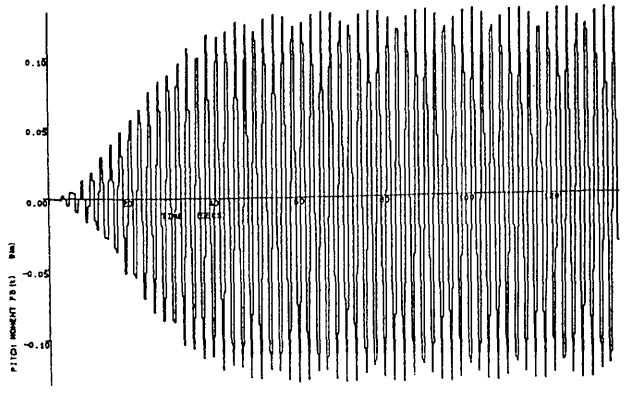

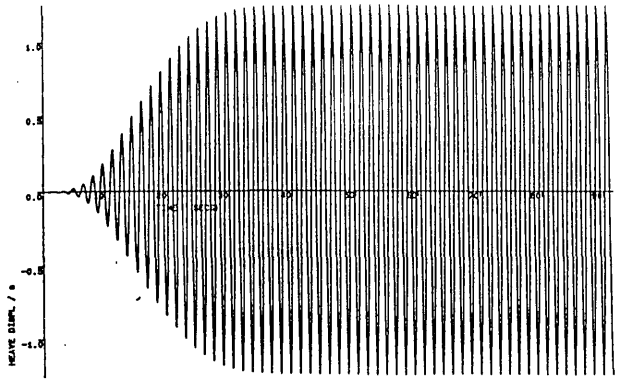

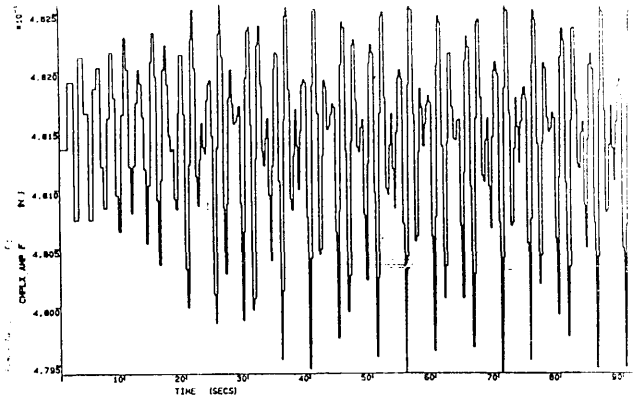

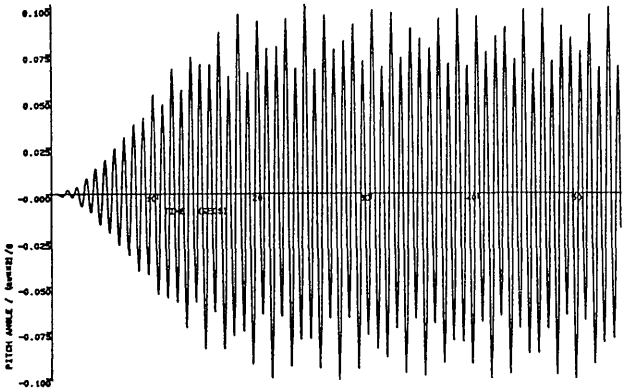

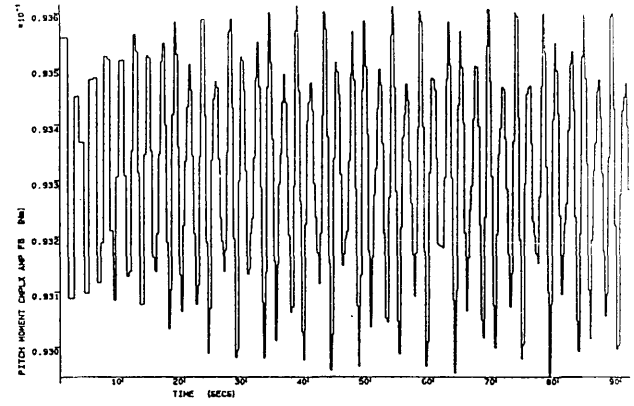

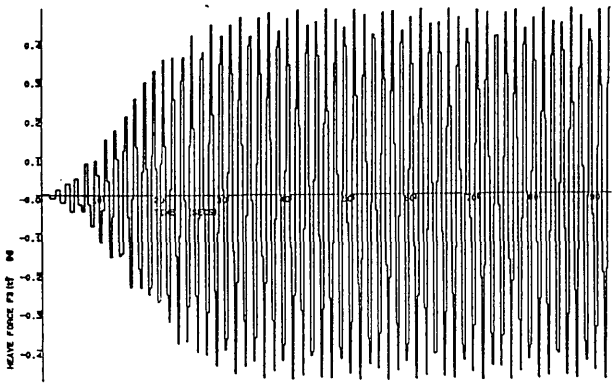

U = 0.5 m/s w = 3.5 rad/s

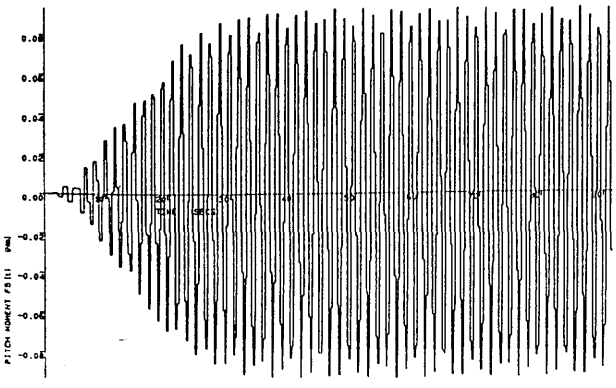

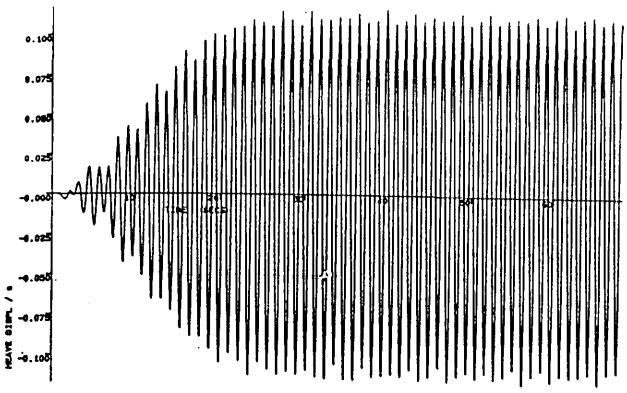

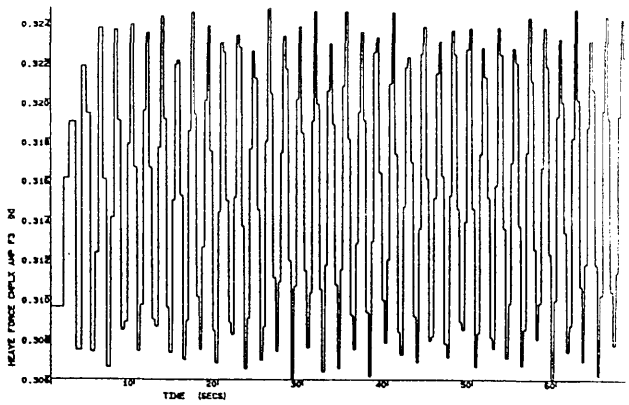

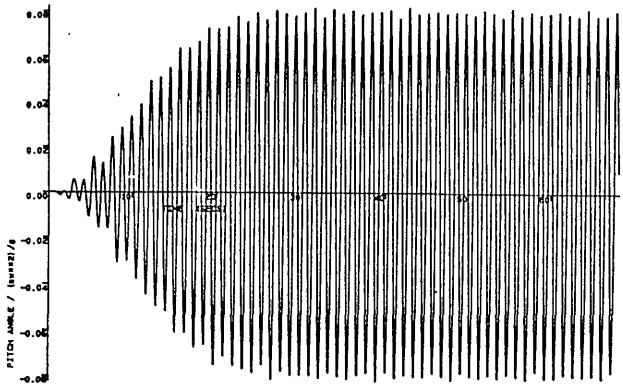

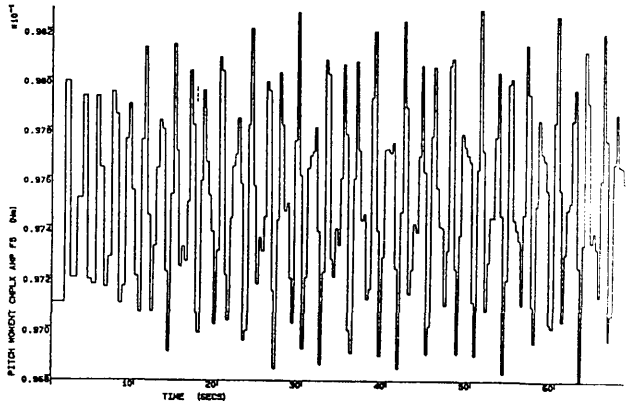

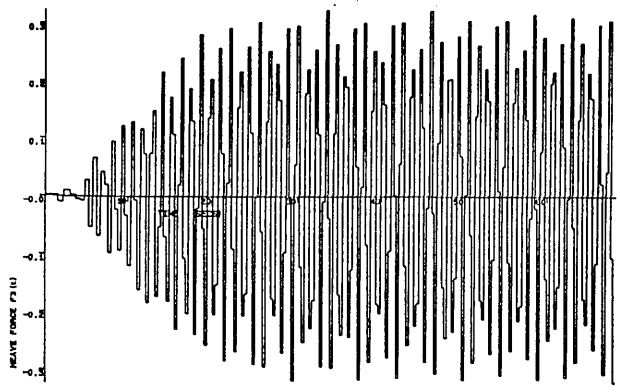

U = 0 m/s w = 4.5 rad/s

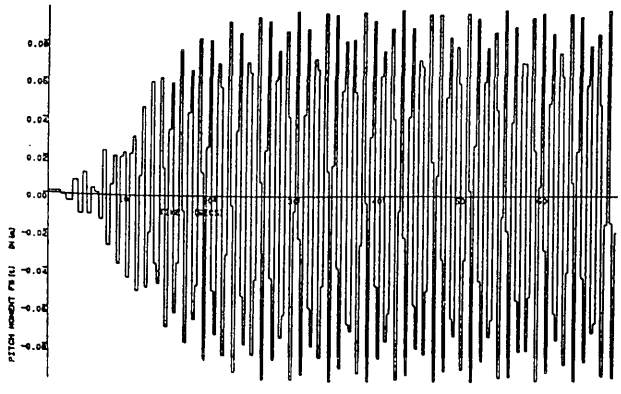

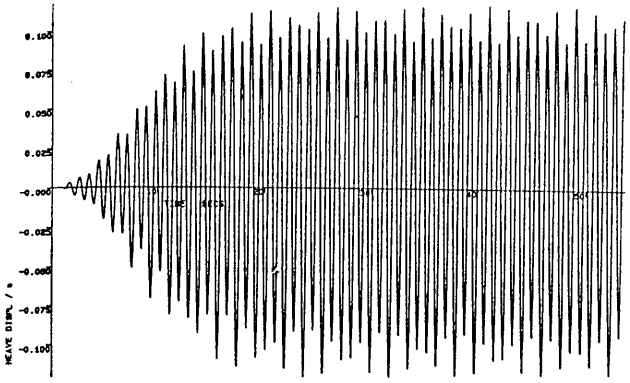

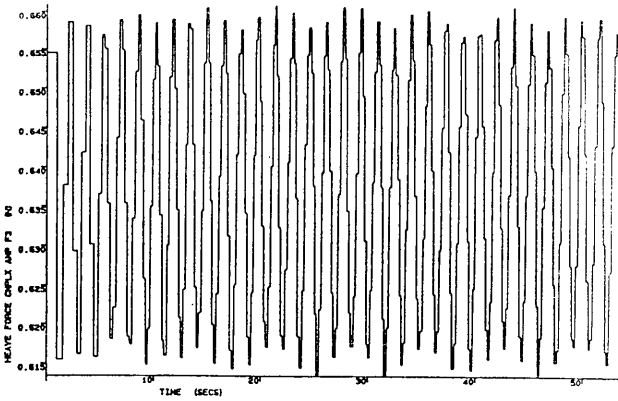

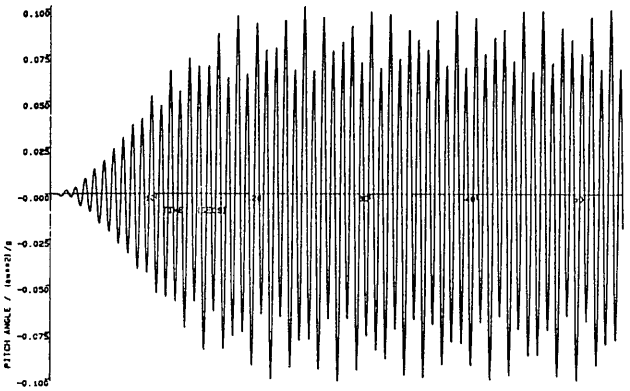

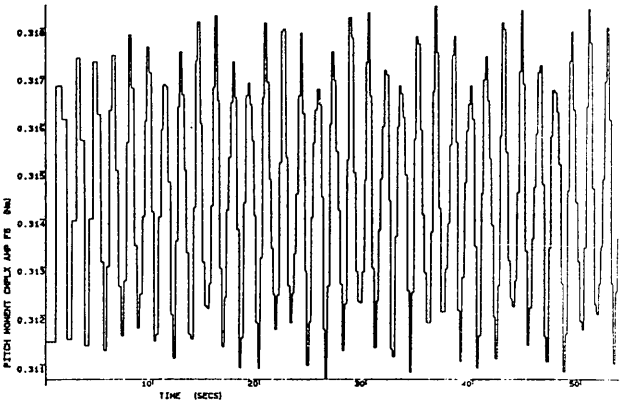

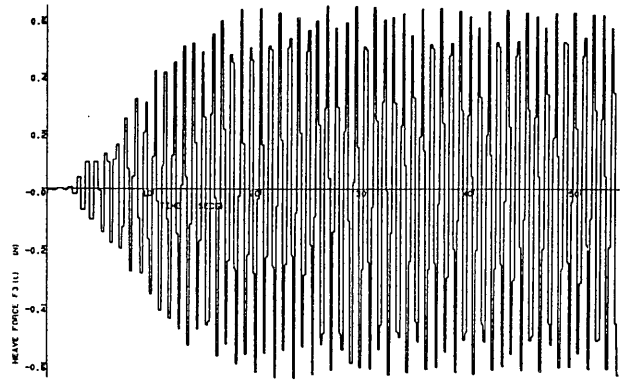

U = 0 m/s w = 5.5 rad/s

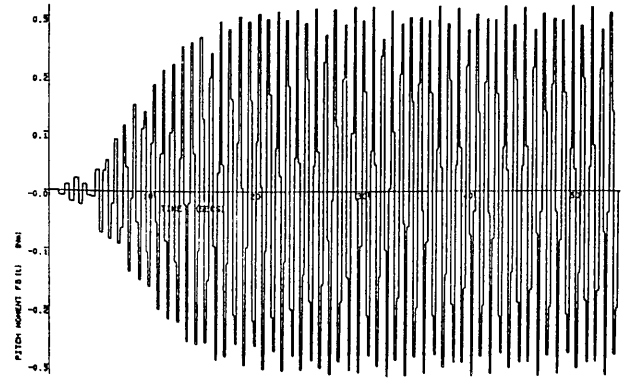

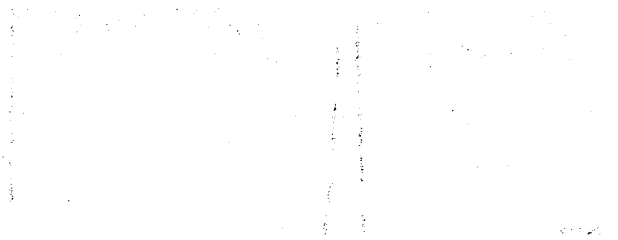

Figure 4.10 Time Domain Solutions (Non-Linear Wave Excitation) Compared with Frequency Domain Solutions

SWATH11, 0.0 and 0.5 ms^{-1}

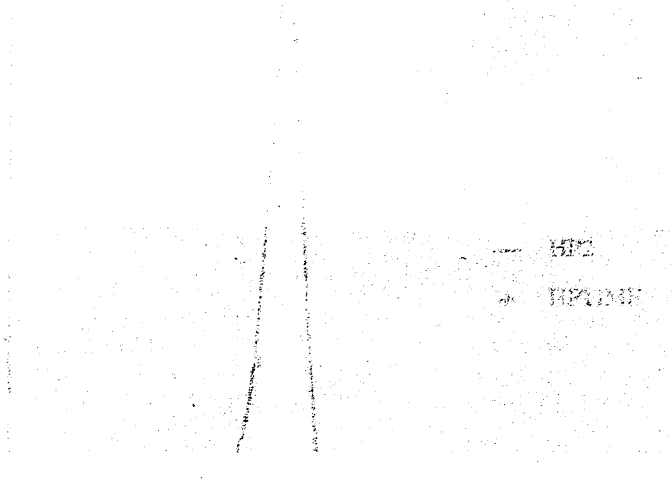

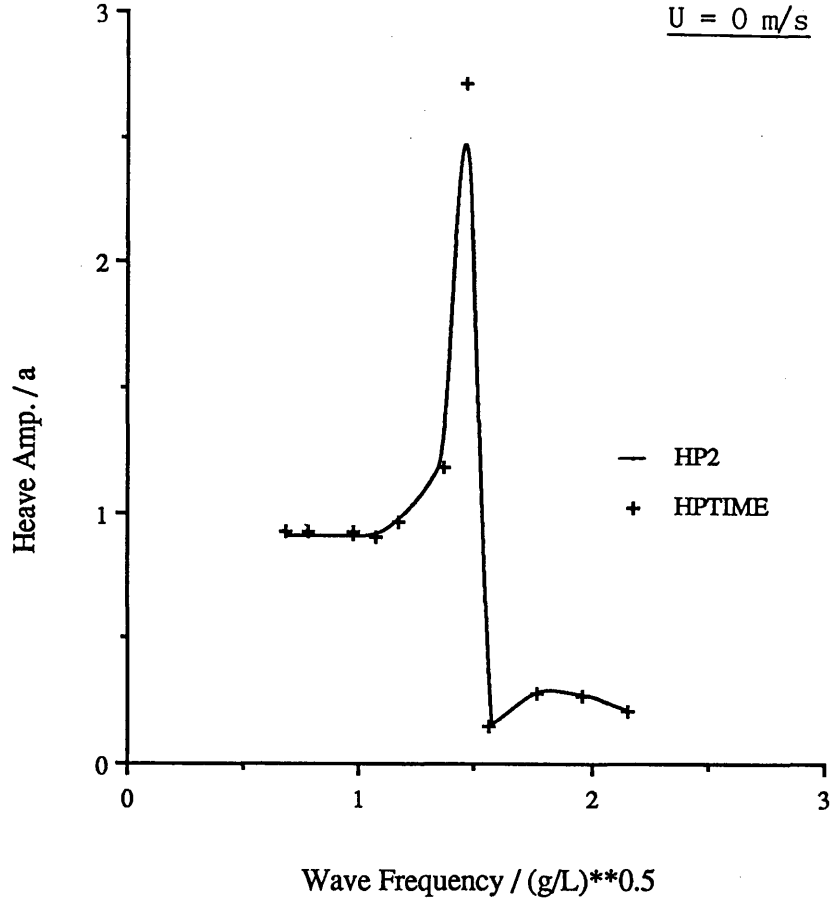
U = 0 m/s
Heave Amp. / a
Wave Frequency / (g/L)**0.5
HP2
HPTIME
0
1
2
3

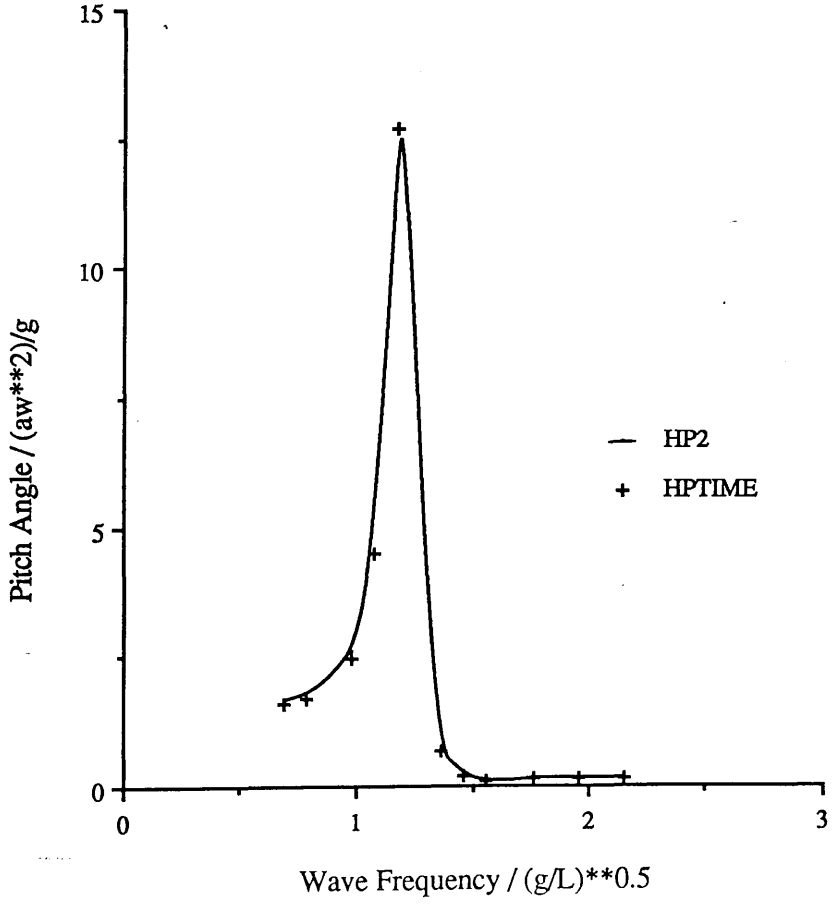
Pitch Angle / (aw**2)/g
Wave Frequency / (g/L)**0.5
HP2
HPTIME
0
5
10
15
0
1
2
3

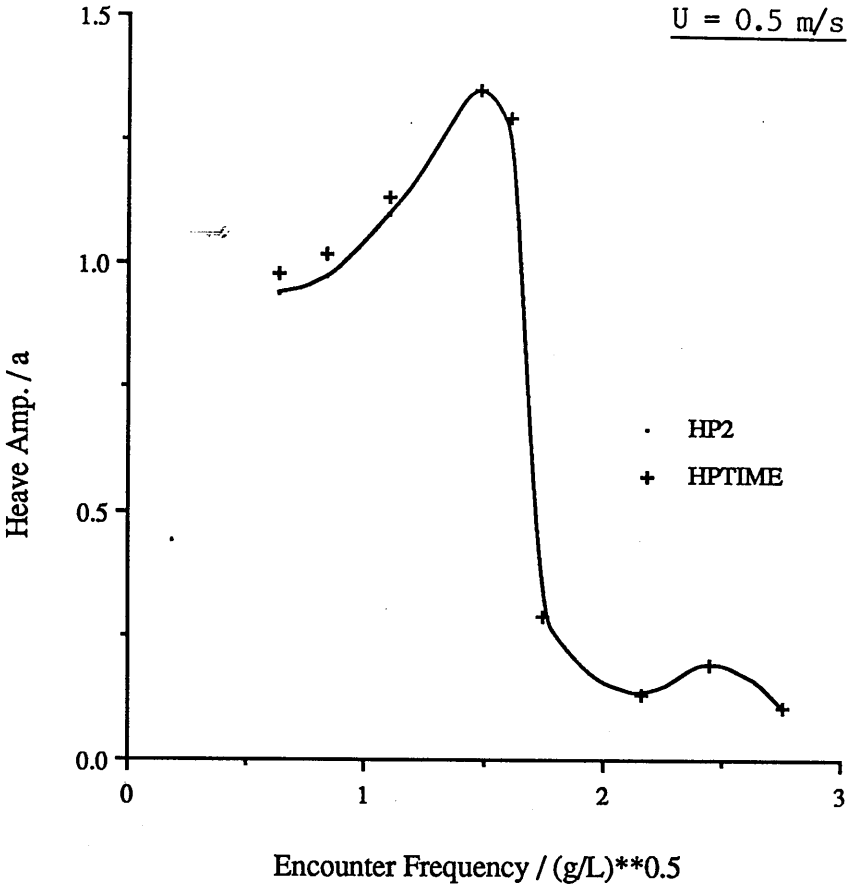
U = 0.5 m/s
Heave Amp. / a
1.5
1.0
0.5
0.0
0
1
2
3
HP2
HPTIME
Encounter Frequency / (g/L)**0.5

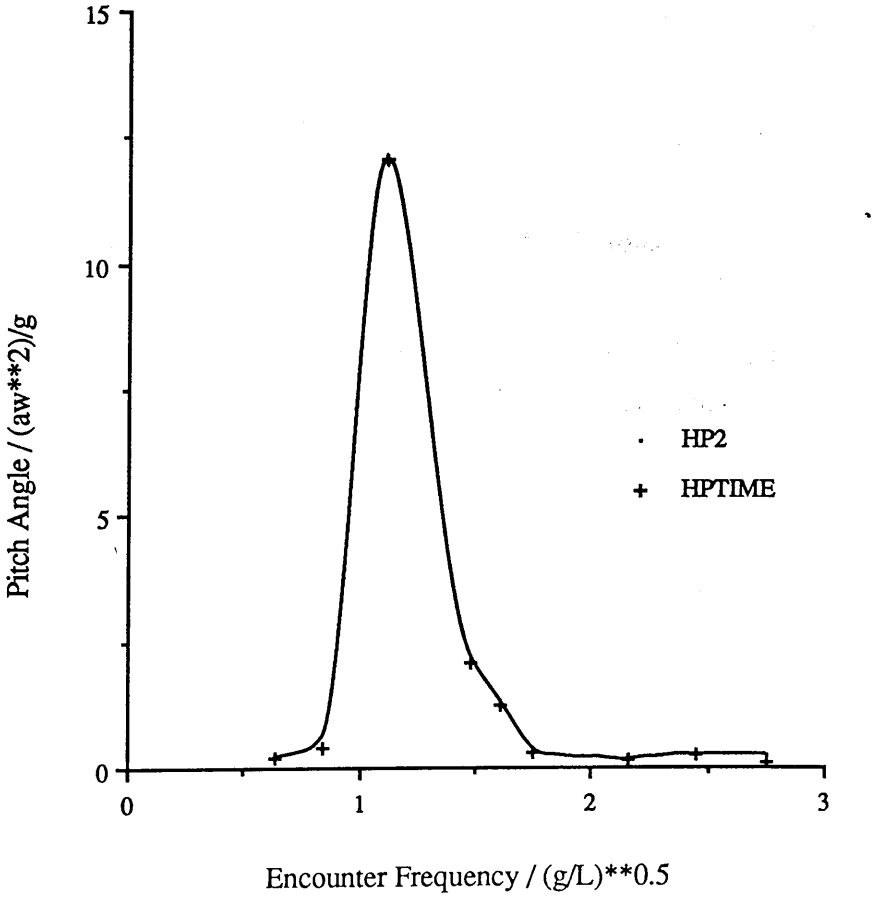
Pitch Angle / (aw**2)/g
15
10
5
0
0
1
2
3
HP2
HPTIME
Encounter Frequency / (g/L)**0.5

CHAPTER 5

NON-LINEAR ADDED MASS, DAMPING AND RESTORING

5.1 Introduction

Further non-linear effects due to the time dependencies of the coupled hydrodynamic and hydrostatic coefficients are assessed and introduced into the time domain model in this chapter. Added mass and damping coefficients are considered before restoring coefficients and methods for introducing the time dependencies of each are presented.Results obtained from the modified time domain computer program are given to illustrate how these additional non-linearities effect the heave and pitch motions of model SWATH11.

5.2 Added Mass and Damping Coefficient Variations

As explained in Chapter 2 the hydrodynamic coefficients of added mass and wave damping represent the fluid forces known as the radiation forces which are generated due to the vessels harmonic motions. These hydrodynamic forces are calculated using the same theoretical approach applied for calculating wave excitaion forces only under different assumed fluid boundary conditions. As a result, relationships with changes in submerged geometry similar to those seen for the wave excitation amplitudes are expected.

5.21 Harmonic Behaviour

Sectional heave added mass and damping values are expected to oscillate harmonically about mean values a_{33}^{m} and b_{33}^{m} with a frequency equal to the wave encounter frequency :

$$a_{33}(t) = a_{33}^{m} + a_{33}^{os}\, e^{-i\omega_e t}$$

$$b_{33}(t) = b_{33}^{m} + b_{33}^{os}\, e^{-i\omega_e t} \qquad (5.1)$$

The oscillatory components a_{33}^{os} and b_{33}^{os} are however expected to be small in amplitude. Indeed for low or even medium amplitude motion displacements, these variations may be difficult to detect.

5.22 Effect of Submergence Depth

Equation (2.37) is the expression for the sectional radiation potential from which resulting motion induced pressure and force are obtained. As the forces , which are given in (2.43), correspond to assumed unit motion velocity and acceleration they represent the strip section hydrodynamic coefficients. Equation (2.37) shows that the sectional added mass and damping coefficients are dependent on submergence depth.

Investigations previously carried out at the University of Glasgow Department of Naval Architecture and Ocean Engineering[43][44] have involved assessing variations in the hydrodynamic coefficients for a number of different hull sections. The predicted trends presented have been obtained by using computer programs which are based on the same Frank Close-fit technique applied in this study.

It has been found in these investigations that, for the fully submerged geometries assessed, at lower wave frequencies the effect of increasing sectional submergence depths is to decrease the added mass of inertia whereas at higher frequencies it increases with increasing depth. As the aspect ratio of the section, defined as B/D (where B is the section breadth and D, the section depth), increases, the wave

frequency at which this behaviour changes decreases. Sectional damping coefficients were found to vary cosiderably with the frequency of motion oscillation and were also found to be influenced significantly by free surface effects. Results suggest that damping effects on fully submerged sections practically disapppear at submergence depths beyond two and a half times the section depth.

In general, these studies show that within the range between zero, at the free surface, and a depth of two and a half times the section depth, variations in sectional hydrodynamic coefficients are apparent.

5.3 Solution Procedure with Non-linear Hydrodynamic Coefficients

An efficient method for modifying the added mass and damping coefficients to represent the vessels changing instantaneous hydrodynamic condition is required.

The importance of reducing the number of calculations performed during the motions solution procedure has been stressed. To avoid applying the computationally lengthy Frank Close-fit technique directly, added mass and damping coefficient variations are introduced into the simulation by using the same approach adopted in Chapter 4 for the wave excitation amplitudes. This involves generating a data base of sectional values and curve fitting polynomial relationships.

Each hull section is analysed in turn. Water surface elevation values E_n are varied over a suitable range and added mass and damping coefficients for each of the corresponding submerged geometries are calculated. By using a curve fitting routine, polynomial expressions of the form :

$$a_n = c_{a1} + c_{a2}E_n + c_{a3}E_n^2 + \ldots$$

and (5.2)

$$b_n = c_{b1} + c_{b2}E_n + c_{b3}E_n^2 + \ldots$$

which relate sectional added mass and damping coefficients with E_n, can be obtained.

Section 4.4 describes how the instantaneous submerged geometry,which is related to motion displacements and wave travel, can be defined in terms of the sectional water surface elevation values. At each time step of the simulation therefore, by inserting the values of E_n into the expressions (5.2), sectional hydrodynamic coefficient values are obtained.

Integration of the sectional coefficients along the vessel length yields total values of coupled added mass and damping coefficients for the whole vessel. Corrections required due to the effects of forward speed are given in equations (2.44). These are applied and the final hydrodynamic coefficients for that instantaneous vessel condition are inserted into the motion equation which are subsequently solved. Heave and pitch solutions obtained together with the modified encountered wave profile represent the conditions for the next time step at $t + dt$. The procedure is repeated for this and subsequent time steps until steady state motion solutions are obtained.

5.4 Non-Linear Restoring Effects

An inherent assumption of linear, frequency domain , ship motion prediction techniques is that restoring characteristics are linear and the coefficients employed correspond to the at rest, still water condition of the craft. Indeed for vessels experiencing small amplitude motions about their mean position and for wall sided craft undergoing larger amplitude motions, this assumption provides a good approximation. It has been shown in previous studies(51 to 56) however that the hydrostatic forces and moments become non-linear for larger amplitude motions. The combined effects of wave shape and dimensions and the vessels' oscillatory motions can produce considerable changes in restoring characteristics.

Variations in restoring characteristics depend on motion related changes in water plane shape . The rates of change of water plane area govern the extent of the restoring non-linearities. For small amplitude motions, the vessel's waterplane area is assumed to be constant which implies that changes in displacement are linear .

For a thorough investigation of more extreme motions and wave loads, variations in the rates of change of displacement cannot be ignored . The method employed to account for non-linear hydrostatic characteristics, involves re-calculating restoring forces and moments at each simulation time step.

5.41 Steady Motion Offset

Vessels designed with flared hull sections, will experience more significant non-linear hydrostatic effects. The extent of these effects will depend on the degree of flare and its distribution along the hull length and over its depth. As motion responses increase the flared part of hull sections effect the hydrostatics for a greater part of the motion cycle and, combined with the longitudinal asymmetry of flare distribution, can cause steady offsets in heave and pitch motion displacements.

Angular motions are normally more sesitive to this non-linear effect. In the cases of vessels with wall sided sections, changes in water-plane area are small and motion offsets will be negligible. Only when experiencing very large motions where sections of haunch become immersed will SWATH vessels demonstrate any steady motion displacement which are induced by non-linear hydrostatic effects.

5.5 Solution Procedure with Non-Linear Restoring

Heave restoring forces and pitch restoring moments can be determined from the instantaneous vessel displacement and LCB position. At each time step, cross sectional areas and area moments which correspond to the vessel's instantaneous submerged geometry can be integrated along the vessel length to obtain values for displacement and LCB.

As described earlier the time dependent submerged geometry is defined by the sectional water surface elevation values, E_n.

Calculating areas of cross-section from design offset data during the solution

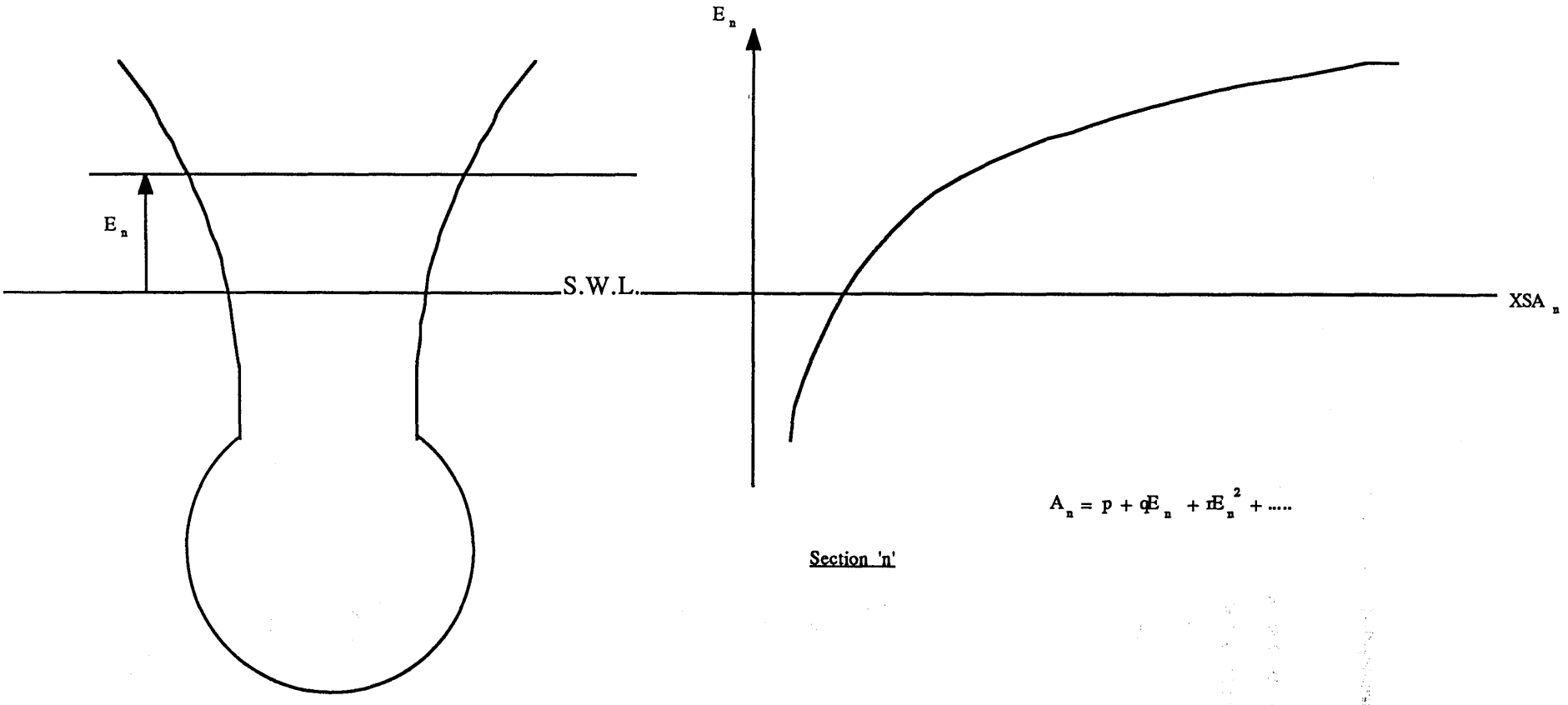

Figure 5.1 Cross Sectional Area Polynomials

procedure would represent a time consuming task for the NAg subroutine used in the simulation. Pre-determined section area polynomial relationships are therefore used to avoid this problem computational burden

Figure 5.1 illustrates how expressions relating cross-section area, A_n with water surface elevation are obtained. A_n values are calculated for a range of E_n values over the strut depth. A curve-fitting routine which will account for any sudden changes in section shape is then applied to give relationships of the form :

$$A_n = p + q\,E_n + r\,E_n^2 + ... \tag{5.3}$$

A_n is constant and independent of E_n for hull sections which do not penetrate the water surface.

During the solution procedure, known values of E_n and equations (5.3) are used to obtain section area values. Together with their moments about the body axis origin, these are integrated along the hull length to yield values for the vessel's displacement and LCB position.

Corresponding heave restoring forces and pitch restoring moments can then be obtained as follows :

$$\begin{aligned} \text{REST 3} &= (\nabla_V(t).\rho - M_{33})\,g \\ \text{REST 5} &= \text{REST 3}\,.\,\text{LCB}(t) \end{aligned} \tag{5.4}$$

these values are inserted into the coupled motion equations :

$$\begin{aligned} (M_{33}+A_{33})\ddot{S}_3(t)+B_{33}\dot{S}_3(t)+A_{35}\ddot{S}_5(t)+B_{35}\dot{S}_5(t) + \text{REST 3} &= F'_3\,e^{-i\omega_e t} \\ (I_{55}+A_{55})\ddot{S}_5(t)+B_{55}\dot{S}_5(t)+A_{53}\ddot{S}_3(t)+B_{53}\dot{S}_3(t) + \text{REST 5} &= F'_5\,e^{-i\omega_e t} \end{aligned} \tag{5.5}$$

which are reduced to their first order differential form and solved.

5.6 Computations with Non-linear Hydrodynamic Coefficients

This Section describes how the time domain computer program has been modified to include non-linear wave excitation effects. This main program structure has been maintained and additional non-linear effects have been introduced by incorporating additional subroutines.

Using the new program, non-linear added mass and damping effects on the coupled heave and pitch motions of model SWATH11 in high anplitude waves have been assessed.

5.61 Structure of Computer Routine

Two new subroutines named SECADM and TOTADM have been written to account for hydrodynamic coefficient Variations.The flow chart shown in figure 5.2 shows how the new routines feature in the main program.

There are no changes to the input data requirements of the command file which activates the main program. An option for the inclusion of non-linear restoring effects will activate the call to subroutine DATABASE. A return to the main program will result if added mass and damping polynomial expressions have been previously calculated.

Subroutines SECMOD and BURAK2 are used to modify the geometry data according to a range of E_n values and to calculate the corresponding added mass and damping coefficients for each section. In the same manner applied for the sectional wave forces, polynomial curves are fitted to section data by the subroutine FITTER. Results are displayed via screen graphics and polynomial coefficints are stored for use in the solution procedure.

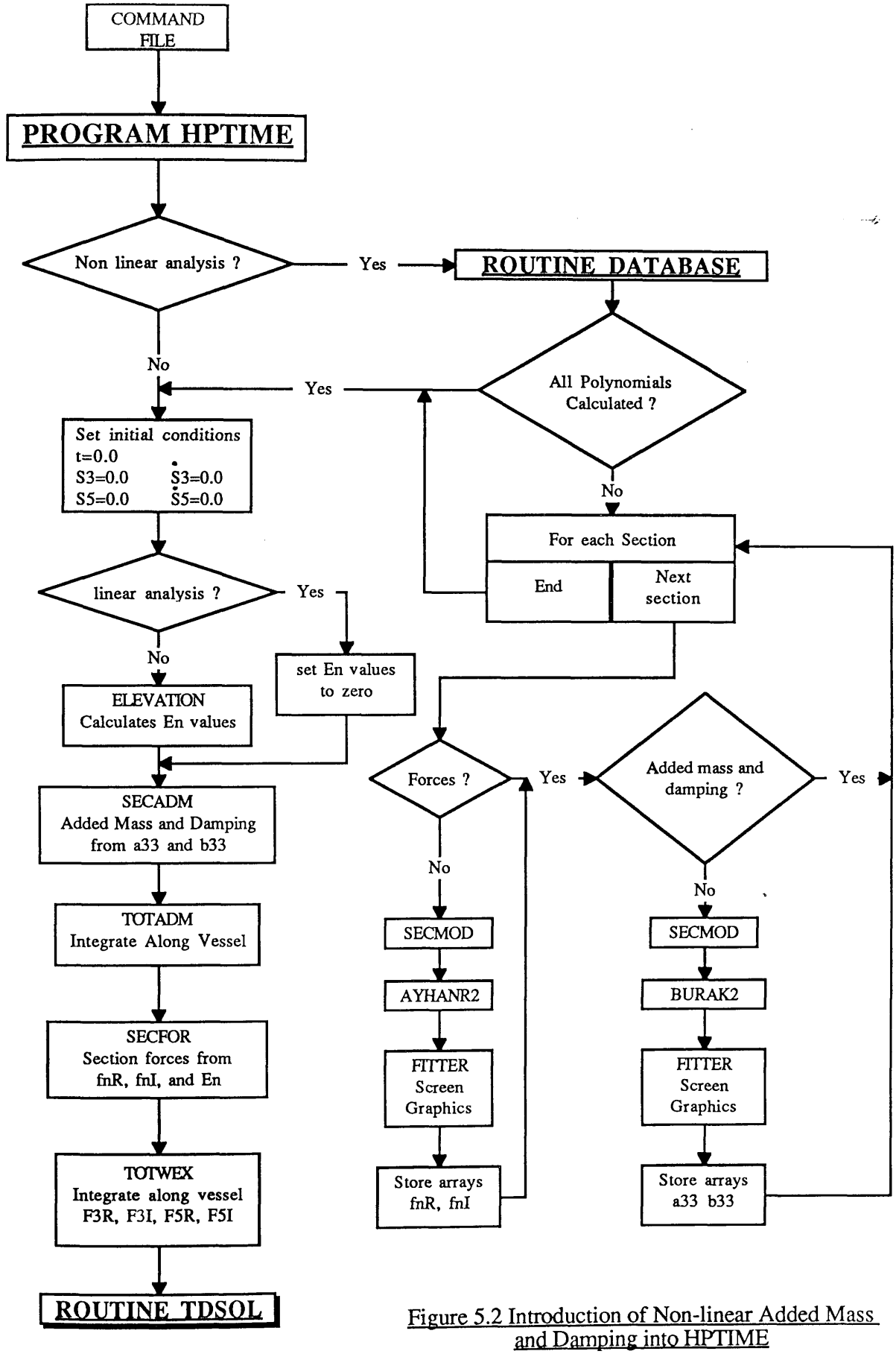

Figure 5.2 Introduction of Non-linear Added Mass and Damping into HPTIME

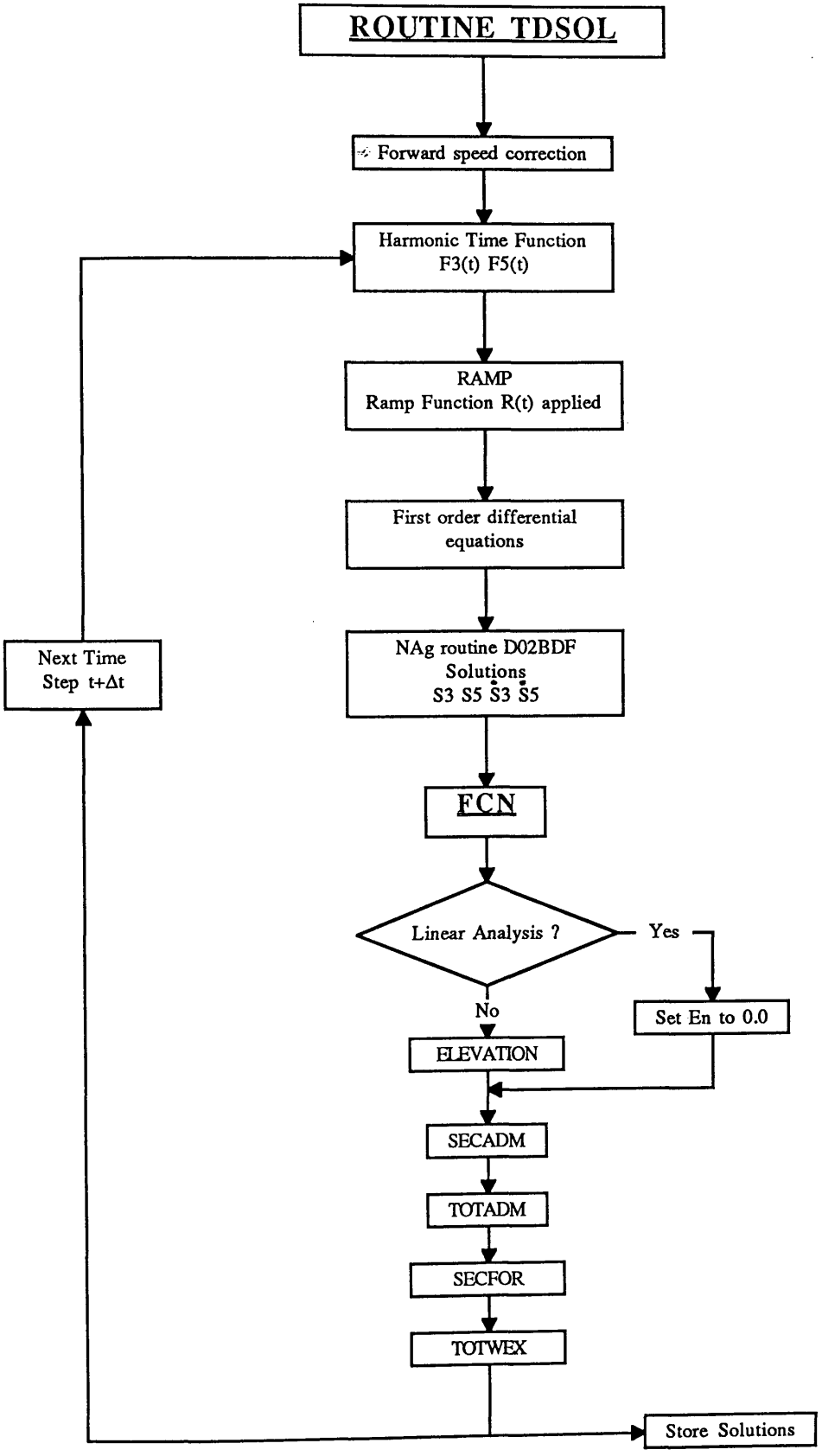

Figure 5.2 (Cont..)

After the return to the main program, initial conditions of the simulation are set and the first time step E_n values are calculated. SECADM applies the sectional polynomial coefficients and produces corresponding added mass and damping values. These values are integrated along the hull length in the subroutineTOTADM which yields total added mass and damping coefficients for the whole vessel.

Forward speed corrections are applied to the hydrodynamic coefficients at the beginning of the solution cycle master routine TDSOL. Ramp functions are applied to the wave exctiation forces and moments . These values together with the hydrodynamic coefficients and the linear hydrostatic coefficients are installed into the first order differential equations of motion which are subsequently solved.

As before, conditions for the next time step are determined from the subroutine FCN. By using the motion solutions and the modified wave profile E_n values are calculated in ELEVATION. Corresponding sectional added mass and damping coefficients are calculated in SECADM which are then integrated along the hull length in TOTADM to give total values for the whole vessel.

The solution procedure is repeated for subsequent time steps until steady state heave and pitch oscillations are obtained.

Figure 5.2 shows that it is possible to run the program to simulate non-linear wave excitation and non-linear added mass and damping conditions simultaneously. Indeed the the structure of the program is such, that in theory , any modifications to the vessels condition can be made at each time step. However, this facility is restricted by computer capacity. Running the program with combinations of non-linear effects is discussed in Chapter 6.

5.62 Analysis of SWATH11

Analysis of model SWATH11 was carried out for a range of wave frequencies between 1.5 and 5.5 $rads^{-1}$. The results presented correspond to a high amplitude wave of 10 cm and are given for the forward speed cases of zero and 0.5 ms^{-1}

5.63 Sectional Coefficient Variations

Figures 5.3 show curve fittied sectional added mass and damping data which are plotted against a range of water surface elevation, E_{n}., values over a range between plus and minus the pontoon hull top side draught. Plots for SWATH11 hull sections 3, 4, 5 and 6 are given for wave frequencies of 1.5, 3.5 and 5.5 rads^{-1}. Attention should be drawn to the small effect that submergence depth has on the sectional hydrodynamic coefficients

5.64 Heave, Pitch and Hydrodynamic Coefficient Time Histories.

Figures 5.4 give the time histories of heave and pitch displacement predictions obtained for SWATH11 over a range of wave frequencies for forward speeds of 0 and 0.5 ms^{-1} . Linear wave excitation corresponding to the force and moment amplitudes of the mean still water geometry has been applied. The exponential ramp function given in equation (3.17) is in effect for the first half of each record. Motion displacements and wave frequencies are non-dimensionalised as described in section 4.64.

Records of in the added mass and damping coefficients A_{33}, B_{33}, A_{55},and B_{55} (pure heave and pure pitch respectively) are given for each case.

The non-dimensionalised amplitudes of motion displacement have been compared with predictions obtained using the equivalent frequency domain linear analysis computer program HP2. Figures 5.5 show the comparisons over the range of model scale wave frequecies between 1.5 and 5.5 rads^{-1}.

5.65 Concluding Remarks

These results show that added mass and damping variations throughout a steady motion cycle are very small. Their minimal non-linear behaviour is seen to have negligible effect on the heave and pitch behavior of SWATH11.

The test exercise has provided confirmation that the technique described above is suitable for introducing some non-linear hydrodynamic restoring effects into SWATH motions simulation.

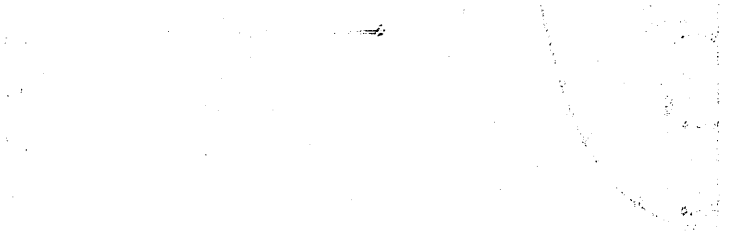

Figures 5.3 Sectional Added Mass and Damping Relationships

SWATH11 Section Nos. 3, 4, 5 and 6

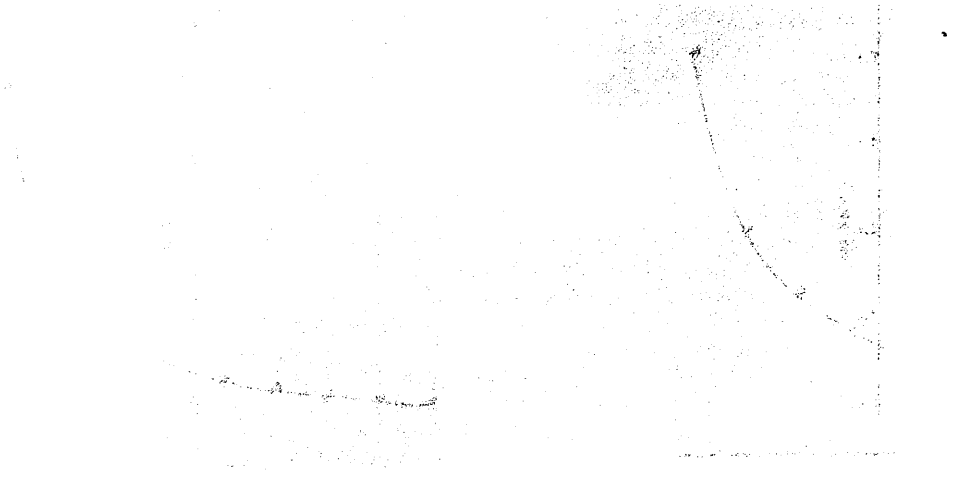

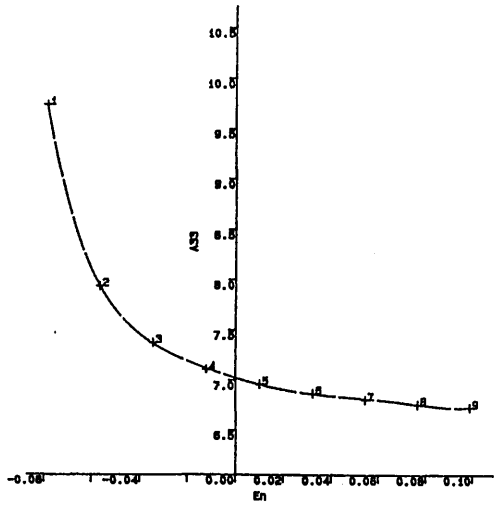

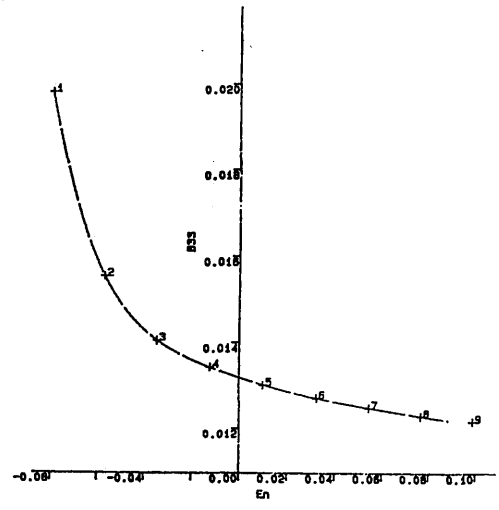

w = 1.5 rad/s

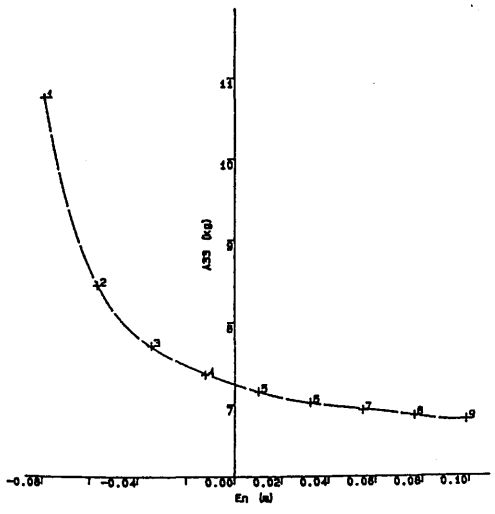

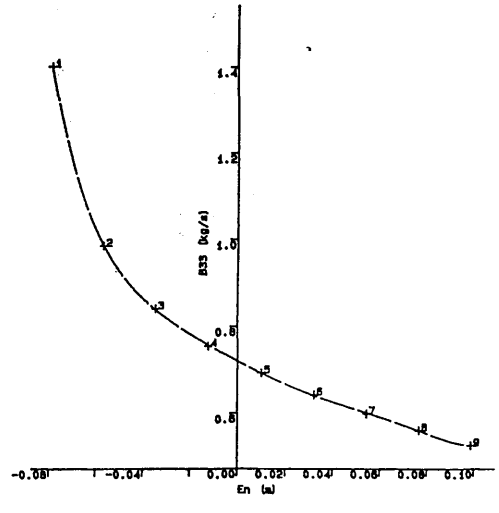

w = 3.5 rad/s

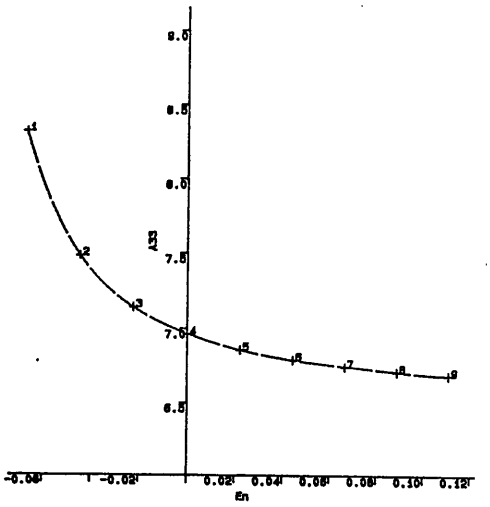

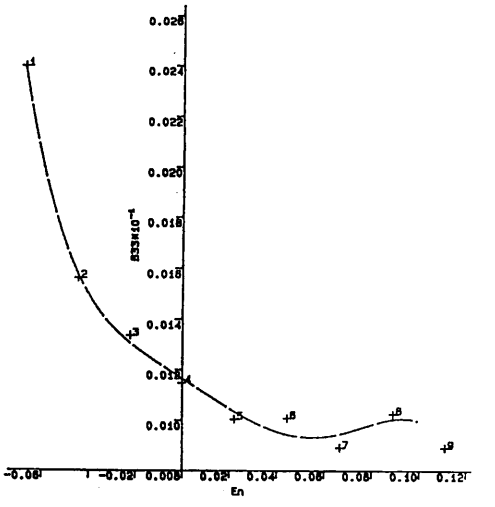

w = 1.5 rad/s

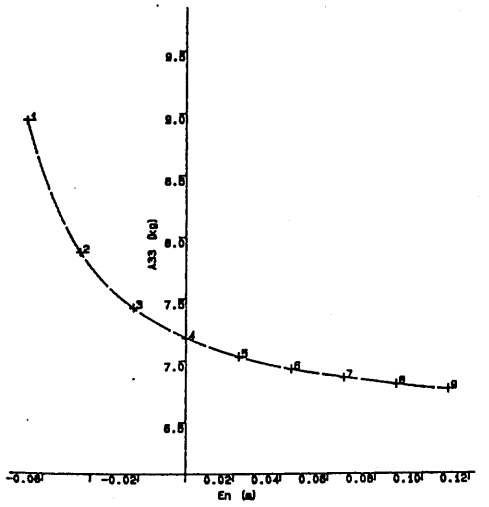

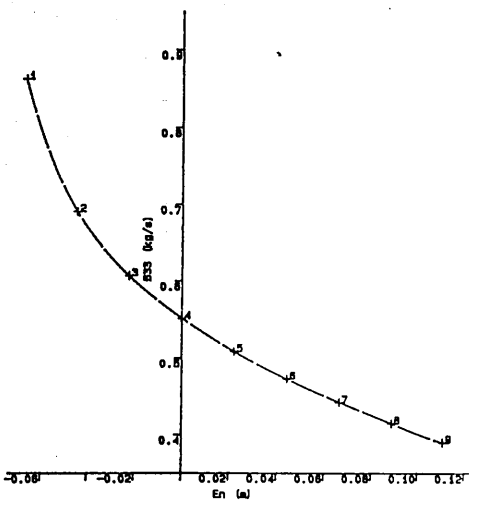

w = 3.5 rad/s

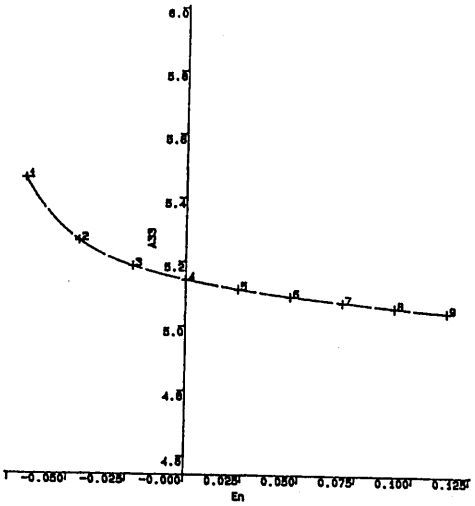

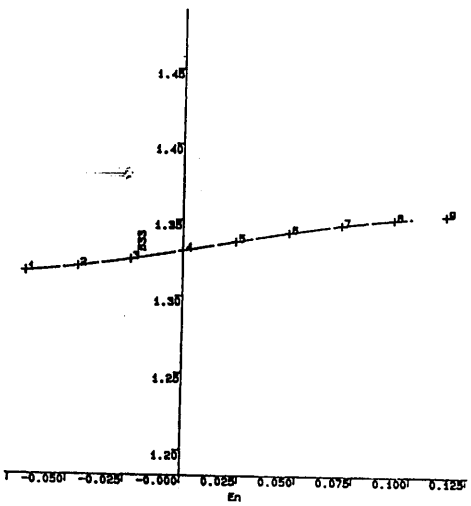

w = 1.5 rad/s

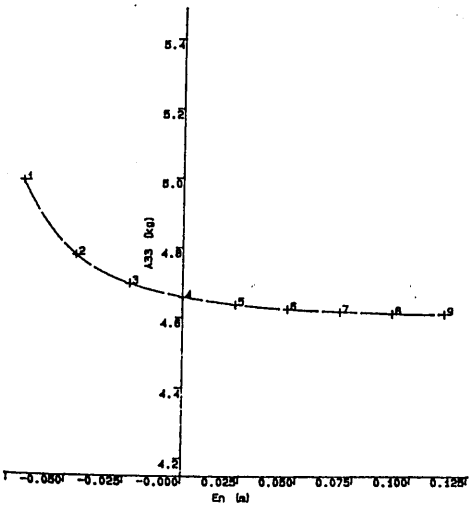

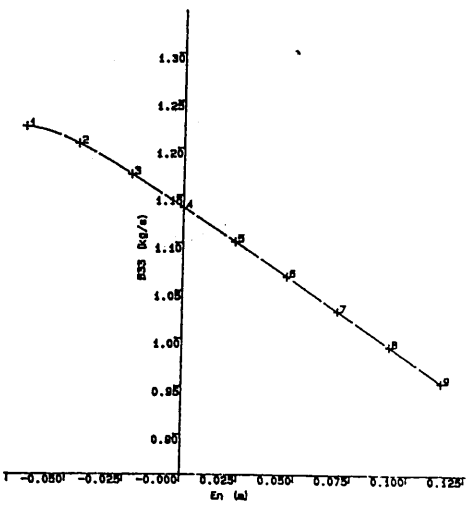

w = 3.5 rad/s

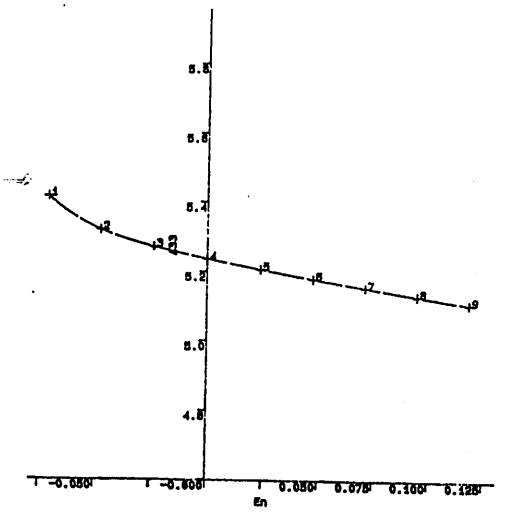

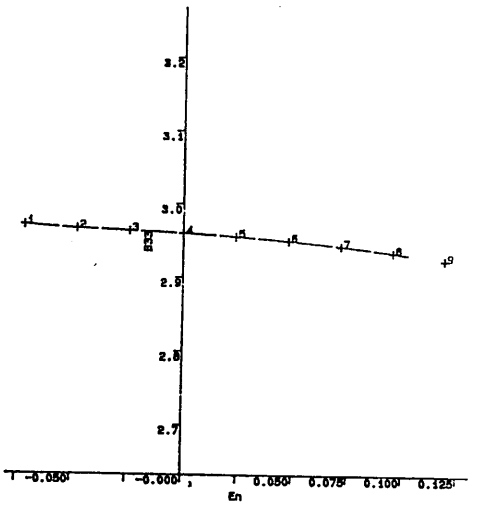

w = 1.5 rad/s

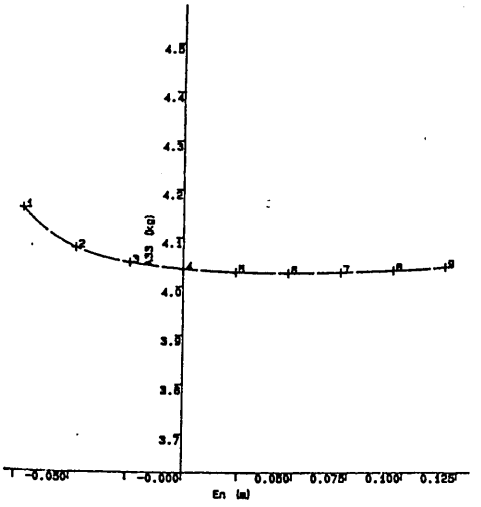

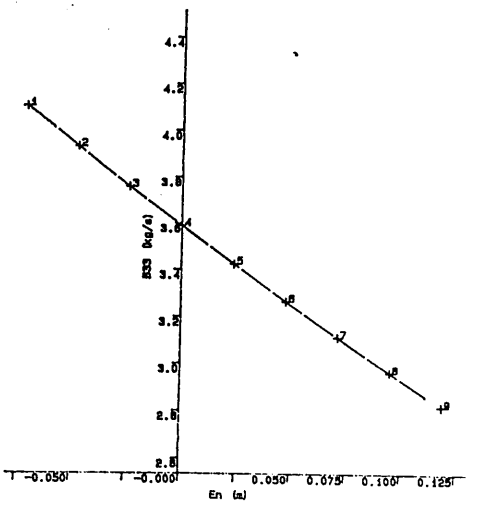

w = 3.5 rad/s

Figures 5.4 Time Domain Solutions with Non-Linear Added Mass and Damping

SWATH11, 0.0 and 0.5ms^{-1}

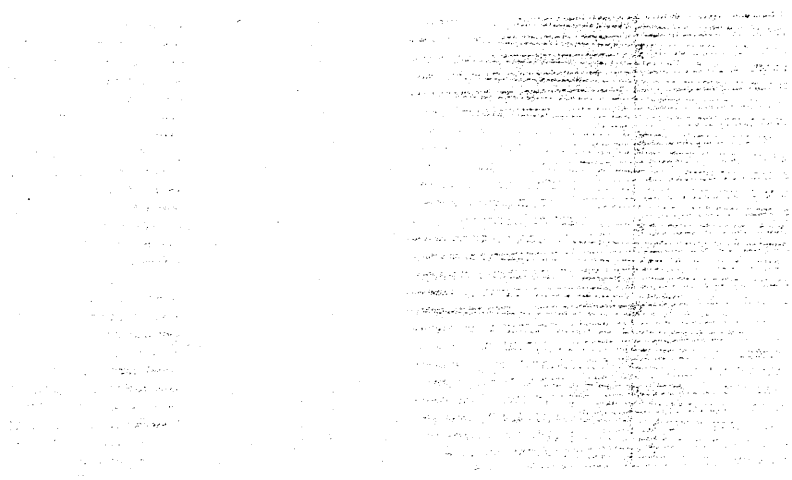

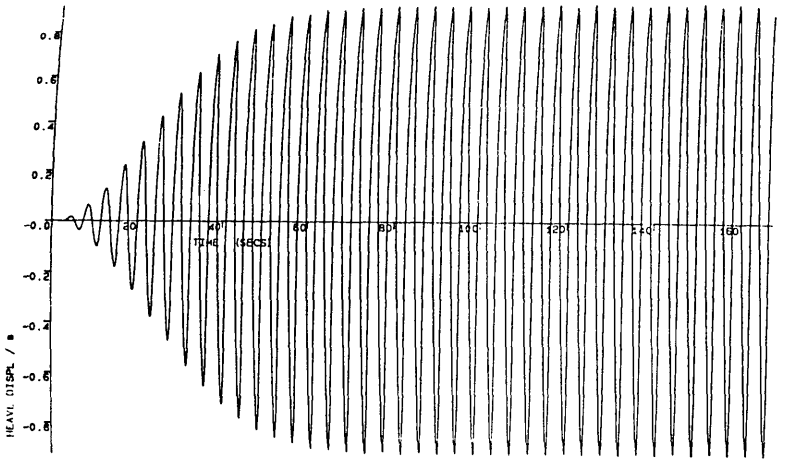

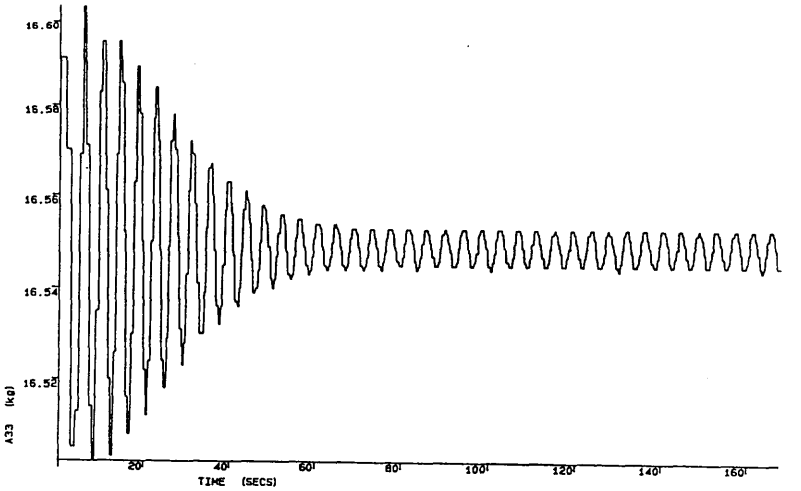

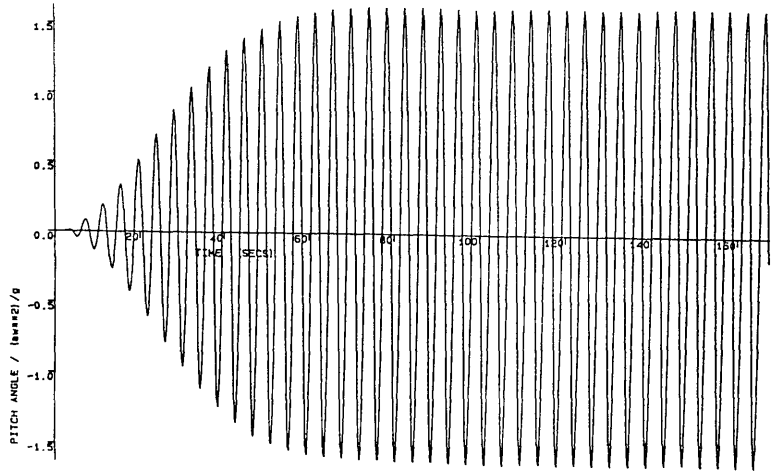

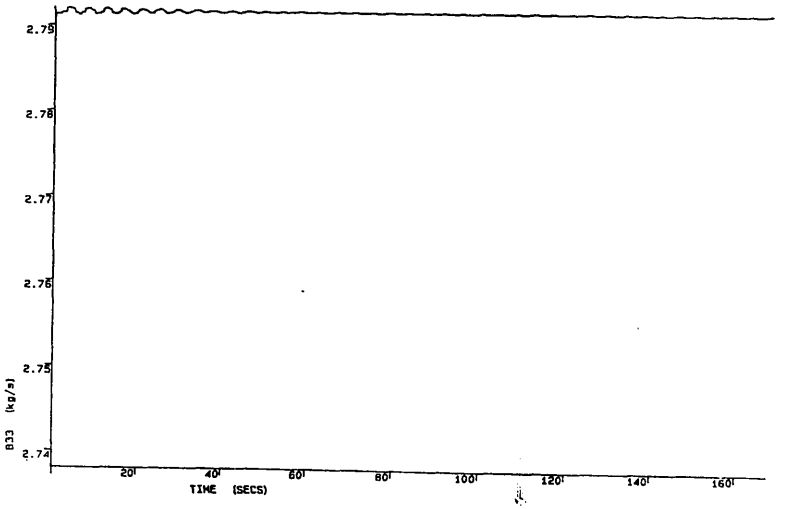

U = 0 m/s w = 1.5 rad/s

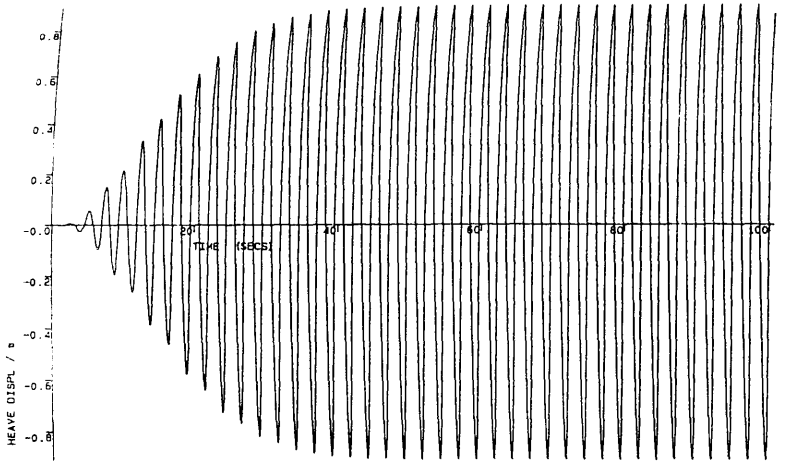

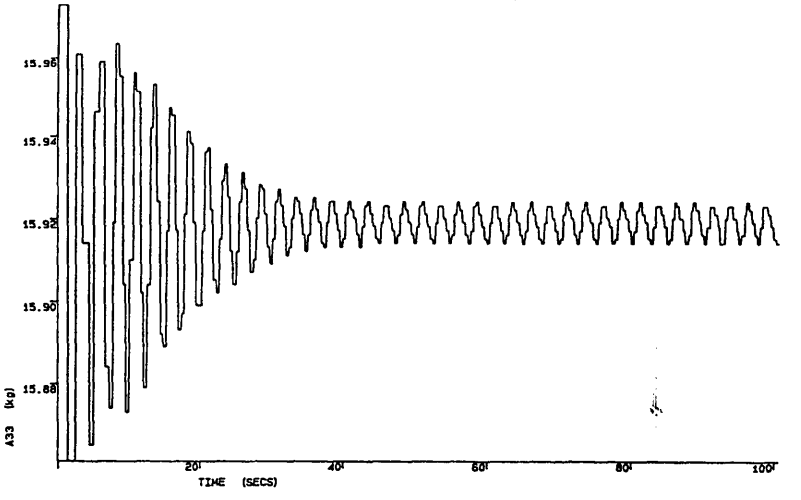

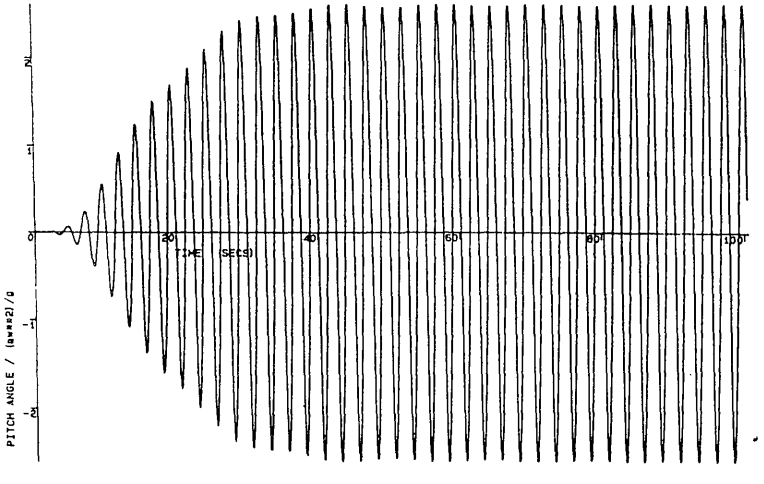

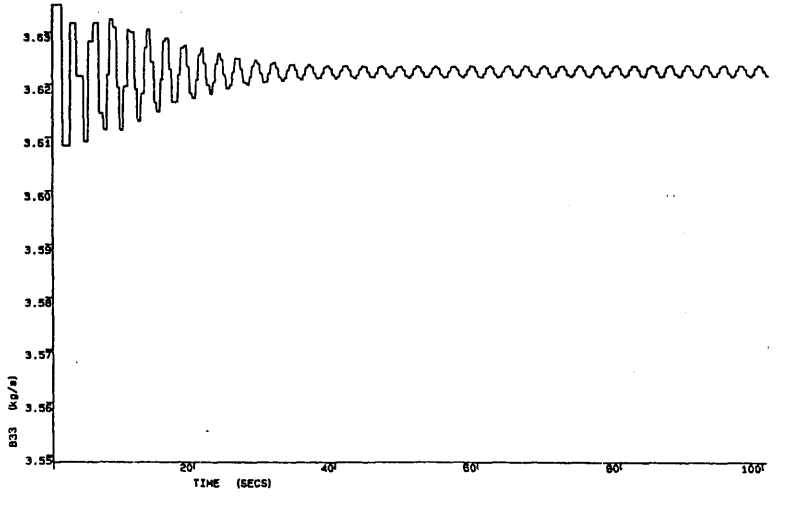

U = 0 m/s w = 2.5 rad/s

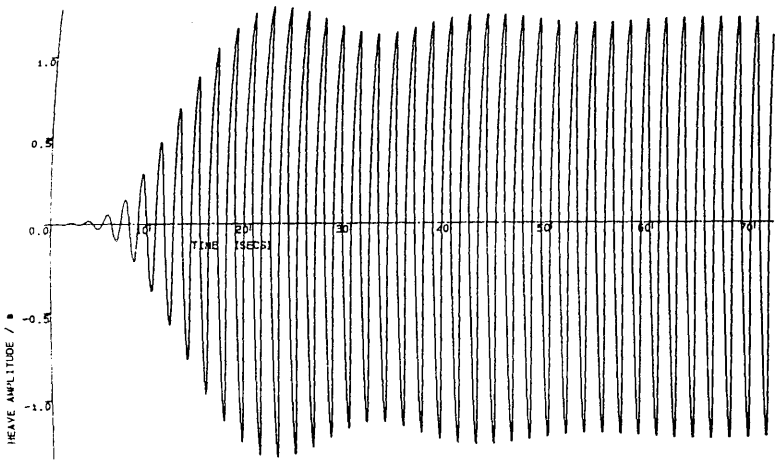

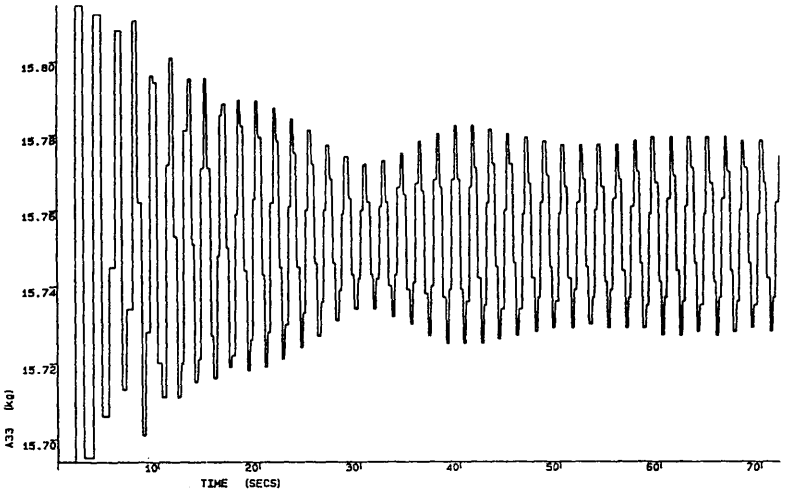

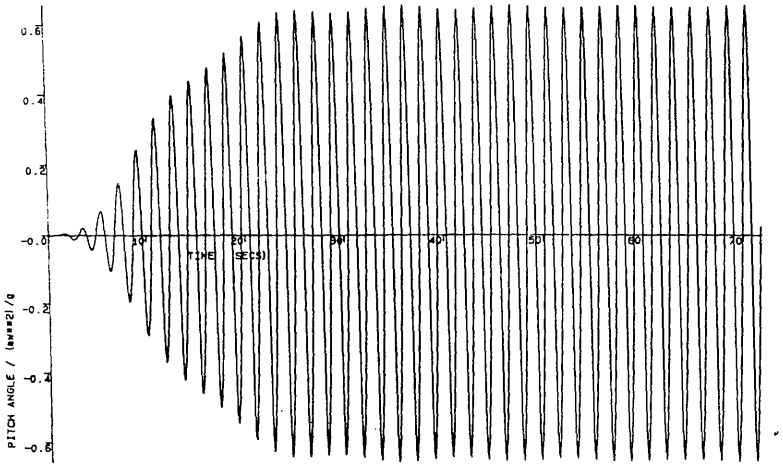

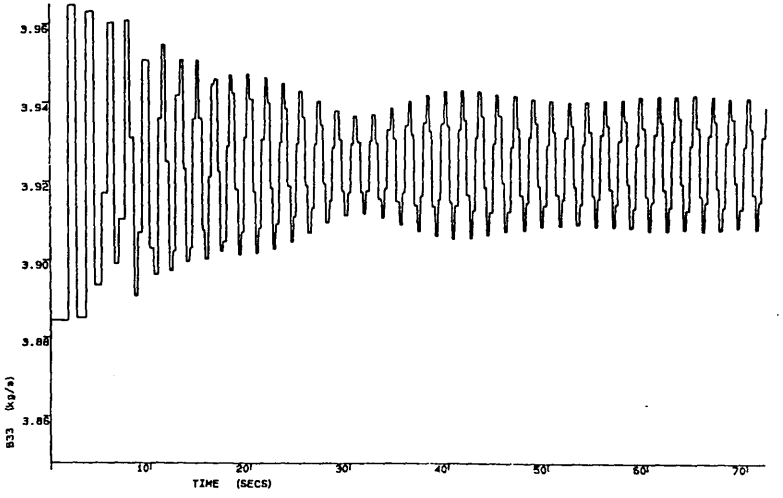

U = 0 m/s w = 3.5 rad/s

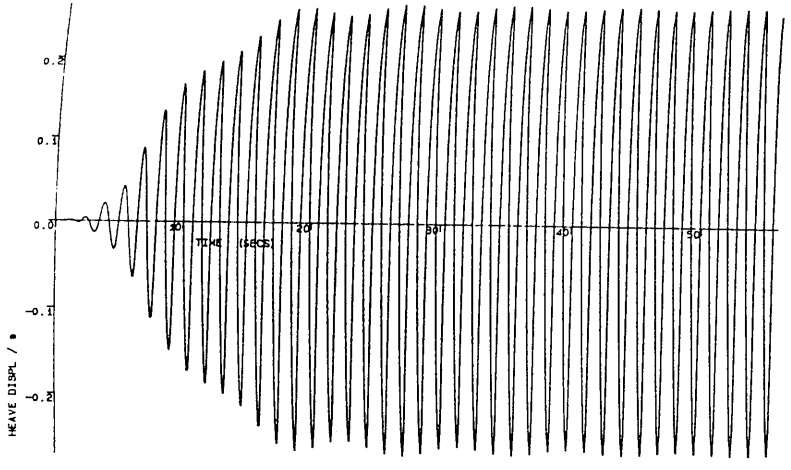

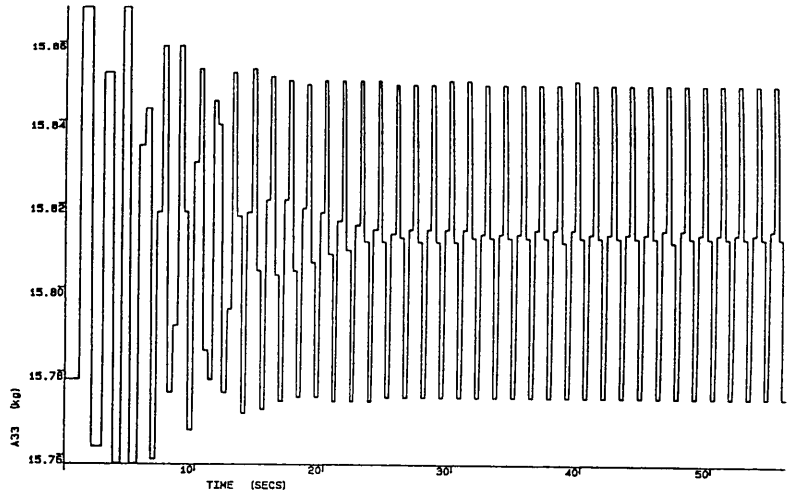

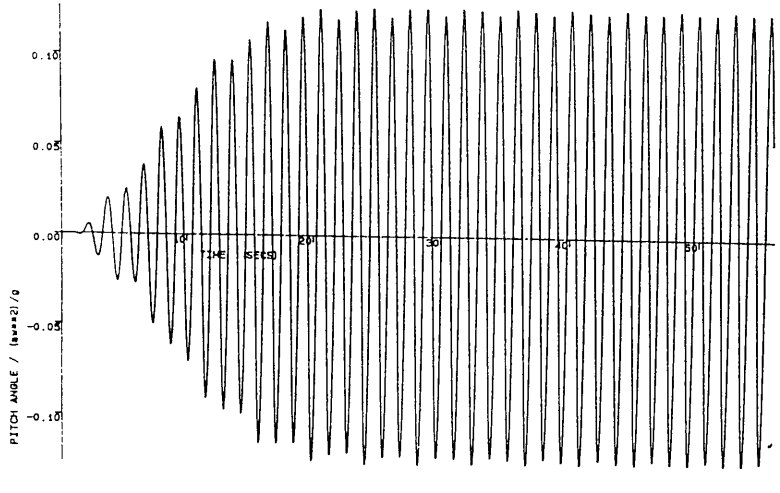

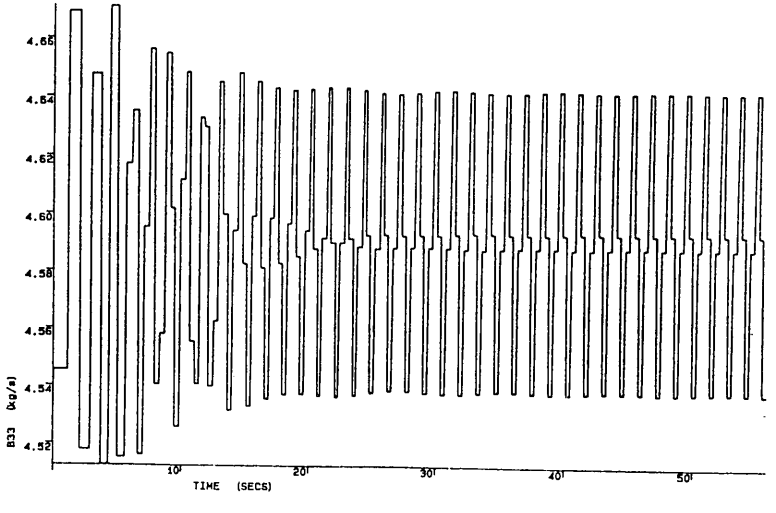

U = 0 m/s w = 4.5 rad/s

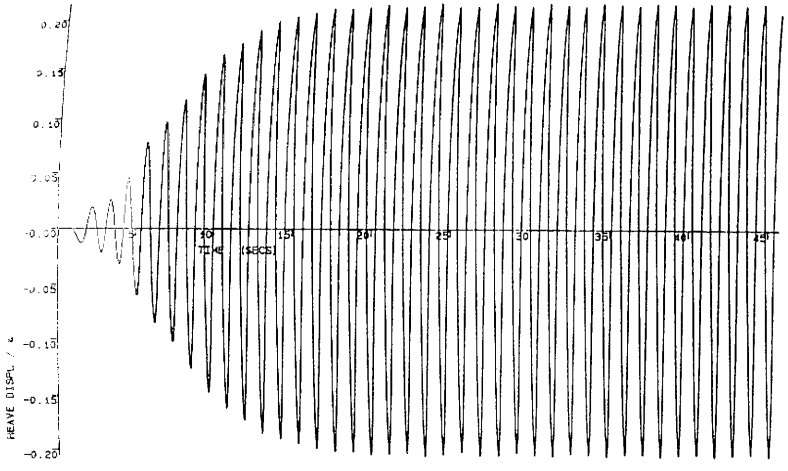

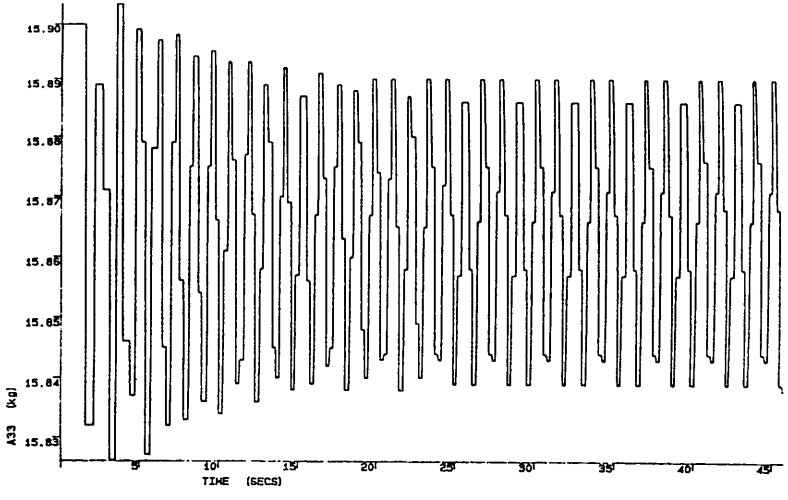

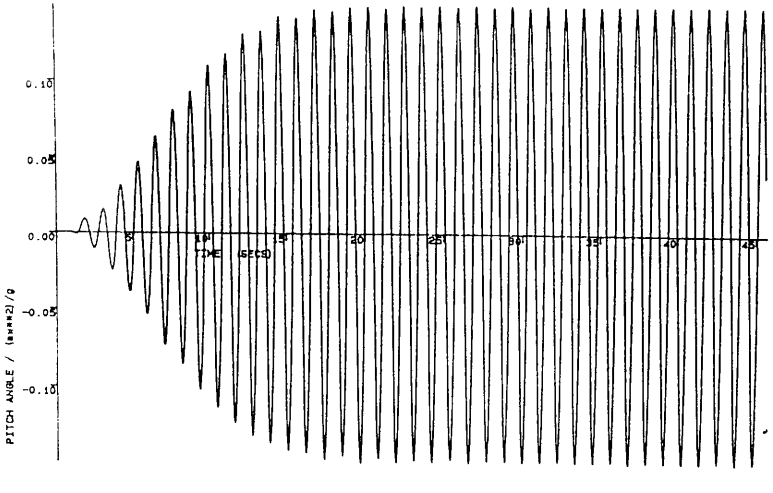

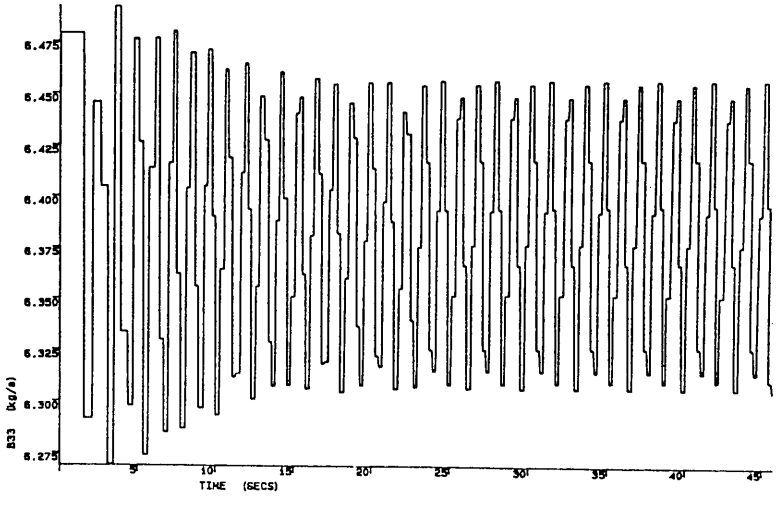

U = 0 m/s w = 5.5 rad/s

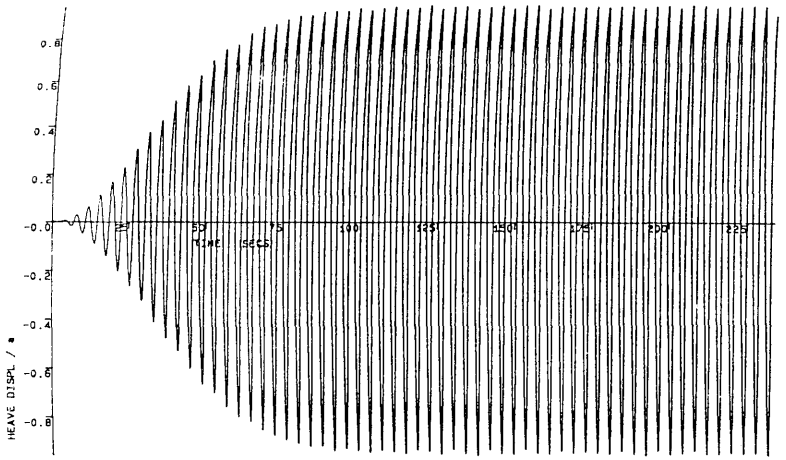

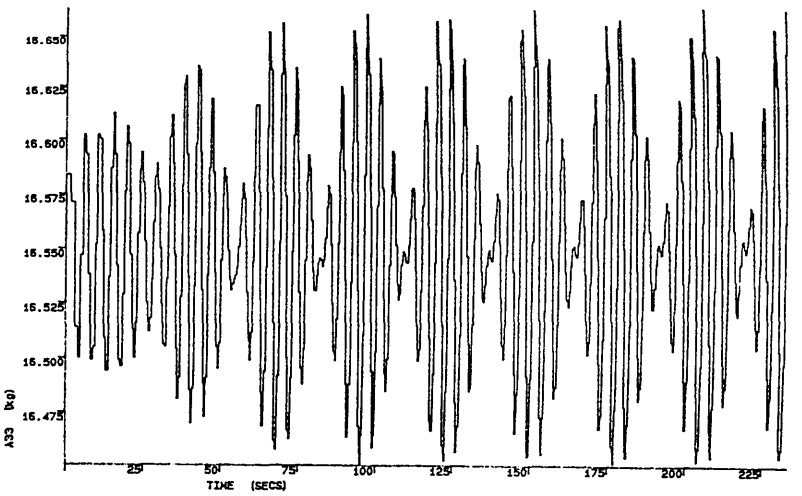

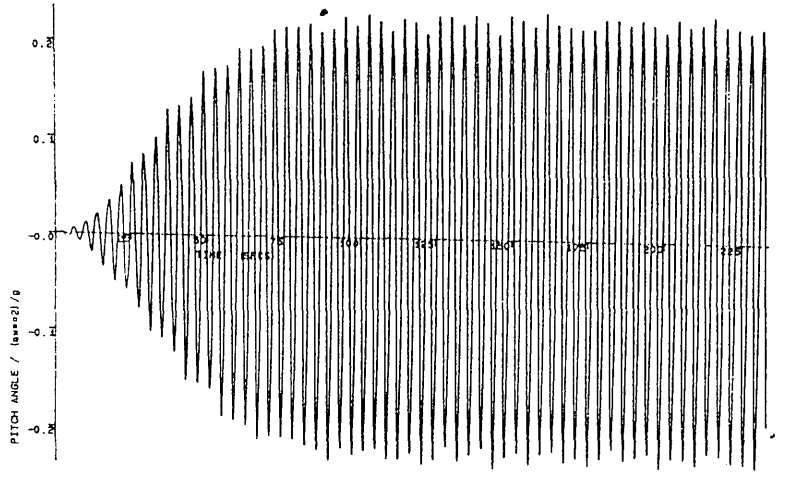

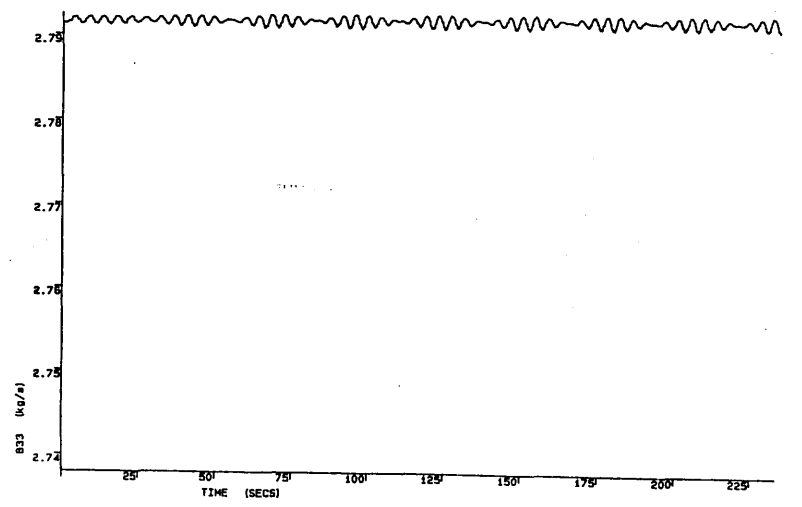

U = 0.5 m/s w = 1.5 rad/s

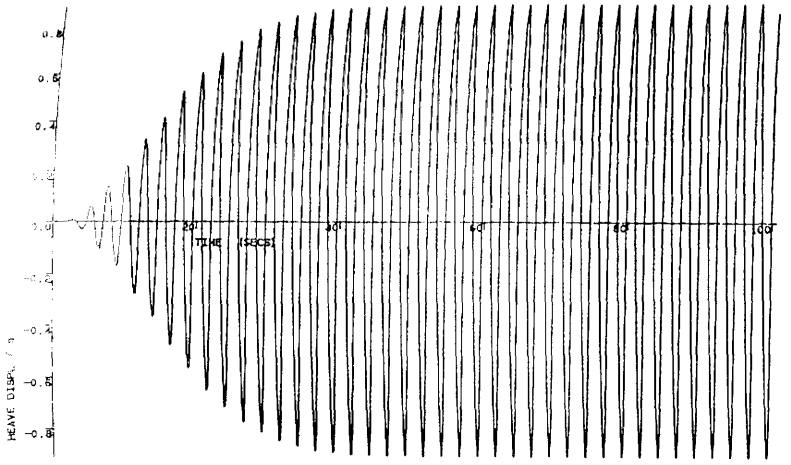

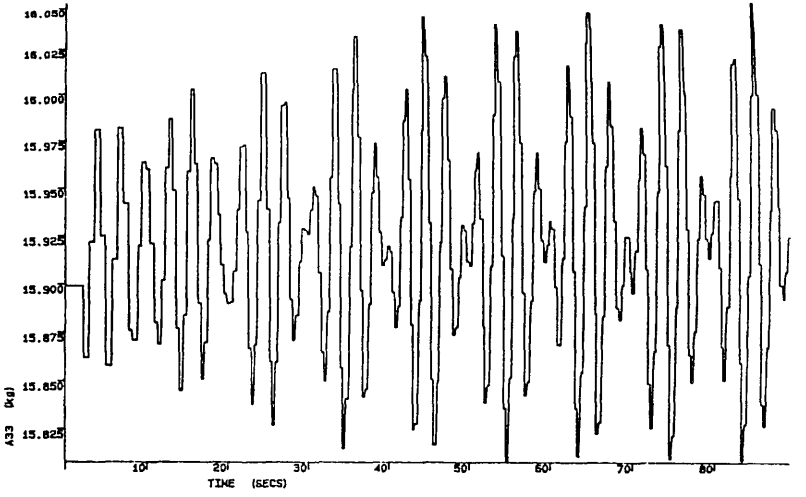

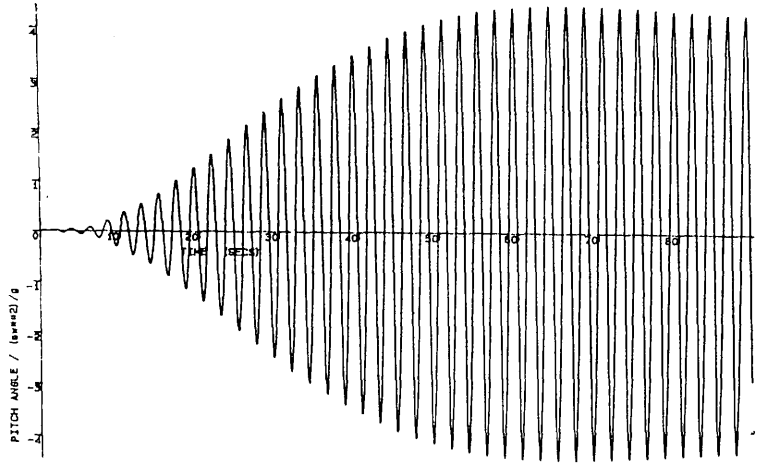

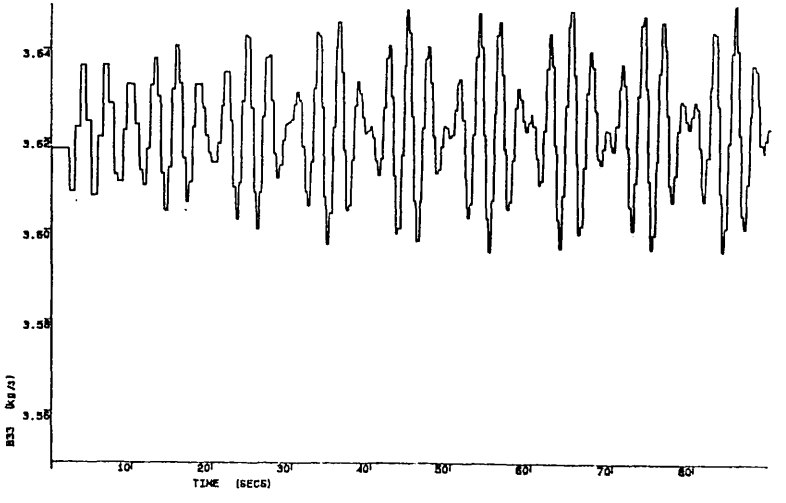

U = 0.5 m/s w = 2.5 rad/s

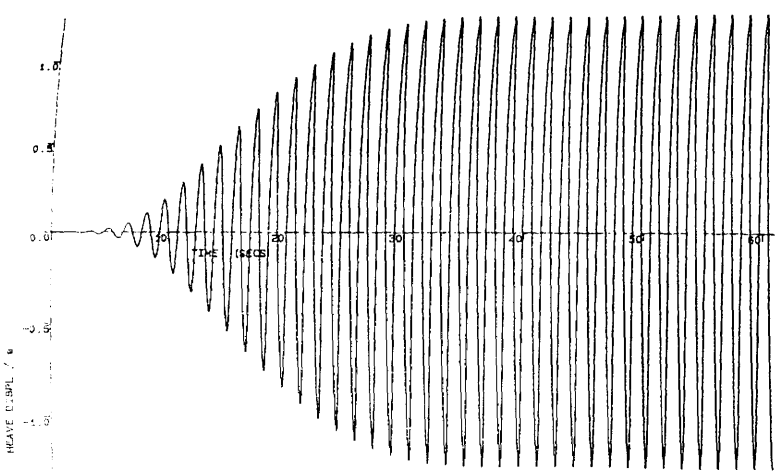

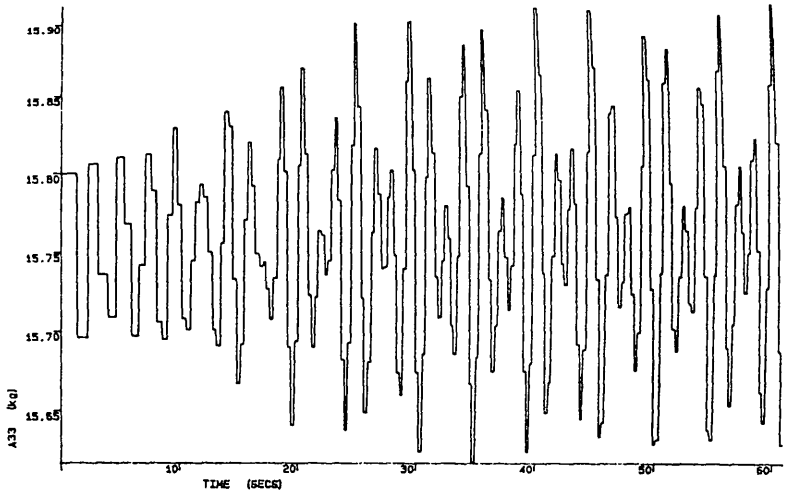

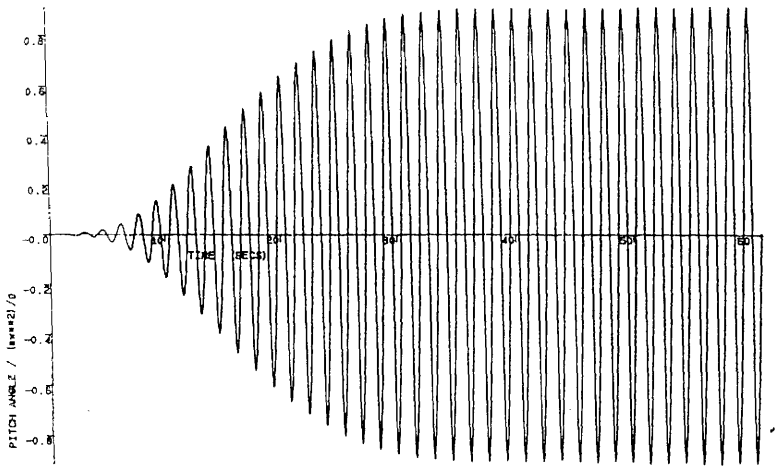

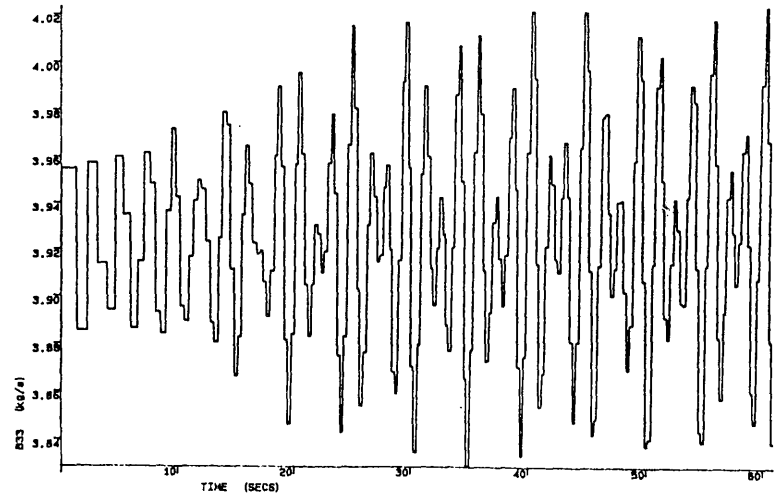

U = 0.5 m/s w = 3.5 rad/s

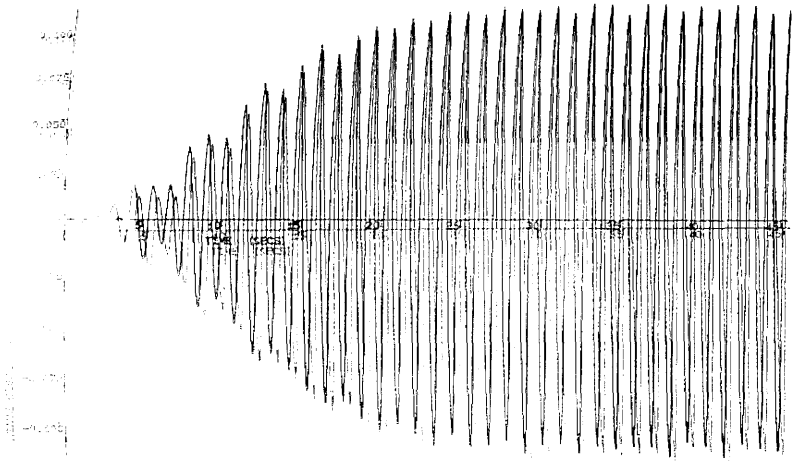

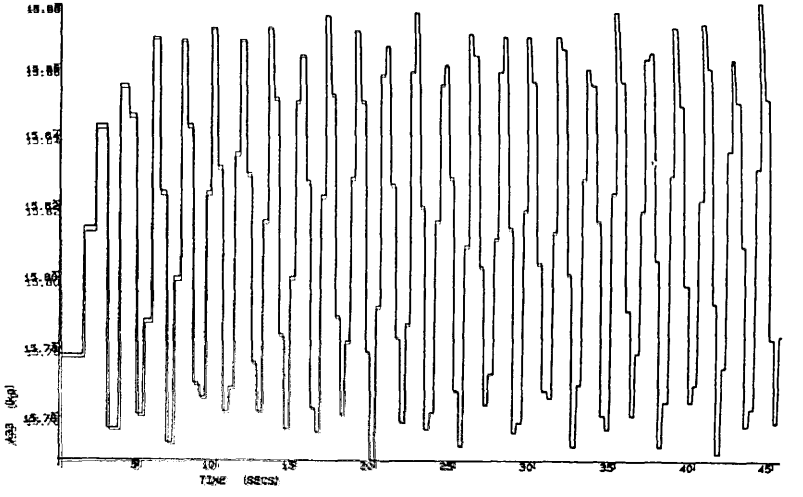

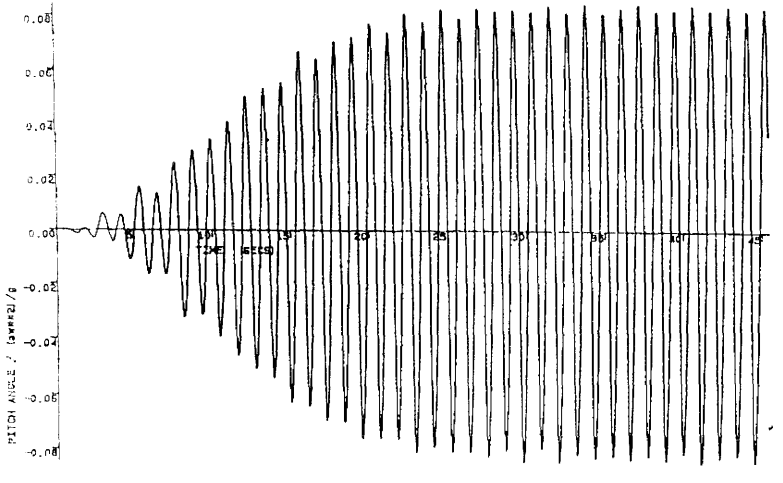

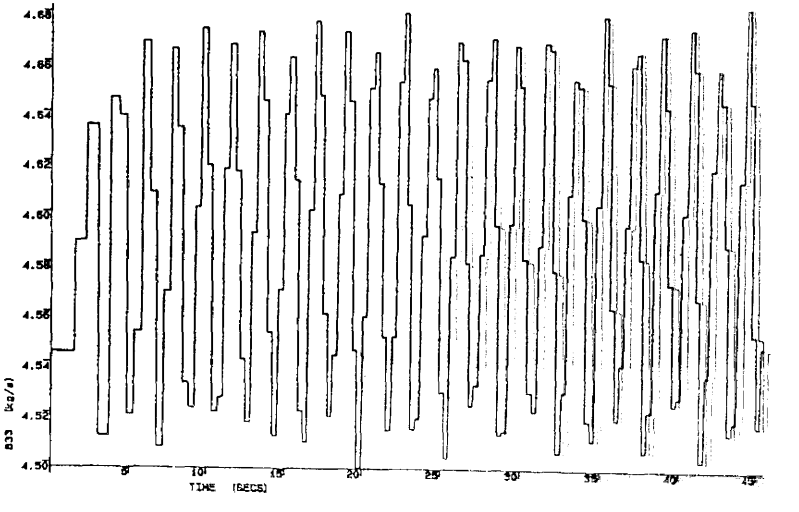

U = 0.5 m/s w = 4.5 rad/s

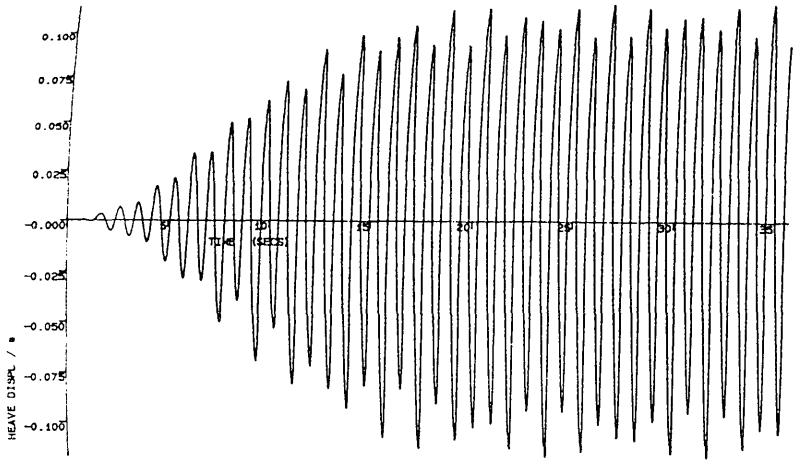

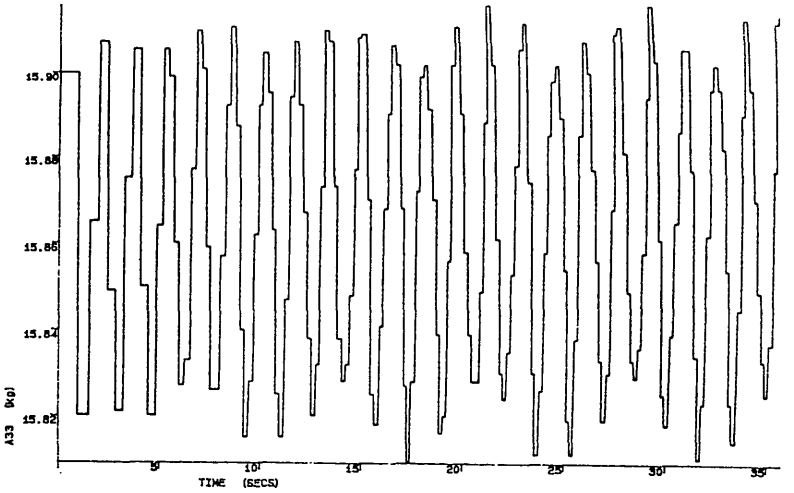

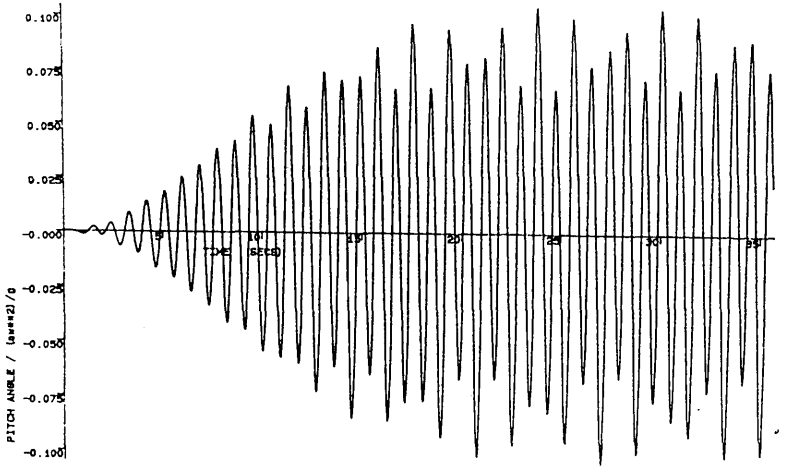

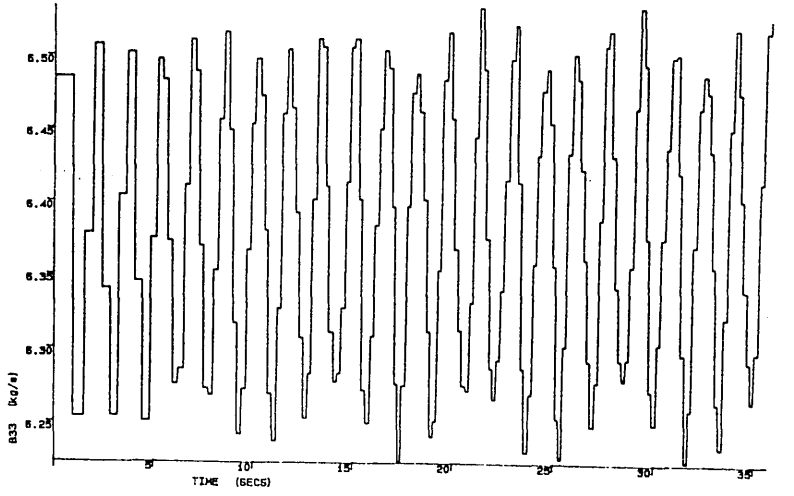

U = 0.5 m/s w = 5.5 rad/s

Figures 5.5 Time Domain Solutions (Non-Linear Added Mass and Damping) Compared with Frequency Domain Solutions

SWATH11, 0.0 and 0.5 ms^{-1}

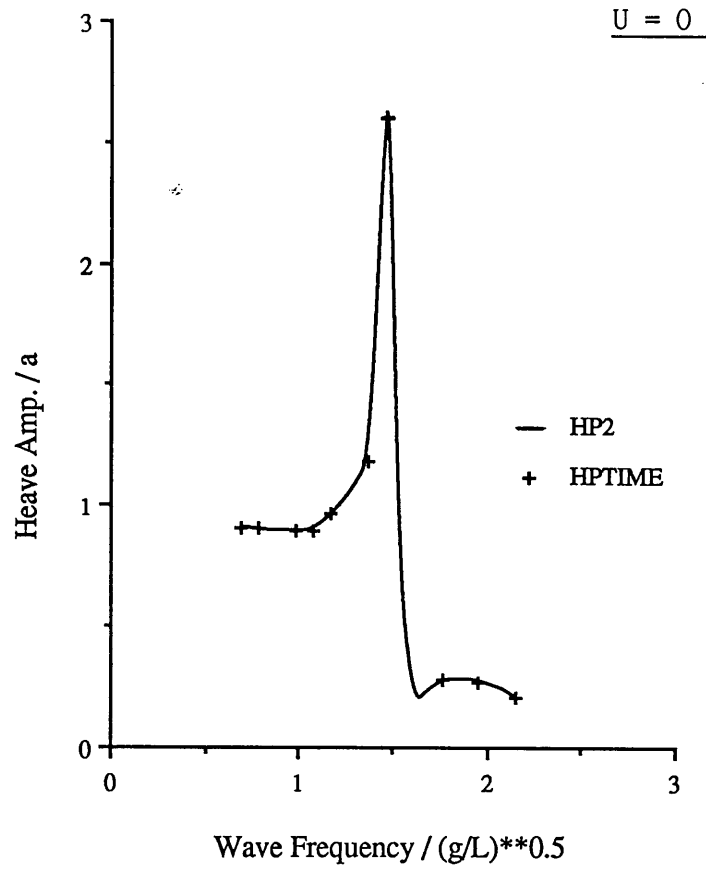
U = 0 m/s
Heave Amp. / a
HP2
HPTIME
Wave Frequency / (g/L)**0.5

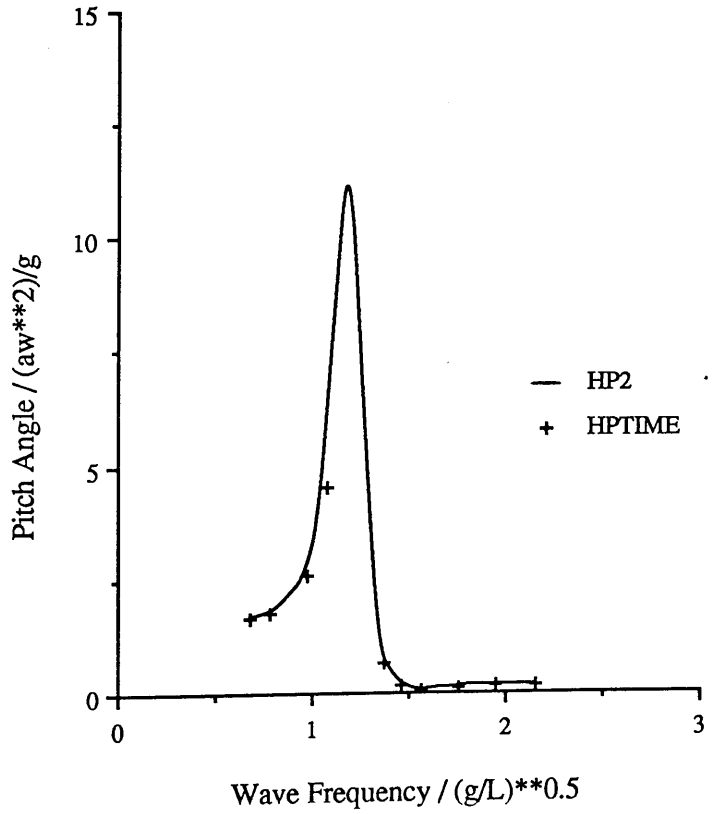
Pitch Angle / (aw**2)/g
HP2
HPTIME
Wave Frequency / (g/L)**0.5

U = 0.5 m/s

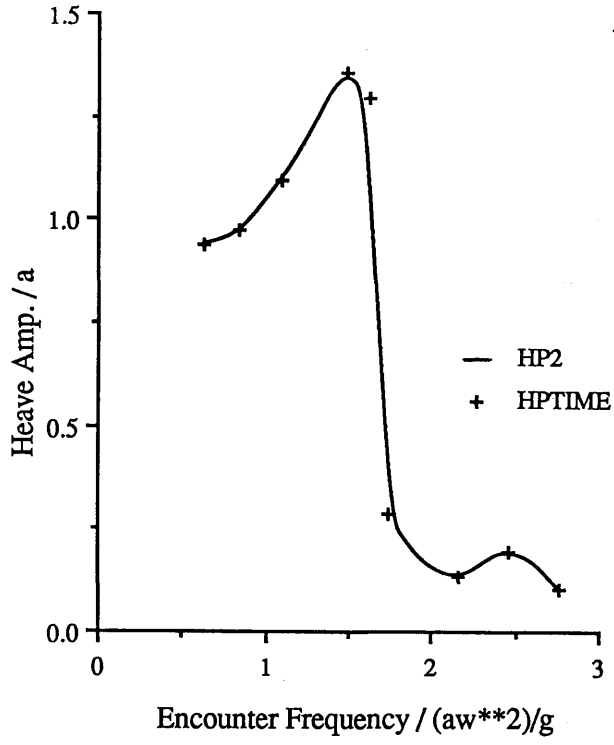
1.5
1.0
0.5
0.0
Heave Amp. / a
0
1
2
3
Encounter Frequency / (aw**2)/g
HP2
HPTIME

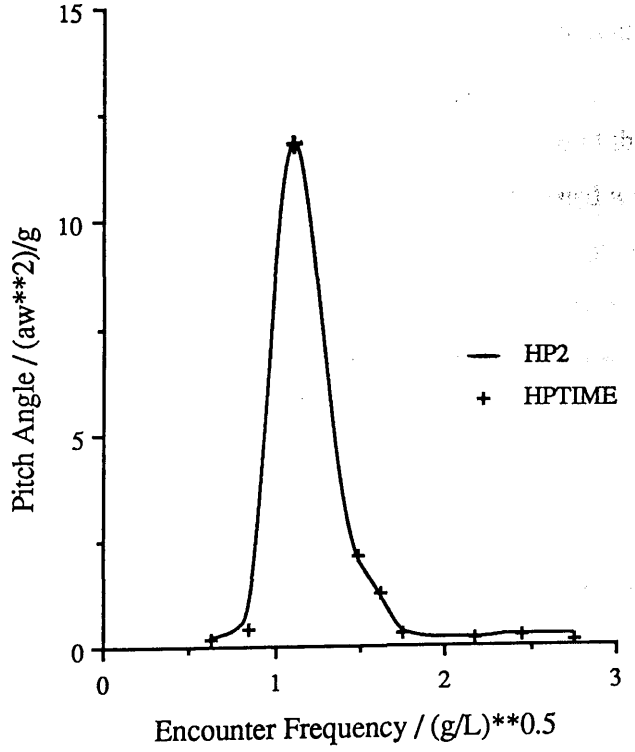
15
10
5
0
Pitch Angle / (aw**2)/g
0
1
2
3
Encounter Frequency / (g/L)**0.5
HP2
HPTIME

5.7 Computations With Non-linear Restoring

The method described for introducing hydrostatic non-linearities into the simulation have been modelled by incorporating new subroutines in the time domain computer program program. Further analysis of model SWATH11 using the modified program gives results which iluustrate the relative significance of non-linear restoring effects.

5.71 Structure of Computer Routine

New subroutines XSAREA and RESTORE have been written to account for non-linear restoring effects. Their location in the main program is shown in figure 5.6. The flow diagram shows that the main program structure is unaltered.

If cross sectional area polynomial relationships have not been previously determined, they are calculated in XSAREA which is called from DATABASE. The polynomial coefficients corresponding to each hull section are stored as common block data for use during the solution procedure. The curve fitting routine applied in FITTER will account for any sudden change in cross section shape.

After returning to the main program, initial conditions of the simulation at time $t = 0$ are set and the corresponding values of E_n are calculated within ELEVATION. Before entering the master solution routine, TDSOL, values of vessel displacement and LCB position for the first time submerged geometry are determined. These are calculated within the subroutine RESTORE which employs the procedure described in section 5.5.

At the beginning of TDSOL, forward speed corrections and harmonic time functions are applied to the hydrodynamic coefficients and wave excitation amplitudes respectively. Motion displacement predictions obtained for the first solution cycle and the altered wave profile define the submerged condition for the next time step. By calling ELEVATION and then RESTORE from the system reconditioning routine, FCN, values of displacement, LCB heave restoring and pitch restoring are obtained

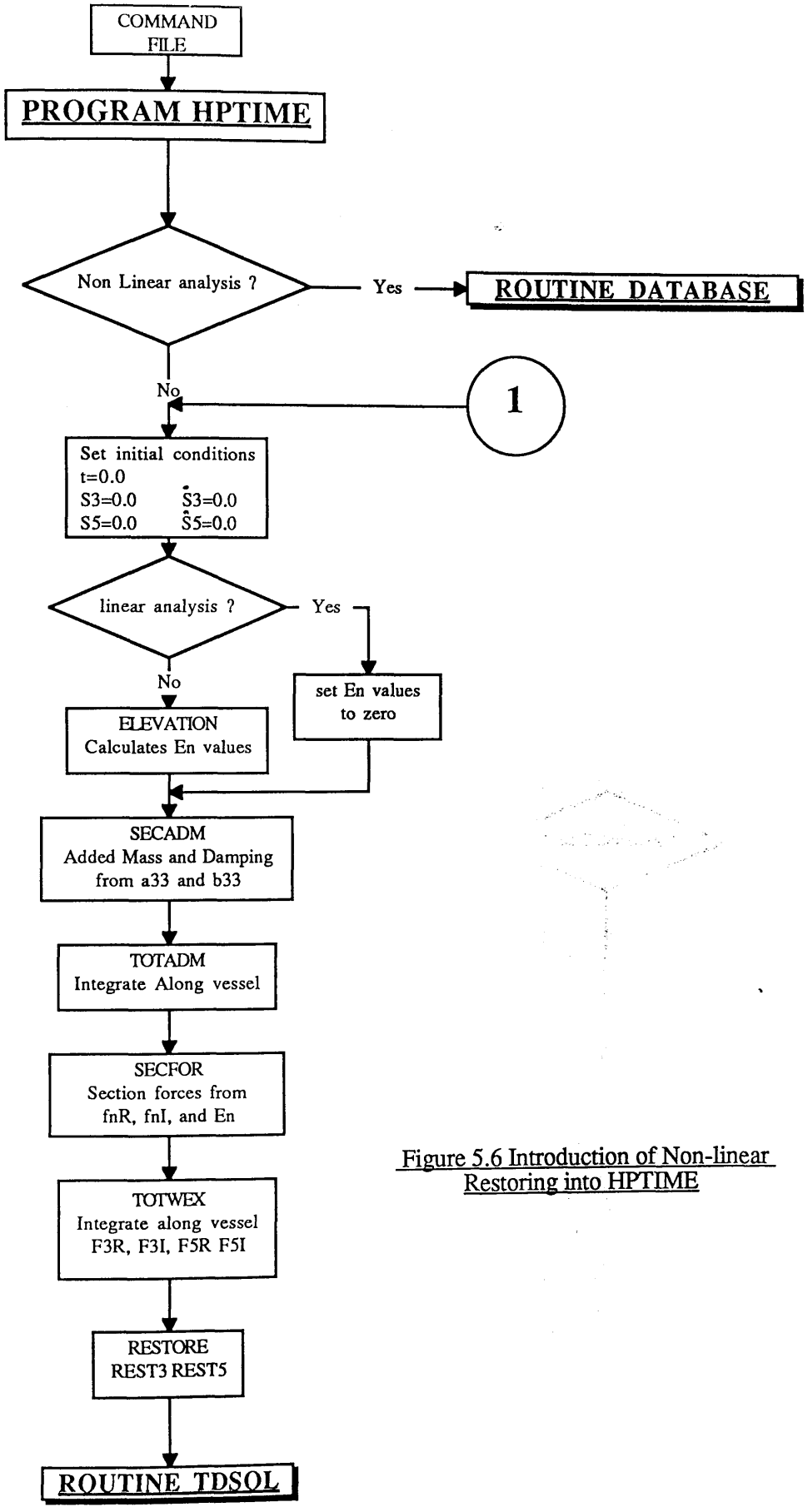

Figure 5.6 Introduction of Non-linear Restoring into HPTIME

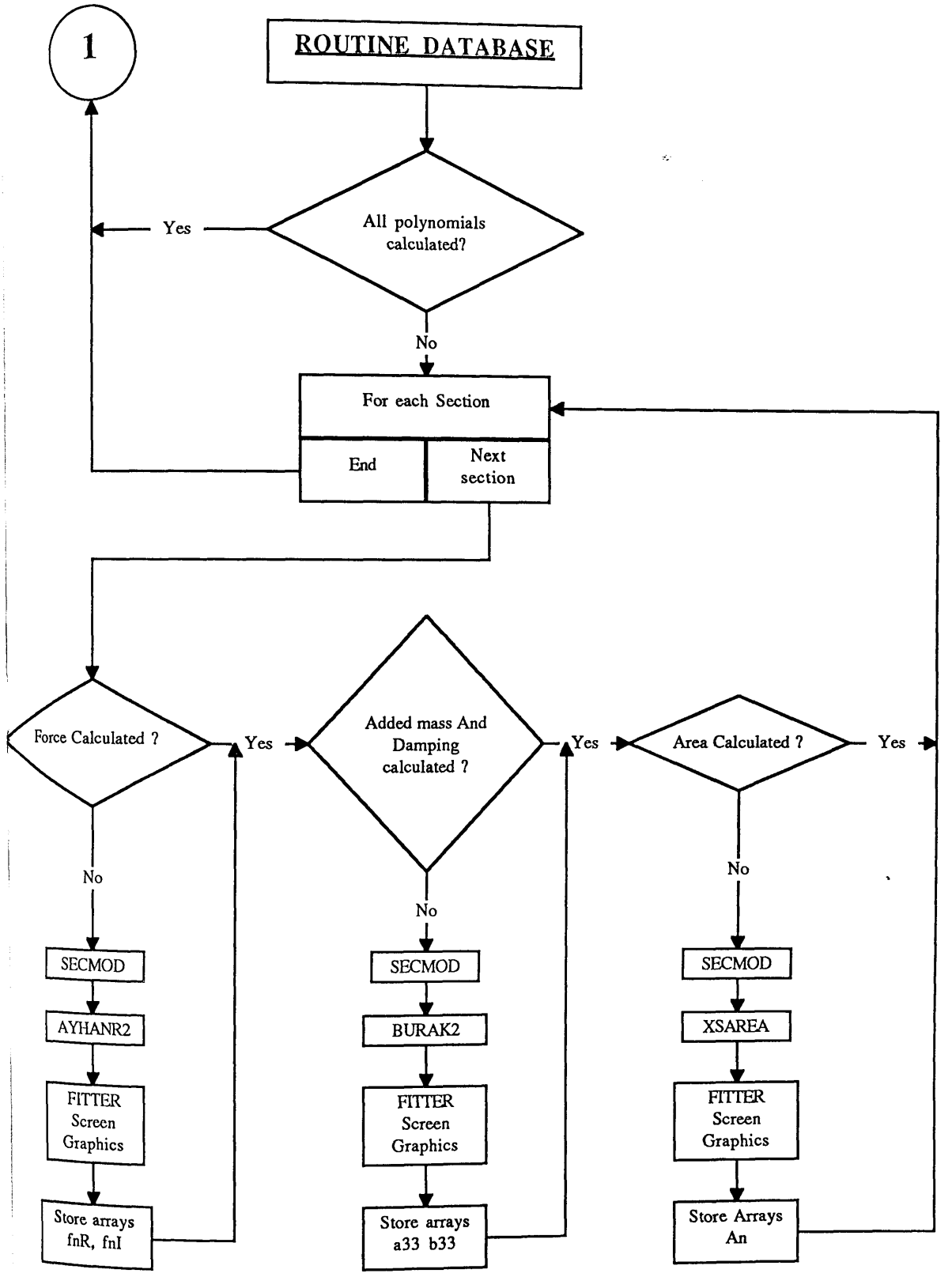

Figure 5.6 (Cont..)

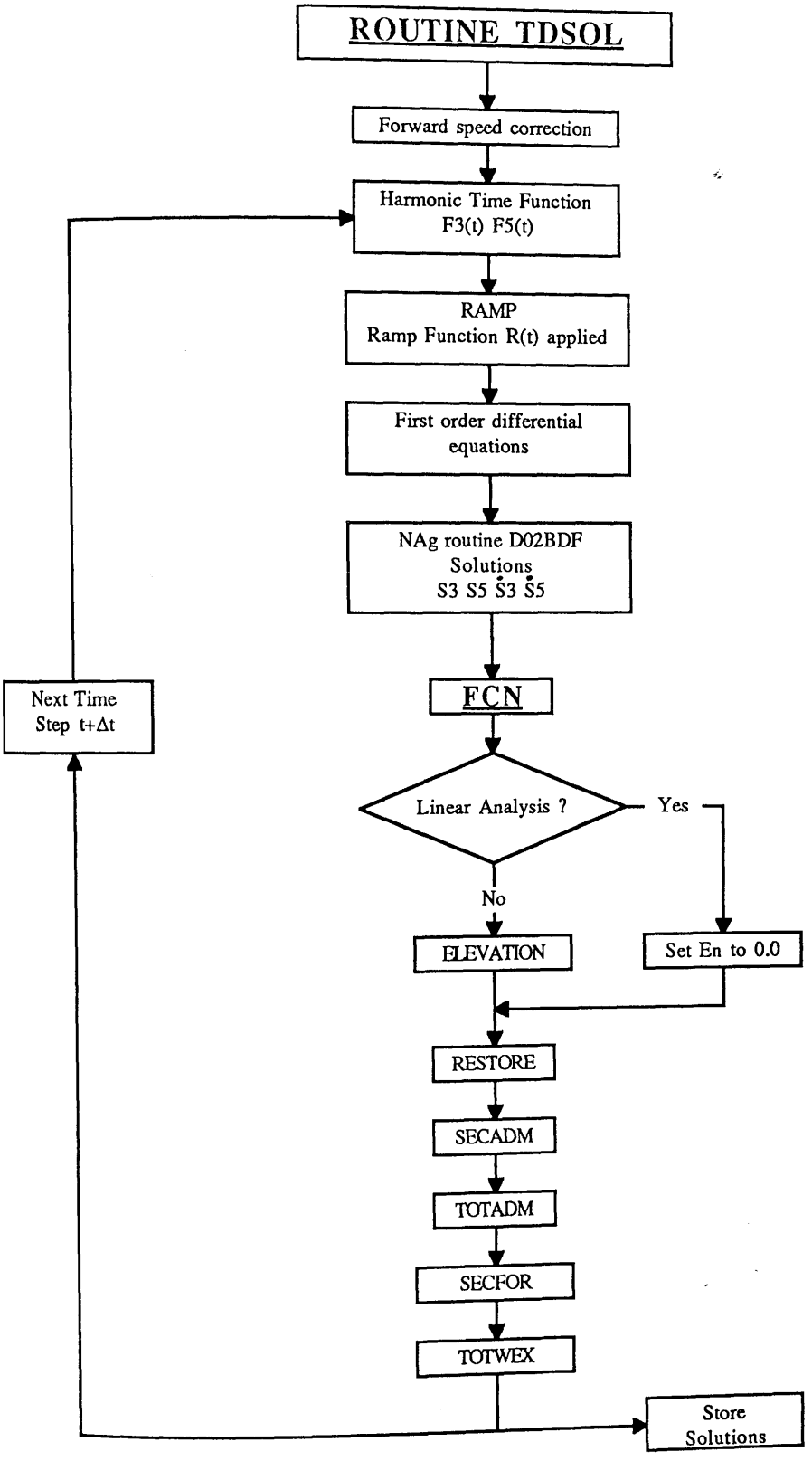

Figure 5.6 (Cont..)

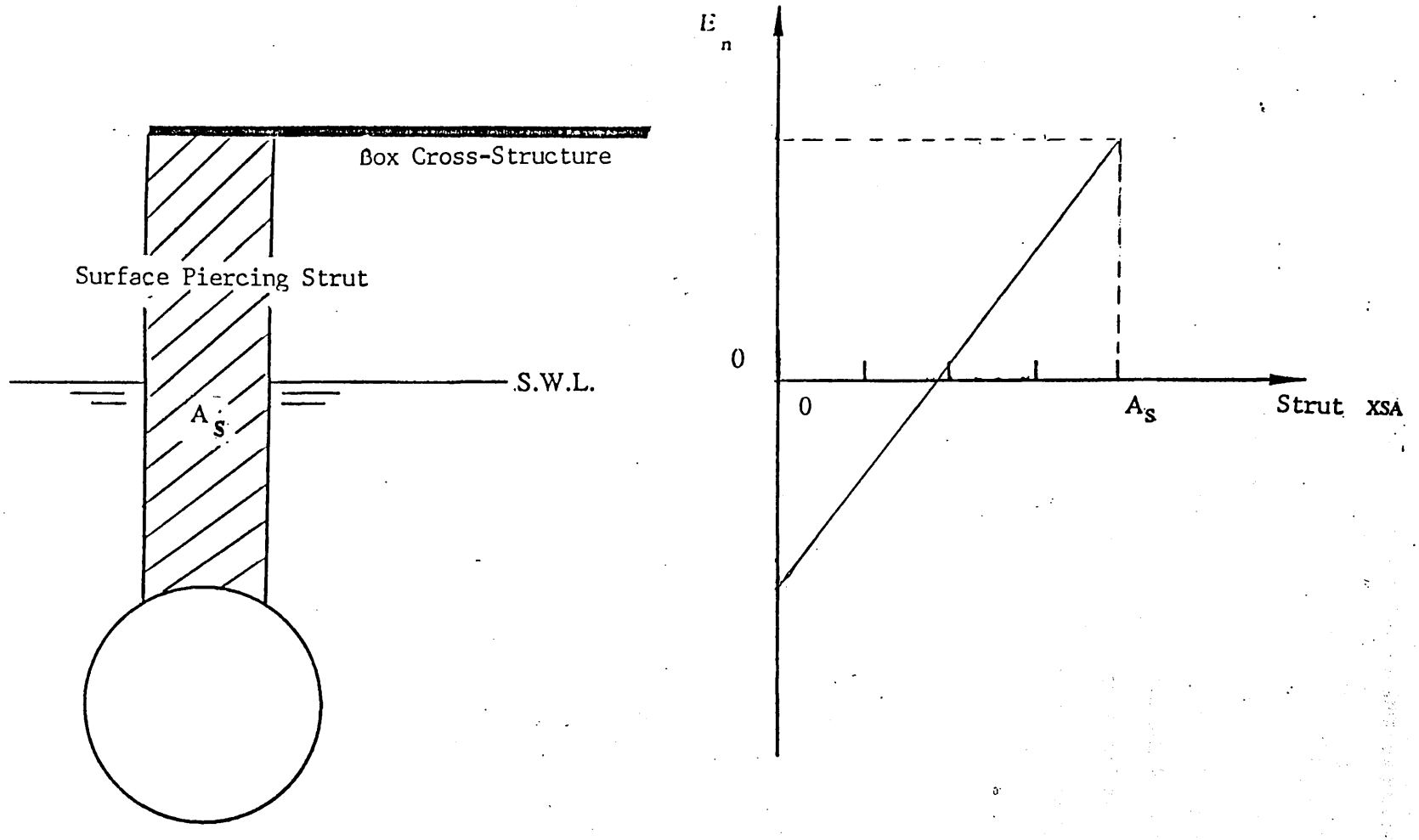

Fig. 5.7 Cross Sectional Area Polynomial - SWATH11

and installed in the motion equations. These are solved and the solutions for t = t + dt obtained. The solution procedure is repeated until constant amplitude heave and pitch solutions are obtained.

5.72 Analysis of SWATH11

Fig. 5.7 illustrates the cross sectional area polynomial relationship for a surface piercing, strut section of SWATH11. As the struts on this design are prismatic over their depth, simple straight line relationships exist between values of water surface elevation and cross section area. Higher order relationships with irregularities will be obtained for more realistic strut sections which have haunch.

Time histories of heave and pitch motion predictions from the analysis of SWATH11 are given in figures 5.8. Motion displacements and wave frequency have been non-dimensionalised by applying the same factors as used previously. Exponential ramp functions applied to the wave excitation forcing funtions are also the same as used before. Their effects can be seen clearly in the first half of each record.of heave restoring force and pitch restoring moment.

Figures 5.9 show comparisons between the response amplitude predictions obtained using time domain, 2-D [5]frequency domain and 3-D [9]frequency domain analysis techniques. Results are given for the range of model scale frequecies of between 1.5 and 5.5 $rads^{-1}$ and for forward speeds of 0 and 0.5ms^{-1}.

Measurements obtained from seakeeping model tests carried out on SWATH11 at the University of Glasgow Hydrodynamics laboratory[8] are presented. These indicate the relative performance of each motion prediction tool over the frequency range.

5.73 Concluding Remarks

Analysis of SWATH11 over the same ranges of wave and forward speed conditions assessed previously has shown that, the effects of non-linear restoring are of more significance than the first two non-linearities assessed.

As expected there were no steady offset effects detected in the heave and pitch results. SWATH11 has surface piercing sections which are prismatic in the body axes z-direction. The wall sided struts are without haunch and have vertical stems. Non-linear hydrostatic effects therefore do not displace the heave or pitch oscillations from their at rest mean position.

The comparison plots in figure 5.9 show that , with the inclusion of non-linear restoring effects, the time domain simulation can give predictions which agree more closely with model test data than predictions obtained from existing 2-D and 3-D frequency domain analysis.

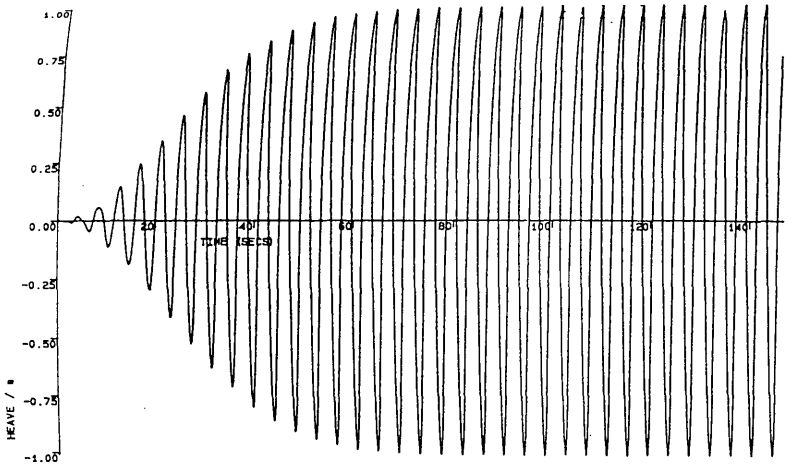

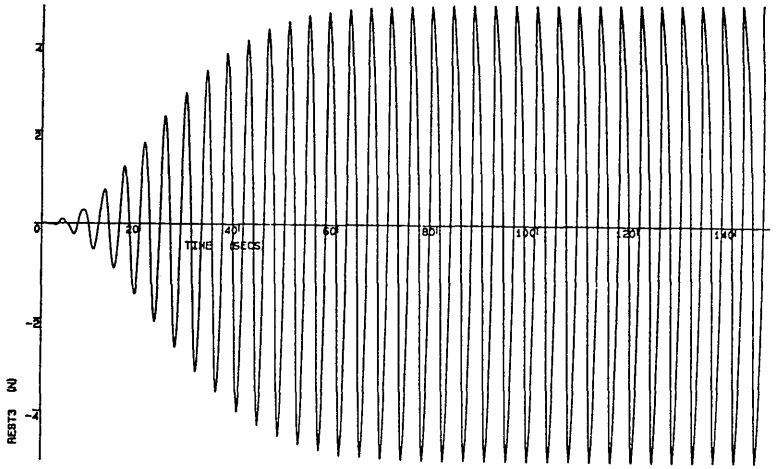

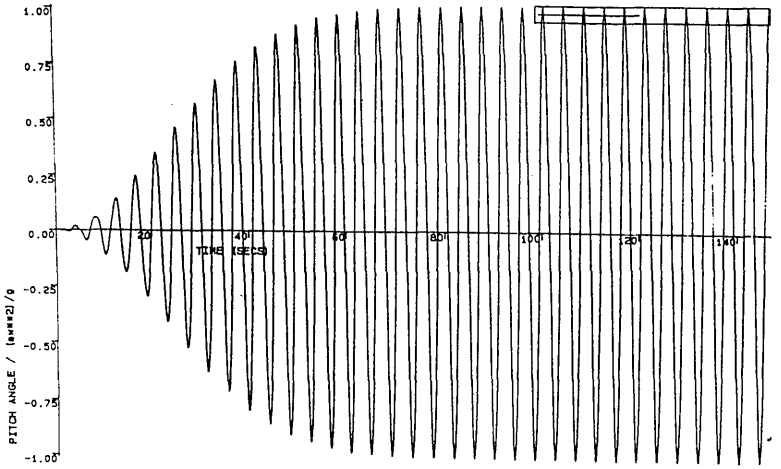

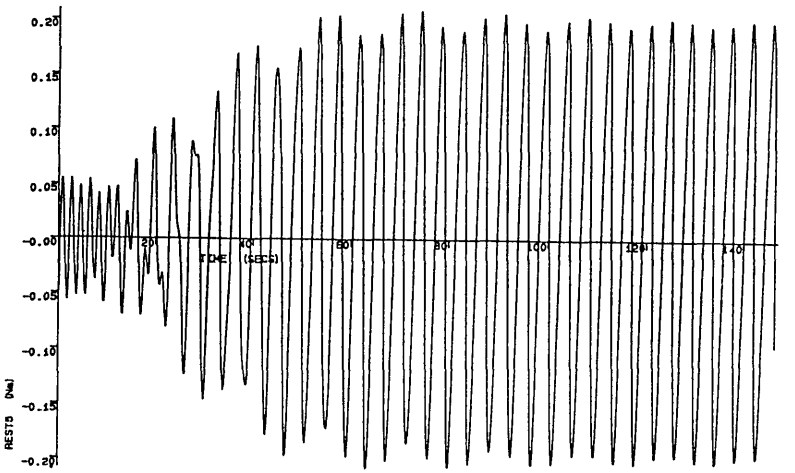

U = 0 m/s w = 1.5 rad/s

Figures 5.8 Time Domain Solutions with Non-Linear Hydrostatic Restoring

SWATH11, 0.0 and 0.5ms^{-1}

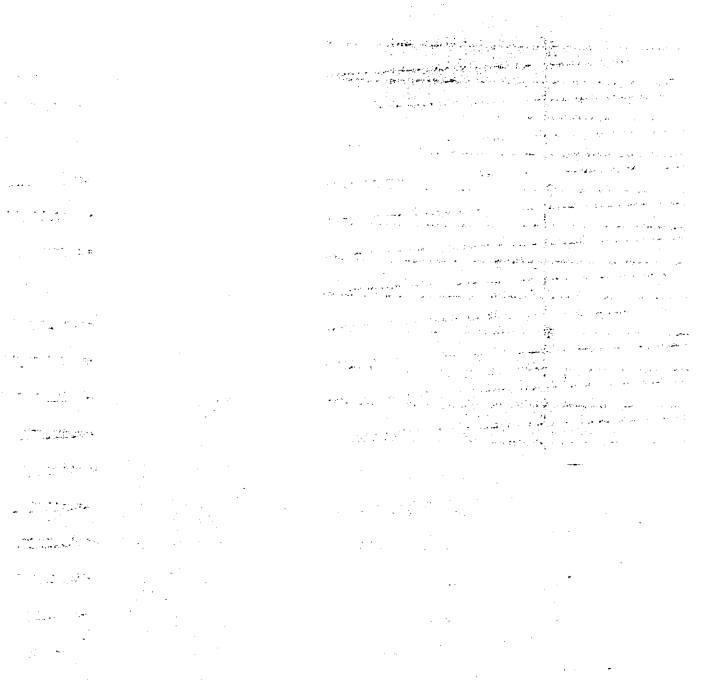

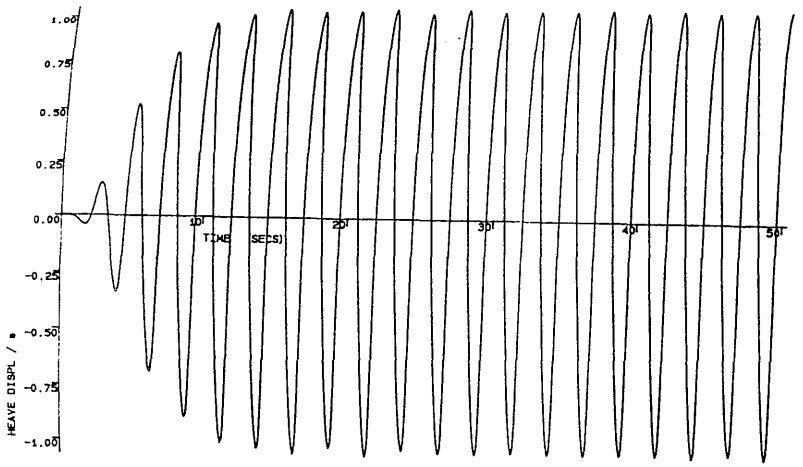

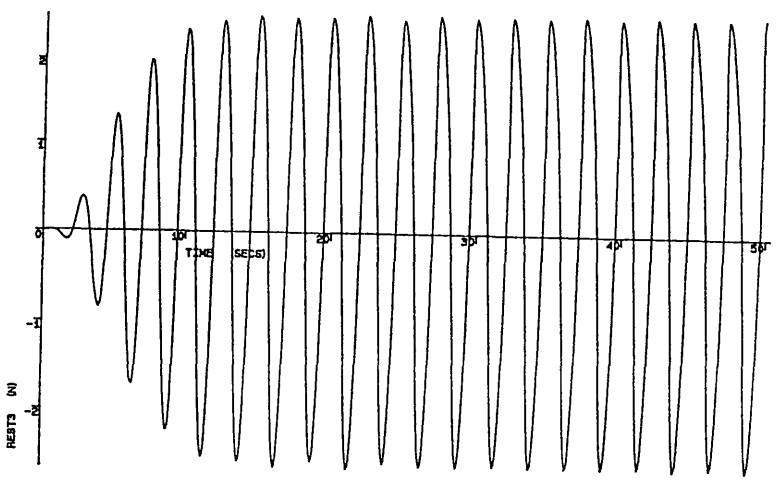

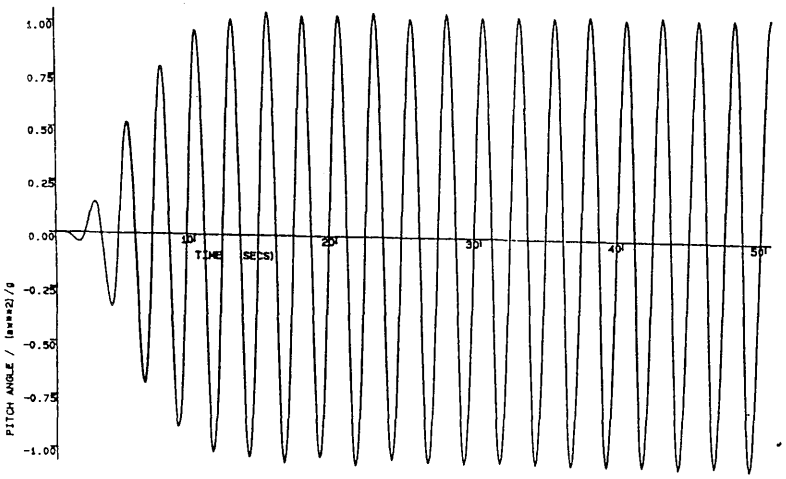

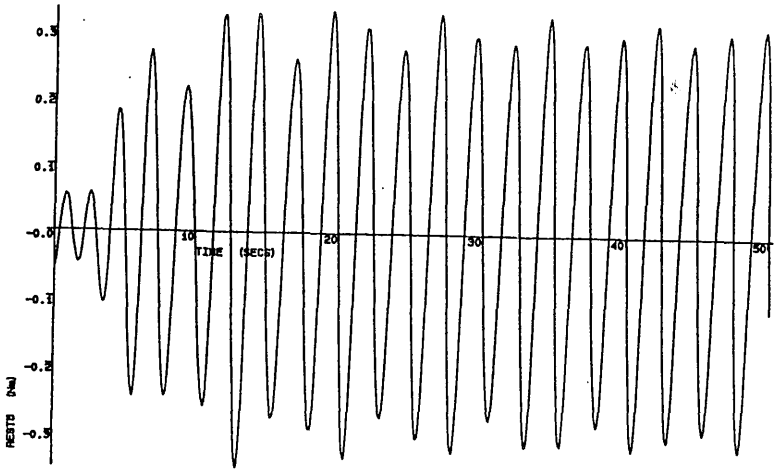

U = 0 m/s w = 2.5 rad/s

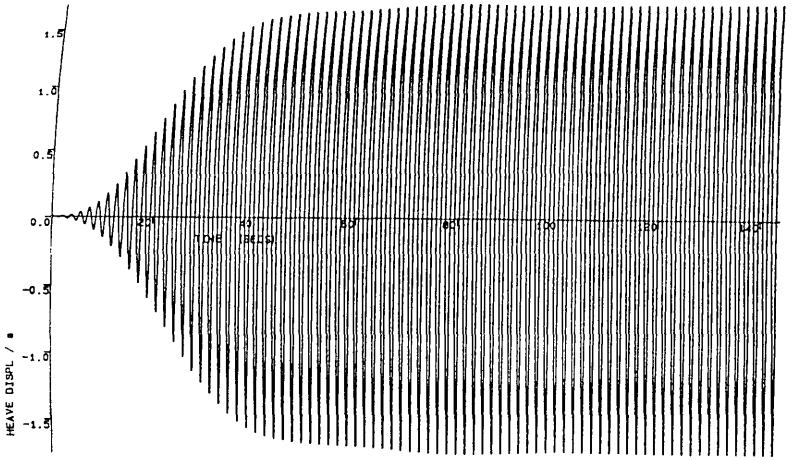

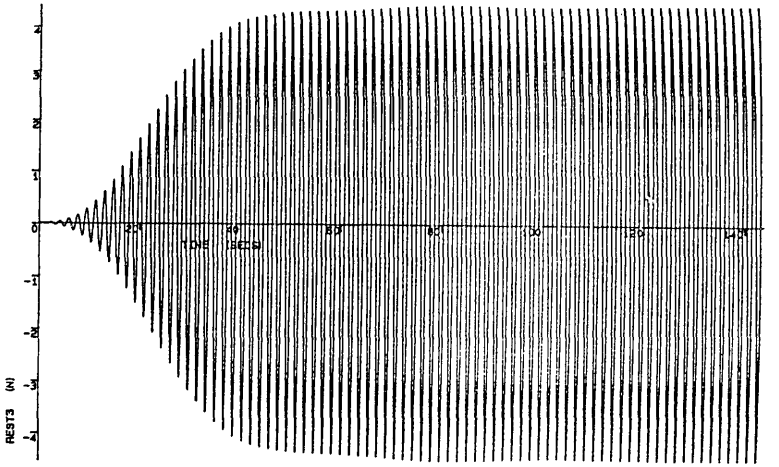

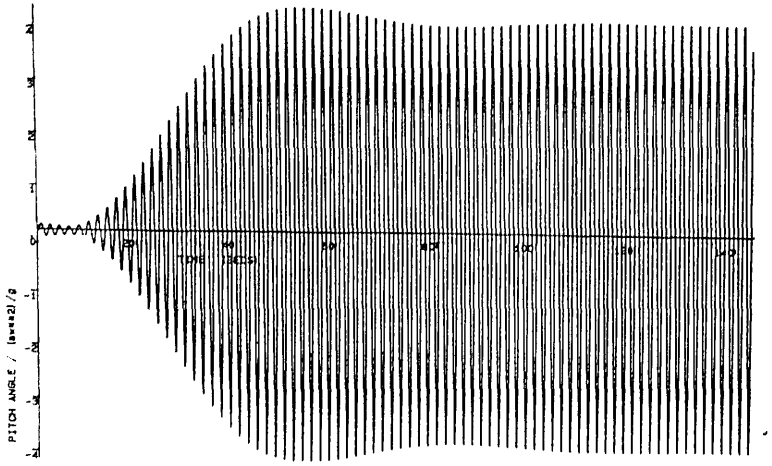

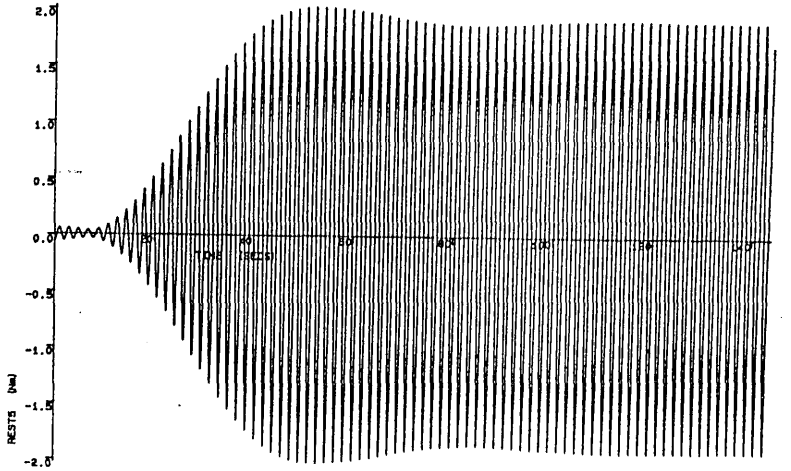

U = 0 m/s w = 3.5 rad/s

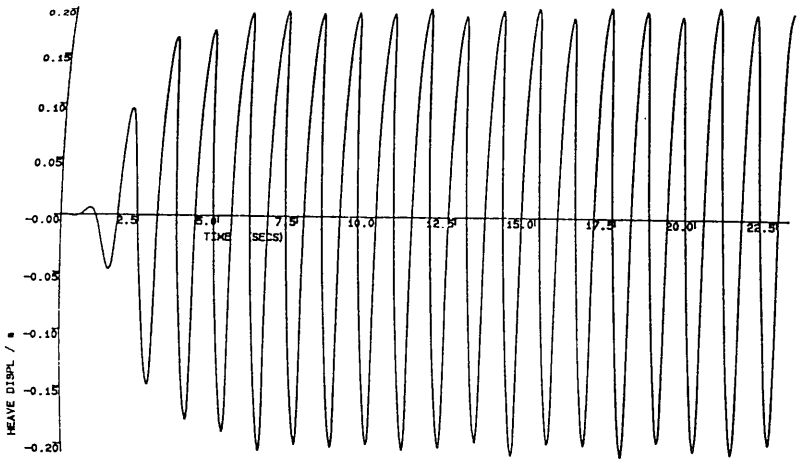

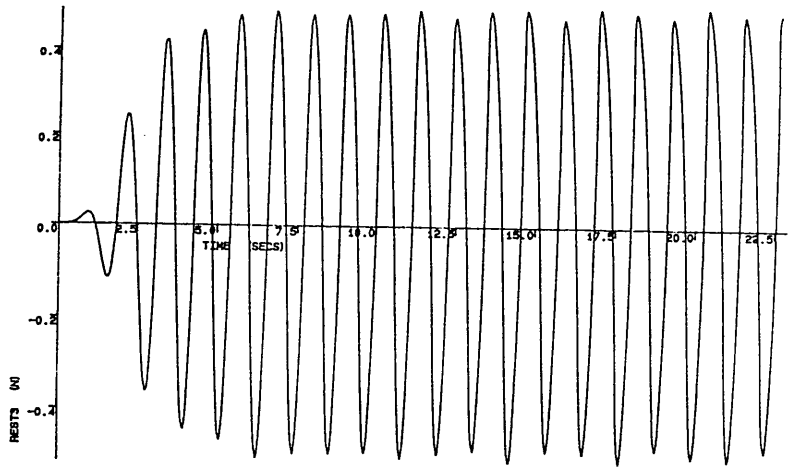

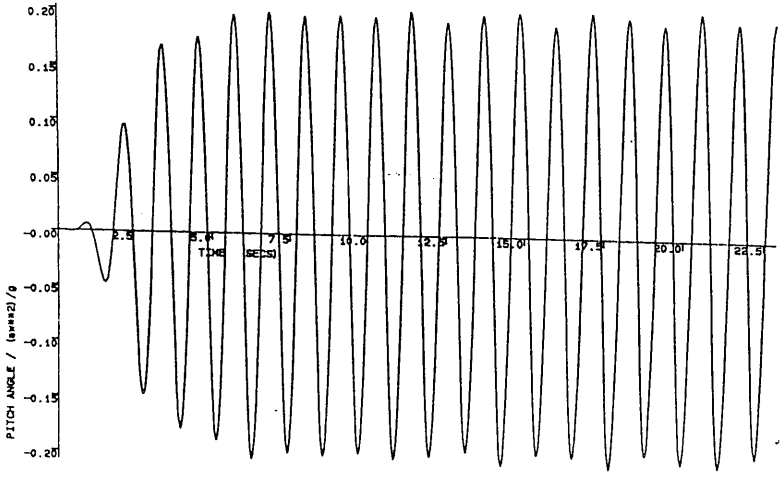

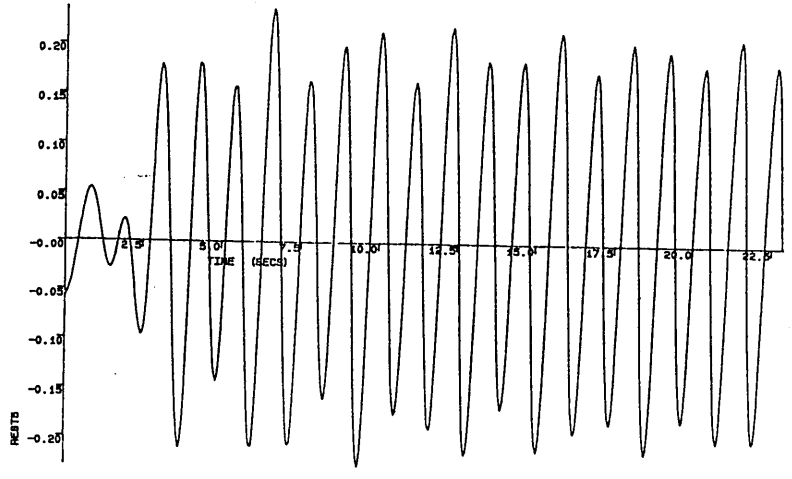

U = 0 m/s $\bar{w}$ = 5.5 rad/s

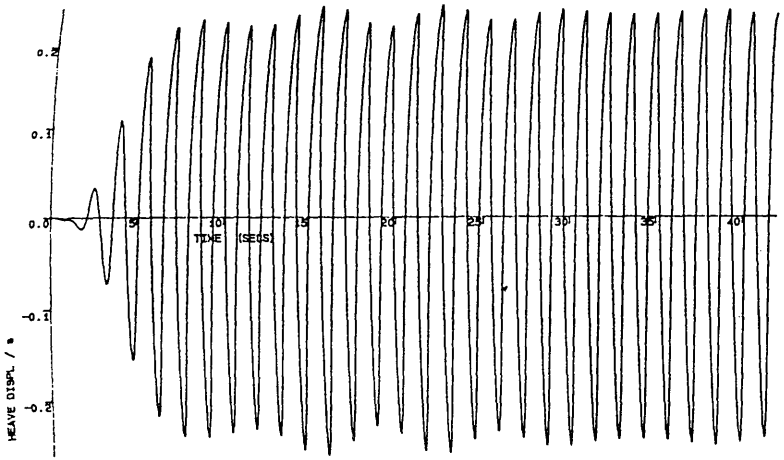

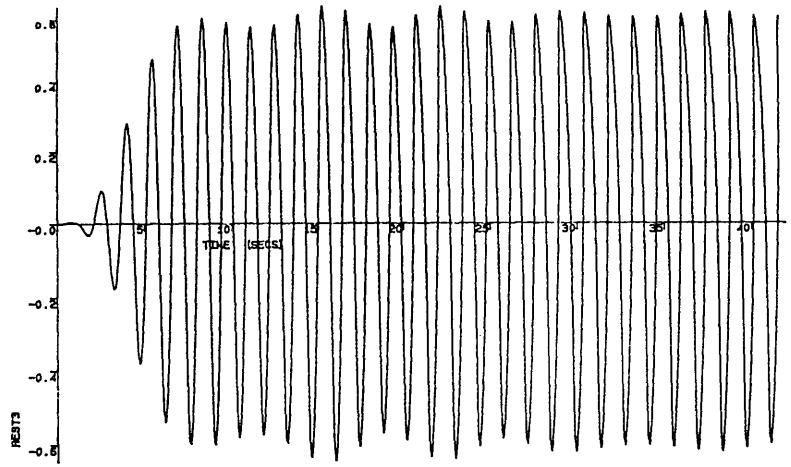

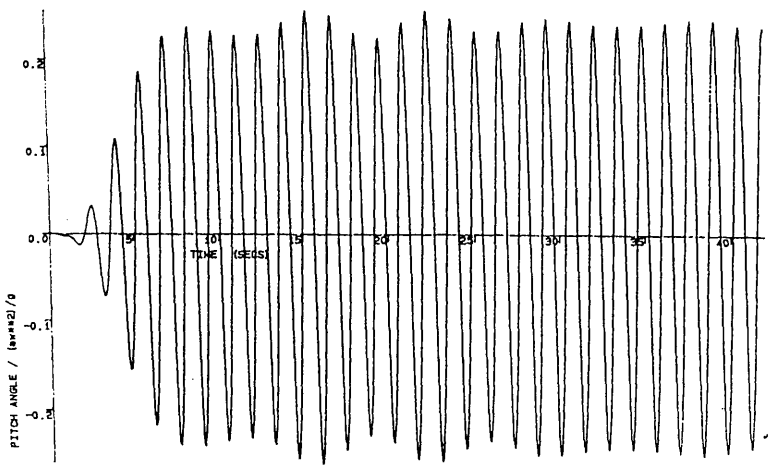

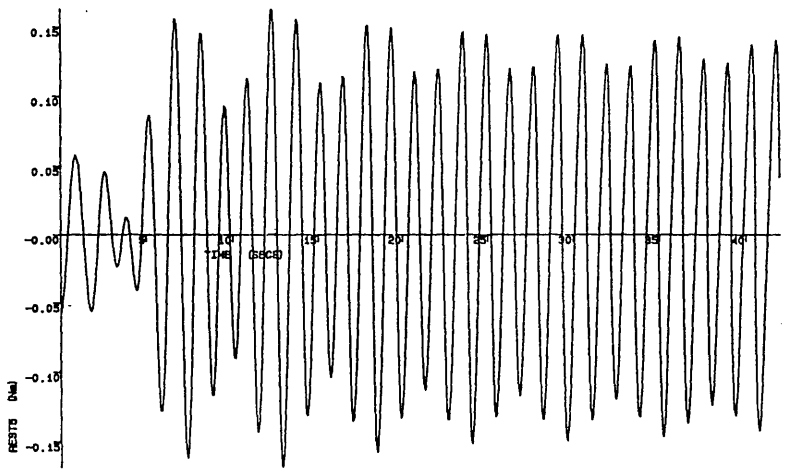

U = 0 m/s w = 4.5 rad/s

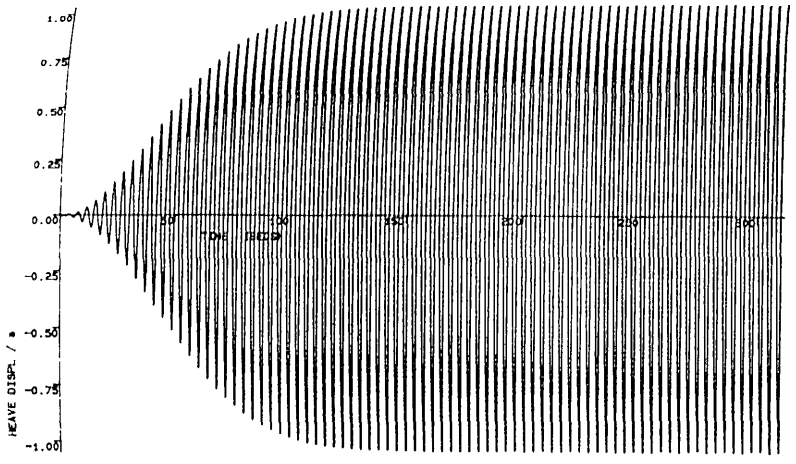

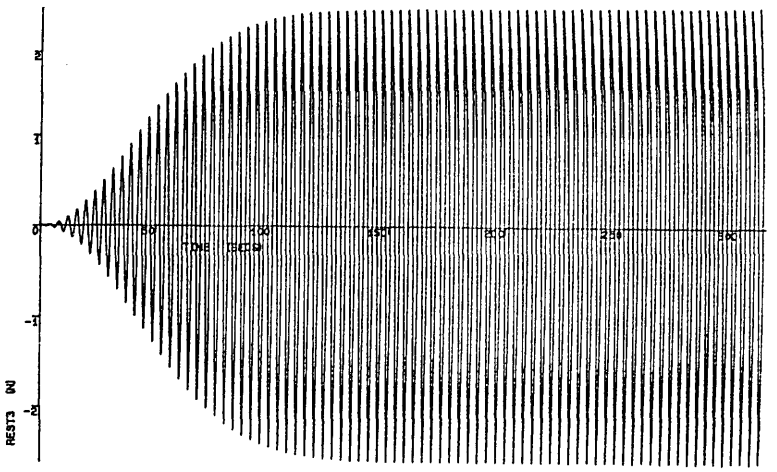

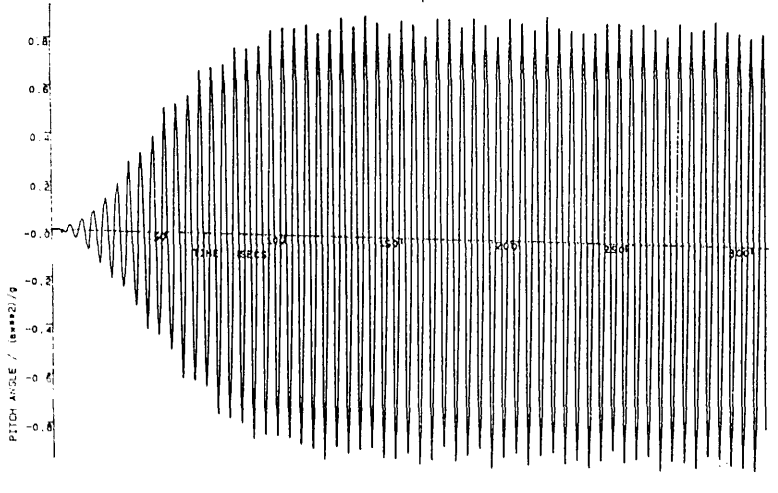

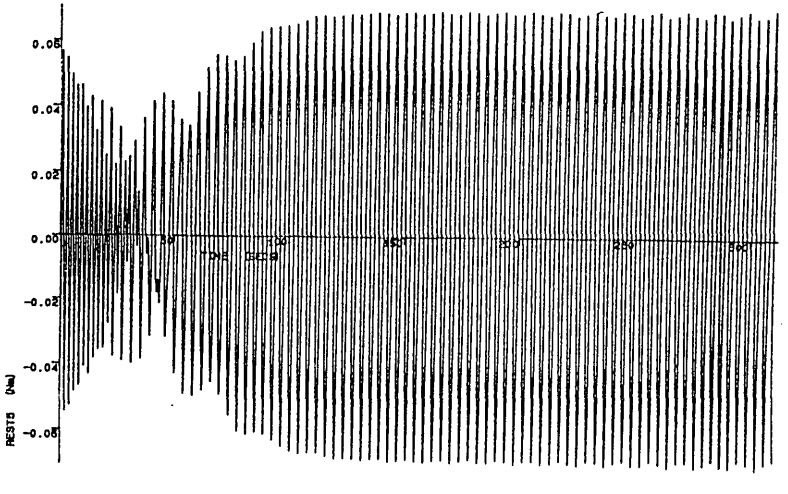

U = 0.5 m/s w = 1.5 rad/s

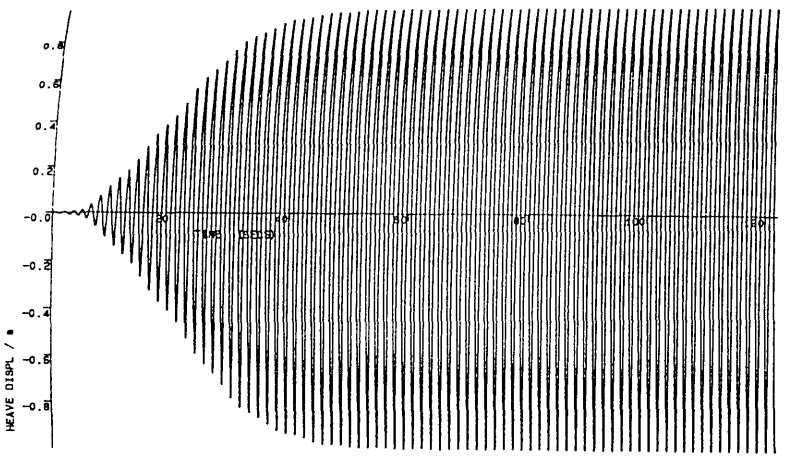

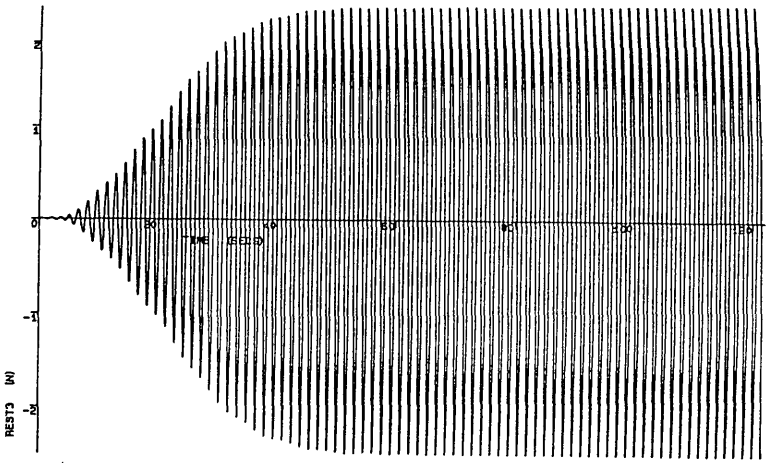

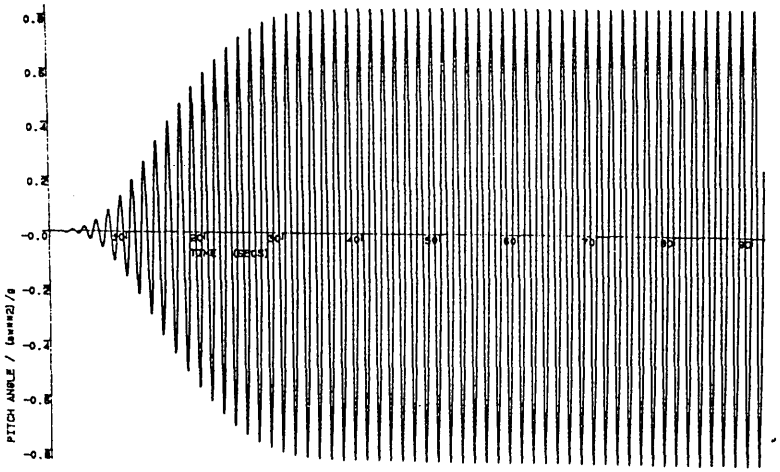

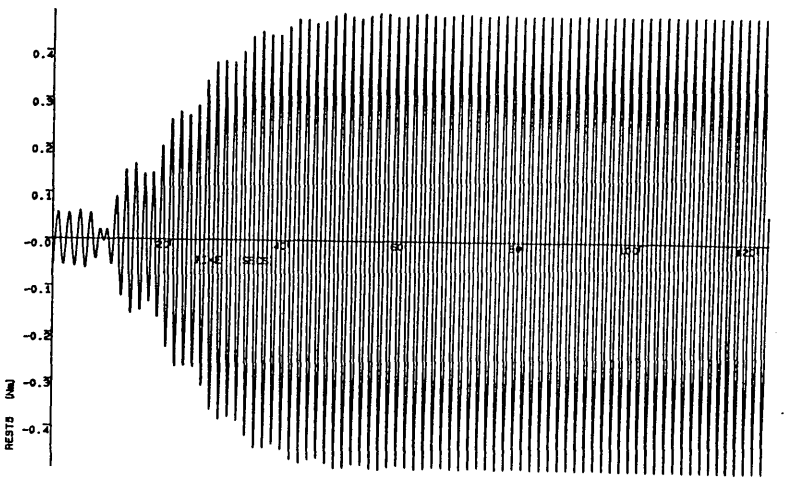

U = 0.5 m/s w = 3.5 rad/ s

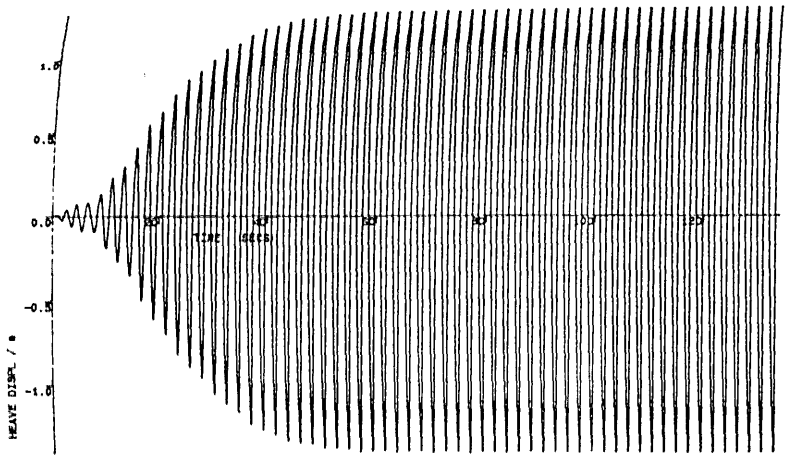

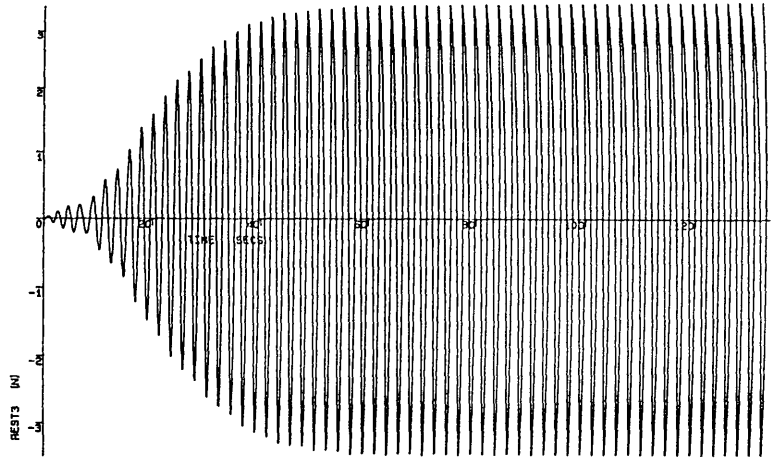

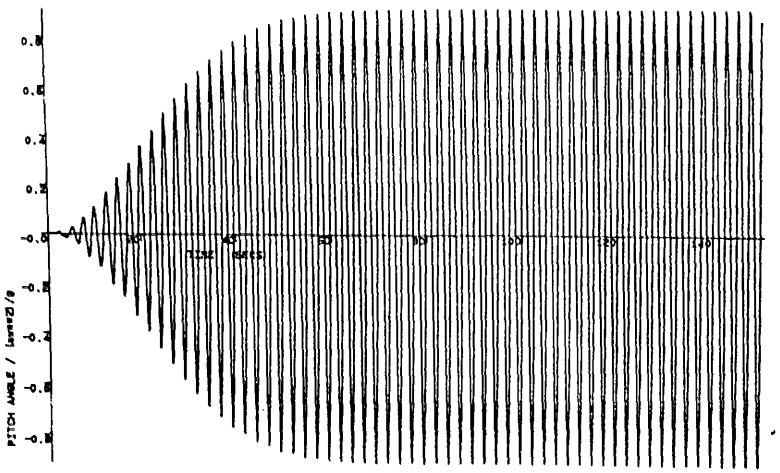

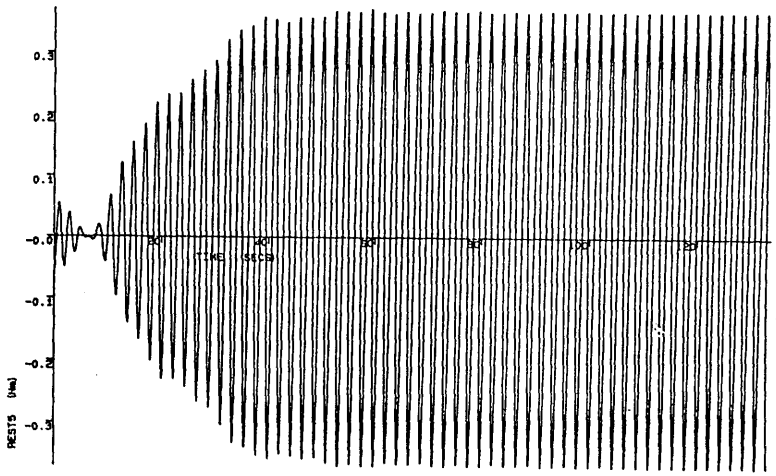

U = 0.5 m/s w = 2.5 rad/s

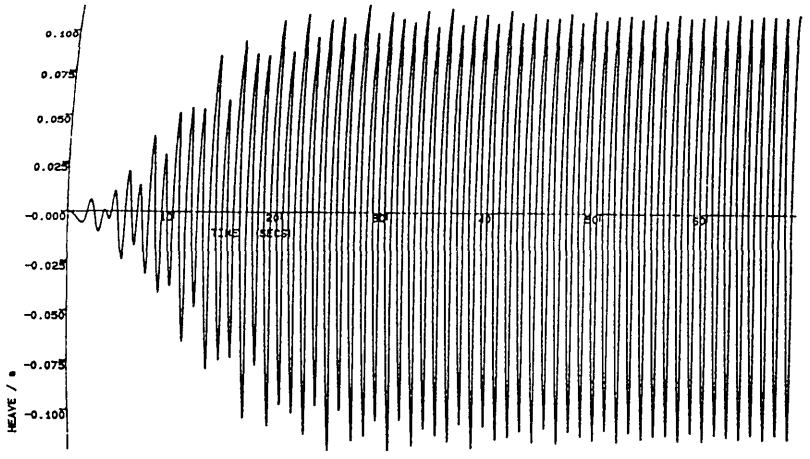

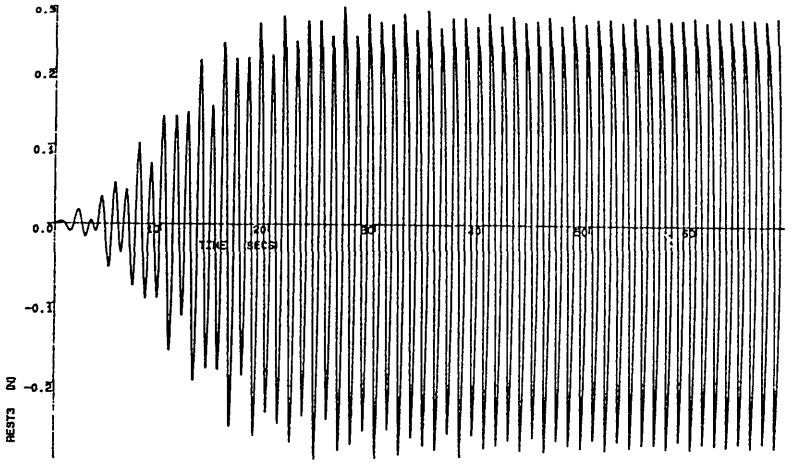

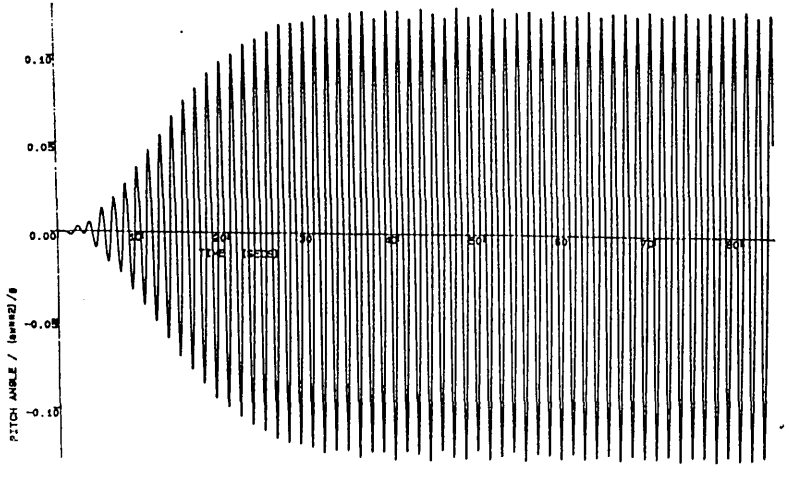

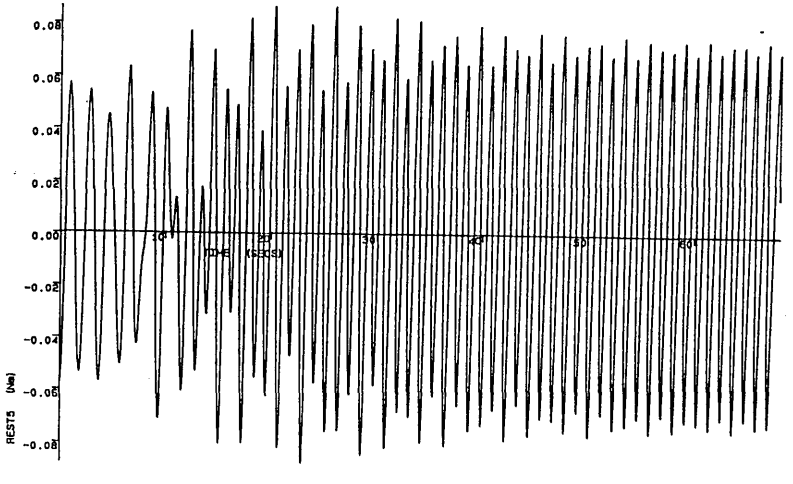

U = 0.5 m/s w = 4.5 rad/s

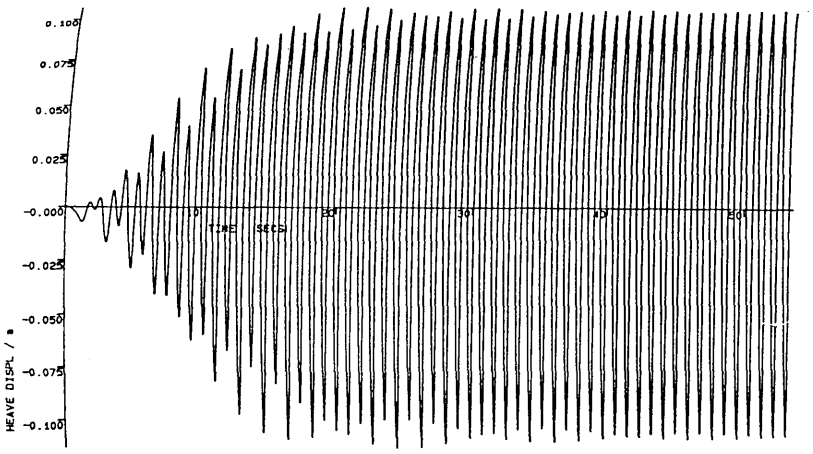

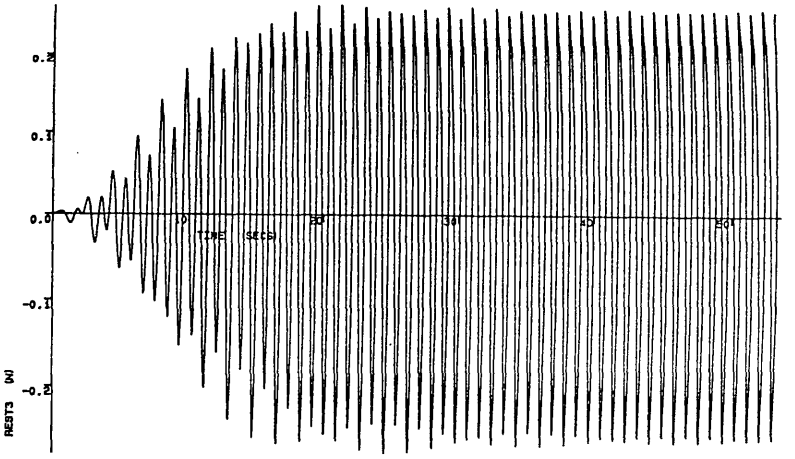

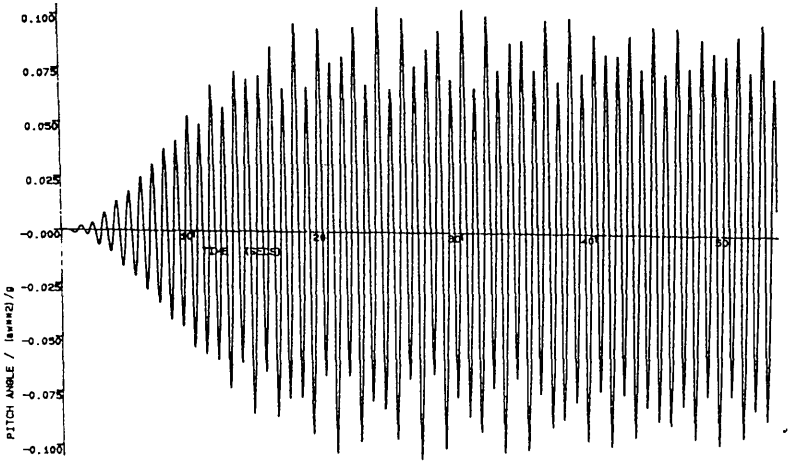

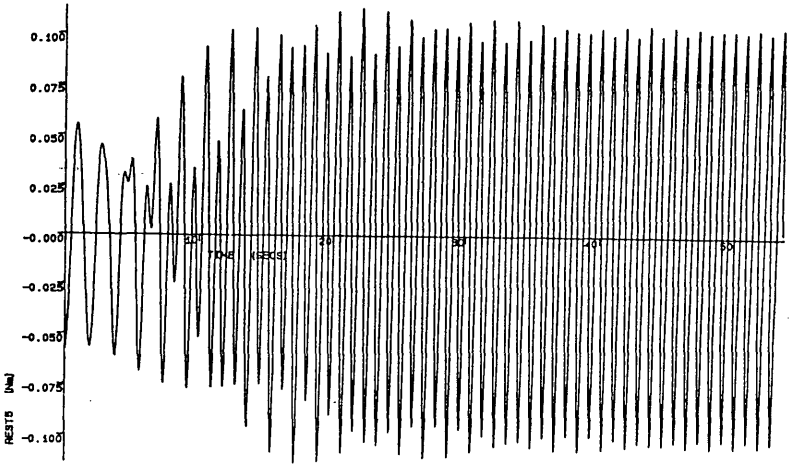

U = 0.5 m/s w = 5.5 rad/s

Figures 5.9 Time Domain Solution (Non-Linear Hydrostatic Restoring) Compared with Frequency Domain Solutions

SWATH11, 0.0 and 0.5 ms^{-1}

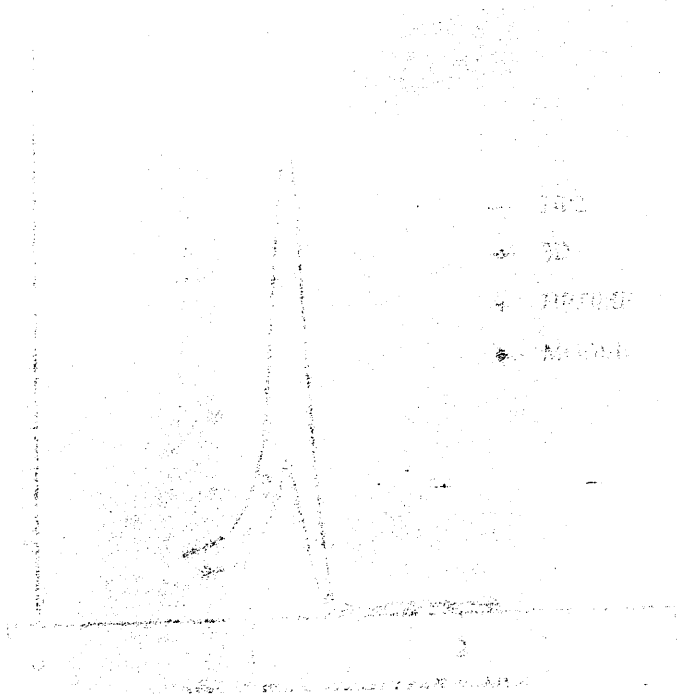

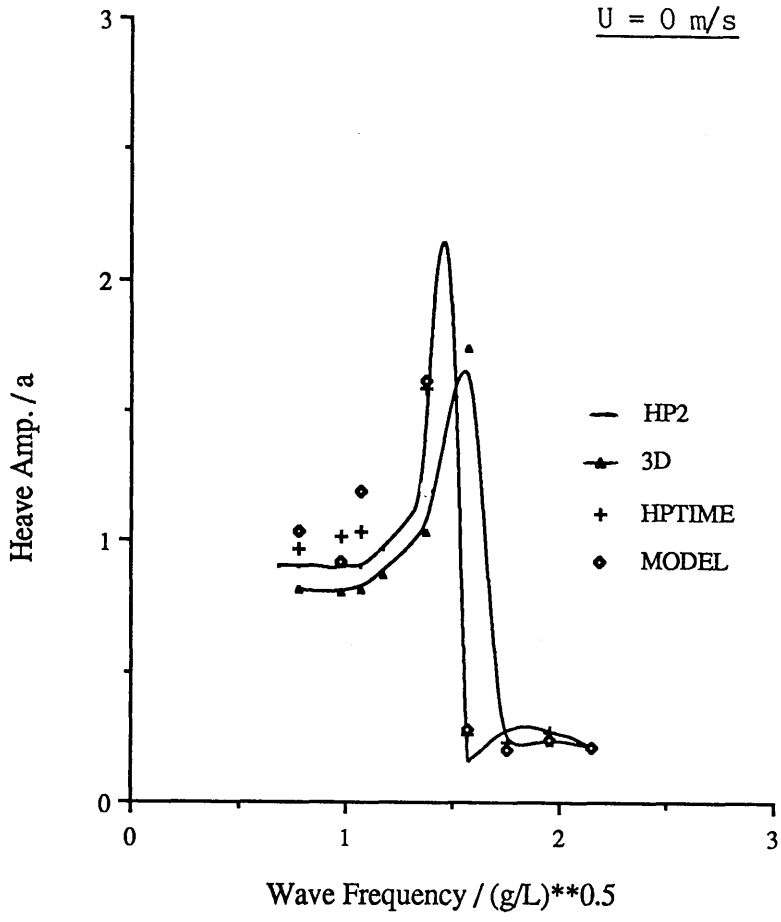
U = 0 m/s
Heave Amp. / a
Wave Frequency / (g/L)**0.5
HP2
3D
HPTIME
MODEL
0
1
2
3

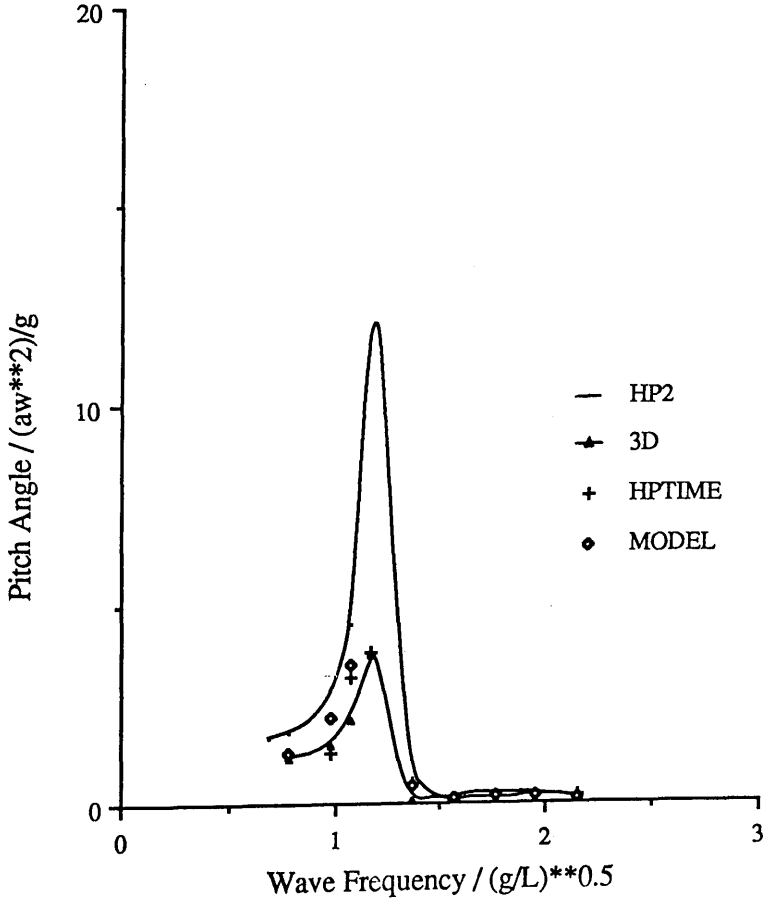
Pitch Angle / (aw**2)/g
Wave Frequency / (g/L)**0.5
HP2
3D
HPTIME
MODEL
0
10
20
1
2
3

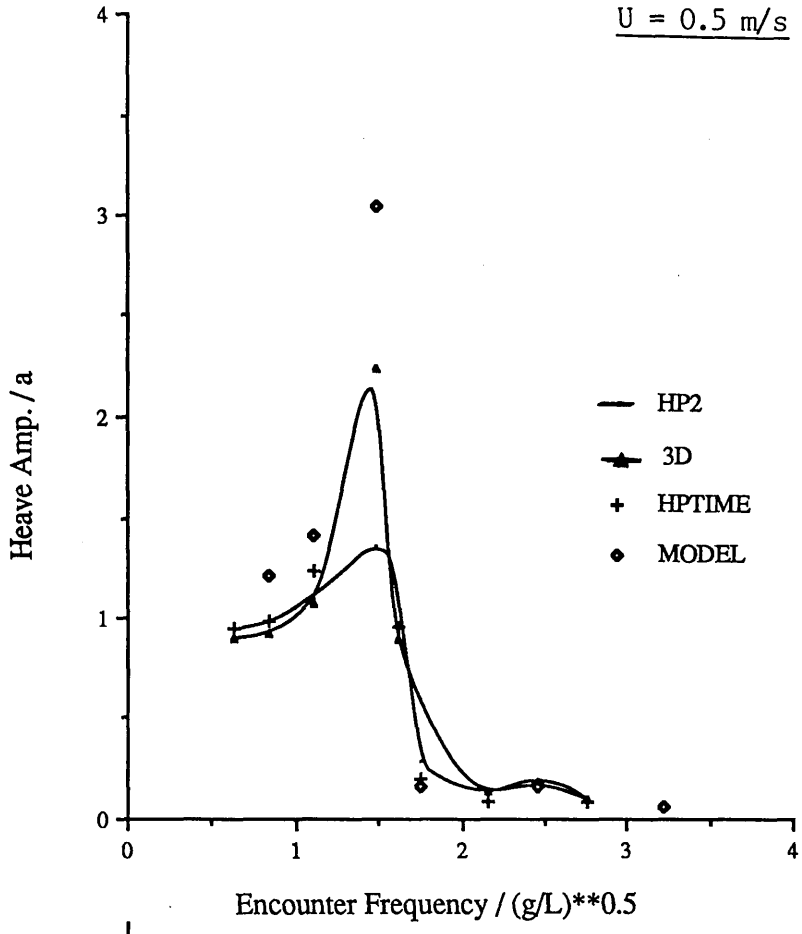
U = 0.5 m/s
Heave Amp. / a
HP2
3D
HPTIME
MODEL
Encounter Frequency / (g/L)**0.5

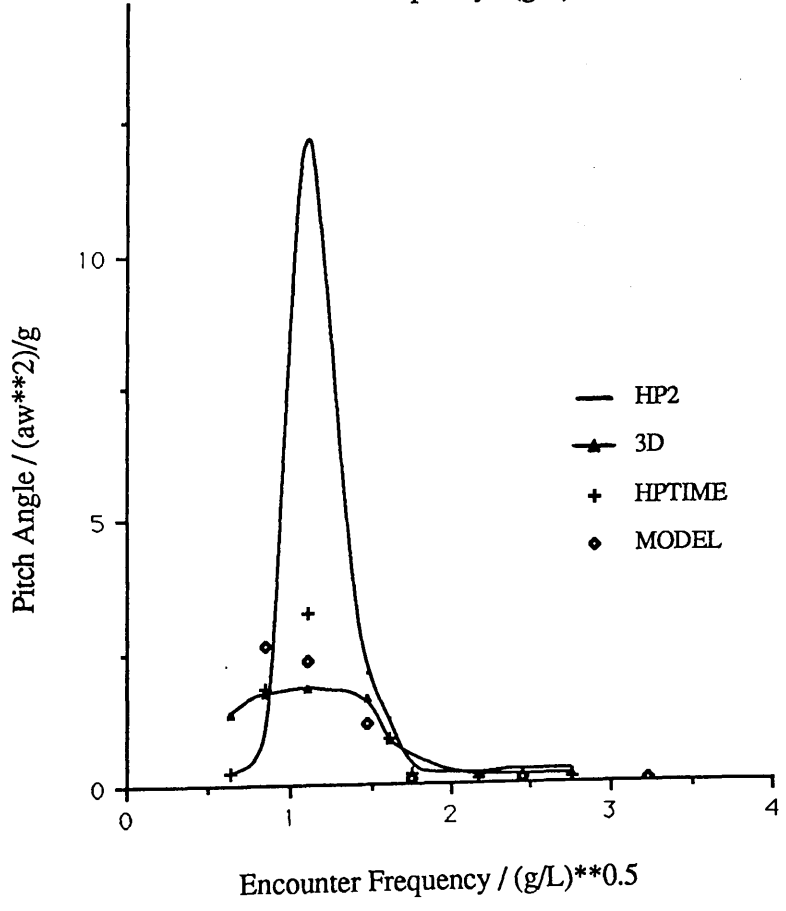
Pitch Angle / (aw**2)/g
HP2
3D
HPTIME
MODEL
Encounter Frequency / (g/L)**0.5

CHAPTER 6

FURTHER DEVELOPMENTS

Additional important non-linear effects will have to be analysed for a full investigation of the behaviour of SWATH vessels. Phenomena which the designer of SWATH vessels cannot afford to ignore include the occurence of cross deck structure slamming and the influence of fin stabiliser control systems. These are discussed in the following with regard to their incorporation into the time domain simulation.

6.1 Fin Stabiliser Motion Control

When travelling at certain angles of trim, all vessels experience a de-stabilising pitch moment known as the 'Munk' moment. This effect is of little concern in the case of conventional mono-hull ships which, because of their large water-plane areas, possess more than adequate hydrostatic pitch restoring characteristics. In such cases the Munk moment is overwhelmed and the vessel remains stable.

For SWATH ships however, the de-stabilising effect is strongly felt. The essence of the concept is its small waterplane area and as a consequence its hydrostatic restoring characteristics in pitch are small. In short a SWATH ship can be described as tender in pitch and it will remain so for large pitch angles.

For this reason , SWATH vessels are prone to large periods of pitch, excessive trim angles and ultimately pitch instability, when operating beyond certain threshhold forward speeds. Such conditions can lead to catastrophic pitch-poling. Additional hazards can occur in severe seas, where it is possible for the vessel to encounter waves of sufficient amplitude to cause slamming on the underside of the cross-deck structure.

SWATH ship safety is obviously jeopardised by these phenomena. Measures to avoid such problems can be taken by introducing stabililising fins. Their effect is to

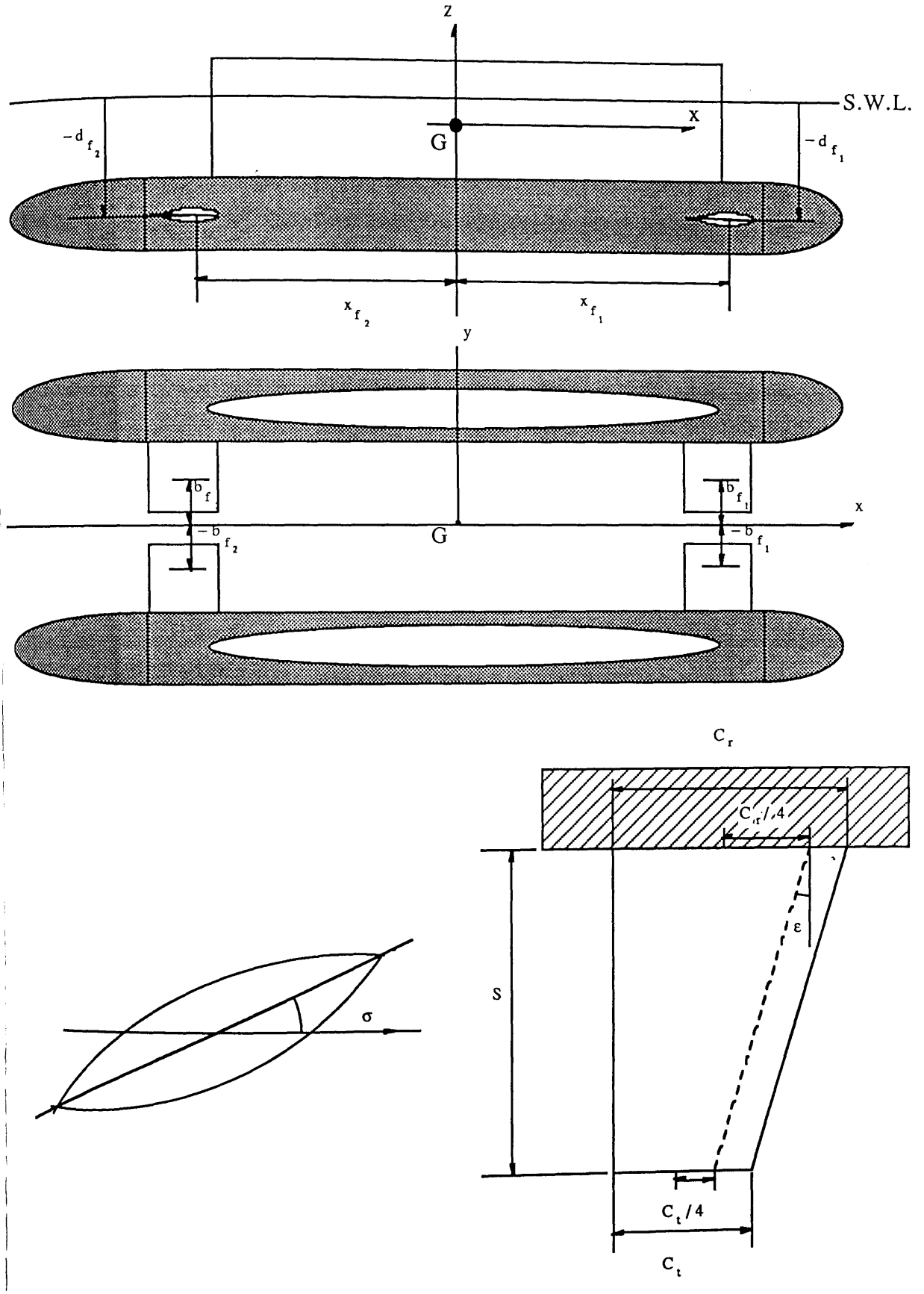

Figure 6.1 Fin Configuration and Notation

contribute to the total pitch restoring moment in a manner analougous to the role of aircraft tail wings. Stabilising fins provide further benefits by contributing to damping in heave, pitch and roll modes modes of motion. If controlable pitch fins are fitted, then further improvements on the allready good seakeeping behaviour of SWATH ships can be acheived.

In previous studies(11) (23) fin effects on SWATH motions have been modelled using frequency domain analysis . In these works the non-linearities of the effect are coped with by applying linearisation assumptions.

To enable the detailed design of SWATH fin -stabiliser control systems, it is important to have a good analytical model which can predict the effects of the non-linear fin control forces. The time domain SWATH motion simulation provides a good means for carrying out such analysis.

A suggested approach to including fin effects into the simulation is described below. The wave excitation and hydrodynamic coefficient corrections given are linearised terms which are used as illustration.

6.11 Theoretical Model

The total force acting on controlable fins which oscillate at the same frequency as the encountered wave can be devided into three components :

(i) the lift force ,

(ii) the inertia force and

(iii) the cross-flow drag force.

Mathematical expressions for these force components can be used to modify the coupled differential equations of motion which may then be solved to yield correspondingly modified heave and pitch responses.

The expressions described which represent the three effects are based on slender body theory. This takes into account pontoon-hull interactions but neglects free

surface effects and assumes that the fully submerged fins have a low aspect ratio.

For the head seas case, the vertical velocity w_z of an incident harmonic wave at the positon (x,y,z) on the submerged hulls is given as :

$$w_z = -i\omega a \exp\left(k_0 z + ik_0 x \cos\mu - ik_0 y \sin\mu\right) e^{-i\omega t} \quad (6.1)$$

where ω, a and k_0 are the incident wave frequency, the wave amplitude and the wave number respectively. μ is the wave heading angle, which is 180 degrees for the head sea case.

Referring to the diagrams given in figure 6.1 the relative vertical velocity of each control fin ,V_{zf} is given as :

$$V_{zf} = \dot{S}_3 - x_f \dot{S}_5 - w_z \quad (6.2)$$

and the fin angle of attack due to the controllable fin angle 'γ'and the heave and pitch motions as :

$$\sigma = \gamma + S_5 + \tan^{-1}\left(\frac{\dot{S}_3 - x_f \dot{S}_5 - w_z}{U}\right) \quad (6.3)$$

(i) Lift Force component

The lift force generated by flow parrallel to the fin chord can be expressed in the following form :

$$f_L = \frac{1}{2} \rho U^2 A_f C_{L\sigma} \sigma \quad (6.4)$$

where A_f is the fin face area and $C_{L\sigma}$ is the angle of attack dependent lift coefficient.

Some of the methods avaiable for determing lift coefficient values involve the use of empirical relationships which are based experimental data(25)

Adopting the method used by Lee and Curphey(11), the lift coefficient can be obtained as follows :

$$C_{L\sigma} = (K_{FH} + K_{HF})C_{L\sigma F} \tag{6.5}$$

where

$$K_{FH} = \frac{C_{L\sigma FH}}{C_{L\sigma F}} \tag{6.6}$$

$$K_{HF} = \frac{C_{L\sigma HF}}{C_{L\sigma F}} \tag{6.7}$$

The subscripts, FH and HF represent the hull induced lift component acting on the fin and the fin induced lift component acting on the hull respectively. F denotes the fin alone.

K_{FH} and K_{HF} are given by :

$$K_{FH} = \frac{2}{\pi(1-\delta)^2}\left[(1+\delta^4)\left\{\frac{1}{2}\tan^{-1}\frac{1}{2}\left(\frac{1}{\delta}-\delta\right)+\frac{\pi}{4}\right\} - \delta^2\left\{\left(\frac{1}{\delta}-\delta\right)+2\tan^{-1}\delta\right\}\right] \tag{6.8}$$

$$K_{HF} = \frac{1}{(1-\delta)^2}\left[(1-\delta^2)^2 - \frac{2}{\pi}\left[(1+\delta^4)\left\{\frac{1}{2}\tan^{-1}\frac{1}{2}\left(\frac{1}{\delta}-\delta\right)+\frac{\pi}{4}\right\} - \delta^2\left\{\left(\frac{1}{\delta}-\delta\right)+2\tan^{-1}\delta\right\}\right]\right] \tag{6.9}$$

with, $\delta = r / r_0$ where r is the hull radius at the fin position and r_0 is the transverse distaince between the hull centre-line and the fin tip

For low aspect ratio fins and given the that effective aspect ratio, A_e, the mean chord c_m and the sweep-back angle, ε are defined as :

$$A_e = \frac{r_0 - \frac{r^2}{r_0}}{c_m} \tag{6.10}$$

$$c_m = \frac{c_t + c_r}{2} \tag{6.11}$$

$$c_m = \frac{c_r - c_t}{4(r_0 - r)} \tag{6.12}$$

(where c_t and c_r are the tip and root chord lengths), it has been shown that the following empirical relationship gives a good approximation for $C_{L\sigma F}$

$$C_{L\sigma F} = \frac{1.8\pi A_e}{1.8 + \cos\varepsilon\sqrt{\frac{A_e^2}{\cos^4\varepsilon} + 4}} \tag{6.13}$$

(ii) Cross-flow Drag force

This component of the total fin force is due to the tendency of fins to shed voticies at their tip, an occurence which is sometimes referred to as 'tip-stall'.

The cross-flow drag f_D is given as :

$$F_D = \frac{1}{2}\rho A_f C_D(\dot{S}_3 - x_f\dot{S}_5 - w_z)\left|\dot{S}_3 - x_f\dot{S}_5 - w_z\right| \tag{6.14}$$

In frequency domain analysis , this expression is linearised using an equivelent linearisation approximation(11)

(iii) Inertia Force

Given that the mass m_f and athe added mass a_{33f} of a fin are obtained from the expressions :

$$m_f = \rho \frac{\pi}{4} s c t \tag{6.15}$$

$$a_{33f} = \rho \frac{\pi}{4} s c^2 \tag{6.16}$$

where s, c and t are the fin span, chord and maximum thickness
then the inertia force f_I generated by the fin due to the accelerations of heave and pitch motions is given as :

$$f_I = (m_f + a_{33f}) (\ddot{S}_3 - x_f \ddot{S}_5) \tag{6.17}$$

Total Force

Summating the three force components, each fin generates a total heave force given by

$$f_T = f_L + f_D + f_I \tag{6.18}$$

The net contribution to the vessel's restoration in the heave mode, F_T can be obtained by summating the total forces generated by each of its stabilising fins.

If there are 'n' fins on each hull then this is given as :

$$F_T = \sum_{j=1}^{n}\Bigg[\frac{\rho}{2}U^2 A_{fj} C_{L\sigma j}\left(2S_5 + \frac{2\left(\dot{S}_3 - x_{fj}\dot{S}_5\right)}{U} - \frac{w_z(b_j) + w_z(-b_j)}{U}\right)$$

$$+ \frac{\rho}{2} A_{fj} C_{Dj}\Big\{\left(\dot{S}_3 - x_{fj}\dot{S}_5 - w_z(b_j)\right)\left|\dot{S}_3 - x_{fj}\dot{S}_5 - w_z(b_j)\right|$$

$$+ \left(\dot{S}_3 - x_{fj}\dot{S}_5 - w_z(-b_j)\right)\left|\dot{S}_3 - x_{fj}\dot{S}_5 - w_z(-b_j)\right|\Big\}$$

$$+ 2\left(m_{fj} + a_{33fj}\right)\left(\ddot{S}_3 - x_{fj}\ddot{S}_5\right)\Bigg] \qquad (6.19)$$

$w_z(b_j)$ and $w_z(-b_j)$ are the incident wave velocities at the port and starboard fin locations shown in figure 6.1

The all important pitch restoring moment, M_T is obtained by summing the moments of each constituant fin heave force, f_{Tj}:

$$M_T = \sum_{j=1}^{n} x_{fj} f_{Tj} \qquad (6.20)$$

In linear motions analysis, fin forces can be incorporated into the coupled heave and pitch equations by modifying the wave excitation terms and by applying the corrections given in table 6.1 to the vessel's hydrodynamic coefficients. Relative wave velocities of the fore and aft fins are represented by V_{zf1} and V_{zf1} respectively. These can be obtained using equation (6.2)

$$A_{33} = 2\,(m_{f1} + a_{33f1}) + 2\,(m_{f2} + a_{33f2})$$

$$A_{35} = -2x_{f1}\,(m_{f1} + a_{33f1}) - 2x_{f2}\,(m_{f2} + a_{33f2})$$

$$A_{53} = -2x_{f1}\,(m_{f1} + a_{33f1}) - 2x_{f2}\,(m_{f2} + a_{33f2})$$

$$A_{55} = -2x_{f1}^{2}\,(m_{f1} + a_{33f1}) + 2x_{f2}^{2}\,(m_{f2} + a_{33f2})$$

$$B_{33} = \rho A_{f1} U C_{L\sigma 1} + \frac{4}{3\pi}\rho A_{f1} C_{D1}\left[V_{zfs1} + V_{xfp1}\right]$$

$$+\rho A_{f2} U C_{L\sigma 2} + \frac{4}{3\pi}\rho A_{f2} C_{D2}\left[V_{zfs2} + V_{xfp2}\right]$$

$$B_{35} = -x_{f1}\rho A_{f1} U C_{L\sigma 1} - x_{f1}\frac{4}{3\pi}\rho A_{f1} C_{D1}\left[V_{zfs1} + V_{xfp1}\right]$$

$$-x_{f2}\rho A_{f2} U C_{L\sigma 2} - x_{f2}\frac{4}{3\pi}\rho A_{f2} C_{D2}\left[V_{zfs2} + V_{xfp2}\right]$$

$$B_{53} = -x_{f1}\rho A_{f1} U C_{L\sigma 1} - x_{f1}\frac{4}{3\pi}\rho A_{f1} C_{D1}\left[V_{zfs1} + V_{xfp1}\right]$$

$$-x_{f2}\rho A_{f2} U C_{L\sigma 2} - x_{f2}\frac{4}{3\pi}\rho A_{f2} C_{D2}\left[V_{zfs2} + V_{xfp2}\right]$$

$$B_{55} = x_{f1}^{2}\rho A_{f1} U C_{L\sigma 1} + x_{f1}^{2}\frac{4}{3\pi}\rho A_{f1} C_{D1}\left[V_{zfs1} + V_{xfp1}\right]$$

$$+x_{f2}^{2}\rho A_{f2} U C_{L\sigma 2} + x_{f2}^{2}\frac{4}{3\pi}\rho A_{f2} C_{D2}\left[V_{zfs2} + V_{xfp2}\right]$$

$$C_{35} = \rho U^{2} A_{f1} C_{L\sigma 1} + \rho U^{2} A_{f2} C_{L\sigma 2}$$

$$C_{55} = -x_{f1}\rho U^{2} A_{f1} C_{L\sigma 1} - x_{f2}\rho U^{2} A_{f2} C_{L\sigma 2}$$

Table 6.1 Corrections Applied to Hydrodynamic and Hydrostatic Coefficients due to Fin Effects

Linearised corrections, F_{3f} and F_{5f}, applied to the heave exciting force and pitch exciting moments respectively are given as follows :

$$F_{3f} = -i\rho\,\omega_e\,a\,U\sum_j A_{fj}\,C_{L\sigma j}\,e^{k_o(-d_j + ix_{fj}\cos\mu - ik_o b_j \sin\mu)}$$

$$- i\rho\,\frac{4}{3\pi}\,\omega_e\,a\sum_j A_{fj}\,C_{Dj}\,e^{k_o(-d_j + ix_{fj}\cos\mu)}$$

$$\left(V_{zfsj}\,e^{ik_o b_j \sin\mu} + V_{zfpj}\,e^{-ik_o b_j \sin\mu}\right) \qquad (6.21)$$

and

$$F_{5f} = -x_{fj}\,F_{3f} \qquad (6.22)$$

Linearisation is not required in the time domain. Non-linearities could be introduced partially at first, by suitably modifying lift and drag coefficients and fin added mass values at each time step to correspond with the instantaneous, relative motions of the fin system.

6.12 Fin Algorithm for 'HPTIME'

Figure 6.2 shows the core solution subroutine TDSOL of the coupled heave and pitch time domain program HPTIME.

As described earlier in the study the subroutine FCN is used to control the motions system reconditioning at each simulation time-step. In addition to the computations carried to account for the non-linear effects assessed in this study, a further fin algorithm , 'FIN' is shown. It is assumed that the geometry and location of

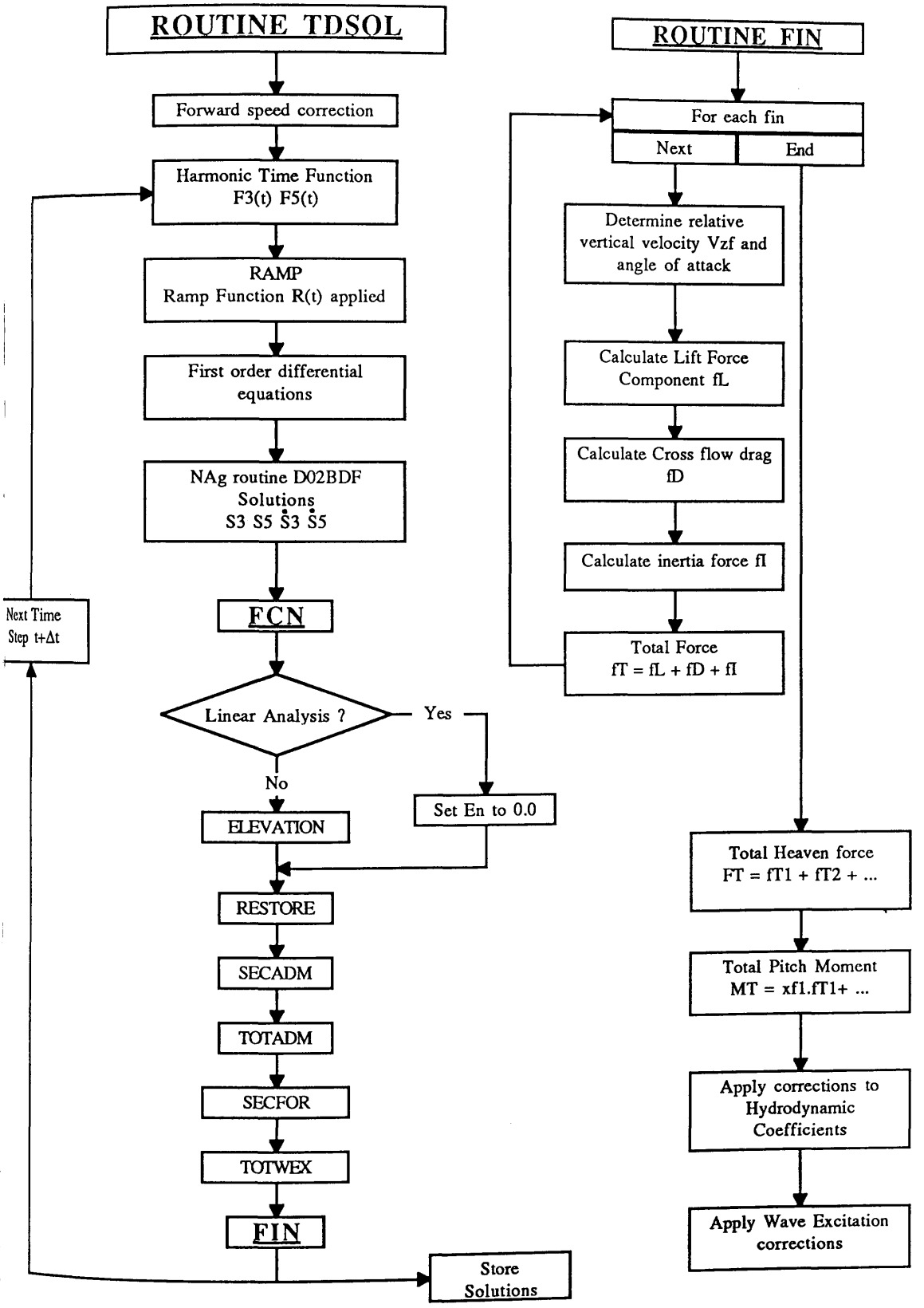

Figure 6.2 Control Fin Algorithm for 'HPTIME'

each control fin is known and that their controlable pitch oscillations are phased correctly to provide positive vessel pitch motion restoration.

Each fin is assessed in turn at each simulation time step. From the histories of the vessel and fin oscillations the instantaneous relative vertical velocity and the fin angle of attack are established. The component lift, cross-flow drag and inertia force components are then calculated and summed to give the total fin force f_T. Values obtained for each fin, are used to determine the total contributions to heave force and pitch moment, F_T and M_T. Suitable corrections are then applied to the motion coefficients and wave excitation terms. These are then returned to FCN and used to obtain solutions for the next simulation time-step.

The performances of different fin stabiliser control systems could eventually be assessed using a version of the program developed in this manner. Such a development would enable the Naval Architect to select an optimum motion control system and feel confident that his SWATH will give a smooth ride.

6.2 Cross Structure Slamming

One of the drawbacks of the SWATH vessel concept is vulnerability to sustaining wave impacts on the underside of its cross-deck structure. Although avoiding action such as speed and heading changes can be taken when operating in sea conditions which cause problematic slamming, it is important to develop methods for assessing the phenomenon so that the tendencies for new SWATH designs to slam can be minimised.

Wave impacts caused by slamming can result in substantial cross-structure loading.which , in turn result in problems concerning local strength, structural fatigue and crew/passenger discomfort.

Analytical techniques are required so that the designer can establish the conditions under which wave impacts occur and can determine the design parameters which have most significant effect on slamming behaviour. Such techniques provide the facility to

predict the magnitude and distribution of wave impact loading. With this information, structural scantlings can be optimised and the ability of the new design to meet specified seakeeping criteria can be assessed.

6.21 Theoretical Approach

For a slam to occur, the contact between the wave surface and the cross-structure underside must exceed a certain threshold relative velocity and the angle of contact must be sufficiently small.

The vertical impact force at the wave impact location can be described as the rate of change of fluid momentum for the wetted area of contact. However the total vertical force due to a slam occurrence includes a buoyant force term due to the immersion of the cross-structure. The buoyant force component can be obtained by integrating the volume of immersion during the slam.

Peak impact loads can be calculated by applying empirical relationships obtained from drop-test data (references 15-22). Alternatively, theoretical models have been developed for determining impact force distributions(49)

In the theory presented by Kaplan for predicting the wave impact component of slamming loads on SWATH type cross-structures.(14) , it can be seen that it is necessary to determine the motion characteristics at the impact location. Velocities and accelerations can be obtained using the pre-slam vessel and wave motions time histories and by assuming average values in the slam force region.

Implementing a slam force model of this nature into the time domain simulation will involve introducing a number of additional calculation steps for the time period of the slam duration. These steps will involve using the relative motions to establish the point of contact and the extent of immersion so that the instantaneous buoyancy and impact components can be calculated. The total slam force can then be resolved in the vertical and horizontal directions to obtain values for the transient slam forces and moments effecting heave and pitch motions. Solution of the motion equations will yield modified relative motions which can then be used to modify the nature of the slam force accordingly.

6.22 Wave Impact Forces

By assuming that the SWATH slam will be similar to a flat plate impacting the water surface, the peak impact pressure can be expressed as (30) :

$$p_{max} = \frac{1}{2}\rho C_n \dot{S}_R^2 \qquad (6.1)$$

The velocity of the structure flat surface S_R relative to the water surface is given by :

$$\dot{S}_R = \frac{(V_x + w_x)\sin S_5 + (V_x + w_x)\cos S_5}{\sin S_5} \qquad (6.2)$$

where V and w are the vessel impact point and wave orbital velocities respectively and x and z denote their components in the horizontal and vertical directions. Drop test empirical relationships such as those derived by Chuang and Milne[17] are required for determining S_R when the solution to (6.2) becomes infinity at the pitch angle, $S_5 = 0$.

From equation (6.1) and given the wetted area of slam impact 'A_S', the impact load normal to the flat structure surface can be written as :

$$F_n = \frac{1}{2}\rho A_S C_n \dot{S}_R^2 \qquad (6.3)$$

The average normal load coefficient C_n can be obtained from experimental data which has been presented in the the form of C_n curves plotted against wetted length.[31]

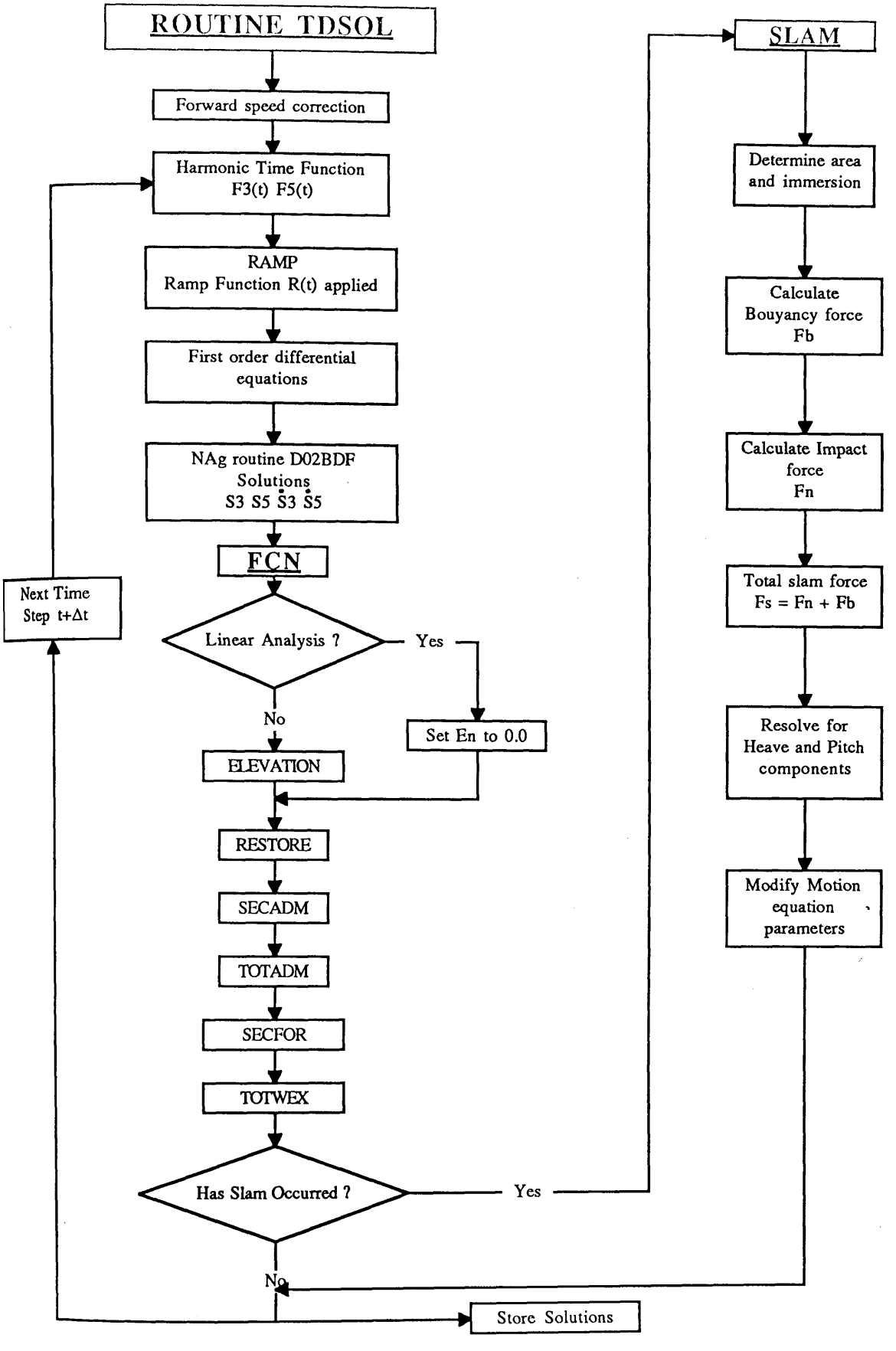

Figure 6.3 Slamming Algorithm for 'HPTIME'

6.23 Slamming Algorithm for HPTIME

This section suggests an approach to incorporating the effects of cross structure slamming into the coupled heave and pitch motion simulation. It is assumed that details of the cross-structure geometry are available and that the only out of balance forces and moments during a slam are due to the impact load and the immersion buoyancy force.

Figure 6.3 shows TDSOL, the core time domain solution routine. Computations are performed at each simulation time step to account the non-linear hydrodynamic and hydrostatic effects presented in this study. These computations are controlled from the subroutine FCN as described earlier. Additional calculations to implement the occurrence of a slam into the simulation are illustrated.

At each simulation time step the vessel's motion displacements and velocities S_3, $\dot{S}_3$, S_5 and $\dot{S}_5$ and the wave profile are known. In the system reconditioning subroutine FCN these values are used to establish whether or not a slam has occurred. Within a new subroutine 'SLAM' the wetted surface area A_S, immersed volume and impact velocity S_R are determined. The buoyancy force component, F_b is then calculated and the impact component, F_n obtained using equation (6.3) and a suitable value for the normal load coefficient. The total slam force given by :

$$F_S = F_b + F_n \tag{6.4}$$

is resolved to obtain heave force and pitch moment components. These values are installed in the motion equations which are solved for the next simulation time step at t + dt. It is assumed, in this model, that the impact component acts throughout the slam duration.

CONCLUDING REMARKS

The important findings of this study and some noteworthy considerations regarding further development work are summarised in the following.

(i) Study Objectives

The aim of this study, "...to develop a theoretical model for predicting the coupled heave and pitch motions of SWATH vessels in the time domain" has been successfully achieved.

In addition, by considering three time dependent effects in turn, an approach to incorporating motion non-linearities has been established.

From here, the simulation technique presented can be further developed to model additional, significantly non-linear, characteristics of SWATH motions. The influence of control fins and the occurrence of cross structure slamming are among the principle concerns during the design of SWATH ships. Methods for introducing these effects have been suggested. With the essential ground work completed, their implementation is expected to be a relatively straight-forward task.

(ii) Prediction Improvements

It has been shown that with the inclusion of non-linear restoring effects, the time domain simulation can give predictions that agree more closely with model test measurements than those obtained from existing 2-D and 3-D frequency domain methods. Improvements of up to 5% of the linear analysis results have been observed for some lower wave frequency cases.The extent of these improvements is expected to be more significant in the analysis of SWATH ships which are of more seaworthy design than SWATH11.

(iii) SWATH11 Motions

This study has shown, that the displacement geometry of SWATH11 is such that the non-linear effects of added mass, damping, and wave excitation are small. Restoring non-linear effects are more apparent. On the whole however, it seems that the non-linear effects studied herein will be of little significance for SWATH vessels which have prismatic struts such as SWATH11.

It should be stressed that any conclusions drawn from the analysis of SWATH11 do not necessarily apply to other SWATH ship designs. In addition, SWATH11 has been analysed in its naked hull form. The addition of stabilising fins will produce very different results.

(iv) Analysis of designs with Haunch and Flare

Since non-linear effects have been built into this SWATH motions model, the predictions which it produces are expected to lie between those given by frequency domain analysis and measurements obtained during model seakeeping tests.

SWATH11 was chosen as the test case in this study because a comprehensive set of model test data is available for this design. In addition, frequency domain SWATH motion prediction techniques developed previously at the University of Glasgow Hydrodynamics Laboratory have been thoroughly tested using the same design.

Comparisons made with the model data and with the linear analysis predictions have served to validate the the developed technique. However as SWATH11 possesses close to linear motion characteristics even in large amplitude waves, it has been difficult to demonstrate clearly the effects of non-linear phenomena.

Unfortunately there is generally a very limited amount of SWATH seakeeping measurement data available and in the interests of validating the linear analysis techniques, tests have been restricted to 'well behaved designs such as SWATH11.

In view of this, there is a requirement for carrying out further extensive model tests on more realistic practical SWATH designs. Studies such as those carried out by MacGregor[46] have shown that the SWATH concept will be compromised by the

practicalities of operational role and design integrity requirements. As a result future designs will be characterised by larger waterplane areas and struts with haunch and flare. These characteristics will result in the vessel experiencing substantially increased non-linear motions.

With such model test data available it will be possible to use the time domain simulation to demonstrate the non-linear effects more clearly.

(v) Comments on Computing

When introducing further non-linear effects into the simulation, great care must be taken to minimise the number of calculations performed during each solution cycle. This is essential if the development work is to be carried out on relatively low capacity computers such as the VAX 11/730 machine used during this study. .

The NAg subroutine used to provide numerical solutions to the motion equations has been shown to be accurate and adequate for this coupled heave and pitch problem. However it is not particularly suitable for non-linear systems. The required amount of CPU time for the same number of solution cycles for a given frequency increases dramatically with the increasing complexity of the non-linear system. As explained earlier this is due to the fact that the subroutine FCN is called for a system definition at each numerical integration step of each time step. There is scope therefore for implementing a numerical solution routine which is more suitable for solving non-linear systems. Such a routine would perform the re-definition calculations once only at the beginning of a solution cycle and store information for use during subsequent integration iterations.

If steady state solutions are to be obtained within reasonable periods of time, computer capacity will impose restrictions on the degree of complexity of the non-linear system. The limitations of the VAX 11/730 are such that although it is possible to run the simulation with all three non-linearities in effect simultaneously, the amounts of

CPU time required are excessive and make it impractical to carry out any valid assessment.

In the summary, the type of computer and choice of numerical solution subroutine used during future development work will have significant influence on the rate of research progress.

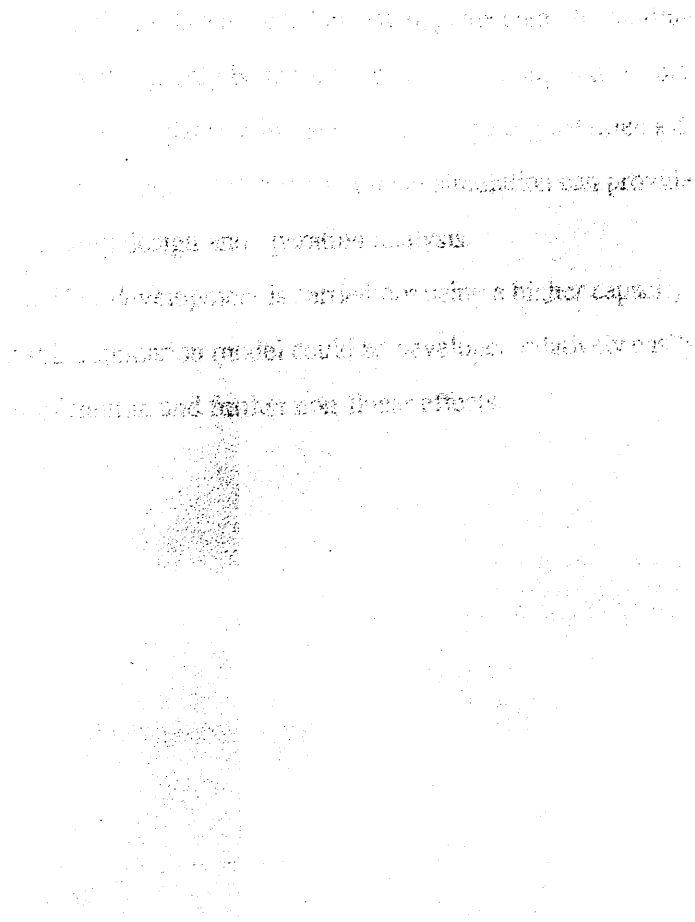

CLOSURE

In addition to covering the essential foundation work required for developing a working and comprehensive SWATH motion prediction technique, the study has provided further indications regarding the nature of SWATH motions in larger amplitude waves. It has been shown that for the example case, the non-linear SWATH motion effects studied are small. Where they have been significant, the predictions obtained from the time domain model offer closer agreement with model test data than those given by existing linear analysis techniques. This is an encouraging development. SWATH11 has prismatic struts and very low water-plane area. Its motions therefore are nearly linear and will certainly be more so than any future practical role SWATH craft. In addition to the essential requirement for investigating the effects described above, the foregoing fact suggests that time domain simulation can provide a valuable tool to aid SWATH ship design and operation analysis.

Given that further development is carried out using a higher capacity computer it is envisaged that this foundation model could be developed relatively easily to include additional modes of motion and further non-linear effects.

References

1. Kim, C. H. Chou, F.S. Tien, D.
'Motions and Hydrodynamic Loads of a Ship Advancing in Oblique Waves'.
Trans. SNAME, Vol. 88 1980, pp 225-256.

2. Salvesen, N. Tuck, E. O. and Faltinsen, O.
'Ship Motions and Sea Loads' Trans. SNAME, Vol. 78 1970.

3. Seren, D. B. and Atlar, M.
'An Overview of the Concepts Employed to Predict the Hydrodynamic Forces Imposed on an Unappended SWATH Ship Proceeding in a Seaway'.
NAOE Report no. 84-63, The University of Glasgow, December 1984.

4. Frank, W.
'On The Oscillation of Cylinders in or below the Free Surface of Deep Fluids'.
DTNSRDC, Report no. 2375, October 1967.

5. Drysdale, L. H.
'Solution of Linear Motion Equation for Coupled Heave and Pitch For a SWATH Ship'. NAOE, Report no. 86-53, The University of Glasgow, December 1986.

6. NAg FORTRAN Library Manual, Mark 11, Numerical Algorithms Group, Oxford, UK, November '83

7. THOMSON, W. T.
'Theory of Vibration With Applications' 2nd. Edition, ISBN 0-04-620012-6, 1984.

8. Djatmiko, E. B.
'Experimental Investigation Into SWATH Ship Motions and Loadings'. M.Sc. Thesis, Department of Naval Architecture and Ocean Engineering, University of Glasgow, November 1987.

9. Zheng, X.
'Prediction of Motion and Wave Loading of Monohull and Twinhull Ships in Waves'. PhD. Thesis, Department of Naval Architecture and Ocean Engineering, University of Glasgow, March 1988.

10. Elsimillawy, N.
'Time-Simulation of Ship Motions'. PhD. Thesis, Department of Naval Architecture and Ocean Engineering, University of Glasgow, July 1984.

11. Lee, C. M. and Curphy, R. M.
'Prediction of Motion, Stability and Wave-load of Small Waterplane-Area, Twin-Hull Ships' Trans. SNAME, Vol. 85, 1977, pp 94-130.

12. Newman, J. N.
'Marine Hydrodynamics', the MIT press, 1977.

13. Hong, Y. S.
'Heave and Pitch Motions of SWATH Ships', Journal of Ship Research, Vol. 30, No.1, March 1986, pp12-25.

14. Kaplan, P.
'Analysis and Prediction of Flat Bottom Slamming Impact of Advanced Marine Vehicles in Waves', International Shipbuilding Progress, Vol. 53, March 1987.

15. Chuang, S. L.
'Experiments on Flat-Bottom Slamming', Journal of Ship Research, March 1966.

16. Chuang, S. L.
'Investigations of Rigid and Elastic Bodies with Water', NSRDC Report No. 3248, February 1970.

17. Chuang, S. L. and Milne, David T.
'Drop Tests of Cones to Assess the Three- Dimensional Effects of Slamming', NSRDC Report No.3543, April 1971.

18. Gerlach, C. Richard,
'Investigation of Water Impact of Blunt Rigid Bodies-Size Scale Effects', Southwest Research Institute, Technical Report No. 2,
Contract No. N00014-67-C-0213 SURI Project No. 02-2036, November 1968.

19. Verhagen, J. H. G.
'The Impact of a Flat Plate on a Water Surface', Journal of Ship Research, December 1967.

20. Lewison G. and Maclean, W. M.
'On the Cushioning of Water Impact by Entrapped Air', Journal of Ship Research, June 1968.

21. 'Comparison of Model and Full-Scale Slamming Data', MPR-351, Contract N00014-71-C-0045, Office of Naval Research. 1971

22. 'Slamming Impact Pressures ', MPR-282, Contract N00014-71-0045, June 1971.

23. Wu, J. Y.
'SWATH Vertical Motion with Emphasis on Fixed Fin Control', Ph.D. Thesis, Glasgow University, Department of Naval Architecture and Ocean Engineering, December 1985.

24. Woolaver, D. A. and Peters, J. B.
'Comparative Ship Performance Sea Trials for the US Coast Guard Cutters *Mellon* and *Cape Corwin* and the US Navy Small Waterplane Area Twin Hull Ship Kaimalino', DTNSRDC Report 80/037, March 1980.

25. Hoerner, F. S. and Borst, H. V.
'Fluid-Dynamic Lift - Practical Information on Aerodynamic and Hydrodynamic Lift', Published by Hoerner, 1975.

26. Hightower, J. D. and Seiple, R. L.
'Operational Experiences with the SWATH Sip SSP Kaimalino' AIAA/SNAME Advanced Marine Vehicles Conference, San Diego, Paper 78- 741, April 1978.

27. Jones M. P.
'Test and Evaluation of Ocean Systems Research 64 SWATH demonstration Craft' Naval Sea Systems Command Detachment, Norfolk, Va, Report 6660-91 Feb. 1982.

28. McCreight, K. Kathryn.
'Assessing the Seaworthiness of SWATH Ships', SNAME Annual Meeting, New York,N.Y., Paper No. 7, November 1987.

29. Atlar M. A.

'Method for Predicting First-Order Hydrodynamic Loads on Single and Twin Sections by the Frank Close-Fit Technique', Glasgow University, Department of Naval Architecture and Ocean Engineering, Report NAOE-85-41, October 1985.

30. Smiley, R.

'A Semi-empirical Procedure for Computing Water Pressure Distribution on Flat and V-Bottom Planing Surfaces During Impact or Planing', NACA TN 2583, December 1951.

31. Arthur, K. Erik.

'A Time Domain Technique for Predicting the Coupled Heave and Pitch Motions of SWATH Ships', Glasgow University, Department of Naval Architecture and Ocean Engineering, Report NAOE-88-23, March 1988.

32. Giannotti, G. Julio.

'Prediction of Slamming Loads for Catamarans', Seventh Annual Offshore Technology Conference, Houston, Texas, Paper No. OTC 2281, May 5-8, 1975.

33. Kim, C. H. Chou, F.

'Wave-Exciting Forces and Moments on an Ocean Platform Fixed in Oblique Seas', OTC Paper No. 1180, Houston, Texas, April 1970.

34. Wehausen, J. V. and Laitone, E. V.

'Surface Waves', Handbuck der Physik, Band IX, Springer Verlag, 1960.

35. Wu, J. Y.

'A Study of the Effect of Fin Size on the Pitching and Heaving of a SWATH Ship', University of Glasgow, Department of Naval Architecture and Ocean Engineering, Report No.NAOE-84-55. 1984.

36. Kim, C. H.

'An Introduction of Water Wave Theory in Ocean Engineering', Stevens Inst. of Tech, Report No. SIT-OE-80-2, NJ,1980.

37. Milne-Thomson, L. M. C.B.E.

'Theoretical Hydrodynamics', 3rd.Edition.

38. Atlar, M. A.

'The SWATH Wave -Load Program Some Aspects of Computer Program SWATHL' University of Glasgow , Department of Naval Architecture and Ocean Engineering, Report No.NAOE-86-55, November 1986.

39. Leitch, E. and Percival, D. J.

'SWATHL User Guide', University of Glasgow , Department of Naval Architecture and Ocean Engineering, MOD Contract Report, 1988.

40. Atlar, M. and Lai, P. S. K.

'A Two-Dimensional Method for Estimating Hydrodynamic Loads and Motions of a Twin-Hulled Semi-Submersible Associated with some Hydrodynamic Aspects in Regular Beam Seas', University of Glasgow , Department of Naval Architecture and Ocean Engineering, Report No.NAOE-85-34, February 1985.

41. Hall, G. and Watt, J. M.
'Modern Numerical Methods for Ordinary Differential Equations', Clarendon Press, Oxford, 1976.

42. Pinkster, J. A.
'Low Frequency Second Order Wave Exciting Forces on Floating Structures', Ph.D Thesis, Wageningen, 1980.

43. Validakis, J. Seren, D. B. and Leitch, E.
'Frequency Dependent Hydrodynamic Coefficient Data for the Heave, Sway and Roll Modes, Part I - Submerged, Symmetrical Single-Hull Sections', University of Glasgow, Department of Naval Architecture and Ocean Engineering, Report No.NAOE-84-02, February 1984.

44. Validakis, J.
'Frequency Dependent Hydrodynamic Coefficient Data for the Heave, Sway and Roll Modes - Part II: Surface Piercing, Single Hull-Strut Combinations', University of Glasgow, Department of Naval Architecture and Ocean Engineering, Report No.NAOE-85-45 Volume II, July 1985.

45. MacGregor, J. R.
'Historical Development of the SWATH Ship Concept', University of Glasgow, Department of Naval Architecture and Ocean Engineering, Report No. NAOE-87-44 November 1987.

46. MacGregor, J. R.
'Concept Design Study of a SWATH SSV', Section Contributed to, Yarrow Shipbuilders, July 1987.

47. 'IKO concepts', Svensk Sjöfarts Tidning, 1988.

48. McGregor, R. C.
'An Illustration of Some SWATH Vessel Characteristics', High Speed Surface Craft Conf., London, May 1983.

49. Gallagher, P.
'Slam Simulations - An Application of Computational Fluid Dynamics', Ph.D Thesis, University of Glasgow, Department of Naval Architecture and Ocean Engineering, May 1985.

50. Bhattacharyya, R.
'Dynamics of Marine Vehicles', John Wiley & Sons, Inc., 1980.

51. Paulding, J. R.
'The Transverse Stability of a Ship in a Longitudinal Seaway', Journal of Ship Research, March 1981.

52. Upahl, E,
'Stability Consideration in a Seaway', Schiffbautechnik, 11 1961, p.441 (Sept.), p.510 (Oct), (BSRA Translation No 1310).

53. Bhattacharyya, R.
'Computer Applications in Hull Form and Stability Calculations', The University of Michigan, The College of Engineering, Department of Naval Architecture and Marine Engineering, No. 038, September, 1969.

54. Martin, J. Kuo, C. and Welaya, Y.
'Ship Stability Criteria Based on Time Varying Roll Restoring Moments', 2nd. Intl. Conf. on Stability of Ships and Ocean Vehicles, Tokyo, October 1982.

55. Helas, G.
'Intact Stability of Ships in Following Waves', 2nd. Intl. Conf. on Stability of Ships and Ocean Vehicles, Tokyo, October 1982.

56. Morrall, A.
'Fishing Vessel Stability and Safety', Proc. Intl. Conf. on Marine Safety, University of Glasgow, September 1983.

57. Choung, M. Lee,
'Prediction of Relative Motion of Ships in Waves' DTNSRDC, MD 20084.

58. Bishop, R. E. D Price, W. G. and Temarel, P.
'On the Hydroelasticity Response of a SWATH to Regular Oblique Waves', Advances in Marine Structures, Paper No. 5, ARE, Dunfermline, Scotland, May 1986.

59. Abbot, I. H. and Von Doenhoff, A. E.
'Theory of Wing Sections', Dover, 1959.

60. Oshima, M. Narita, H. and Kunitake Y.
'Development of the Semi-Submersible Catamaran (SSC)', AIAA/SNAME, Advanced Marine Vehicles Conference, 1979.

61. 'Mesa 80: Mitsui Semi-Submersible Catamaran as a Fast Ferry', Motor Ship, July 1980.